TRANSIENT WAVEFORM SYNTHESIS FOR RADAR TARGET DISCRIMINATION

By

Che-I Chuang

A DISSERTATION

Submitted to
Michigan State University
in partial fulfillment of the requirements
for the degree of

DOCTOR OF PHILOSOPHY

Department of Electrical
Engineering and Systems
Science

1983

ABSTRACT

TRANSIENT WAVEFORM SYNTHESIS FOR RADAR TARGET DISCRIMINATION

By

Che-I Chuang

A new scheme for radar detection and discrimination, the transient waveform synthesis method, is investigated. This scheme consists of synthesizing an aspect-independent waveform for the incident radar signal which excites the target in such a way that the return radar signal from the target contains only a single resonance mode of that target in the late-time period. When the incident waveform synthesized to excite a particular natural mode of a known preselected target is applied to a different target, the return signal will be significantly different from that of the expected natural mode. The wrong target can thus be discriminated.

Three kinds of targets, a normally oriented infinite cylinder, a pair of skew-coupled wires and a system of crossed wires are investigated. Both integral-equation and differential-equation approaches are used to search for the natural resonance modes of the targets. Impulse responses are then computed using these natural modes and the sigularity expansion method (SEM). A complete procedure for synthesizing the required incident radar signal is developed and used to synthesize the waveform for single-mode excitation.

To confirm the applicability of the waveform-synthesis scheme, the synthesized incident waveform is convolved with the impulse response of the target. Numerical results are given to demonstrate target-discrimination sensitivity based on this method. An experimental study is described later, and the results are compared with the theory.

To My Grandfather
Mr. Chang Chuang

ACKNOWLEDGMENTS

The author wishes to express sincere appreciation to his academic advisor, Dr. Kun-Mu Chen, for his assistance and guidance throughout this study. A special note of thanks is due Dr. Dennis P. Nyquist for his generous support and valuable comments during the course of this work.

The author also gratefully acknowledges the special assistance provided by Dr. Byron C. Drachman.

Finally, the author thanks his parents, Mr. and Mrs. Bee-Shang Chuang, and his wife, Hwei-Hsin, for their understanding and encouragement.

TABLE OF CONTENTS

TABLE OF CONTENTS continued

TABLE OF CONTENTS continued

LIST OF TABLES

LIST OF FIGURES

LIST OF FIGURES continued

LIST OF FIGURES continued

LIST OF FIGURES continued

LIST OF FIGURES continued

LIST OF FIGURES continued

LIST OF FIGURES continued

CHAPTER 1

INTRODUCTION

In recent years, research on radar target identification and discrimination utilizing transient electromagnetic waveforms has been conducted by a number of workers [1-8]. One interesting scheme is to irradiate a target with a simple waveform such as an impulse, a step or a ramp signal, and then analyze the scattered field from the target in terms of natural resonance modes of the target. It is known that the waveform of the scattered field is aspect-dependent, but the set of natural resonance frequencies extracted from the scattered field is independent of the aspect angle [9-13]. Using this property, a target can be identified if the extracted set of natural frequencies is compared with the collection of known data on the natural frequencies of various targets. Two different targets can also be discriminated if the two sets of natural frequencies are compared. An inherent limitation of this scheme arises from the presence of noise in the return signal and the associated difficulty of accurately extracting natural frequencies of the target.

In this thesis, an inverse scheme, to be called the "transient waveform synthesis" method, is investigated. Instead of analyzing the field scattered by the target in terms of its natural resonance modes, this new scheme sythesizes the waveform of the incident radar signal in such a way that, when it excites the target, the return radar signal contains only a single natural mode of the target. It will be shown in the following chapters that when the incident radar signal sythesized to excite a particular natural mode of a preselected target is applied to a different target, the return signal will be different from that of the expected natural mode. A "wrong" target can therefore be discriminated from an "expected" target. The following sections discuss more about some theoretical background of this scheme.

1.1 Singularity Expansion Method (SEM) [9, 14]

The SEM was advanced by Carl Baum as a means of treating transient and broadband electromagnetic scattering problem. This development was based on the results from many experiments in which different scatterers were illuminated by transient electromagnetic fields. It was observed during the later-time period (i.e., when the target is not under direct illumination of the exciting field) that the response of the scatterer appeared to consist of a superposition of damped sinusoidal oscillations for which frequencies and damping constants are related to the geometry of the scatterer. The SEM was developed to explore the possibility of expressing any external scattering response as a summation of damped sinusoids of which frequencies and damping constants are characterized by the scatterer in a similar way as the internal response of a cavity.

By using the contour integral in the attempt to inverse-tranform the scattered field in Laplace-transform domain, it was found [9] that the time-domain scattered field can be expressed in terms of the singularities associated with its transform. It has been shown that for finite size objects in free space consisting of perfect conductors with constitutive parameters suitably constrained in their complex s-plane properties, the response has only poles as singularities in the s-plane [15, 16]. In this thesis all except one target are finite-size, so we consider only pole singularities which depend only upon the geometry of the target. The target in Chapter 3 is not finite-size and possesses a branch-cut singularity. It is found, however, that the response related to the branch-cut singularity can be approximated as a sum of two exponentially-decaying functions and thus belongs to the category of natural-mode response with zero frequencies. Therefore, for the targets we aim to study, the damped-sinusoids dominate the late-time response. It is extremely important to note that the natural frequency (i.e.. $s = \sigma + j\omega$ σ = damping constant and $\omega = 2\pi \times$ frequency) depends only on the target geometry. Thus once determined, they characterize the target for any excitation and can be used for target discrimination.

1.2 Aspect-Independent Property of Waveform-Synthesis Method

The simplest case of this radar waveform synthesis scheme has been studied by Chen [17] for the case of a thin wire irradiated by a radar pulse at normal incidence. For this case, it is possible to synthesize a required waveform for the incident radar signal to excite a single-mode return response at all post-incidence times. When this study is generalized to oblique incidence, difficulties are encountered in obtaining a realizable required incident waveform for exciting a single-mode, scattered field. Furthermore, the incident radar signal appears to be aspect-dependent. This difficulty arises because there exists a finite transit time for an obliquely-oriented wire, i.e., a finite time for an impulse to pass the wire. The impulse response of this wire consists of an early-time, forced response in addition to the sum of natural modes which describes a normally oriented wire. This early-time, forced impulse response is difficult to approximate analytically, and consequently is responsible for problems encountered when synthesizing an incident radar signal to excite a single-mode, scattered field at all post-incidence times.

To overcome this difficulty, we have concentrated on the behavior of the late-time response of targets and have found a scheme to synthesize the required waveform for an incident radar signal of finite duration to excite a single-mode, scattered field in the late-time period (where the early-time inpulse response is not required, since that period has elapsed). More significantly, this synthesized incident radar signal is found to be aspect-independent. The details of this scheme are discussed in Chapter 2. Then we apply this scheme in Chapter 3 for a target of infinite cylinder in which the exact solution exists and in Chapters 4 and 5 for coupled wires in which the integral equations are used to solve the problem. Chapter 6 discusses the time-domain scatting range for experiments related to this research. In addition to the waveform synthesis scheme, impulse response of the target is computed so that a detailed study of transient electromagnetics is complete for each example. We conclude this thesis in Chapter 7 by summarizing this scheme from the system point of view and showing some potential problems of this scheme.

CHAPTER 2

DEVELOPMENT OF THE BASIC EQUATIONS

This chapter is concerned with the development of fundamental equations, boundary conditions, and synthesis procedure that will be used repeatedly in later chapters. Section 2.1 concerns the linear-system models for a target-discrimination system and defines the problem. Section 2.2 illustrates the scheme for target discrimation and develops the basic equations associated with it. Section 2.3 discusses the required computations involved in this problem and derives the integral equations with boundary conditions included. Finally, Section 2.4 uses the previous work to obtain a complete procedure for solving this problem numerically.

2.1 Linear-System Models of a Target-Discrimination System

There are two equivalent schemes for target discrimination as depicted in Figure 2.1. The scheme on the left is the original waveform-synthesis method: it transmits the required incident radar signal, which is synthesized for monomode excitation, to the target. The right, expected target will yield a monomode return signal while the wrong target will not. The scheme shown on the right is the alternative implementation: the required incident signal for monomode excitation is synthesized and stored in the computer momory. An incident radar signal with some convenient waveform (provided it possesses the desirable frequency component)

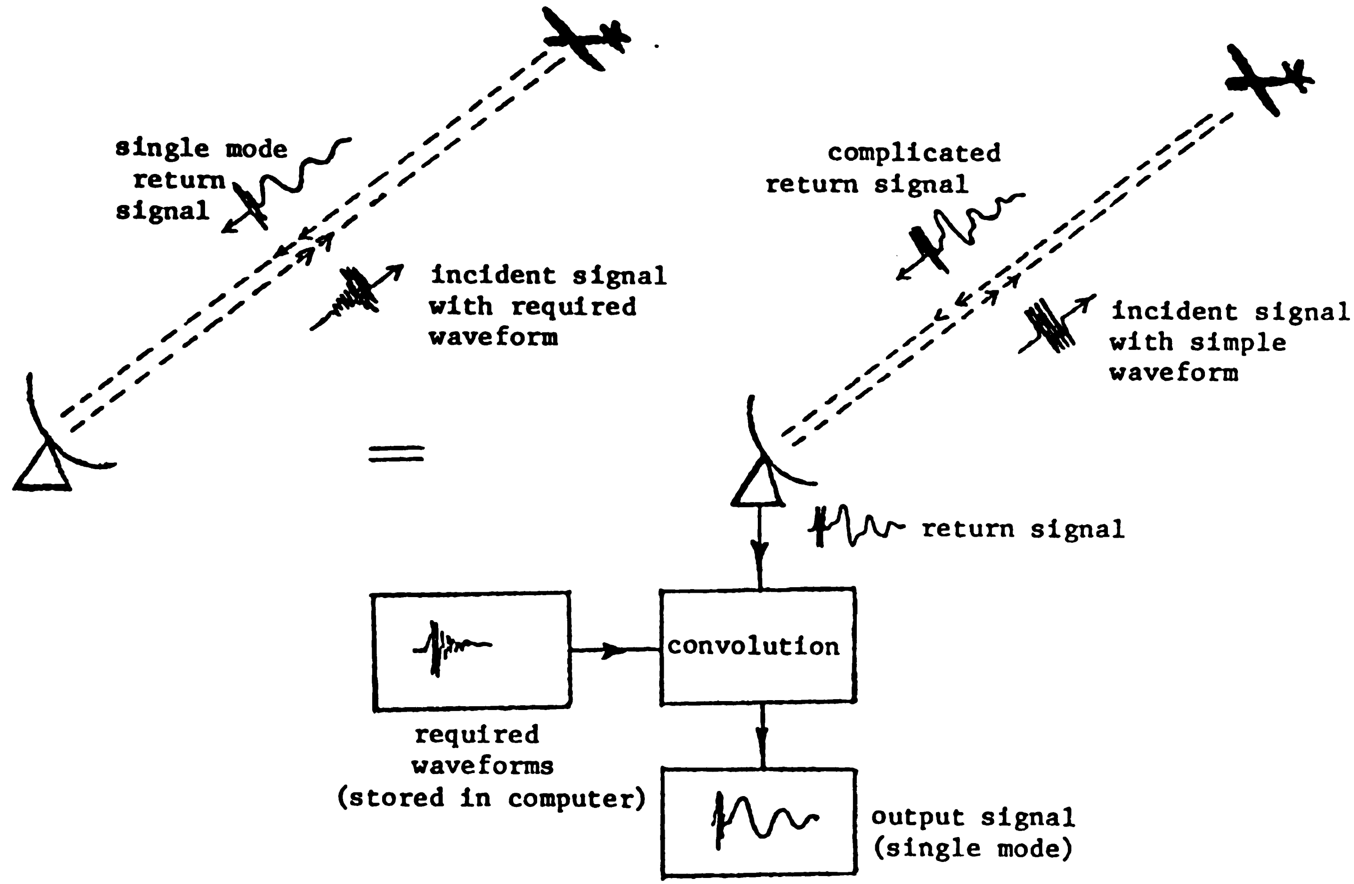

Figure 2.1 Two equivalent arrangements for target discrimination.

excites the target, which yields a return signal with an irregular waveform. The return signal is convolved numerically with the stored, required incident signal. The convolved output signal will display a single natural mode of the target (a pure damped sinusoid) if the target is the expected one; the return signal from a different target will not produce the expected natural mode after convolution.

To define the problem, consider the linear-system models in Figure 2.2. The model on the left corresponds to the scheme on the left of Figure 2.1: the input $E^e(t)$ is the synthesized, required waveform for monomode excitation, the system is represented by the impulse response of the target, h(t), while the output, $E^s(t)$, is the backscattered electric field from the target. The input/output relation is $E^s(t) = E^e(t) * h(t)$. The model on the right is the linear-system representation of the alternative scheme: the input, $E^r(t)$, is the radar return from the target, the system is now represented by $E^e(t)$, which is synthesized and stored in a computer for numerical convolution, while the output, $E^o(t)$, is the result of the convolution between $E^r(t)$ and $E^e(t)$. Therefore, the input/output relation of this model is $E^o(t) = E^r(t) * E^e(t)$.

$$E^e(t) \longrightarrow \underset{\text{(Target)}}{\boxed{h(t)}} \longrightarrow E^s(t) \qquad\qquad E^r(t) \longrightarrow \underset{\text{(Computer)}}{\boxed{E^e(t)}} \longrightarrow E^o(t)$$

Figure 2.2. The linear-system models of two equivalent synthesis schemes for target discrimination.

The problem is thus defined as follows:

(1) For model on the left of Figure 2.2:

Synthesize $E^e(t)$ so that in the late-time period, the output, 2.2

ex

E[

res

imp

fir

whe

$E^s(t) = E^e(t) * h(t)$ will be a single natural mode of the target.

(2) For model on the right of Figure 2.2:

Synthesize $E^e(t)$ so that in the late-time period, the output, $E^o(t) = E^r(t) * E^e(t)$, will be a single natural mode of the target.

It is specified that $E^e(t)$ is of finite duration T_e and $h(t)$, $E^r(t)$ are sums of natural modes in the late-time period for $t \geq 2T_t$, where T_t is the one-way transit time for the signal to pass the whole target.

2.2 Waveforem-Synthesis Scheme

2.2.1 Single-Mode Excitation

For the purpose of synthesizing the required waveform for monomode excitation, we consider the model of the alternative scheme. Since $E^r(t)$ is a representation of radar return from the target, $h(t)$ (impulse response) is a special case of $E^r(t)$ when the incident waveform is an impulse function, therefore, the second model in Section 2.1 includes the first model.

From the discussion in Chapter 1, $E^r(t)$ can be expressed as

$$E^r(t) = E^r(t,\theta) = \xi(t,\theta) + \sum_{n=1}^{n} a_n(\theta)\, e^{\sigma_n t} \mathrm{Cos}(\omega_n t + \varphi_n(\theta)) \quad (2.1)$$

where

$\xi(t,\theta)$ = forced response which exists only during the period $0 \leq t \leq 2T_t$,

$\sum_{n=1}^{n} a_n(\theta)e^{\sigma_n t}\, \mathrm{Cos}(\omega_n t + \varphi_n(\theta))$ = the sum of natural modes which exists for all t,

$a_n(\theta)$ = aspect-dependent amplitude of the nth natural mode,

$\varphi_n(\theta)$ = aspect-dependent phase angle of the nth natural mode.

θ = aspect angle,

$\sigma_n + j\omega_n = S_n$ = the nth natural frequency,

with $N \to \infty$ theorectically, and finite for late-time consideration.

The output, $E^o(t,\theta)$, can be expressed, based on the convolution theorem, as $E^o(t,\theta) = E^r(t,\theta) * E^e(t)$

$$= \int_o^t E^e(t')E^r(t-t', \theta)dt' \tag{2.2}$$

The integration limits are o and t respectively because both $E^e(t)$ and $E^r(t,\theta)$ are causal functions. Substitution of equation (2.1) into equation (2.2) leads to

$$E^o(t,\theta) = \int_o^t E^e(t') \{\xi(t-t',\theta) + \sum_{n=1}^{n} a_n(\theta)\, e^{\sigma_n(t-t')}$$

$$\cdot \mathrm{Cos}[\omega_n(t-t') + \varphi_n(\theta)]\}dt' .$$

For the late-time period of $t \geq T_e + 2T_t$, the upper-limit becomes T_e since $E^e(t') = o$ for $t' \geq T_e$, and the forced response term does not contribute to the integral because

$$\xi(t-t',\theta) = o \quad \text{for} \quad o \leq t' \leq T_e \quad \text{if} \quad t \geq T_e + 2T_t.$$

The property of $\xi(t,\theta) = o$ for $t \geq 2T_t$ has been used. The output waveform in the late-time period then becomes

$$E^{o}(t,\theta) = \int_{o}^{T_e} E_e(t')\{\sum_{n=1}^{N} a_n(\theta)e^{\sigma_n(t-t')}\text{Cos}[\omega_n(t-t') + \varphi_n(\theta)]\}dt' \qquad (2.3)$$

$$\text{for} \quad t \geq T + 2T_t .$$

Equation (2.3) can be rewritten as

$$E^{o}(t,\theta) = \sum_{n=1}^{N} a_n(\theta)e^{\sigma_n t}\{A_n \text{Cos}[\omega_n t + \varphi_n(\theta)]$$

$$+ B_n \text{Sin}[\omega_n t + \varphi_n(\theta)]\} \qquad (2.4)$$

where the coefficients A_n and B_n are given as

$$\begin{Bmatrix} A_n \\ \\ B_n \end{Bmatrix} = \int_{o}^{T_e} E^{e}(t')\, e^{-\sigma_n t'} \begin{Bmatrix} \text{Cos}\omega_n t' \\ \\ \text{Sin}\omega_n t' \end{Bmatrix} dt' \qquad (2.5)$$

It is important to observe that A_n and B_n are independent of the aspect angle θ, and it is possible to choose a proper $E^{e}(t)$ in such a way that all the coefficients vanish except one. By doing so $E^{o}(t,\theta)$ will consist of a single natural mode even though it is still aspect-dependent.

2.2.2 Required Signals and Output Waveforms

Now that it is possible to choose an aspect-independndt $E^{e}(t)$ to excite a single-mode $E^{o}(t,\theta)$, let's construct $E^{e}(t)$ with a linear combination of basis functions as

$$E^{e}(t) = \sum_{m=1}^{2N} d_m f_m(t) \qquad (2.6)$$

where $\{f_m(t)\}$, $m = 1,2,\ldots,2N$ is a set of basis functions such as pulse functions, impulse functions, Fourier cosine functions and nautralmode functions; d_m are unknown coefficients to be determined based on the condition of single-mode excitation of $E^o(t,\theta)$.

Substituting (2.6) in (2.5) leads to

$$
\begin{aligned}
A_n &= \sum_{m=1}^{2N} M_{nm}^c \, d_m \\
B_n &= \sum_{m=1}^{2N} M_{nm}^s \, d_m
\end{aligned}
\qquad (2.7)
$$

where

$$
\begin{Bmatrix} M_{nm}^c \\ M_{nm}^s \end{Bmatrix} = \int_o^{T_e} f_m(t')\, e^{-\sigma_n t'} \begin{Bmatrix} \mathrm{Con}\,\omega_n t' \\ \mathrm{Sin}\,\omega_n t' \end{Bmatrix} dt' \qquad (2.8)
$$

It is observed that M_{nm}^c's and M_{nm}^s's are explicit functions of T_e, incident radar pulse duration, and T_e is a parameter of freedom which can be varied to obtain a desirable waveform for $E^e(t)$. The effect of changing T_e and basis functions will be examined later.

Expression (2.7) can be rewritten in matrix form as

$$
\begin{bmatrix} A_n \\ \hline B_n \end{bmatrix} = \begin{bmatrix} M_{nm}^c \\ \hline M_{nm}^s \end{bmatrix} \begin{bmatrix} d_m \end{bmatrix} \qquad \begin{aligned} n &= 1,2,\ldots,N \\ m &= 1,2,\ldots,2N \end{aligned} \qquad (2.9)
$$

In equation (2.9), $[M_{nm}]$ matrix is of $2N \times 2N$ order, and $[d_m]$ and $\begin{bmatrix} A_n \\ \hline B_n \end{bmatrix}$ are two $2N$ column matrices.

To obtain a single-mode, output waveform (e.g. the jth mode), we can set

$B_j = 1$ and $B_n = o$ for $n \neq j$ and $A_n = o$ for all n.

and solve equation (2.9) to get

$$\begin{bmatrix} d_m \end{bmatrix} = \begin{bmatrix} M^c_{nm} \\ ------ \\ M^s_{nm} \end{bmatrix}^{-1} \begin{bmatrix} A_n \\ ---- \\ B_n \end{bmatrix} \tag{2.10}$$

by choosing T_e so that $\det[M_{nm}] \neq 0$. $[d_m]$ can then be easily determined and $E^e(t)$ is obtained from equation (2.4) to be

$$E^o(t,\theta) = a_j(\theta)e^{\sigma_j t} \operatorname{Sin}(\omega_j t + \varphi_j(\theta)) . \tag{2.11a}$$

Similarly, we can set $A_j = 1$ and $A_n = 0$ for $n \neq j$, $B_n = o$ for all n to get

$$E^o(t,\theta) = a_j(\theta)\, e^{\sigma_j t} \operatorname{Cos}(\omega_j t + \varphi_j(\theta)) . \tag{2.11b}$$

It is noted that with this synthesized $E^e(t)$, the output waveform after convolution, $E^o(t,\theta)$, remains single-mode for any aspect angle θ, even though the amplitude $a_j(\theta)$ and the phase angle $\varphi_j(\theta)$ vary with θ. In other words, when this synthesized $E^e(t)$ is convolved with the radar return, $E^r(t)$, the output signal contains only a single natural mode for any aspect angle as long as $a_j(\theta)$ is not zero.

2.3 Required Computations and Integral Equations

2.3.1 Required Computations

It is obvious from Section 2.2 that search of the natural frequencies is an important task in synthesizing the required waveform. Natural frequencies can be obtained theoretically or experimentally.

In this report, the efforts are concentrated mainly on the theoretical aspects for some simple targets. For those targets which are so complicated that theorectical computations become almost impossible, experimetal approaches such as Prony's method [12] are desirable.

As far as the theoretical methods are concerned, there are basically two approaches; the first one is the differential-equation approach for some idealized structures while the other is the integral-equation approach for those targets that the analytical formulation is impossible. In Chapter 3 we will discuss an example of the first approach, while in Chapters 4 and 5 the second approach is used.

The differential-equation approach is based on Maxwell's equations. The only difference now is that instead of using Fourier transform, we will solve the Maxwell's equations in the Lapalace-transform domain to handle the trasient nature of this problem. As for the integral-equation approach, there is more involved: it is necessary to match the boundary conditions to obtain the integral equation(s) and then solve it (them) numerically; and to make the numerical procedure more stable, we usually need to convert the electric field integral equation to the Hallen-type integral equation [18]. Therefore, Section 2.3.2 is devoted to the derivation of some basic integral equations and their boundary conditions which will be used repeatedly in Chapters 4 and 5.

So long as we get the natural frequencies, the required excitation, $E_e(t)$, can be determined from equations (2.6) and (2.10) with an optimal T_e and proper choices of basis functions. For the waveform-synthesis, our job is done. However, to complete the transient scattering research, it is desirable to compute the impulse response of the target. Once computed, any transient response can be obtained by convolving it with the incident waveform. If this impulse response is convolved with the required waveform, $E_e(t)$, the expected response can be observed.

To determine the impulse response, we apply SEM and the moment method to the integral equations. After obtaining the natural frequencies, we compute the natural mode currents and the coupling coefficients which are related to the residues of natural modes. Induced current is constructed based upon these coefficients and natural mode currents. Scattered field is then determined from the induced current.

2.3.2 Integral Equations

In this section, we will first derive an E-field integral equation (EFIE) for transient surface current excited on a perfectly-conducting body by a transient incident-wave EM field, then use this result in a relatively general, coupled wires systems to get the coupled EFIE's. Finally we will demonstrate an easy way to convert EFIE's to coupled Hallen-type integral equations.

Let's consider the geometry as shown in Figure 2.3 for a general, perfectly-conducting body illuminated by a transient, incident plane-wave, $\vec{E}^i(\vec{r},t)$, which excites, on the body surface, the induced current $\vec{K}(\vec{r},t)$ and charge, $\sigma(\vec{r},t)$. The induced current and charge, in turn, maintain a scattered wave, $\vec{E}^s(\vec{r},t)$. Our objective here is to derive an integral equation for the unknown current by matching the boundary condition on the surface so that the total tangential E-field on the surface is zero,

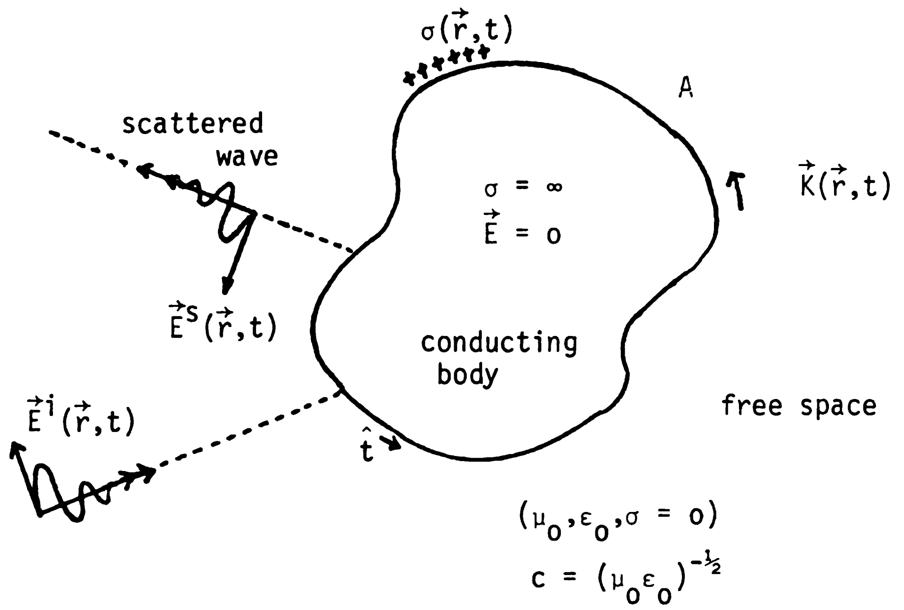

Figure 2.3. A perfectly-conducting body is illuminated by a transient plane-wave, incident field.

$\hat{t}\cdot(\vec{E}^{i}(\vec{r},t) + \vec{E}^{s}(\vec{r},t)) = o$ ... for all $\vec{r} \in A$ of perfectly-conducting body (2.12)

Where $\hat{t}$ is the unit vector tangent to the body surface. We use Laplace transform to handle the transient behavior, and express $\tilde{\vec{E}}^{s}(\vec{r},s)$ in terms of scalar and vector potentials,

$$\tilde{\vec{E}}^{s}(\vec{r},s) = -\nabla\tilde{\Phi}(\vec{r},s) - s\,\tilde{\vec{A}}(\vec{r},s) \tag{2.13}$$

where

$$\tilde{\Phi}(\vec{r},s) = \int_A \frac{\tilde{\sigma}(\vec{r}',s)}{\varepsilon_o 4\pi R} e^{-\gamma R}\, dA' = \text{scalar potential} \tag{2.14}$$

$$\tilde{\vec{A}}(\vec{r},s) = \int_A \frac{\mu_o \tilde{\vec{K}}(\vec{r},s)}{4\pi R} e^{-\gamma R}\, dA' = \text{vector potential} \tag{2.15}$$

and $\gamma \equiv \frac{s}{c}$ = complex propagation constant.

The conservation of change in Laplace-transform domain leads to

$$\nabla\cdot\tilde{\vec{K}}(\vec{r},s) = -s\tilde{\sigma}(\vec{r},s)\ . \tag{2.16}$$

Substituting equation (2.16) into equation (2.14), we express scalar potential in terms of source $\tilde{\vec{K}}(\vec{r},s)$,

$$\tilde{\Phi}(\vec{r},s) = \int_A \frac{-\frac{1}{s}\nabla'\cdot\tilde{\vec{K}}(\vec{r}',s)}{\varepsilon_o 4\pi R} e^{-\gamma R}\, dA'\ . \tag{2.17}$$

Equations (2.17), (2.15) and (2.13) give us a relation between $\tilde{\vec{E}}^{s}(\vec{r},s)$ and $\tilde{\vec{K}}(\vec{r},s)$,

$$\tilde{\vec{E}}^{s}(\vec{r},s) = \frac{1}{s\varepsilon_o}\nabla\Big[\int_A \frac{\nabla'\cdot\tilde{\vec{K}}(\vec{r}',s)}{4\pi R} e^{-\gamma R}\, dA'$$

$$-s\,\mu_o \int_A \frac{\tilde{\vec{K}}(\vec{r}',s)}{4\pi R} e^{-\gamma R}\, dA'\Big]\ . \tag{2.18}$$

The combination of equation (2.18) and boundary condition (2.12) leads to

$$- \hat{t}\cdot\vec{\tilde{E}}^{i}(\vec{r},s) = \frac{1}{s\varepsilon_o}\ \hat{t}\cdot\nabla\left[\int_A \frac{\nabla\cdot\vec{\tilde{K}}(\vec{r}\,',s)}{4\pi R}\ e^{-\gamma R}\ dA'\right]$$

$$- s\mu_o\left[\int_A \frac{\hat{t}\cdot\vec{\tilde{K}}(\vec{r}\,',s)}{4\pi R}\ e^{-\gamma R}\ dA'\right] \quad \text{for} \quad \vec{r}\in A, \qquad (2.19)$$

rearranging equation (2.19) we finally get

$$\int_A [\nabla'\cdot\vec{\tilde{K}}(\vec{r}\,',s)(\hat{t}\cdot\nabla) - r^2\ \hat{t}\cdot\vec{\tilde{K}}(\vec{r}\,',s)]\frac{e^{-\gamma R}}{4\pi R}\ dA'$$

$$= -\varepsilon_o s\ \hat{t}\cdot\vec{\tilde{E}}^{i}(\vec{r},s) \quad \text{for all} \quad \vec{r}\in A\ . \qquad (2.20)$$

This is EFIE for unknown $\vec{\tilde{K}}(\vec{r},s)$ induced on A in Laplace-transform domain.

Let's consider the coupled wires system as shown in Figure 2.4, the wires may or may not be crossed.

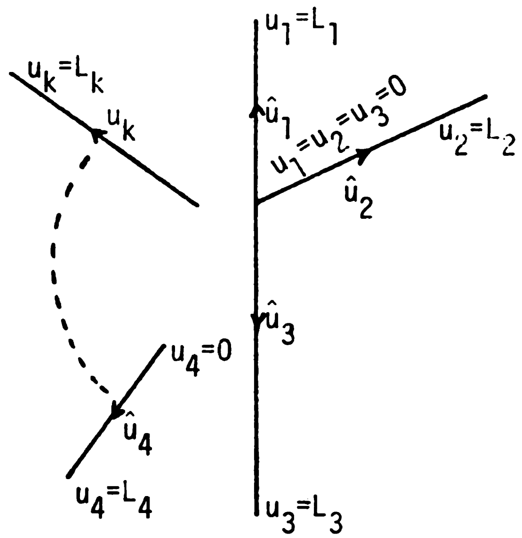

Figure 2.4. A general coupled wires system

Equation (2.20) becomes

$$\int_\Gamma \nabla'\cdot\vec{I}(\vec{r}',s)(\hat{t}\cdot\nabla) - \gamma^2\hat{t}\cdot\vec{I}(\vec{r}',s)\ \frac{e^{-\gamma k}}{4\pi R}\,d\ell' = -\varepsilon_o s\hat{t}\cdot\vec{E}^i(\vec{r},s) \qquad (2.21)$$

where Γ is the contour of integration; note that surface integral becomes a line integral after the thin wire approximation. Since $\nabla'\cdot\vec{I}_\ell(u_\ell',s) = \frac{\partial I_\ell(u_\ell',s)}{\partial u_\ell'}$ --- for $\ell = 1,2,\ldots,K$, and $\hat{t}\cdot\nabla = \frac{\partial}{\partial u_k}$ for $k = 1,2,\ldots,K$, equation (2.21) can then be rewritten as

$$\sum_{\ell=1}^{K}\int_o^{L_\ell}\left[\frac{\partial I_\ell}{\partial u_\ell'}\ \frac{\partial}{\partial u_k} - \gamma^2(\hat{u}_k\cdot\hat{u}_\ell)\ I_\ell(u_\ell',s)\right]\frac{e^{-\gamma R_{k\ell}}}{4\pi R_{k\ell}}\,du_\ell'$$

$$= -\varepsilon_o s\ \hat{u}_k\cdot\vec{E}^i(u_k,s) \text{ --- for } 0 \le u_k \le L_k,\ k = 1,2,\ldots,K \qquad (2.22)$$

where $R_{k\ell} = R(u_k,u_\ell')$ for $(k,\ell) = 1,2,\ldots,K$

$$= |u_k\hat{u}_k - (\vec{d}_{k\ell} + u_\ell'\hat{u}_\ell)|$$

$$= \sqrt{u_k^2 + u_\ell'^2 - 2u_k u_\ell'(\hat{u}_k\cdot\hat{u}_\ell) - 2\vec{d}_{k\ell}\cdot(u_k\hat{u}_k - u_\ell'\hat{u}_\ell) + d_{k\ell}^2}\ ,$$

$\vec{d}_{k\ell}$ = the vector from the origin for u_k to the origin for u_ℓ.
To handle the thin-wire approximation at the source-point singularily $u_\ell' = u_k$ when $\ell = k, d_{k\ell} = o$, the wire raduis a_k^2 is included in the above formulation such that $R_{kk}'(u_k,u_k') = a_k$. Then $R_{k\ell}$ becomes

$$R_{k\ell}(u_k,u_\ell') \approx \sqrt{u_k^2 + u_\ell'^2 - 2u_k u_\ell'(\hat{u}_k\cdot\hat{u}_\ell) - 2\vec{d}_{k\ell}\cdot(u_k\hat{u}_k - u_\ell'\hat{u}_\ell) + d_{k\ell}^2 + a_k^2} \qquad (2.23).$$

Physically, we consider the field point u_k to be on the wire surface while source point u_ℓ' to be located along the wire axis for the thin-wire approximation. The leading integral terms in equation (2.22) can be modified by evaluating the integral by parts in the u'_ℓ variable so that I_ℓ instead of $\frac{\partial I_\ell}{\partial u_\ell}$ appears as unknown:

$$\int_0^{L_\ell} \frac{\partial I_\ell}{\partial u'_\ell}(u'_\ell,s) \frac{\partial}{\partial u_k} \frac{e^{-\gamma R_{k\ell}}}{4\pi R_{k\ell}} du'_\ell = I_\ell(u'_\ell,s) \frac{\partial}{\partial u_k} \frac{e^{-\gamma R_{k\ell}}}{4\pi R_{k\ell}} \Bigg|_{u'_\ell = 0}^{u'_\ell = L_\ell}$$

$$- \int_0^{L_\ell} I_\ell(u'_\ell,s) \frac{\partial^2}{\partial u_k \partial u'_\ell} \frac{e^{-\gamma R_{k\ell}}}{4\pi R_{k\ell}} du'_\ell \tag{2.24}$$

If we define

$$W_{k\ell}(u_k) \equiv I_\ell(L_\ell^-,s) \frac{e^{-\gamma R_{k\ell}(u_k,L_\ell)}}{4\pi R_{k\ell}(u_k,L_\ell)} - I_\ell(o^+,s) \frac{e^{-\gamma R_{k\ell}(u_k,o)}}{4\pi R_{k\ell}(u_k,o)} \tag{2.25}$$

then expressions (2.22) (2.24) and (2.25) lead to

$$\sum_{\ell=1}^{K} \{-\int_0^{L_\ell} I_\ell(u'_\ell,s)[\frac{\partial^2}{\partial u_k \partial u'_\ell} + \gamma^2(\hat{u}_k \cdot \hat{u}_\ell)] \frac{e^{-\gamma R_{k\ell}}}{4\pi R_{k\ell}} du'_\ell + \frac{\partial W_{k\ell}}{\partial u_k}(u_k)\}$$

$$= -\varepsilon_o s \hat{u}_k \cdot \tilde{\vec{E}}^i(u_k,s) \text{ --- for } 0 \leq u_k \leq L_k,\ k = 1,2,\ldots,K\,. \tag{2.26}$$

This is the basic set of coupled EFIE's we will be using in Chapters 4 and 5.

Examing closely equation (2.26), we can see that the kernel function of this EFIE involves a second partial derivative. This term, when applying the moment method solution, will introduce discontinuity in the basis function of charge, and thus cause some undesirable features such as the sensitivity to changes in the number of partitions and the initial guess in root searching. To avoid the unstable characteristics of EFIE, we derive, in the following, the Hallen-type integral equations in which the kernel functions possess no derivatives.

Equations in (2.26) are integro-differential equations. They can be reduced to pure integtal equations of the Hallen type by first converting them to an inhomogeneous ODE which can be solved to provide the desired result.

In the $\ell = k$ integral term of the coupled system of EFIE's,

$$\frac{\partial^2}{\partial u_k \partial u_k'} \frac{e^{-\gamma R_{kk}}}{4\pi R_{kk}} = - \frac{\partial^2}{\partial u_k^2} \frac{e^{-\gamma R_{kk}}}{4\pi R_{kk}} ,$$

so that this term is singled out for the special attention,

$$\int_0^{L_k} I_k(u_k',s)[\frac{\partial^2}{\partial u_k^2} - \gamma^2] \frac{e^{-\gamma R_{kk}}}{4\pi R_{kk}} du_k' + \sum_{\ell=1}^{K} \{\frac{\partial w_{k\ell}(u_k)}{\partial u_k}$$

$$- (1-\delta_{\ell k}) \int_0^{L_\ell} I_\ell(u_\ell',s) [\frac{\partial^2}{\partial u_k \partial u_\ell'} + \gamma^2(\hat{u}_k \cdot \hat{u}_\ell)] \frac{e^{-\gamma R_{k\ell}}}{4\pi R_{k\ell}} du_\ell'\}$$

$$= -\varepsilon_0 s \, \hat{u}_k \cdot \tilde{\vec{E}}^i(u_k,s) \tag{2.27}$$

where $\delta_{\ell k} = o$ for $\ell \neq k$; $\delta_{\ell k} = 1$ for $\ell = k$.

The trick is to modify the differential operator of the second integral term (by adding and subtracting an appropriate factor) to indentify an operator which is common with that of the first integral term,

$$[\frac{\partial^2}{\partial u_k \partial u_\ell'} + \gamma^2(\hat{u}_k \cdot \hat{u}_\ell)] \frac{e^{-\gamma R_{k\ell}}}{4\pi R_{k\ell}} = - [\frac{\partial^2}{\partial u_k^2} - \gamma^2] \frac{e^{-\gamma R_{k\ell}}}{4\pi R_{k\ell}} (\hat{u}_k \cdot \hat{u}_\ell)$$

$$+ \frac{\partial}{\partial u_k} [\frac{\partial}{\partial u_\ell'} + \frac{\partial}{\partial u_k} (\hat{u}_k \cdot \hat{u}_\ell)] \frac{e^{-\gamma R_{k\ell}}}{4\pi R_{k\ell}}$$

and

$$[\frac{\partial}{\partial u'_\ell} + \frac{\partial}{\partial u_k}(\hat{u}_k\cdot\hat{u}_\ell)]\,\frac{e^{-\gamma R_{k\ell}}}{4\pi R_{k\ell}} = \frac{d}{dR_{k\ell}}\,\frac{e^{-\gamma R_{k\ell}}}{4\pi R_{k\ell}}\,[\frac{\partial}{\partial u'_\ell} + \frac{\partial}{\partial u_k}(\hat{u}_k\cdot\hat{u}_\ell)]R_{k\ell}$$

$$= \frac{d}{dR_{k\ell}}\,\frac{e^{-\gamma R_{k\ell}}}{4\pi R_{k\ell}}\,\frac{u'_\ell - u_k(\hat{u}_k\cdot\hat{u}_\ell) + \vec{d}_{k\ell}\cdot\hat{u}_\ell + [u_k - u'_\ell(\hat{u}_k\cdot\hat{u}_\ell) - \vec{d}_{k\ell}\cdot\hat{u}_k](\hat{u}_k\cdot\hat{u}_\ell)}{R_{k\ell}}$$

$$= \frac{d}{dR_{k\ell}}\,\frac{e^{-\gamma R_{k\ell}}}{4\pi R_{k\ell}}\,\frac{u'_\ell[1-(\hat{u}_k\cdot\hat{u}_\ell)^2] + d_{k\ell}\cdot[\hat{u}_\ell - \hat{u}_k(\hat{u}_k\cdot\hat{u}_\ell)]}{R_{k\ell}} \quad .$$

By defining

$$g_{k\ell}(u_k,u'_\ell,s) \equiv \frac{d}{dR_{k\ell}}\,\frac{e^{-\gamma R_{k\ell}}}{4\pi R_{k\ell}}\,\frac{u'_\ell[1-(\hat{u}_k\cdot\hat{u}_\ell)^2] + \vec{d}_{k\ell}\cdot[\hat{u}_\ell - \hat{u}_k(\hat{u}_k\cdot\hat{u}_\ell)]}{R_{k\ell}}, \qquad (2.28)$$

equation (2.27) can be converted to

$$[\frac{\partial^2}{\partial u_k^2} - \gamma^2]\sum_{\ell=1}^{K}\int_0^{L_\ell} I_\ell(u'_\ell,s)\,\frac{e^{-\gamma R_{k\ell}}}{4\pi R_{k\ell}}\,(\hat{u}_k\cdot\hat{u}_\ell)du'_\ell$$
$$+ \sum_{\ell=1}^{K}\{\frac{\partial w_{k\ell}(u_k)}{\partial u_k} - (1-\delta_{\ell k})\int_0^{L_\ell} I_\ell(u'_\ell,s)\,\frac{\partial g_{k\ell}(u_k,u'_\ell,s)}{\partial u_k}\,du'_\ell\}$$
$$= -\varepsilon_0 s\,\hat{u}_k\cdot\tilde{\vec{E}}^i(u_k,s) \quad . \qquad (2.29)$$

Recall that an inhomogeneous ODE in the following form

$$(-\frac{\partial^2}{\partial u^2} - \gamma^2)\psi(u) = f(u)$$

can be solved [19] as

$$\psi(u) = C_1 \cosh \gamma u + C_2 \text{ sink } ru + \frac{1}{\gamma}\int_0^u f(\xi)\sinh \gamma(u-\xi)d\xi$$

Therefore (2.29) can be solved as inhomogeneous ODE to be

$$\sum_{\ell=1}^{K} \int_0^{L_\ell} I_\ell(u'_\ell,s) \frac{e^{-\gamma R_{k\ell}}}{4\pi R_{k\ell}} (\hat{u}_k\cdot\hat{u}_\ell)du'_\ell$$

$$= C'_{1k} \cosh \gamma u_k + C'_{2k} \sinh \gamma u_k + \frac{1}{\gamma}\int_0^{u_k} d\xi \sinh[\gamma(u-\xi)]$$

$$\{ \sum_{\ell=1}^{N} [(1-\delta_{k\ell}) \int_0^{L_\ell} I_\ell(u'_\ell,s) \frac{\partial g_{k\ell}(\xi,u'_\ell,s)}{\partial\xi} du'_\ell$$

$$- \frac{\partial w_{k\ell}(\xi)}{\partial\xi}] - \varepsilon_o s \, \hat{u}_k\cdot\vec{\tilde{E}}^i(\xi,s)\} \tag{2.30}$$

The two terms involving $\frac{\partial}{\partial\xi}$ can be integrated by parts to give:

$$\frac{1}{\gamma}\int_0^{u_k} d\xi \sinh[\gamma(u-\xi)]\{ \sum_{\ell=1}^{K} [(1-\delta_{k\ell}) \int_0^{L_\ell} I_\ell(u'_\ell,s) \frac{\partial g_{k\ell}(\xi,u'_\ell,s)}{\partial\xi} du'_\ell - \frac{\partial w_{k\ell}(\xi)}{\partial\xi}]\}$$

$$= \sum_{\ell=1}^{N} \int_0^{L_\ell} du'_\ell \, I_\ell(u'_\ell,s)(1-\delta_{k\ell}) \left[\frac{g_{k\ell}(\xi,u'_\ell,s) \sinh \gamma(u_k-\xi)}{\gamma}\right|_{\xi=o}^{\xi=u_k}$$

$$+ \int_0^{u_k} g_{k\ell}(\xi,u'_\ell,s) \cosh \gamma(u_k-\xi)d\xi] - \sum_{\ell=1}^{K} \left.\frac{w_{k\ell}(\xi) \sinh \gamma(u_k-\xi)}{\gamma}\right|_{\xi=o}^{\xi=u_k}$$

$$+ \int_0^{u_k} w_{k\ell}(\xi) \cosh \gamma(u_k-\xi)d\xi] \tag{2.31}$$

where

$$\left.\frac{g_{k\ell}(\xi,u'_\ell,s) \sinh \gamma(u_k-\xi)}{\gamma}\right|_{\xi=o}^{\xi=u_k} = -\frac{g_{k\ell}(o,u'_\ell,s) \sinh \gamma u_k}{\gamma}$$

$$\left.\frac{w_{k\ell}(\xi) \sinh \gamma(u_k-\xi)}{\gamma}\right|_{\xi=o}^{\xi=u_k} = -\frac{w_{k\ell}(o) \sinh \gamma u_k}{\gamma} \; . \tag{2.32}$$

The terms associated with expressions in (2.32) and last term in (2.31) are simply proportional to cosh γu_k and sink γu_k, and therefore we can redefine constants C'_{1k} and C'_{2k} to be C_{1k} and C_{2k}. Equation (2.30) is thus reduced to

$$\sum_{\ell=1}^{K} \int_{0}^{L_\ell} I_\ell(u'_\ell,s) \left[\frac{e^{-\gamma R_{k\ell}}}{4\pi R_{k\ell}} (\hat{u}_k\cdot\hat{u}_\ell) - (1-\delta_{k\ell}) \int_0^{u_k} g_{k\ell}(\xi,u'_\ell,s) \cosh\gamma(u_k-\xi)\, d\xi\right] du'_\ell$$

$$= C_{1k}\cosh\gamma u_k + C_{2k}\sinh\gamma u_k - \frac{\varepsilon_0 s}{\gamma}\int_0^{u_k} \hat{u}_k\cdot\tilde{\vec{E}}^i(\xi,s)\sinh\gamma(u_k-\xi)d\xi \qquad (2.33)$$

Defining
$$K_{k\ell}(u_k|u'_\ell,s) \equiv \frac{e^{-\gamma R_{k\ell}}}{4\pi R_{k\ell}}(\hat{u}_k\cdot\hat{u}_\ell) - (1-\delta_{k\ell})\int_0^{u_k} g_{k\ell}(\xi,u'_\ell,s)\cosh\gamma(u-\xi)d\xi \qquad (2.34)$$

leads to

$$\sum_{n=1}^{K}\int_0^{L_\ell} I_\ell(u'_\ell,s)\, K_{k\ell}(u_k|u'_\ell,s)du'_\ell$$

$$= C_{1k}\cosh\gamma u_k + C_{2k}\sinh\gamma u_k - \frac{\varepsilon_0 s}{\gamma}\int_0^{u_k}\hat{u}_k\cdot\tilde{\vec{E}}^i(\xi,s)\sinh\gamma(u_k-\xi)d\xi$$

$$\text{for } 0 \le u_k \le L_k \quad \text{and } k = 1,2,\ldots,K. \qquad (2.35)$$

This set of integral equations has kernel functions which possess no derivatives, however, there are integration terms involved. This is a more stable set of IE's but with the increased cost of computer execution time and storage since the integration terms not only take much more computation, but also destroy the symmetry of the matrix which is obtained from employing the moment nethod. With this trade-off we use Hallen-type IE's to find the natural modes while EFIE's are used to determined the coupling coefficients.

There are unknown constants introduced in equation (2.35). The way to determine them is to exploit the boundary conditions. For those wires with no cross, the constants are considered as 2K unknowns with 2K currents on the wire ends vanishing and thus dropped out of the unknowns. The case of crossed wires is more complicated, we will discuss more in Chapter 5. Basically the boundary conditions used to determine unknown constants are: [20]

1) continuity of scalar potential across the junctions,

2) continuity of vector potential across the junctions,

3) zero current at the wire ends,

4) Kirchhoff's current law at junctions.

Conditions 1), 3) and 4) are sufficient to solve the problem, while condition 2) will further simplify the problem for the case with wire segments aligned in the same line.

2.4 Problem-solving Procedure.

The procedure used in later chapters to solve the problem and to synthesize the required waveform, $E^e(t)$, is outlined as follows.

1. Based upon the Maxwell's equaitons and boundary conditions to form the appropriate differential equations or integral equaitons in the Laplace-transform domain, set $\tilde{\vec{E}}^i(\vec{r},s) = o$ for natural response.

2. Solve the differential equations analytically or use the moment method to form a matrix equation,

$$AI = o \quad (2.36)$$

3. Set det(A) as a function of s, then use Muller's or Newton's method to determine its zeros, which are the natural frequencies. Solve (2.36) after finding natural frequencies to determine the natural mode current, $\nu_n(u)$, for nth mode.

4. Using SEM [14] to compute the coupling coefficients as

$$a_n(s) = \frac{\int_\Gamma S(u,s)\nu_n(u)du}{\int_\Gamma \int_\Gamma \nu_n(u)\nu_n(u')\{\frac{d}{ds}[K(u|u',s)]\}_{s=s_n} du'du} \quad (2.37)^{1}$$

where

$$S(u,s) = -\varepsilon_o s\, \hat{u}_k\cdot\tilde{\vec{E}}^i(u_k,s) - \sum_{\ell=1}^{K} \frac{\partial w_{k\ell}}{\partial u_k}(u_k) \quad \text{for} \quad o \le u_k \le L_k$$

$$k = 1,2,\ldots,K$$

= forcing function or source function,[2]

$K(u|u',s)$ is the kernel function in (2.26),

Γ represents the whole contour of integration in equation (2.26),

the induced current is then expressed as $I(u,s) = \sum_{n=1}^{N} a_n(s)\nu_n(u)(s-s_n)^{-1}$ (2.38)

5. The impulse response of scattered field is computed from the vector potential which is maintained by the impulse response of the induced current. We will discuss this more in Chapters 4 and 5.

6. The required waveform is synthesized by the process described in Section 2.2.

7. To check the results, we use discrete convolution or FFT to convolve $E^e(t)$ with $h(t)$.

8. Perform the transient EM experiments which will be discribed in Chapter 6, to check the impulse response.

---

[1]In Baum's formulation, the denominator has $\mu_n(u)$ instead of $\nu_n(u)$, where $\mu_n(u)$ is the solution of $JA = o$; $\mu_n(u) = \nu_n(u)$ for the case of symmetric matrix A. This is true for those cases we want to discuss if we consider EFIE's.

[2]It can be easily seen from equation (2.26).

These are the major steps used to solve this problem. We will solve a differential equation for an infinite cylinder in which an exact analytical solution exists, in Chapter 3. In Chapter 4, a skew coupled wires system with no cross is considered. We then consider a system of crossed wires in Chapter 5 as a crude model of airplane. The experimental study of this problem is discussed in Chapter 6.

CHAPTER 3

INFINITE CYLINDER

The waveform-synthesis method is applied here to a target consisting of a thick, perfectly-conducting, infinite cylinder illuminated by a transient, normally-incident, transversely-polorized plane wave. Using a spectral approach in the Laplace-transform domain, the current induced on the cylinder and its backscatter-field transfer function are first calculated in Section 3.1. By inverse transforming its transfer function, the impulse response of the target is obtained in Section 3.2. It is found that this response consists of a discrete spectrum comprised of a residue series in natural resonance modes augmented by a series of continuous-spectrum terms arising from a branch-cut integration; the impulse response of the infinite cylinder can not be constructed as a pure SEM series. The late-time impulse response is subsequently approximated in closed form in Section 3.3 and used to obtain the late-time backscattered field excited by an incident field with arbitrary waveshape. Based upon the latter representation of the backscattered field, the incident waveform required to excite a monomode return radar signal is synthesized.

It is demonstrated in Section 3.4 that an optimal incident radar signal can be synthesized which excites (by convolution with the impulse response) a monomode return signal from the cylinder in its late-time period. When an optimal signal,synthesized to excite a particular natural mode of a given cylinder, illuminates a cylinder of slightly different radius, the resulting return signal is found to differ from the expected monomode response. The "wrong" cylinder is therefore sensitively discriminated from the "expected" one. Applicability of the radar waveform synthesis method to implement target identification is therefore demonstrated.

3.1 Induced Current and Backscattered Field

An infinite, perfectly-conducting cylinder of radius "a" is illuminated by a normally-incident, transient, plane-wave radar signal with its electric field polorized perpendicular to the cylinder axis as indicated in Figure 3.1. The incident field is expressed as

$$\vec{E}^i(\vec{r},t) = \hat{y}\ u[t-(x+a)/c]F[t-(x+a)/c] \tag{3.1}$$

where $F(t)$ is an unknown waveform function to be synthesized subject to the criterion that it excite single, natural-mode backscatter from the cylinder. Laplace transforming yields

$$\tilde{\vec{E}}^i(\vec{r},s) = L\{\vec{E}^i(\vec{r},t)\} = \hat{y}\ \tilde{F}(s)e^{-\gamma(x+a)} \tag{3.2}$$

where $\tilde{F}(s) = L\{F(t)\}$ and $\gamma = s/c$ is the complex propagation constant. The total EM field excited about the cylinder by $\vec{E}^i$ consists of a wave, transverse-magnetic (TM) to its direction of propagation, with

$$\tilde{\vec{E}}(\vec{r},s) = \hat{r}\ \tilde{E}_r(r,\varphi,s) + \hat{\varphi}\ E_\varphi(r,\varphi,s) \tag{3.3}$$

$$\tilde{\vec{H}}(\vec{r},s) = \hat{z}\ \tilde{H}_z(r,\varphi,s)$$

where $\tilde{\vec{E}}(\vec{r},s)$ and $\tilde{\vec{H}}(\vec{r},s)$ satisfy Maxwell's equations in Laplace-transform domain,

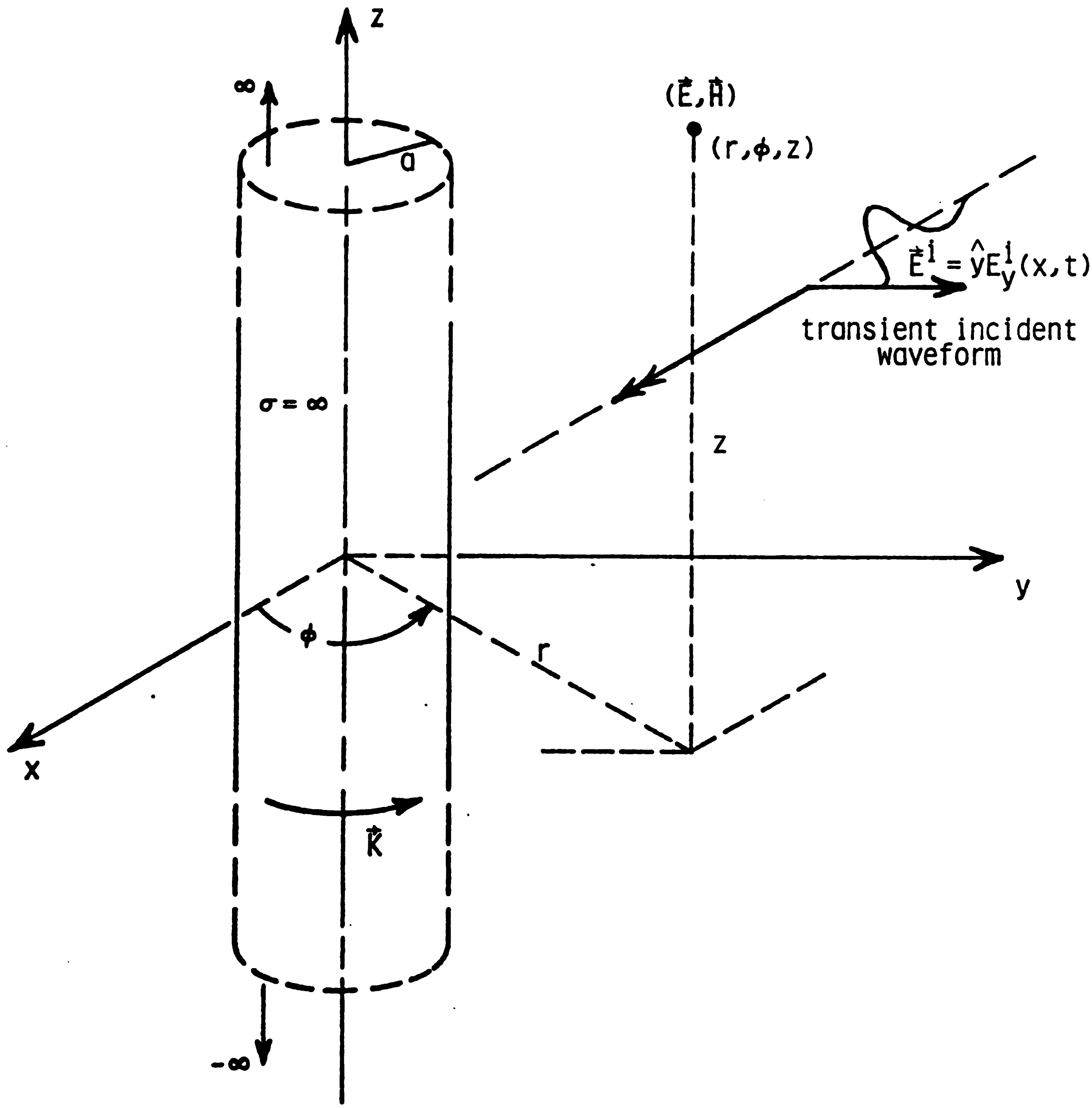

Figure 3.1 Configuration of an infinite, perfectly-conducting cylinder illuminated by a transient, normally-incident, transversely-polarized plane wave.

$$\left.\begin{aligned}\nabla\times\tilde{\vec{E}}(\vec{r},s) &= -\mu_o s\,\tilde{\vec{H}}(\vec{r},s)\\ \nabla\times\tilde{\vec{H}}(\vec{r},s) &= \epsilon_o s\,\tilde{\vec{E}}(\vec{r},s)\end{aligned}\right\} . \tag{3.4}$$

Equation (3.4) leads to

$$\left.\begin{aligned}\tilde{E}_r &= \frac{1}{\epsilon_o s r}\,\frac{\partial\tilde{H}_z}{\partial\varphi}\\ \tilde{E}_\varphi &= \frac{-1}{\epsilon_o s}\,\frac{\partial\tilde{H}_z}{\partial r}\end{aligned}\right\} \tag{3.5}$$

and

$$\frac{1}{r}\left[\frac{\partial}{\partial r}(r\tilde{E}_\varphi) - \frac{\partial}{\partial\varphi}\tilde{E}_r\right] = -\mu_o s\tilde{H}_z \quad . \tag{3.6}$$

Subsitute Equation (3.5) into equation (3.6), we get

$$\nabla^2\tilde{H}_z - \gamma^2\tilde{H}_z = o. \tag{3.7}$$

Total field $\tilde{\vec{E}}$ can be expressed as $\tilde{\vec{E}} = \tilde{\vec{E}}^i + \tilde{\vec{E}}^s$, where $\tilde{\vec{E}}^s$ is the scattered field maintained by induced surface current excited on the cylinder, and satisfies the boundary condition

$$\hat{\Phi}\cdot\tilde{\vec{E}}\,(r=a,\Phi,s) = o. \tag{3.8}$$

Incident fields $\tilde{E}^i_\Phi$, $\tilde{H}^i_z$ can be expressed in cylindrical coordinates by a plane-wave expansion [21] in the cylindrical-wave function solutions to equations (3.5) and (3.7) which are bounded in the origin as

$$\begin{aligned}\tilde{E}^i_\varphi &= \tilde{F}(s)\ e^{-\gamma a}\ e^{-\gamma r\cos\Phi}\cos\Phi \\ &= \sum_{n=o}^{\infty} I'_n(\gamma r)\ [A_n(s)\cos(n\Phi)]\end{aligned} \tag{3.9}$$

with unknown Fourier coefficients $A_n(s)$. Exploit orthogonality to determine $A_n(s)$,

$$I_n'(\gamma r)\,\frac{2\pi}{\epsilon_n}\,A_n(s) = \tilde{F}(s)\,e^{-\gamma a}\int_{-\pi}^{\pi} e^{-\gamma r\cos\Phi}\,\text{Cos}\Phi\,\text{Cos}(n\Phi)d\Phi \tag{3.10}$$

where ϵ_n is Neumann's number ($\epsilon_o = 1$; $\epsilon_n = 2$, $n > o$). From [22],

$$I_n(z) = \frac{1}{\pi}\int_{o}^{\pi} e^{z\text{Cos}\theta}\,\text{Cos}(n\theta)d\theta \tag{3.11}$$

by differentiation,

$$I_n'(z) = \frac{1}{\pi}\int_{o}^{\pi} e^{z\text{Cos}\theta}\,\text{Cos}\theta\,\text{Cos}(n\theta)d\theta \tag{3.12}$$

Therefore, equation (3.10) becomes,

$$I_n'(\gamma r)\,\frac{2\pi}{\epsilon_n}\,A_n(s) = \tilde{F}(s)\,e^{-\gamma a}2\pi I_n'(-\gamma r)$$

$A_n(s)$ can be determined as

$$A_n(s) = -(-1)^n\epsilon_n\tilde{F}(s)\,e^{-\zeta} \tag{3.13}$$

where $\zeta \equiv \gamma a$ and $-(-1)^n = \dfrac{I_n'(-\gamma r)}{I_n'(\gamma r)}$ as can be easily seen from equation (3.12). $\tilde{E}_\varphi^i$ and $\tilde{H}_z^i$ are thus expressed as

$$\left.\begin{aligned} \tilde{E}_\varphi^i &= -\tilde{F}(s)\,e^{-\zeta}\sum_{n=o}^{\infty}(-1)^n\epsilon_n\,I_n'(\gamma r)\text{Cos}(n\Phi) \\ \tilde{H}_z^i &= \frac{\tilde{F}(s)e^{-\zeta}}{Zo}\sum_{n=o}^{\infty}(-1)^n\epsilon_n\,I_n(\gamma r)\text{Cos}(n\Phi) \end{aligned}\right\} \tag{3.14}$$

where $Z_o = (\mu_o/\epsilon o)^{\frac{1}{2}}$.

A similar expansion of the scattered field, in cylindrical-wave-function solutions to equiations (3.5) and (3.7) which satisfy the radiation condition, provides

$$\tilde{E}_\Phi^s = \sum_{n=0}^{\infty} a_n(s)K_n'(\gamma r)\text{Cos}(n\Phi) \tag{3.15}$$

with unknown Fourier coefficients $a_n(s)$. Satisfaction of boundary condition (3.8) requires $\tilde{E}^s_\Phi(a,\varphi,s) = -\tilde{E}^i_\varphi(a,\varphi,s)$, which yields upon substitution of expressions of (3.14) and (3.15)

$$\sum_{n=o}^{\infty} a_n(s)K_n'(\zeta)\mathrm{Cos}(n\Phi) = \tilde{F}(s)e^{-\zeta} \sum_{n=o}^{\infty} (-1)^n\epsilon_n I_n'(\zeta)\mathrm{Cos}(n\Phi)$$

leading to coefficients

$$a_n(s) = \tilde{F}(s)e^{-\zeta} \frac{(-1)^n\epsilon_n I_n'(\zeta)}{K_n'(\zeta)} \tag{3.16}$$

Therefore the scattered electric and magnetic fields can be determine form equations (3.15), (3.16) and (3.5) as

$$\left.\begin{aligned} \tilde{E}^s_\Phi &= \tilde{F}(s)e^{-\zeta} \sum_{n=o}^{\infty} \frac{(-1)^n\epsilon_n I_n'(\zeta)}{K_n'(\zeta)} K'(\gamma r)\mathrm{Cos}(n\Phi) \\ \tilde{H}^s_z &= -\frac{\tilde{F}(s)e^{-\zeta}}{Z_o} \sum_{n=o}^{\infty} \frac{(-1)\epsilon_n I_n'(\zeta)}{K_n'(\zeta)} K(\gamma r)\mathrm{Cos}(n\Phi) \end{aligned}\right\} \tag{3.17}$$

Induced current excited on the cylinder by $\tilde{\vec{E}}^i$ is obtained as $\tilde{\vec{K}}(\Phi,s) = \hat{r} \times \hat{z}\, \tilde{H}_z(a,\varphi,s) = -\hat{\varphi}[\tilde{H}^i_z(a,\varphi,s) + \tilde{H}^s_z(a,\varphi,s)]$, which provides

$$\tilde{K}_\varphi(\varphi,s) = -\frac{\tilde{F}(s)e^{-\zeta}}{Z_o} \sum_{n=o}^{\infty} (-1)^n\epsilon_n \left[\frac{I_n(\zeta)K_n'(\zeta)-I_n'(\zeta)K_n(\zeta)}{K_n'(\zeta)}\right] \mathrm{Cos}(n\Phi)$$

$$= \frac{\tilde{F}(s)e^{-\zeta}}{Z_o\zeta} \sum_{n=o}^{\infty} \frac{(-1)^n\epsilon_n}{K_n'(\zeta)} \mathrm{Cos}(n\Phi) \tag{3.18}$$

where in the latter expression the Wronskian for modified Bessel functions $I_n(\zeta)K_n'(\zeta) - I_n'(\zeta)K_n(\zeta) = -\zeta^{-1}$ has been exploited. The radiation-zone scattered field is finally obtained as

$$\tilde{E}^{sr}_\varphi(r,\varphi,s) = \tilde{E}^s_\varphi(r\to\infty,\varphi,s)$$

$$\sim -\tilde{F}(s)e^{-\zeta(R+1)} \sqrt{\frac{\pi}{2R}} \sum_{n=o}^{\infty} \frac{(-1)^n\epsilon_n I_n'(\zeta)}{\sqrt{\zeta}\, K'_n(\zeta)} \mathrm{Cos}(n\Phi) \tag{3.19}$$

where $R = r/a$ is a normalized radial coordinate.

Natural-mode solutions are those $\tilde{K}_\varphi \neq o$ and $\tilde{E}_\varphi \neq o$ which can exist as solutions to the homogeneous problem when $\tilde{F}(s) = o$. It is clear from the expressions (3.18) and (3.19) that normalized natural frequencies $\zeta_{n\ell}$ satisfy the characteristic equaiton

$$K_n'(\zeta_{n\ell}) = o \tag{3.20}$$

for the $n\ell$'th natural mode, where $\zeta_{n\ell}$ is the ℓ'th complex root of $K_n' = o$. Natural frequencies $s_{n\ell}$ are subsequently recovered as $s_{n\ell} = c\,\zeta_{n\ell}/a$.

Complex roots to $K_n'(\zeta) = o$ can be counted by Watson's [23] method, and were found by Luke [24] to number $n+[1-(-1)^n]/2$. Note that $k_o'(\zeta)$ possesses no roots. Coefficients in the power series representation for $K_n'(\zeta)$ are real for ζ not on its branch cut, consequently [25] the roots occur in complex-conjugate pairs. It follows from the fundamental form of the modified Bessel's equation that these roots are simple zeros. Details on computation of the $\zeta_{n\ell}$ (Using Newton's method and computing K_n' from integral representations of K_n and I_n) were reported in [26]. Other method (Using Muller's method and computing K_n' from a software of Bessel function [27]) also yields exactly the same results. All such roots are found to have negative real parts, and the distribution of approximately 200 of the $\zeta_{n\ell}$ in the second quadrant of the complex ζ-plane is displayed in Figure 3.2; a symmetric distribution exists in the third quadrant. The roots are observed to be distributed along layers of constant ℓ which are ordered by index n as indicated. Table 3.1 displays all roots to $n = 19$

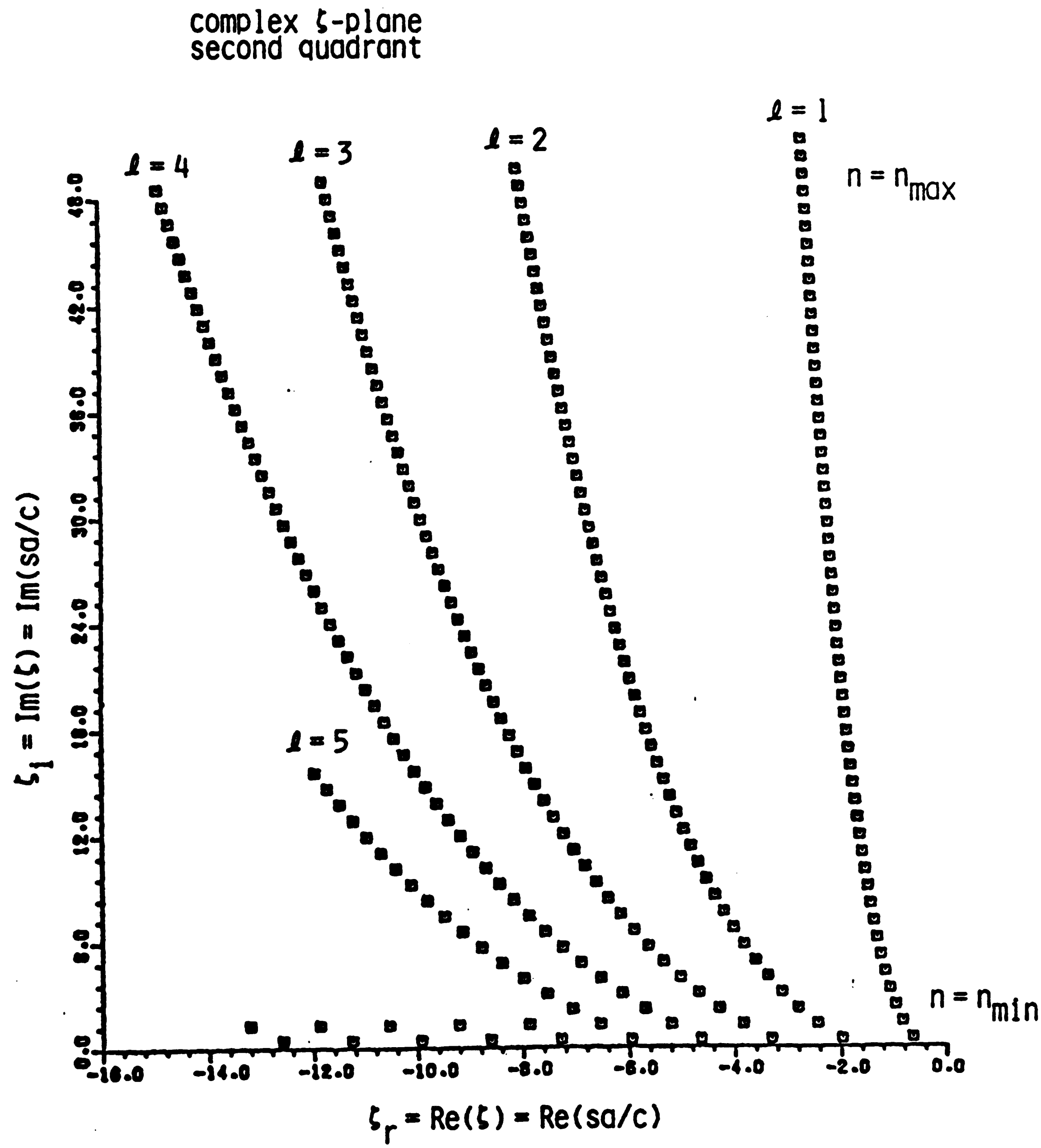

Figure 3.2 Distribution of the roots $\zeta_{n\ell} = (\zeta_r)_{n\ell} + j(\zeta_i)_{n\ell}$ to $K_n'(\zeta) = 0$ in the second quadrant of the complex ζ-plane.

Table 3.1. Complex roots $\zeta_{n\ell} = (\zeta_r)_{n\ell} + j(\zeta_i)_{n\ell}$ to $K_n'(\zeta) = 0$; all roots to n=19 for first three layers $\ell = 1,2,3$.

	$\ell = 1$ roots of 1'st branch		$\ell = 2$ roots of 2'nd branch		$\ell = 3$ roots of 3'rd branch	
n	$-\zeta_r$	$\pm\zeta_i$	$-\zeta_r$	$\pm\zeta_i$	$-\zeta_r$	$\pm\zeta_i$
1	.64355	.50118				
2	.83455	1.4344				
3	.96756	2.3739	1.9816	.44080		
4	1.0728	3.3221	1.2441	1.1323		
5	1.1612	4.2769	2.8037	2.2119	3.3098	.43637
6	1.2383	5.2366	3.1082	3.1094	3.8394	1.3104
7	1.3071	6.2002	3.3730	4.0142	4.2871	2.1891
8	1.3694	7.1667	3.6087	4.9252	4.6784	3.0733
9	1.4267	8.1358	3.8221	5.8415	5.0280	3.9628
10	1.4797	9.1069	4.0176	6.7625	5.3453	4.8574
11	1.5293	10.080	4.1985	7.6876	5.6367	5.7565
12	1.5759	11.054	4.3672	8.6162	5.9069	6.6597
13	1.6200	12.030	4.5255	9.5480	6.1592	7.5667
14	1.6618	13.007	4.6749	10.483	6.3962	8.4772
15	1.7017	13.985	4.8165	11.420	6.6200	9.3908
16	1.7398	14.964	4.9512	12.359	6.8323	10.307
17	1.7763	15.943	5.0798	13.301	7.0345	11.226
18	1.8114	16.924	5.2029	14.245	7.2275	12.148
19	1.8452	17.905	5.3210	15.190	7.4124	13.072

for the first three layers $\ell = 1,2,3$.

3.2 Impulse Response

The backscattered field along $\Phi = \pi$ can be expressed from equation (3.19) as

$$\tilde{\vec{E}}^{sb}(r,s) = \hat{\varphi}\,\tilde{\vec{E}}^{sr}_{\varphi}(r,\pi,s) = \hat{y}\,\tilde{F}(s)\sqrt{\frac{\pi}{2R}}\,e^{-\zeta(R-1)}H(s) \quad (3.21)$$

where transfer function $H(s)$ is defined as

$$H(s) = \sum_{n=o}^{\infty} \epsilon_n H_n(s) \quad (3.22a)$$

with

$$H_n(s) = \frac{e^{-2\zeta} I_n'(\zeta)}{\sqrt{\zeta}\, K_n'(\zeta)} \quad . \quad (3.22b)$$

In expression (3.22), the ratio of Bessel functions behaves asymptotically for large ζ as $I_n'(\zeta)/K_n'(\zeta) \propto \exp(2\zeta)$; the time-shifting factor $\exp(-2\zeta)$ has been included in equation (3.22) to annul that behavior at $\zeta \to \infty$ and thus facilitate the inverser transformation of $H_n(s)$. Physically this introduces in equation (3.20) the right time-shifting factor $\exp[-\zeta(R-1)]$ which corresponds to the time-delay between the "turn-on" times of incident field and backscattered field observed at normalized radial coordinate R.

Apart from pure amplitude and time-shift factors, the normalized impulse response of the cylinder is obtained from expression (3.20) with $F(s) = 1$ as

$$h(t) = L^{-1}\{H(s)\} = \sum_{n=o}^{\infty} \epsilon_n h_n(t) \quad (3.23)$$

with

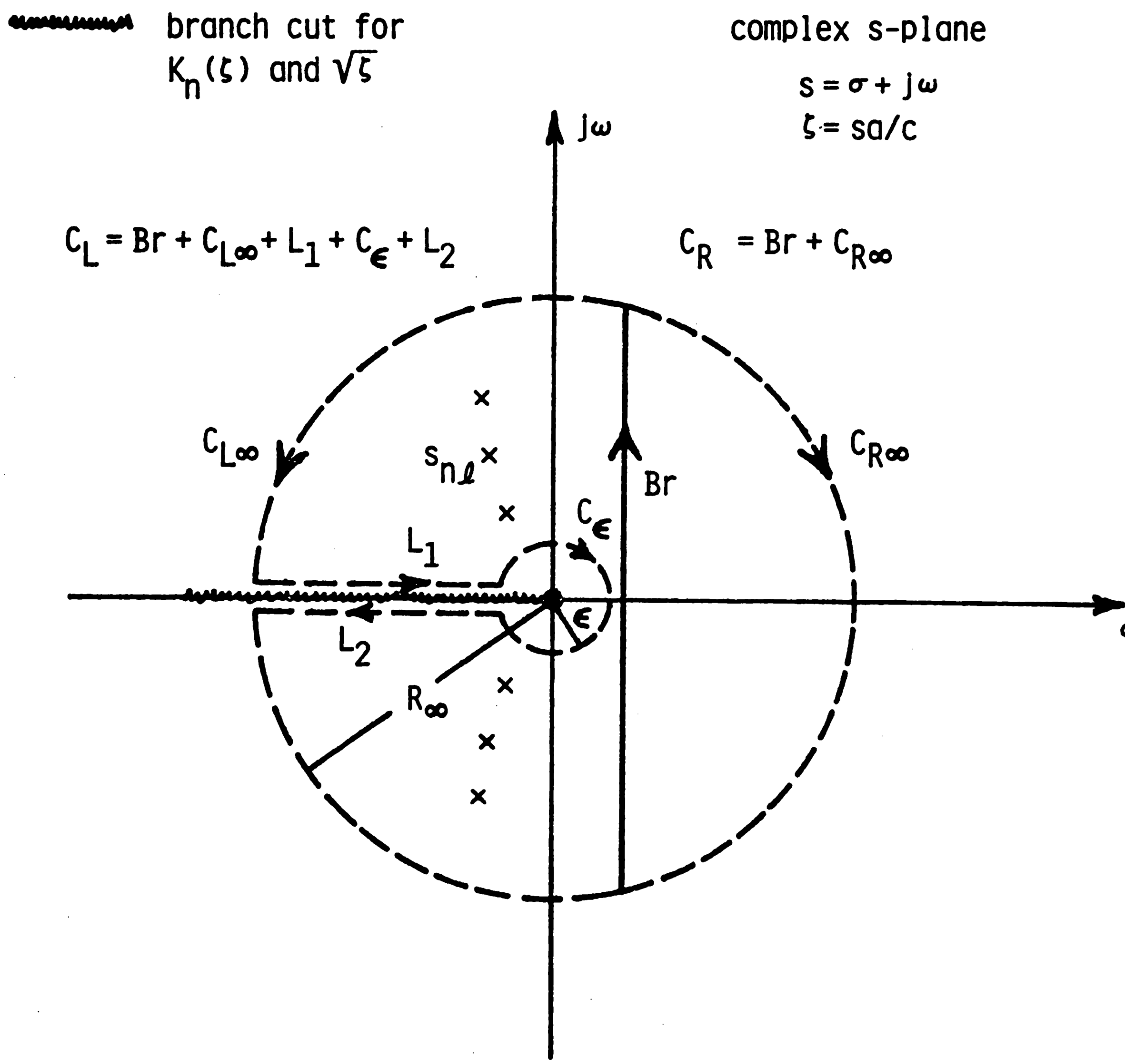

Figure 3.3 Integration contours in the complex-frequency plane appropriate for evaluation of $h_n(t) = \mathscr{L}^{-1}\{H_n(s)\}$; the branch cut is appropriate for $K_n(\zeta)$ and $\sqrt{\zeta}$.

$$h_n(t) = L^{-1}\{H_n(s)\} = \frac{1}{2\pi j}\int_{Br} H_n(s)\, e^{st}\, ds \quad . \tag{3.24}$$

The appropriate Bromwich contour and associated integration contours in the complex s-plane are indicated in Figure 3.3. For $t < o$, Br is closed in the right half plane along $C_{R\infty}$; since C_R encloses no singular points then

$$h_n(t) = -\frac{1}{2\pi j}\lim_{R\to\infty}\int_{C_{R\infty}} H_n(s)\, e^{st}\, ds = o \text{ --- } t < o\,, \tag{3.25}$$

vanishing of equation (3.25) can be easily shown using large-argument asymptotic forms of modified Bessed functions.

For $t > o$, Br is closed along $C_{L\infty} + L_1 + C_\epsilon + L_2$ to form the closed contour C_L. It is easily demonstrated that the contribution from $C_{L\infty}$ and C_ϵ vanishes, since

$$\lim_{R\to\infty}\int_{C_{L\infty}} H_n(s)\, e^{st}\, ds = \lim_{\epsilon\to o}\int_{C_\epsilon} H_n(s)\, e^{st}\, ds = o$$

by large and small argument approximations respectively. C_L encloses all the simple poles $s_{n\ell}$, $n > o$, at which $K_n'(\zeta_{n\ell}) = o$ such that

$$h_n(t) = \sum_\ell R_{n\ell} - \frac{1}{2\pi j}\left[\int_{L_1} H_n(s)\, e^{st}\, ds + \int_{L_2} H_n(s)\, e^{st}\, ds\right] \text{ --- } t > 0 \tag{3.26}$$

where $R_{n\ell}$ is the residue of the simple pole at $s_{n\ell}$

$$R_{n\ell} = \left.\frac{e^{st}\, e^{-2\zeta}\, I_n'(\zeta)}{\frac{d}{ds}[\sqrt{\zeta}\, K_n'(\zeta)]}\right|_{\zeta=\zeta_{n\ell}} = (\frac{c}{a}) \left.\frac{e^{\zeta(\tau-2)} I_n'(\zeta)}{\frac{d}{d\zeta}[\sqrt{\zeta}\, K_n'(\zeta)]}\right|_{\zeta=\zeta_{n\ell}}$$

$$= (\frac{c}{a}) \left.\frac{e^{\zeta(\tau-2)} I_n'(\zeta)}{\sqrt{\zeta} K_n''(\zeta) + \frac{1}{2\sqrt{\zeta}} K_n'(\zeta)}\right|_{\zeta=\zeta_{n\ell}}$$

$$= (\frac{c}{a}) \frac{e^{\zeta_{n\ell}(\tau-2)}\, I_n'(\zeta_{n\ell})}{\sqrt{\zeta_{n_\ell}}\, K_n''(\zeta_{n\ell})} \tag{3.27}$$

with rormalized frequency $\zeta_{n\ell} = s_{n\ell} a/c$ and normalized time $\tau = t/(a/c)$, $\left.\frac{1}{2\sqrt{\zeta}} K_n'(\zeta)\right|_{\zeta=\zeta_{n\ell}} \to o$ since $K_n'(\zeta_{n\ell}) = o$. From modified Bessel equation [22],

$$Z^2 K_n''(z) + z\, K_n'(z) - (z^2 + n^2) K_n(z) = o,$$

we get the following,

$$K_n''(\zeta_{n\ell}) = \frac{(\zeta_{n\ell}^2 + n^2) K_n(\zeta_{n\ell}) - \zeta_{n\ell} K_n'(\zeta_n)}{\zeta_{n\ell}^2}$$

$$= [1 + (\frac{n}{\zeta_{n\ell}})^2] K_n(\zeta_{n\ell}) \tag{3.28}$$

therefore,

$$R_{n\ell} = (\frac{c}{a}) \frac{e^{\zeta_{n\ell}(\tau-2)}\, I_n'(\zeta_{n\ell})}{[1+(\frac{n}{\zeta_{n\ell}})^2]\sqrt{\zeta_{n\ell}} K_n(\zeta_{n\ell})} \; . \tag{3.29}$$

Exploiting appropriate analytic continuation [22] of I_n' and K_n', the contributions from line integrals along the branch cut of $\sqrt{\zeta}$ and $K_n'(\zeta)$ can be evaluated as

$$\int_{L_1} H_n(s)e^{st}\,ds = \int_{-\infty+j\Delta}^{o+j\Delta} \frac{e^{-2\zeta} I_n'(\zeta)}{\sqrt{\zeta}\; K_n'(\zeta)} e^{st}\,ds \text{ ---- as } \Delta \to o^+$$

$$= \left(\frac{c}{a}\right) \int_o^\infty \frac{e^{-\zeta(\tau-2)} I_n'(-\zeta)}{\sqrt{-\zeta}\; K_n'(-\zeta)}\, d\zeta$$

$$= \left(\frac{c}{a}\right) \frac{(-1)^{n+1}}{j} \int_o^\infty \frac{e^{-\zeta(\tau-2)} I_n'(\zeta)}{\sqrt{\zeta}[(-1)^{n+1} K_n'(\zeta) + j\pi I_n'(\zeta)]}\, d\zeta$$

$$\int_{L_2} H_n(s)e^{st}ds = \int_{o-j\Delta}^{-\infty-j\Delta} \frac{e^{-2\zeta} I'_n(\zeta)}{\sqrt{\zeta}\; K_n'(\zeta)} e^{st}ds \text{ --- as } \Delta \to o^+$$

$$= -\left(\frac{c}{a}\right) \int_o^\infty \frac{e^{-\zeta(\tau-2)} I_n'(-\zeta)}{\sqrt{-\zeta}\; K_n'(-\zeta)}\, d\zeta$$

$$= -\left(\frac{c}{a}\right) \frac{(-1)^{n+1}}{-j} \int_o^\infty \frac{e^{-\zeta(\tau-2)} I_n'(\zeta)}{\sqrt{\zeta}[(-1)^{n+1} K_n'(\zeta) - j\pi I_n'(\zeta)]}\, d\zeta$$

Where ζ is the real variable $\zeta = \sigma a/c$ ($j\omega = o$ on real axis) in the resulting integrals. The impulse response finally becomes

$$h(\tau) = \sum_{n=o}^{\infty} \epsilon_n h_n(\tau)$$
$$= u(\tau)\left(\frac{c}{a}\right)\left[\sum_{n=o}^{\infty} \sum_{\ell=1}^{\substack{n/2(\text{even } n)\\(n+1)/2(\text{odd } n)}} 2\mathrm{Re}\{a'_{n\ell} e^{\zeta_{n\ell}\tau}\} + \mathcal{I}_n'(\tau)\right] \tag{3.30}$$

Where the sum over ℓ includes only those $\zeta_{n\ell}$ with positive imaginary parts and

$$a'_{n\ell} = \frac{\epsilon_n\, e^{-2\zeta_{n\ell}}\, I_n'(\zeta_{n\ell})}{[1+(\frac{n}{\zeta_{n\ell}})^2]\sqrt{\zeta_{n\ell}} K_n(\zeta_{n\ell})} \tag{3.31}$$

$$I_n'(\tau) = \frac{\epsilon_n}{\pi} \int_o^\infty \frac{I_n'(\zeta)K_n'(\zeta)}{\sqrt{\zeta}[K_n'^2(\zeta) + \pi^2 I_n'(\zeta)]} e^{-\zeta(\tau-2)} d\zeta \tag{3.32}$$

It is observed that this impulse response consists of a discrete-spectrum series of pure natural modes $\exp[(\zeta_r)_{n\ell}\tau] \, \mathrm{Cos}[(\zeta_i)_{n\ell}\tau + \varphi_{n\ell}]$ augmented by the series of continuous-spectrum integral terms $I_n'(z)$ which comprise non-oscillatory functions having an essentially decaying-exponential nature.

The impulse response is computed for $\tau > 2$, where the various series can be appropriately truncated. The series of continuous-spectrum integral terms is found to converge rapidly, and retention of only the leading 10 terms provides adequate accuracy. In these integral terms, contributions from the neighborhood of the singularity at $\zeta = o$ are calculated analytically using small-argument approximations of required Bessel functions, while the upper integral limit is truncated for the remaining numerical integration because all significant contributions from the integrand are found to occur for $\zeta < 5$. All significant contributions to the discrete-spectrum residue series of natural modes are provided by the $\ell = 1$ layer of complex natural frequencies $\zeta_{n\ell}$, while layers with $\ell > 1$ provide negligible contribuiton for $\tau > 2$. The latter series is computed by summing the first 19 terms numerically while obtaining an approximate representation for the remaining terms to $n = \infty$. Layer index $\ell = 1$ is subsequently dropped for brevity. A study of natural frequencies ζ_n and the associated residue coefficients a_n' for large n indicates that the frequency difference $\Delta\zeta = \zeta_n - \zeta_{n-1}$ $= (-0{,}034 + j\ 0,\ 98)$ and residue ratio $A = a_n'/a_{n-1}' = 1{,}0607 \exp\,(j67.55^o)$ approach constant values for $n \geq 19$, i.e., the roots of layer $\ell = 1$

are distributed approximately along a straight line with equal spacing. Those terms having $n > 19$ can therefore be approximated as a geometric progression and summed in closed form. The predominant $\ell = 1$ residue series therefore leads to

$$\sum_{n=1}^{\infty} 2\mathrm{Re}\{a'_{n1}\, e^{\zeta_{n1}\tau}\} \approx 2\mathrm{Re}\{\sum_{n=1}^{19} a'_n\, e^{\zeta_n\tau} + \frac{a'_{19}\, e^{\zeta_{19}\tau} A\, e^{\Delta\zeta\tau}}{1-Ae^{\Delta\zeta\tau}} \tag{3.33}$$

with $a'_{19}\exp(\zeta_{19}\tau) = 3.320\exp(j94.94^{o})\exp[(-1.845 + j17.9)\tau]$. This approximation was described in [28] where it was used to quantify the impulse response of a conducting sphere.

Figure 3.4 indicates the normalized impulse response and its constituent components. Table 3.2 shows the poles of the first layer and their corresponding residues. The series of continuous-spectrum integral terms provides an important contribution during the early-time period, where it largely annuls the contribution by the discrete natural-mode residue series which has opposite sign during that period. The specular reflection behavior near $\tau = o$ is thus obvious (Figure 3.4 has the phase inverted). The residue series provides the anticipated, well-known creeping-wave contribution. It is noted that the approximate sum of terms for $n > 19$ is an important contribution in the latter series, since the leading 19 terms alone result in an impulse response having an incorrect superposed oscillation. The present impulse response agrees well with the earlier approximation by Moffatt [29] over the time interval considered.

3.3 Incident Waveform Synthesis for Monomode Backscatter

The late-time or free-response period in the backscatter signal from a target illuminated by a transient waveforem of finite duration

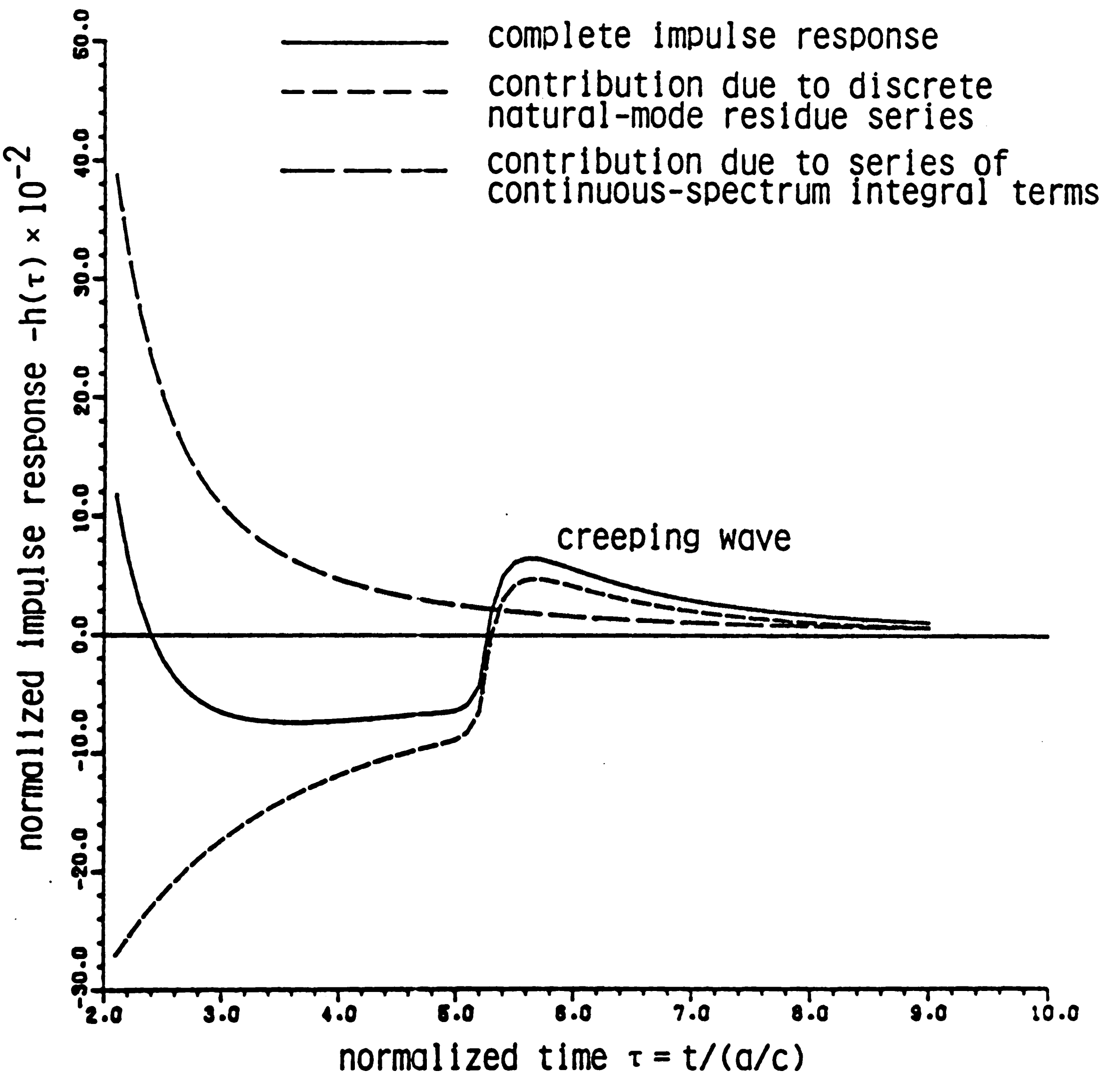

Figure 3.4 Normalized impulse response of an infinite cylinder illuminated by a normally-incident, transversely-polarized, impulsive plane-wave field.

Table 3.2 Poles of the first layer of natural modes and corresponding residues used to compute approximated impulse response of infinite cylinder.

	poles of 1'st branch (ℓ=1) $\zeta_{n1}=\sigma_{n1}+j\omega_{n1}$		residues at ζ_{n1} $a_{n1}=a^r_{n1}+ja^i_{n1}$	
n	σ_{n1}	ω_{n1}	a^r_{n1}	a^i_{n1}
1	-.6435	.5012	.2407	-.4415
2	-.8345	1.434	.6099	.0932
3	-.9676	2.374	.1442	.7440
4	-1.073	3.322	-.7707	.4583
5	-1.161	4.277	-.8034	-.6535
6	-1.238	5.237	.3760	-1.114
7	-1.307	6.200	1.318	-.0495
8	-1.369	7.167	.5769	1.346
9	-1.427	8.136	-1.151	1.131
10	-1.480	9.107	-1.612	-.7188
11	-1.529	10.08	.0790	-1.920
12	-1.576	11.05	1.962	-.6911
13	-1.620	12.03	1.484	1.685
14	-1.662	13.01	-1.080	2.158
15	-1.702	13.98	-2.578	-.2002
16	-1.740	14.96	-.8475	2.630
17	-1.776	15.94	2.250	-1.898
18	-1.811	16.92	2.779	1.440
19	-1.845	17.90	-.2857	3.308

T_e is well defined, e.g., Jones [30]. If the initial response (arising from the incident wavefront first striking the target) occurs at $t = o$, then the late time period begins at $t = T_e + 2T_t$ where T_t is the one-way transit time for the wavefront to sweep across the target. Thus the late-time period of the impulse response begins at $\tau = 4$ in the present problem.

It is found that during, and just prior to, the late-time period, for $\tau > 3$, the series of real, decaying, continuous-spectrum integral terms in the impulse response (3.30) can be approximated by two real-exponential terms while the discrete natural-mode series for $n > 19$ can be approximated by a pair of damped-sinusoidal terms; consequently that response can be expressed as

$$h(\tau) = u(\tau) \left[\sum_{n=1}^{N_m} a_n e^{\sigma_n \tau} \mathrm{Cos}(\omega_n \tau + \phi_n) + I(\tau) + R(\tau) + C(\tau) \right] . \quad (3.34)$$

The residue series include $N_m (N_m = 19$ for all numerical results subsequently presented) terms arising from the first layer $(\ell = 1)$ of natural-frequency roots from Figure 3.2. Natural modes contributed by the higher-order layers $(\ell > 1)$ are insignificant during that late-time period due to their rapid exponential decay. Empirical approximations to the integral sum and the residue series for $n > N_m$, valid for $\tau > 3$, are

$$I(\tau) = -0.083\, e^{-0.95(\tau-3)} - 0.025\, e^{-0.36(\tau-3)} \quad (3.35)$$

$$R(\tau) = -0.026\, e^{-1.09(\tau-3)} \mathrm{Cos}[18.85(\tau-3)] - 0.016\, e^{-1.22(\tau-3.1)} \mathrm{Cos}[17.95(\tau-3.1)] \quad (3.36)$$

while $C(\tau)$ is a correction term required for $\tau < 3$ to compensate for the approximations inherent in $I(\tau)$ and $R(\tau)$. The approximated impulse response with $C(\tau) \approx o$ assume for the late-time period is compared in Figure 3.5 to the relatively accurate representation obtained from equation (3.30) and displayed previously in Figure 3.4. The two real-exponential terms in $I(\tau)$ can be regarded as limiting natural modes having vanishing angular frequency and subsequently be included in the residue series along with the damped sinusoids contributed by $R(\tau)$. If $N = N_m + 4$, then the impulse response becomes

$$h(\tau) = u(\tau) \sum_{n=1}^{N} a_n e^{\sigma_n \tau} \mathrm{Cos}(\omega_n \tau + \varphi_n) + C(\tau) \tag{3.37}$$

The backscattered-field waveform $E^s(\tau)$ excited by an incident field waveform $E^e(\tau)$ having finite dimation τ_e is obtained through the convolution theorem as

$$\begin{aligned} E^s(\tau) &= \int_o^{\tau_e} E^e(\tau') \, h(\tau-\tau') \, d\tau' \quad \text{for} \quad \tau > \tau_e \\ &= \int_o^{\tau_e} E^e(\tau') u(\tau-\tau') \{ \sum_{n=1}^{N} a_n e^{\sigma_n(\tau-\tau')} \mathrm{Cos}[\omega_n(\tau-\tau') + \varphi_n] + C(\tau-\tau') \} d\tau \end{aligned}$$

Since $C(\tau-\tau') \approx o$ for $\tau > \tau_e + 3$, then during the late-time period the previous expression becomes

$$\begin{aligned} E^s(\tau) &= \int_o^{\tau_e} E^e(\tau') \sum_{n=1}^{N} a_n e^{\sigma_n(\tau-\tau')} \mathrm{Cos}[\omega_n(\tau-\tau') + \varphi_n] d\tau' \\ &= \sum_{n=1}^{N} a_n e^{\sigma_n \tau} [A_n \mathrm{Cos}(\omega_n \tau + \varphi_n) + B_n \mathrm{Sin}(\omega_n \tau + \varphi_n)] \end{aligned} \tag{3.38}$$

valid for $\tau > \tau_e + 3$, where

$$\begin{Bmatrix} A_n \\ \\ B_n \end{Bmatrix} = \int_o^{\tau_e} E^e(\tau') \, e^{-\sigma_n \tau'} \begin{Bmatrix} \mathrm{Cos}\omega_n \tau' \\ \\ \mathrm{Sin}\omega_n \tau' \end{Bmatrix} d\tau' \tag{3.39}$$

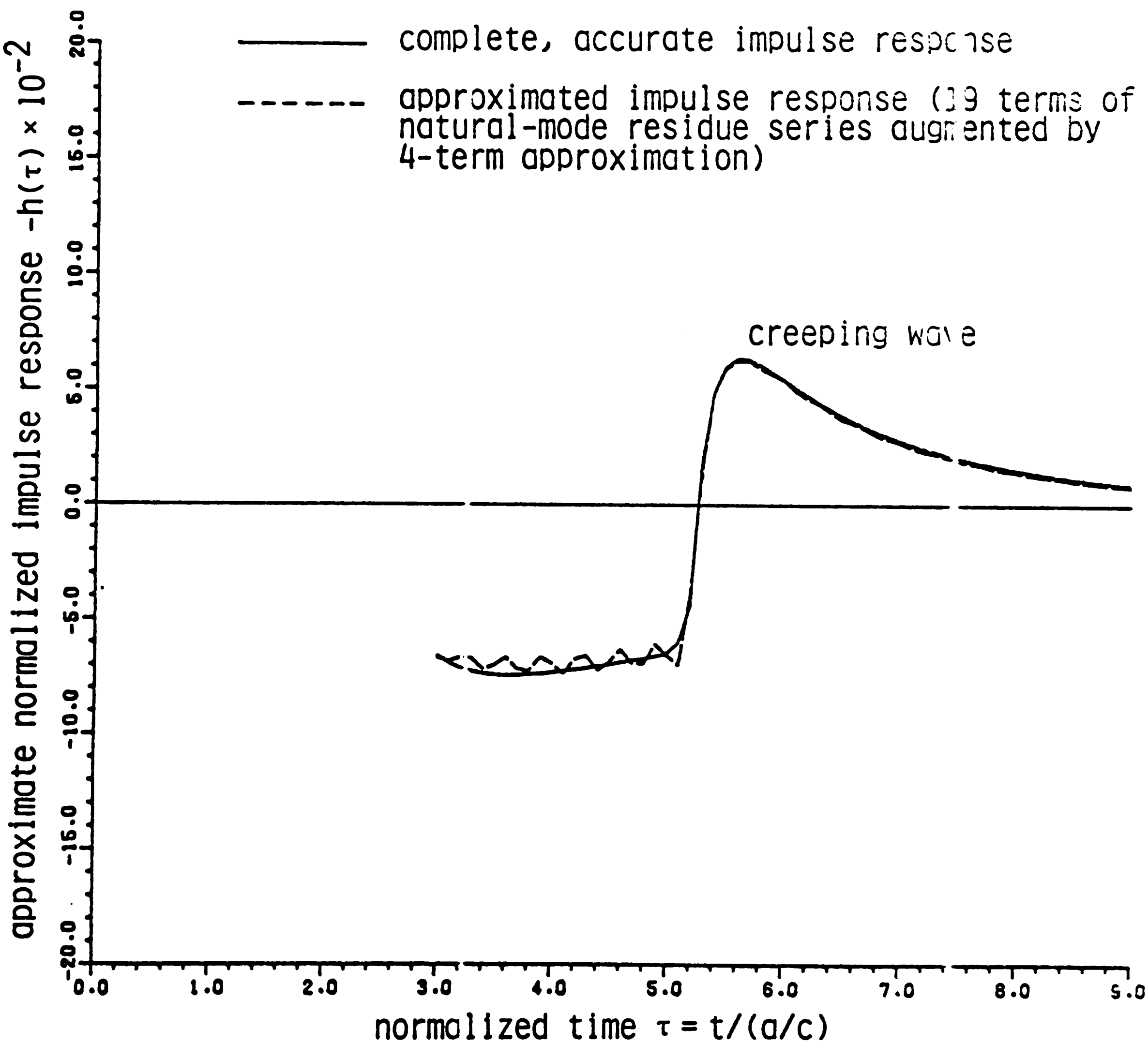

Figure 3.5 Approximate normalized, late-time impulse response of an infinite cylinder; utilized for synthesis of incident waveform to excite monomode backscatter.

It is desired to synthesize an incident waveform $E^e(\tau)$ which excites only a single natural-mode scattered-field response $E^s(\tau)$ from equation (3.38) during the late-time period. The desired E^e can be expanded in terms of some basis functions as indicated in Section 2.2. The basis functions used are pulse functions, the results of numerical computations will be discribed in the next section.

3.4 Numerical Results for Incident-Waveform Synthesis and Target Discrimination

Incident waveforms required to excite monomode backscatter consisting of purely the first or second natural modes of the infinite-cylindrical target are synthesized according to the procedure described in Chapter 2. The finite duration of the incident wavefore is chosen initially, based upon experience with thin-cylinder targets [13], as one normalized period of the cylinder's first natural mode; this choice leads to $\tau_e = 1/f_1 = 2\pi/(\zeta_i)_{11} = 2\pi/0.5012 = 12.54$. The late-time response, upon which the synthesis procedure was based, occurs during $\tau \gtrsim \tau_e + 3 = 15.54$; numerical results for the late-time, backscattered-field response are therefore presented for $\tau \geq 15.5$.

The incident signal required during $0 \leq \tau \leq 12.54$ to excite a purely first-mode ($\zeta_1 = -.6435 + j.5012$) response is indicated in Figure 3.6 along with the resulting monomode response for $\tau \geq 15.5$. It is noted that the return signal, which was obtained by convolving the synthesized incident waveforem with approximate impulse response (2.34), indeed consists of a first natural mode in the late-time period. The early-time return signal (not constrained by the synthesis procedure) exhibits an irregular waveform, and is omitted for the sake of clarity.

Also shown in the same figure in dashed line is the return signal from a wrong-cylinder target with 10% smaller radius, it is found that the response of the preselected cylinder consists of the desired first natural mode while that from the wrong target cannot be identified as a single natural mode. Figure 3.7 indicates similar results for the incident waveform required (with $\tau_e = \frac{1}{f_1}$) to excite purely second-mode ($\zeta_2 = -.8345 + j1.434$) backscatter and the resulting late-time return signals from right and wrong targets. For $\tau_e = \frac{1}{f_1}$ as chosen in Figures 3.6 and 3.7, it is found that the late-time response occures after $\tau = \tau_e + 3 = 15.54$ while the negative real part of the natural frequencies are so large that the signal is very small after such a long time. This may cause serious problem when, in the practical situation, the signal is contaminated by noise. Therefore, it is desirable to synthesize the required incident waveform with shorter duration. We tried different τ_e and found that the waveform may be optimal when τ_e is in the order of $(0.55 - 0.70)1/f_1$: If τ_e is too small, the required waveform oscillates quite rapidly and the matrix in equation (2.9) has a large condition number [31] indicating an ill-conditioned situation in synthesis procedure while a large τ_e causes the small signal-to-noise ratio as indicated above. The require incident waveform with $\tau_e = \frac{2}{3}\frac{1}{f_1}$ and the resulting late-time return signals from right and wrong targets are indicated in Figure 3.8 for the first mode excitation and in Figure 3.9 for the second mode excitation. It is clear that with this τ_e, the return signal is much stronger than that from $\tau_e = \frac{1}{f_1}$ and thus easier for us to indentify and discriminate the target. The required waveforms with $\tau_e = 0.594 \frac{1}{f_1}$ to excite the first mode and the

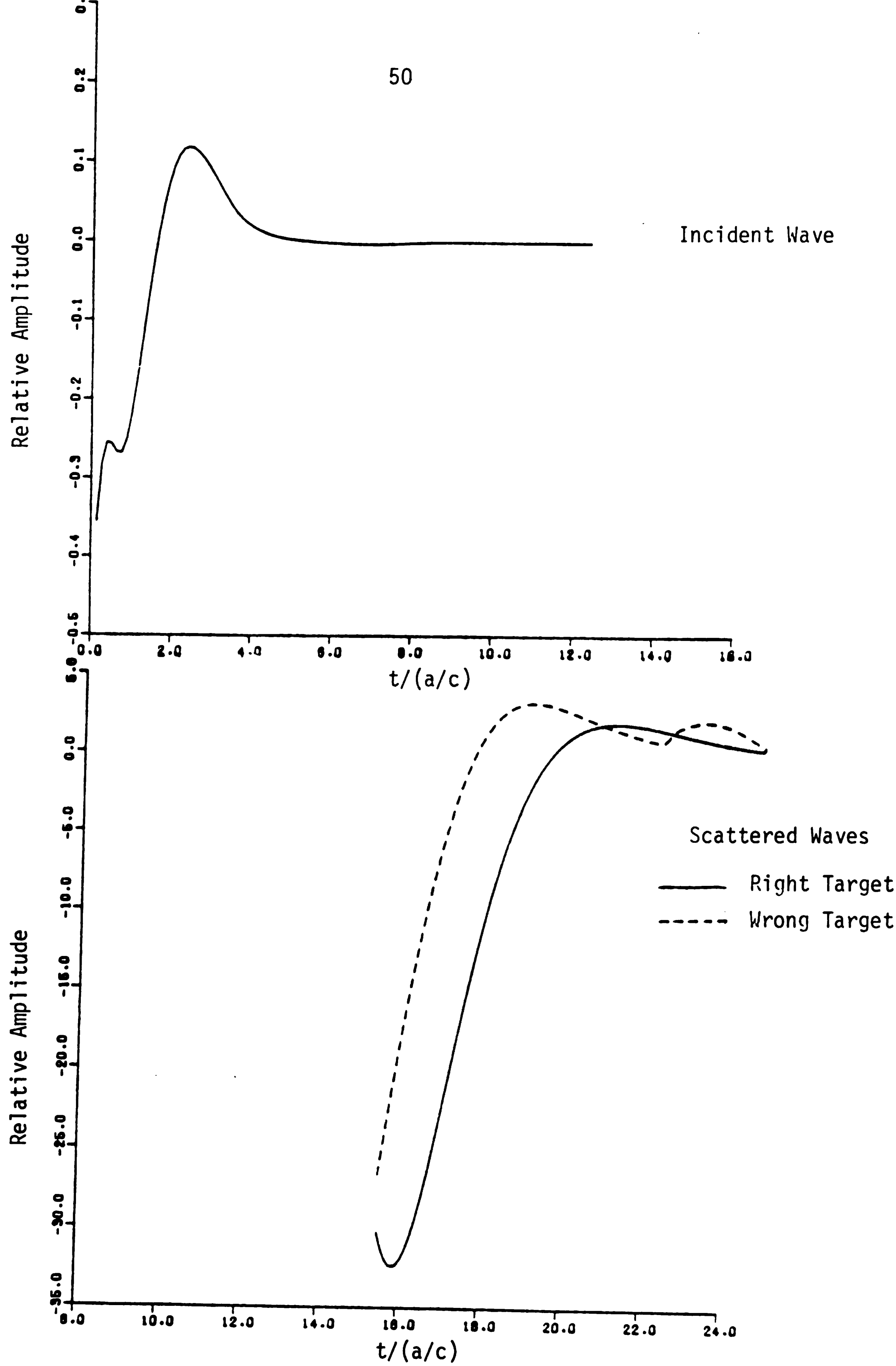

Figure 3.6. Synthesized incident waveform required to excite monomode backscatter in the first natural mode of an infinite cylinder and the resulting monomode scattered wave along with return waveform from a target with 10% smaller radius.

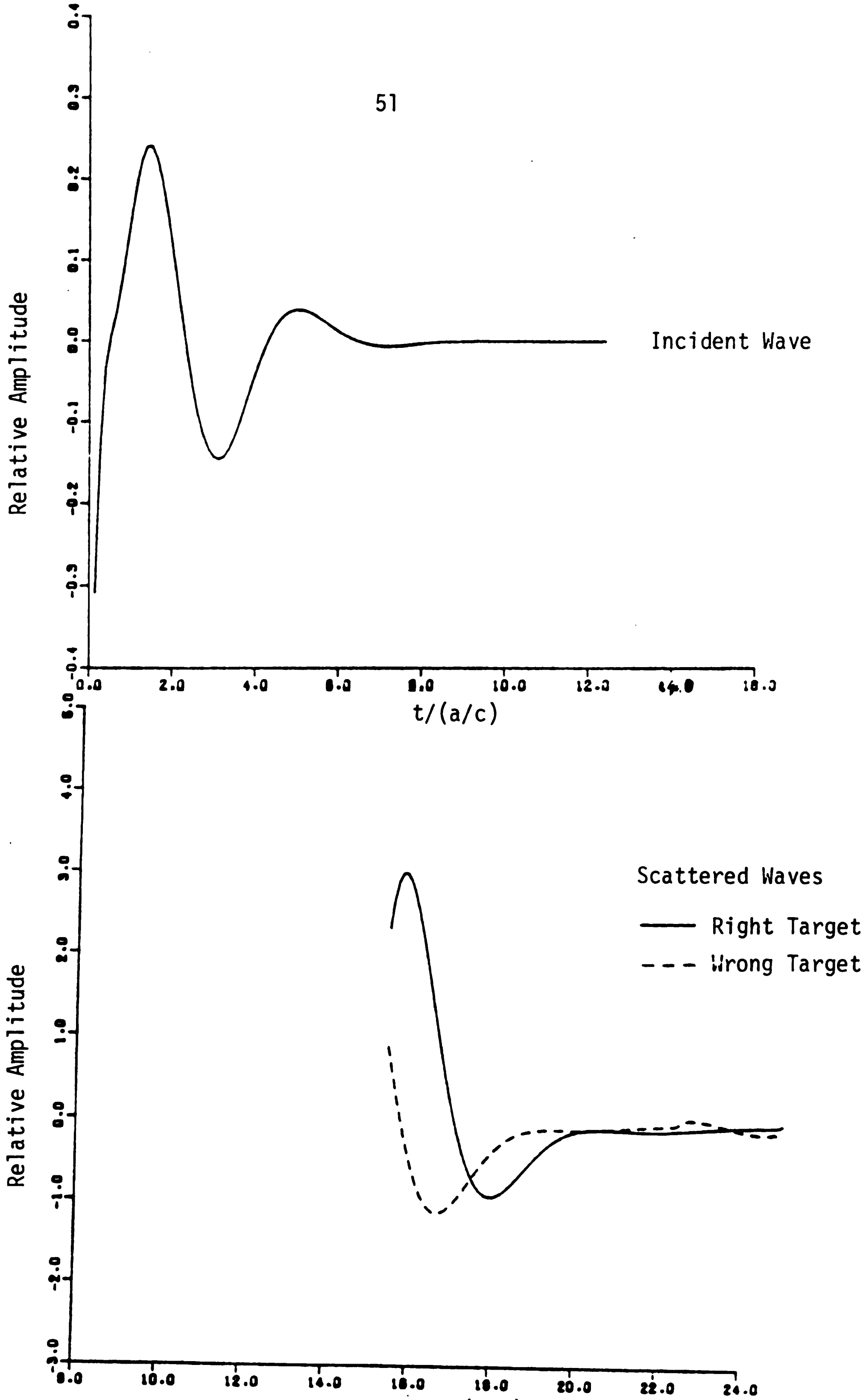

Figure 3.7. Synthesized incident waveform required to excite monomode backscatter in the second natural mode of an infinite cylinder and the resulting monomode scattered wave along with return waveform from a target with 10% smaller radius.

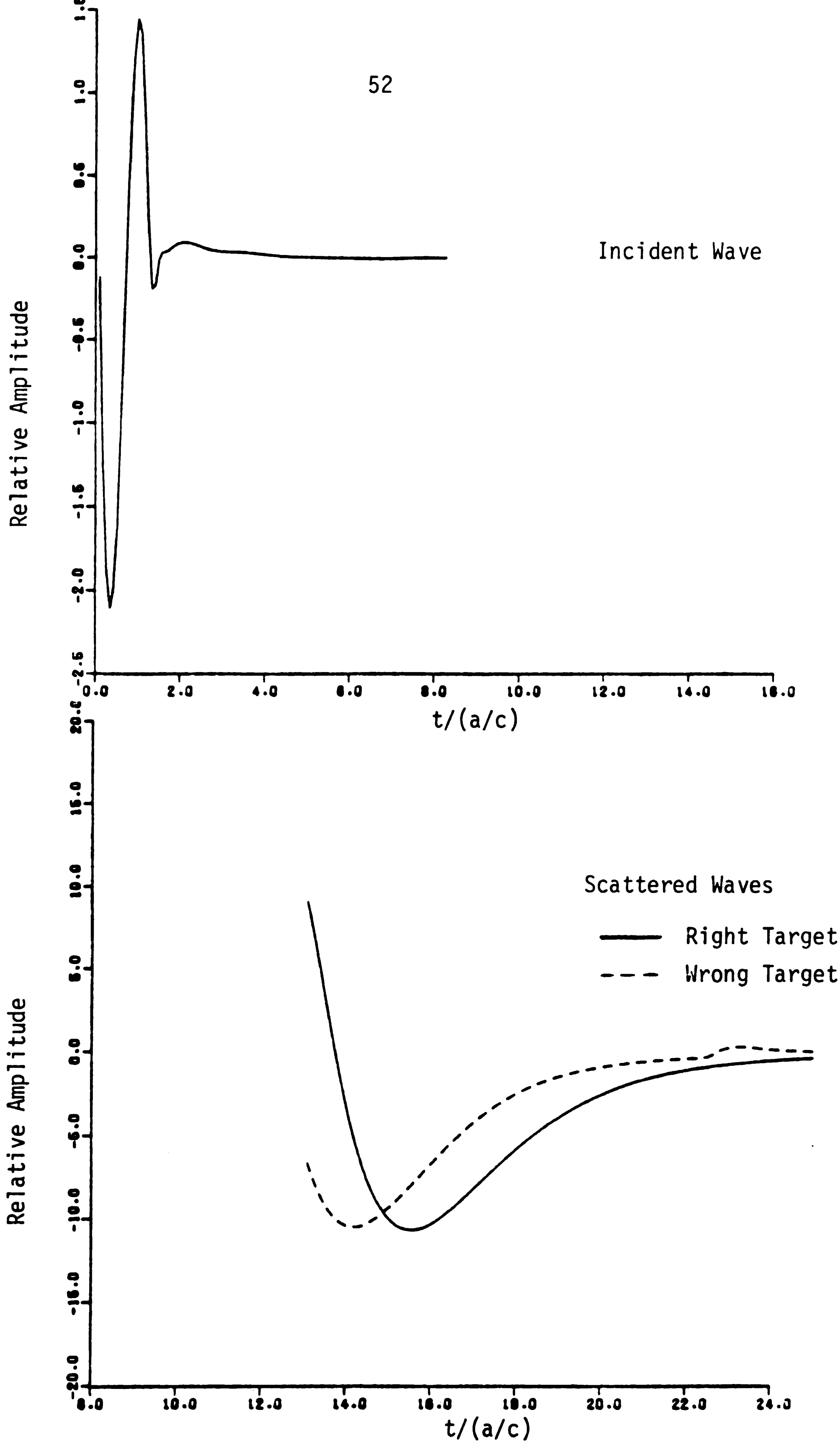

Figure 3.8. Synthesized and scattered waveforms for the first mode excitation similar to Figure 3.6 except a shorter τ_e.

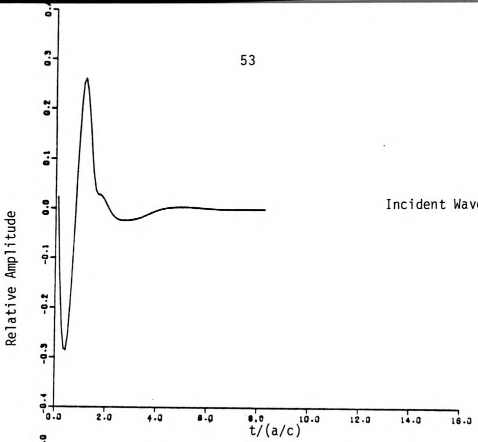

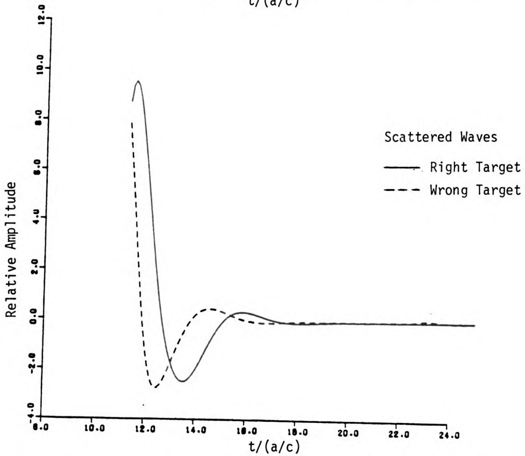

Figure 3.9. Synthesized and scattered waveforms for the second mode excitation similar to Figure 3.7 except a shorter τ_e.

second mode are shown in Figures 3.10 and 3.11 for comparision. It is obvious that they are very similar to those with $\tau_e = \frac{2}{3}\frac{1}{f_1}$, and therefore the resulting radar returns are not computed. The possibility of using different basis functions will be discussed later.

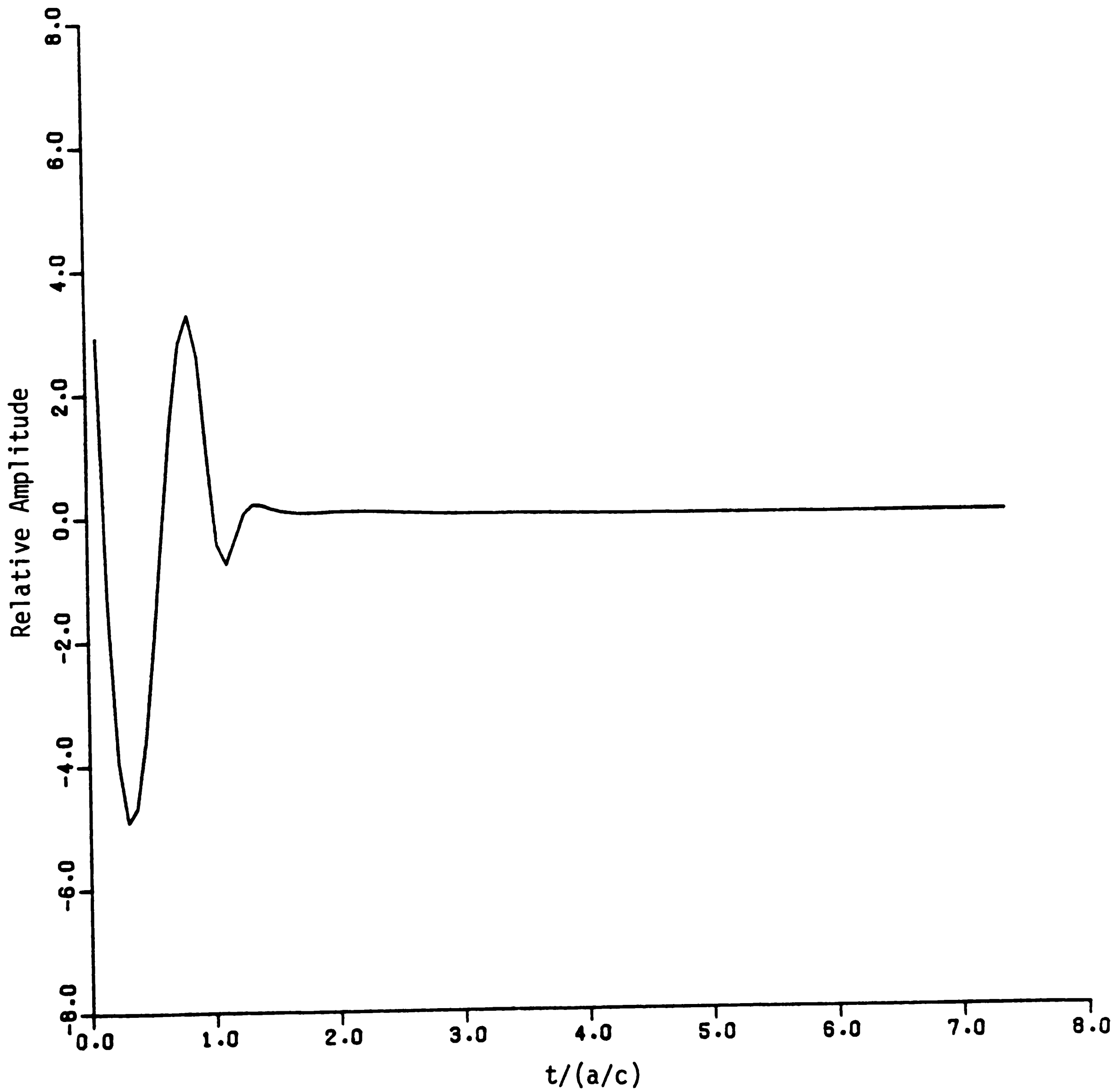

Figure 3.10. Synthesized incident waveform required to excite monomode backscatter in the first natural mode of an infinite cylinder with $\tau_e = 0.594 \frac{1}{f_1}$.

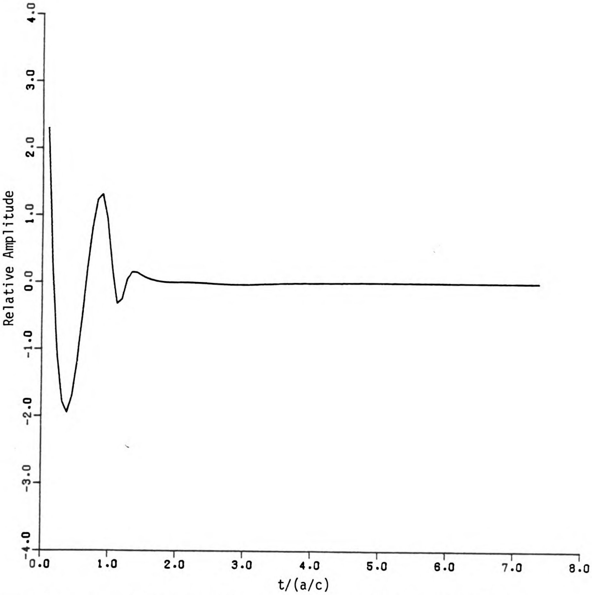

Figure 3.11. Synthesized incident waveform required to excite monomode backscatter in the second natural mode of an infinite cylinder with $\tau_e = 0.594 \frac{1}{f_1}$.

CHAPTER 4

SKEW-COUPLED WIRES

We apply the waveform-synthesis method and SEM to a target, consisting of a pair of skew-coupled, perfectly-conducting thin wires, which is illuminated by a transient, obliquely-incident, plane wave. The geometry of the problem is defined in Section 4.1 that also specifies the incident field. The integral equations descussed in Section 2.3.2 are applied to this geometry and described in detail in Section 4.2. The induced currents on the two wires are decomposed into symmetric and antisymmetric components to reduce the coupled integral equations into single integral equation for each mode. The numerical computation is thus simplified. The integral equations are solved in Section 4.3 to obtain the induced currents. Section 4.3.1 concerns with the natural modes by solving the homogeneous integral equations while Section 4.3.2 uses these natural modes to compute the coupling coefficient associated with each mode. The induced currents are obtained by carrying out the numerical computations of coupling coefficients and inverse Laplace-transform in Section 4.3.3. These induced currents are used in Section 4.4 to compute the vector potentials which, in turn, generate the back-scattered field. Some general formulas are derived first in Section 4.4 and then the specializations of parameters are made in Section 4.5 to determine the impulse response of a few special cases. Some of the cases are related to the experiments which will be described in Chapter 6. Finally, Section 4.6 demonstrates the numerical results of waveform-synthesis and its application to the radar target discrimination. Computer simulations by numerically convolving the synthesized incident waveforms with the impulse responses of the right and wrong targets are shown to indicate applicability of this waveform-symthesis scheme in practical situations.

4.1 Geometry of Problem

A pair of skew-coupled, perfectly-conducting thin wires with radii "a", lengths L, orientation angles α and distance 2d are illuminated by an obliquely-incident, transient, plane-wave radar signal at an angel φ as depicted in Figure 4.1. The incident field is expressed as

$$\vec{E}^{i}(\vec{r},t) = \hat{\zeta}\, F(t- \frac{\hat{k}\cdot\vec{r}}{c}) \tag{4.1}$$

where $\hat{\zeta} = \zeta_x\hat{x} + \zeta_y\hat{y} + \zeta_z\hat{z}$ = the unit polarization vector of the incident field,

$\vec{r} = x\,\hat{x} + y\,\hat{y} + z\,\hat{z}$ = the position vector,

$\hat{k} = k_x\,\hat{x} + k_y\,\hat{y} + k_z\,\hat{z}$ = the unit propagation vector,

with $\hat{k}\cdot\hat{\zeta} = o$;

and $F(t)$ is an unknown waveform function to be synthesized based on the requirement that $\vec{E}^{i}(\vec{r},t)$ excites a single-mode scattered field in the late-time period. The tangential components of $\vec{E}^{i}(\vec{r},t)$ on the wires, in their Laplace-transform, are

$$\tilde{E}^{i}_{tanj}(u_j,s) = (\zeta_y \cos\alpha-(-1)^j\,\zeta_z \sin\alpha)\,\tilde{F}(s) \exp\{-\gamma[k_y u_j \cos\alpha-(-1)^j k_z(d + u_j \sin\alpha)]\} \tag{4.2}$$

$o \le u_j \le L$, $j = 1,2$ for wire #1 and #2 respectively,

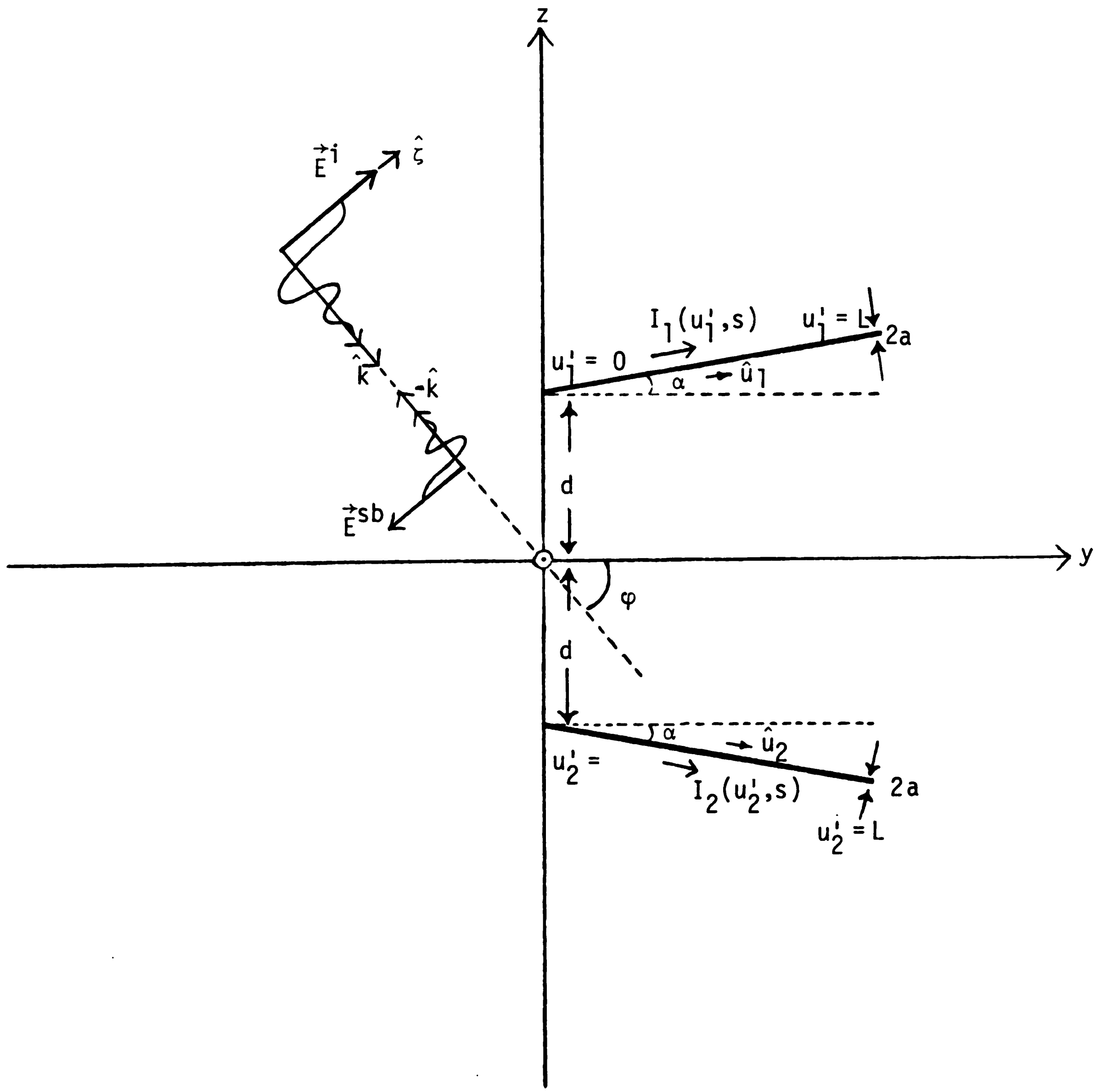

Figure 4.1. Two thin wires oriented at an angle are illuminated by an incident radar signal.

where $\tilde{F}(s) = \mathcal{L}\{F(t)\}$ and $\gamma = \frac{s}{c}$ is the complex propagation constant. These electric fields excite transient induced currents on the wires, and induced currents, in turn, generate a transient backscattered electric field. Our goal is to synthesize an aspect-independent waveform $F(t)$ for monomode excitation.

4.2 Integral Equations

To simplify this problem, we decompose the induced currents into symmetric and antisymmetric components, i.e.,

$$\left.\begin{aligned} I_1 &= I_s + I_a \\ I_2 &= I_s - I_a \end{aligned}\right\} \tag{4.3}$$

where I_s is the symmetric current which is the same in both wires while I_a is the antisymmetric current which flows in opposite directions with equal amplitude in both wires. After this simplification, each mode needs only one integral equation instead of two coupled integral equations in two unknown currents, I_1 and I_2. By matching the boundary condition on the perfectly-conducting wire surfaces so that the total tangential electric field, $E_{tan} = E^i_{tan} + E^s_{tan}$, equals zero there, we obtain the electric field integral equations (EFIF) from equation (2.26) as

$$\sum_{\ell=1}^{2} \{- \int_o^L I_\ell(u'_\ell, s) \left[\frac{\partial^2}{\partial u_j \partial u'_\ell} + \gamma^2(\hat{u}_j \cdot \hat{u}_\ell)\right] \frac{e^{-\gamma R_{j\ell}}}{4\pi R_{j\ell}} du'_\ell$$

$$+ \frac{\partial W_{j\ell}}{\partial u_j}(u_j)\} = -\varepsilon_o \, s \, \tilde{E}^i_{tan_j}(u_j,s) \; \ldots \text{ for } \; o \leq u_j \leq L \quad j = 1,2 \tag{4.4}$$

$$\text{where } W_{j\ell}(u_j) \equiv I_\ell(L^-,s) \frac{e^{-\gamma R_{j\ell}(u_j,L)}}{4\pi R_{j\ell}(u_j,L)} - I_\ell(o^+,s) \frac{e^{-\gamma R_{j\ell}(u_j,o)}}{4\pi R_{j\ell}(u_j,o)} = 0, \tag{4.5}$$

since $I_\ell(L^-,s) = I_\ell(o^+,s) = o$ at the wire ends.

By defining $S_j(u_j,s) \equiv -\varepsilon_o s\, \tilde{E}^i_{\tan_j}(u_j,s)$, $j = 1,2$ (4.6) as forcing functions, and dropping j,ℓ subscripts, we can rewrite equation (4.4) as

$$\left.\begin{aligned}\int_o^L I_1(u,s)\,K(u|u',s)du' + \int_o^L I_2(u,s)\,K_2(u|u',s)du' = S_1(u,s)\\ \int_o^L I_1(u,s)\,K_2(u|u',s)du' + \int_o^L I_2(u,s)\,K(u|u',s)du' = S_2(u,s)\end{aligned}\right\} \quad (4.7)$$

where
$$\left.\begin{aligned}K(u|u',s) &= -\left[\frac{\partial^2}{\partial u\partial u'} + \gamma^2\right]\frac{e^{-\gamma R(u,u')}}{4\pi R(u,u')} = \text{self-kernel},\\ K_2(u|u',s) &= -\left[\frac{\partial^2}{\partial u\partial u'} + \gamma^2 \operatorname{Cos} 2\alpha\right]\frac{e^{-\gamma R_2(u,u')}}{4\pi R_2(u,u')} = 2\alpha\text{-coupling kernel},\end{aligned}\right\} \quad (4.8)$$

with
$$\left.\begin{aligned}R(u,u') &= [(u-u')^2 + a^2]^{\frac{1}{2}},\\ R_2(u,u') &= \{(u-u')^2 \operatorname{Cos}^2\alpha + [2d + (u+u')\sin\alpha]^2 + a^2\}^{\frac{1}{2}}.\end{aligned}\right\} \quad (4.9)$$

From addition and subtraction of two equations in (4.7) and equation (4.3), we get the following equations,

$$\left.\begin{aligned}&\int_o^L I_s(u,s)K_s(u|u',s)\,du' = S_s(u,s) \quad \text{for symmetric modes}\\ &\int_o^L I_a(u,s)\,K_a(u|u',s)du' = S_a(u,s) \quad \text{for antisymmetric modes}\end{aligned}\right\} \quad (4.10)$$

$u \in [o,L]$,

where
$$\left.\begin{aligned}K_s(u|u',s) = K(u|u',s) + K_2(u|u',s)\\ K_a(u|u',s) = K(u|u',s) - K_2(u|u',s)\end{aligned}\right\}, \quad (4.11)$$

and

$$S_s(u,s) = \tfrac{1}{2}\,[S_1(u,s) + S_2(u,s)]$$
$$S_a(u,s) = \tfrac{1}{2}\,[S_1(u,s) - S_2(u,s)] \tag{4.12}$$

Coupled EFIE's in (4.7) are thus decoupled.

For the convenience of numerical computation, we obtain Hallen-type integral equations from (2.35) as

$$\int_o^L I_1(u',s)\,K_h(u|u',s)du' + \int_o^L I_2(u',s)\,K_{h2}(u|u',s)du'$$
$$= C_{11}\,\text{Cosh}\,\gamma u + C_{21}\,\sinh\gamma u - \frac{\varepsilon_o s}{\gamma}\int_o^u \tilde{E}^i_{tan_1}(\xi,s)\sinh\gamma(u-\xi)d\xi$$
$$\int_o^L I_1(u',s)\,K_{h2}(u|u',s)du' + \int_o^L I_2(u',s)\,K_h(u|u',s)du' \tag{4.13}$$
$$= C_{12}\cosh\gamma u + C_{22}\sinh\gamma u - \frac{\varepsilon_o s}{\gamma}\int_o^u \tilde{E}^i_{tan_2}(\xi,s)\,\sinh\gamma(u-\xi)d\xi$$
$$\text{for}\quad o \le u \le L$$

where $K_h(u|u',s) = \dfrac{e^{-\gamma R}}{4\pi R}$ = self Hallen-type kernel,

$$K_{h2}(u|u',s) = \frac{e^{-\gamma R_2}}{4\pi R_2}\,\text{Cos}\,2\alpha - \int_o^u g_2(\xi,u',s)\,\text{Cosh}\,\gamma(u-\xi)d\xi \tag{4.14}$$

= 2α - coupling Hallen-type kernel

with $$g_2\,(\xi,u',s) = \frac{d}{dR_2(\xi,u')}\,\frac{e^{-\gamma R_2(\xi,u')}}{4\pi R_2(\xi,u')}\;\frac{u'\sin^2 2\alpha + 2d\,\sin\alpha(1+\text{Cos}\,2\alpha)}{R_2(\xi,u')}. \tag{4.15}$$

Similar to the process of decoupling EFIE's, by adding and subtracting two equations in (4.13) and using definitions in (4.3) and (4.6), we get the following decoupled Hallen-type integral equations,

$$\int_o^L I_s(u',s)\, K_{hs}(u|u',s) = C_{1s} \cosh \gamma u + C_{2s} \sinh \gamma u + \frac{1}{\gamma}\int_o^u S_s(\xi,s) \sinh \gamma(u-\xi)d\xi \quad \text{for symmetric modes}$$

$$\int_o^L I_a(u',s)\, K_{ha}(u|u',s) = C_{1a} \cosh \gamma u + C_{2a} \sinh \gamma u + \frac{1}{\gamma}\int_o^u S_a(\xi,s) \sinh \gamma(u-\xi)d\xi \quad \text{for antisymmetric modes} \tag{4.16}$$

$u \in [o,L]$,

where $C_{1s} = \frac{C_{11} + C_{12}}{2}$, $C_{1a} = \frac{C_{11} - C_{12}}{2}$, $C_{2s} = \frac{C_{21} + C_{22}}{2}$, $C_{2a} = \frac{C_{21} - C_{22}}{2}$ $\Bigg\}$ = arbitrary constants,

$$\left.\begin{aligned} K_{hs}(u|u',s) &= K_h(u|u',s) + K_{h2}(u|u',s) \\ K_{ha}(u|u',s) &= K_h(u|u',s) - K_{h2}(u|u',s). \end{aligned}\right\} \tag{4.17}$$

Equations (4.16) are the integral equations to be used for finding the natural modes while equations (4.10) are used to compute the coupling coefficients [9] which are necessary in obtaining the impulse response.

4.3 Induced Currents

4.3.1. Natural Modes

Natural-mode solutions are those modes which exist as the solutions to the homogeneous problem with $\tilde{F}(s) = o$. By applying moment method [32], the integral equations in (4.16) are converted to a pair of matrix equations as

$$\left.\begin{aligned} A_s(s)\ I_s &= 0 \\ A_a(s)\ I_a &= 0 \end{aligned}\right\} \tag{4.18}$$

where

$$I_s = \begin{bmatrix} C_1 \\ I_2 \\ I_3 \\ \cdot \\ \cdot \\ \cdot \\ I_{NP} \\ C_2 \end{bmatrix}_s \qquad I_a = \begin{bmatrix} C_1 \\ I_2 \\ I_3 \\ \cdot \\ \cdot \\ \cdot \\ I_{NP} \\ C_2 \end{bmatrix}_a$$

for symmetric and antisymmetric modes respectively.

Note that in this solution the wire is partitioned into NP partitions with $I_1 = I_{NP+1} = 0$ for the current near the wire ends and subsequently dropped from the unknown colunm matrix while C_1 and C_2 are included as unknowns. The detail of partitioning the wire is shown in Figure 4.2.

For the purpose of getting nontrivial solutions for I_s and I_a, matrices $A_s(s)$ and $A_a(s)$ must be singular, and therefore the natural frequency is that s which satisfies

$$\left.\begin{aligned} \det\,[A_s(s)] &= 0 \quad \text{for symmetric mode} \\ \det\,[A_a(s)] &= 0 \quad \text{for antisymmetric mode.} \end{aligned}\right\} \tag{4.19}$$

Both Newton's and Muller's methods are used to search for the roots of equations (4.19), NP = 10n is used for the nth mode. Once we've found

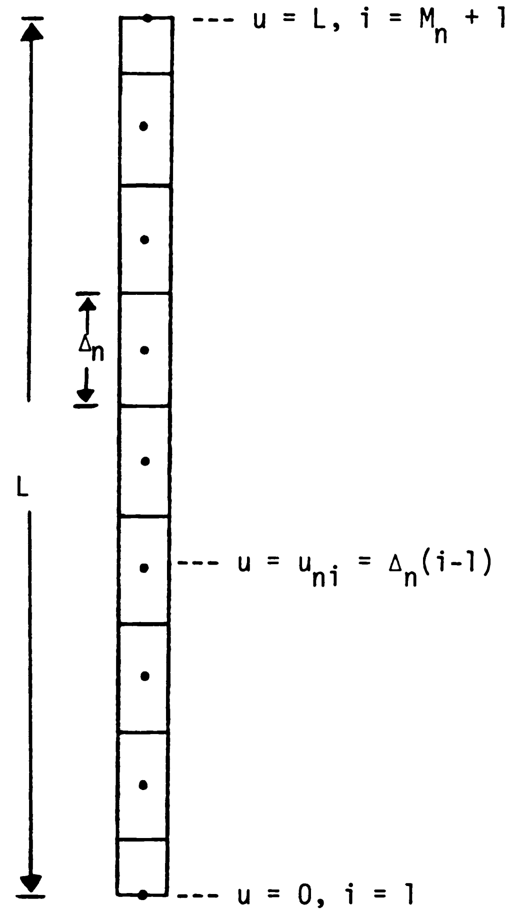

Np = # of partitions = M_n for the nth mode

$$\Delta_n = \frac{L}{M_n} = \frac{L}{10n}$$

Figure 4.2. Partitioning of the wire for moment-method solution using pulse-function expansion.

$s_n = \sigma_n + j\omega_n$ to be a root, its complex-congugate, s_n^*, is also a root, since equations in (4.19) have real coefficients. Therefore, for those numerical results we'll show below, only those roots which are in the second quadrant are demonstrated explicitly, and the natural modes are in the form of $A_n e^{\sigma_n t} \cos(\omega_n t + \varphi_n)$, where A_n and φ_n depend on the aspect-angle (which, in turn, depends on $\hat{\zeta}$ and $\hat{k}$).

In the following, some natural-frequency distributions with $L/a = 200$ are demonstrated with different parameter varied. Figures 4.3 and 4.4 are the distributions of the first 10 natural frequencies in the first layer with $d/L = 0.5$ and $\alpha = 0^o$, 30^o, 60^o and 90^o together with the first 10 natural frequencies for the isolated wire. Figure 4.3 is for antisymmetric modes and Figure 4.4 for symmetric modes. The distributions of roots with different angles are so close to the roots of the isolated wire that it is not easy to make any conclusion about the coupling effect due to different angles. In Figure 4.5, we plot the trajectories of the first antisymmetric and symmetric roots with $L/a = 200$, $d/L = 0.5$, with changing α. It is obvious that they are converging to the first root of the isolated wire as α increases; this is reasonable since increasing α reduces the coupling between the wires. The other interesting observation is that the root of the isolated wire is roughly the average of the roots of antisymmetric and symmetric modes. We see about the same property appears in Figure 4.6 for the second modes. The effect on the first antisymmetric mode for $L/a = 200$, $\alpha = 0^o$, 30^o, 60^o and 90^o by changing d is reflected in Figure 4.7; there are spiral-like trajectories with a largest "radius" for the case of $\alpha = 0^o$ and the $\alpha = 90^o$ case smallest. This is again a demonstration of a smaller coupling for a larger angle. Another important observation is that as

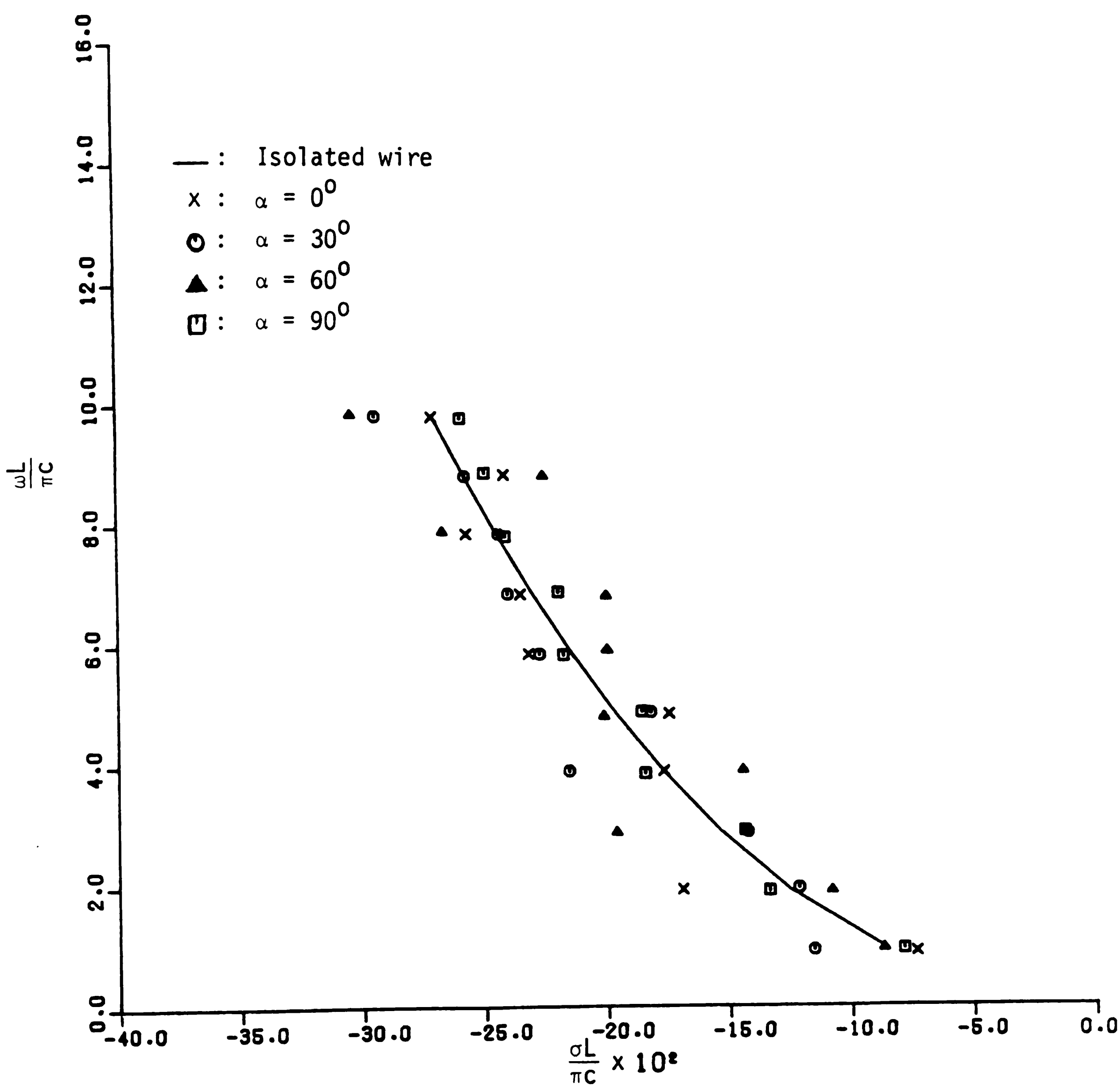

Figure 4.3. Locations of the first 10 natural frequencies of the first layer of the antisymmetric modes for the two coupled wires with $L/a = 200$, $d/L = 0.5$ and for $\alpha = 0^o$, 30^o, 60^o and 90^o.

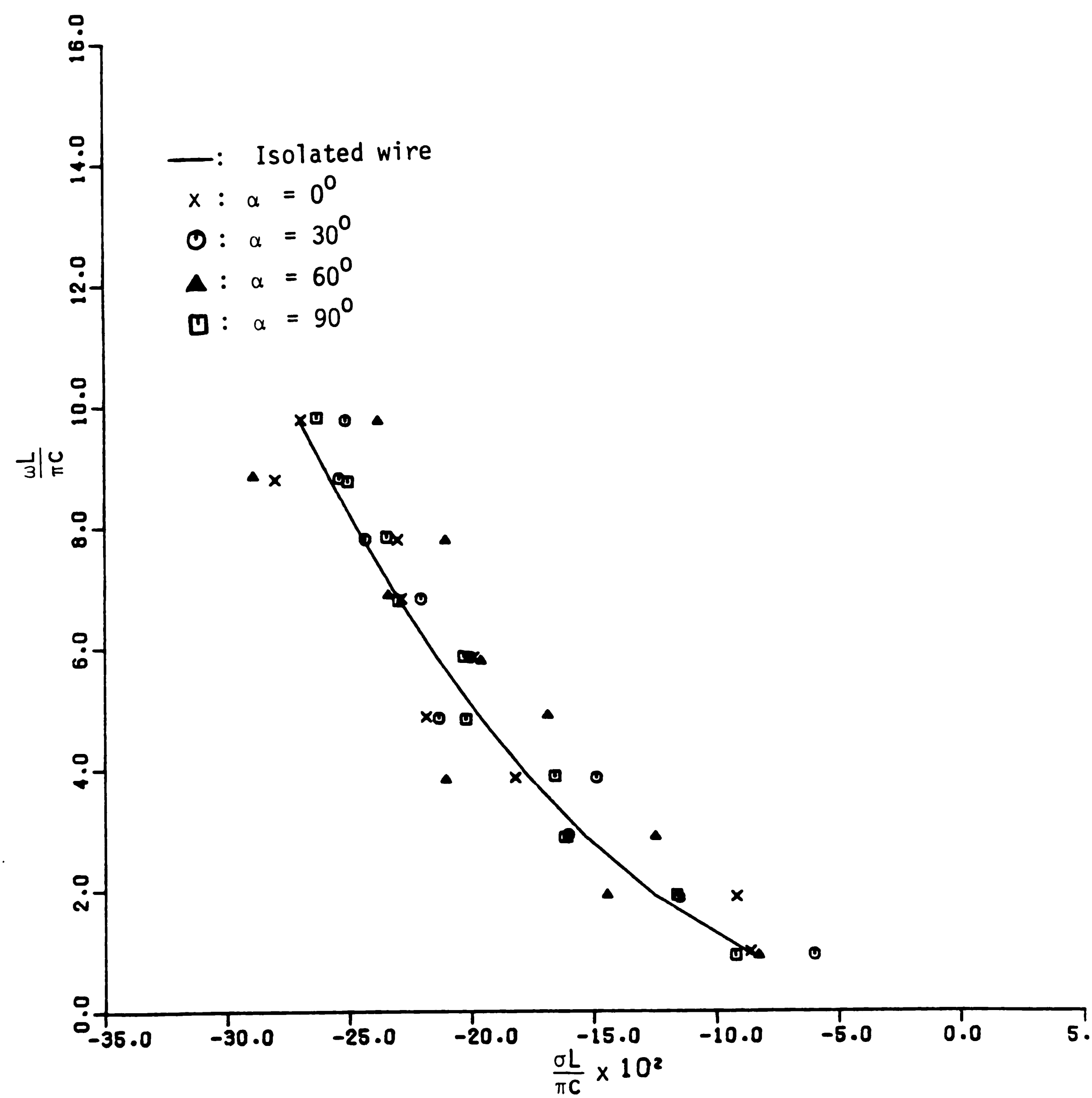

Figure 4.4. Locations for the first 10 natural frequencies of the first layer of the symmetric modes for the two coupled wires with $L/a = 200$, $d/L = 0.5$ and for $\alpha = 0^0$, 30^0, 60^0 and 90^0.

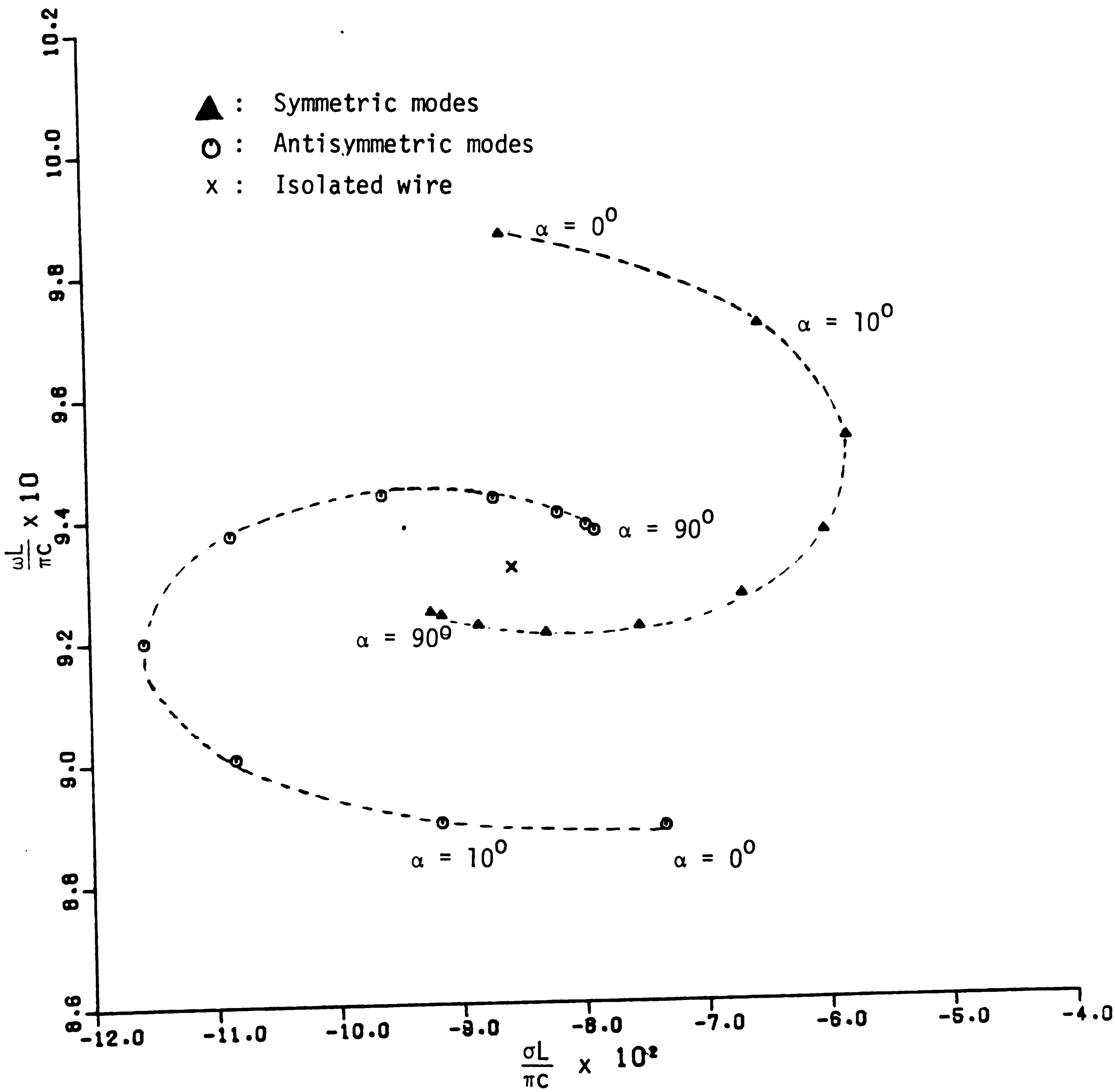

Figure 4.5. Locations of the first natural frequencies of the symmetric and antisymmetric modes vary as functions of the orientation angle ; L/a = 200 and d/L = 0.5.

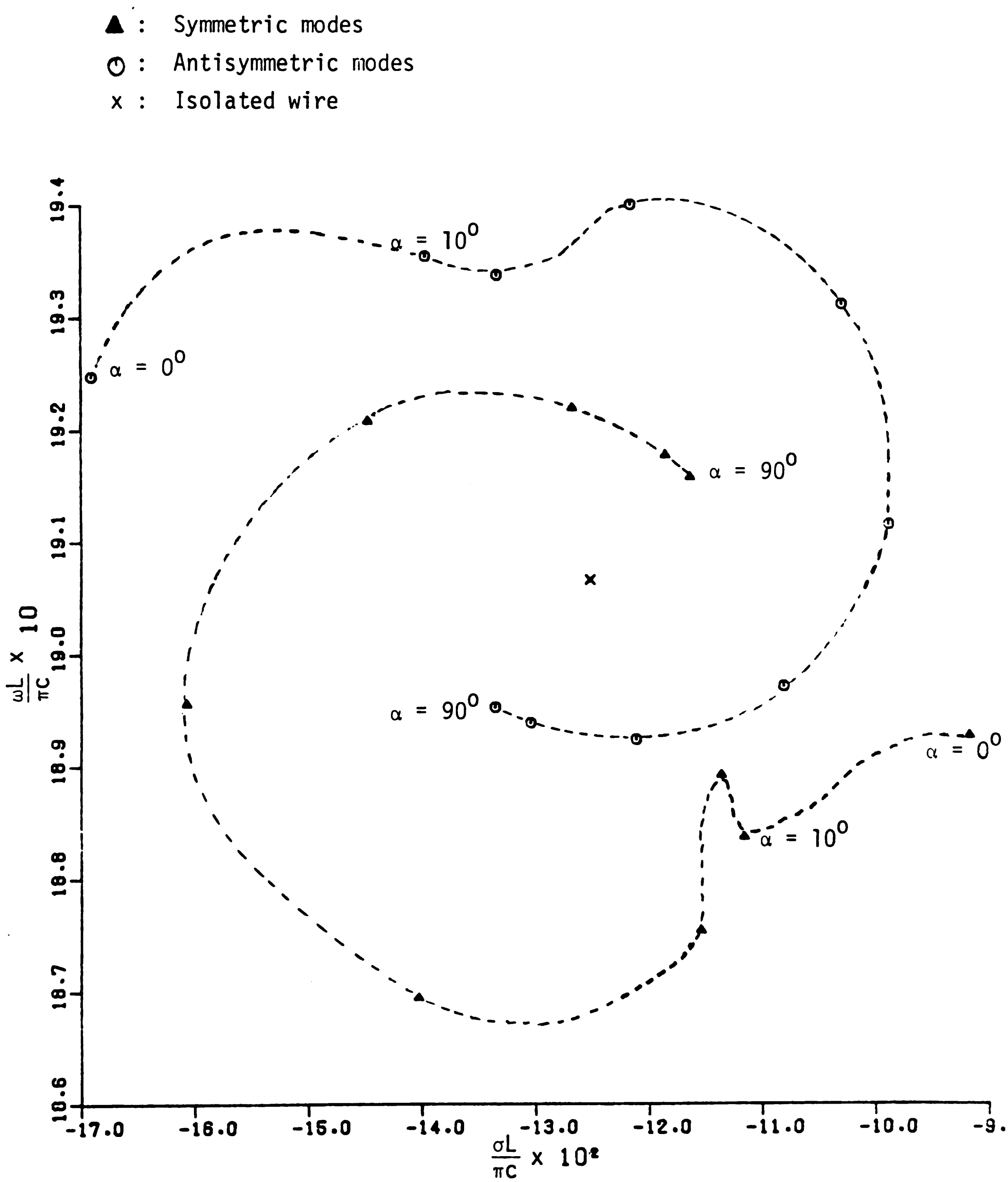

Figure 4.6. Locations of the second natural frequencies of the symmetric and antisymmetric modes vary as functions of the orientation angle ; L/a = 200 and d/L = 0.5.

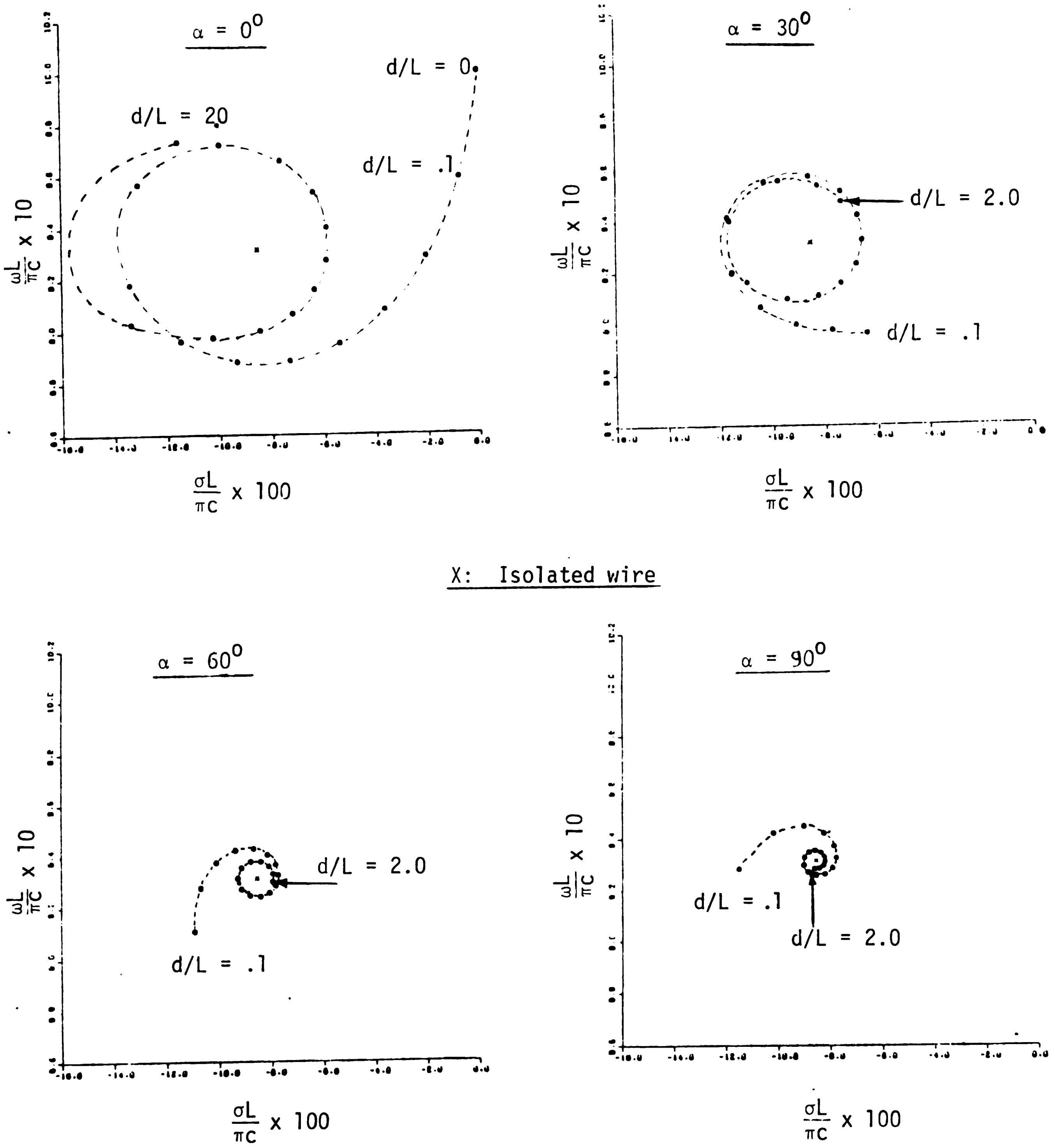

Figure 4.7. Locations of the first natural frequencies of the anti-symmetric mode vary as functions of the spacing between wires for $\alpha = 0^0$, 30^0, 60^0 and 90^0 and with $a/L = 1/200$.

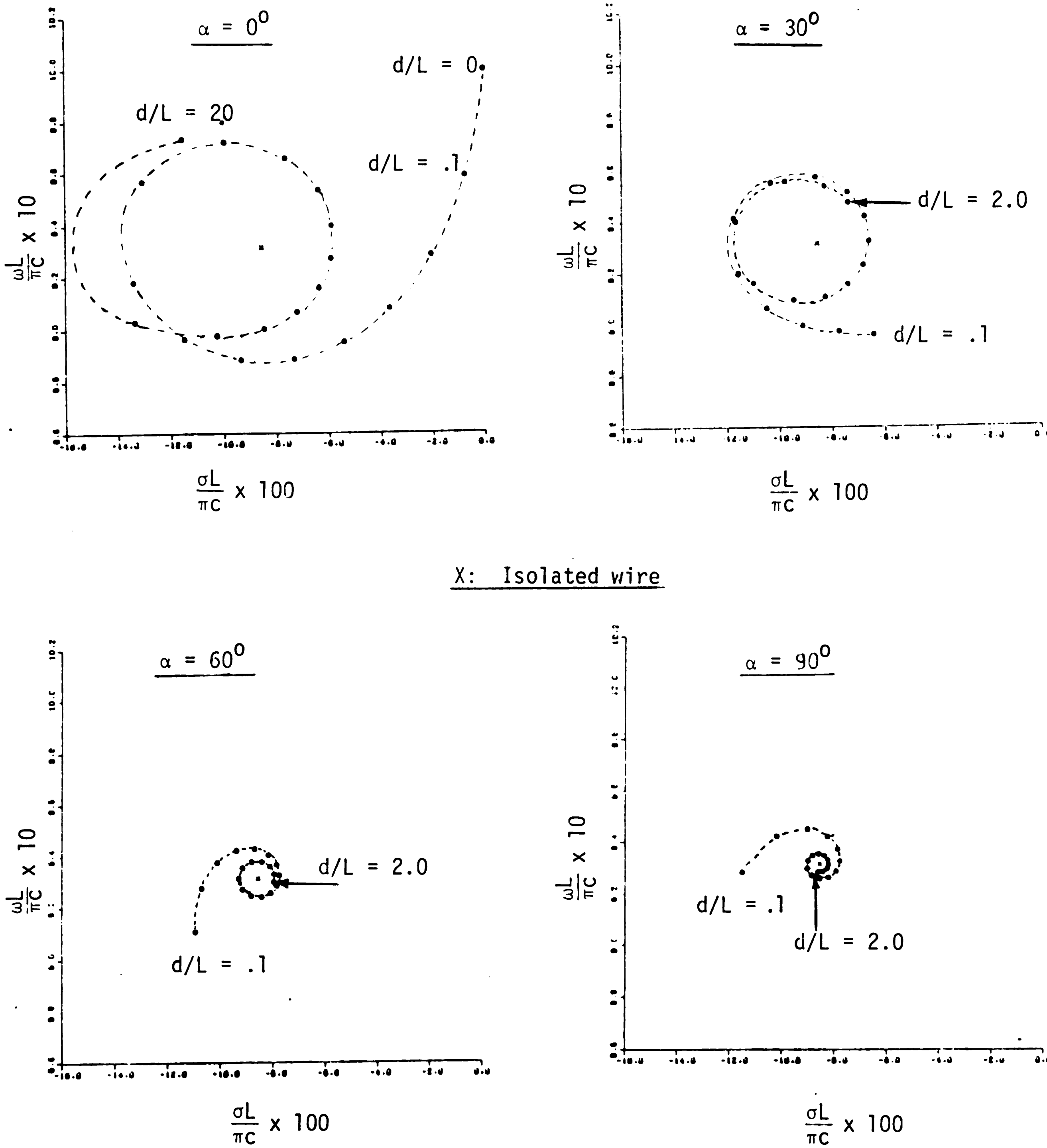

Figure 4.7. Locations of the first natural frequencies of the anti-symmetric mode vary as functions of the spacing between wires for $\alpha = 0^{o}$, 30^{o}, 60^{o} and 90^{o} and with $a/L = 1/200$.

the distance becomes larger and larger, the coupling between the wires decreases, and subsequently the root becomes closer and closer to that of an isolated wire. This figure is compared with the result in [33] in which only a wire over ground plane and thus only antisymmetric modes exist. Figures 4.8, 4.9 and 4.10 are demonstrations of how symmetric and antisymmetric natural frequencies change as d changes for the first, the second and the third mode, respectively, with $\alpha = 0^{o}$. It is found that for higher order modes the "radii" of spirals become smaller and smaller and converge faster to the root of the isolated wire.

To complete the natural-mode solution, we must compute the natural-mode currents associated with the natural frequencies. The way to compute them is to substitute the roots we've found into (4.18) and solve the homogeneous equations by eliminating one equation (one row of matrix) and setting a particular segment of the current (the best choice is the segment which has the maximum current; if this choice happens to be zero-current segment, then the solution will blow up) to be one and moving the corresponding column to the right hand side with the negative sign. Some results for different modes, different angles with $L/a = 200$, $d/L = 0.5$ are shown in Figures 4.11 - 4.13, they are also compared with pure sinusoidal current distribution which is approximately the case for the isolated wire.It is seen that the imaginary part of natural-mode currents are affected more by the coupling. Compare Figures 4.5 and 4.6 for the coupling effect.

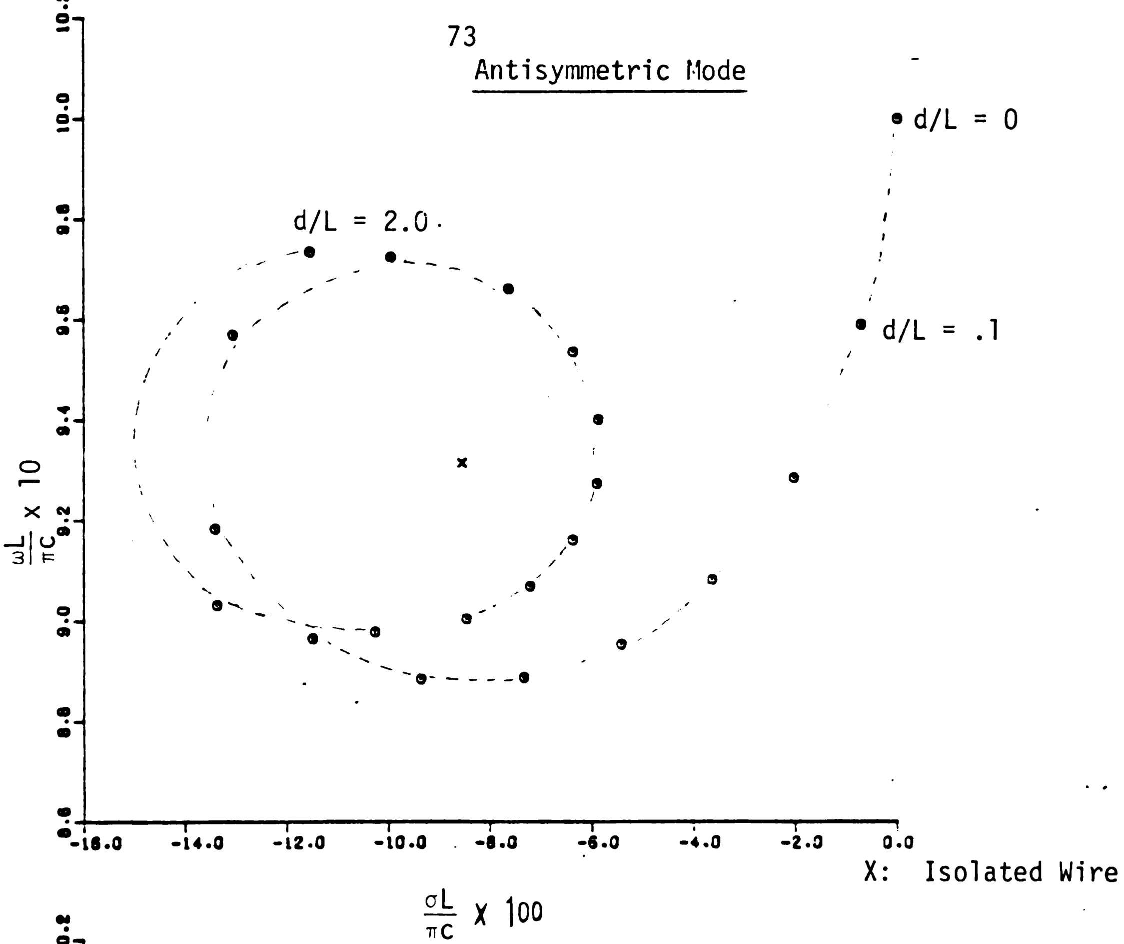

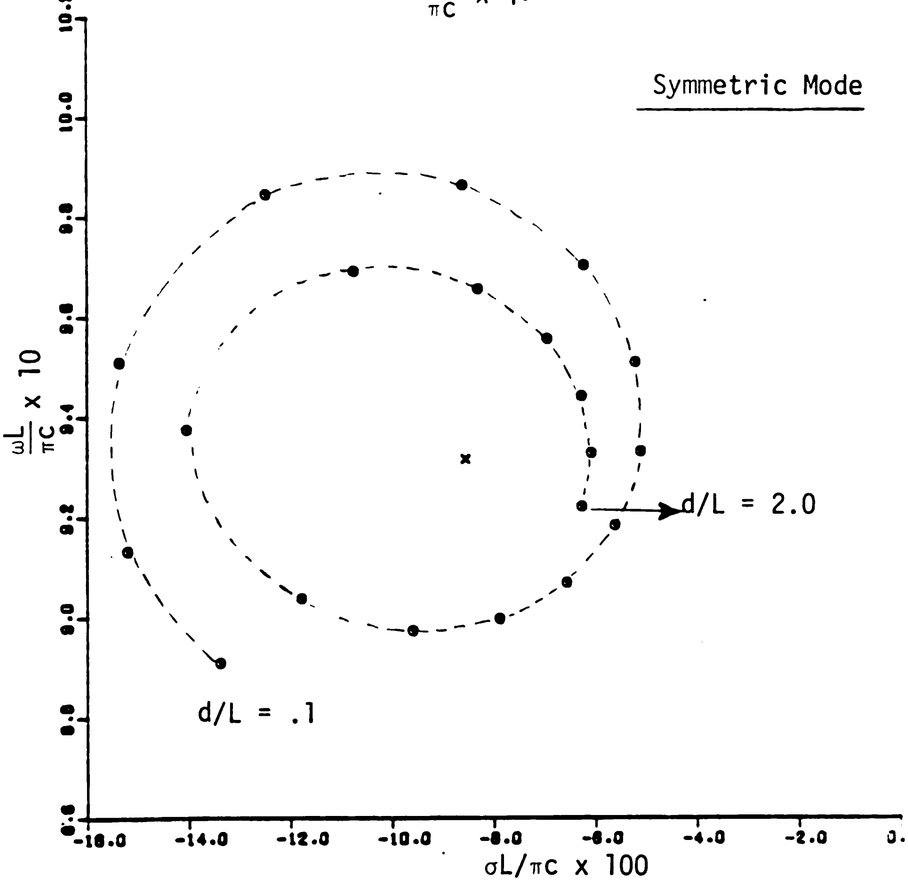

Figure 4.8. Locations of the first natural frequencies of antisymmetric mode vary as functions of d/L for $\alpha = 0^{0}$ and a/L = 1/200.

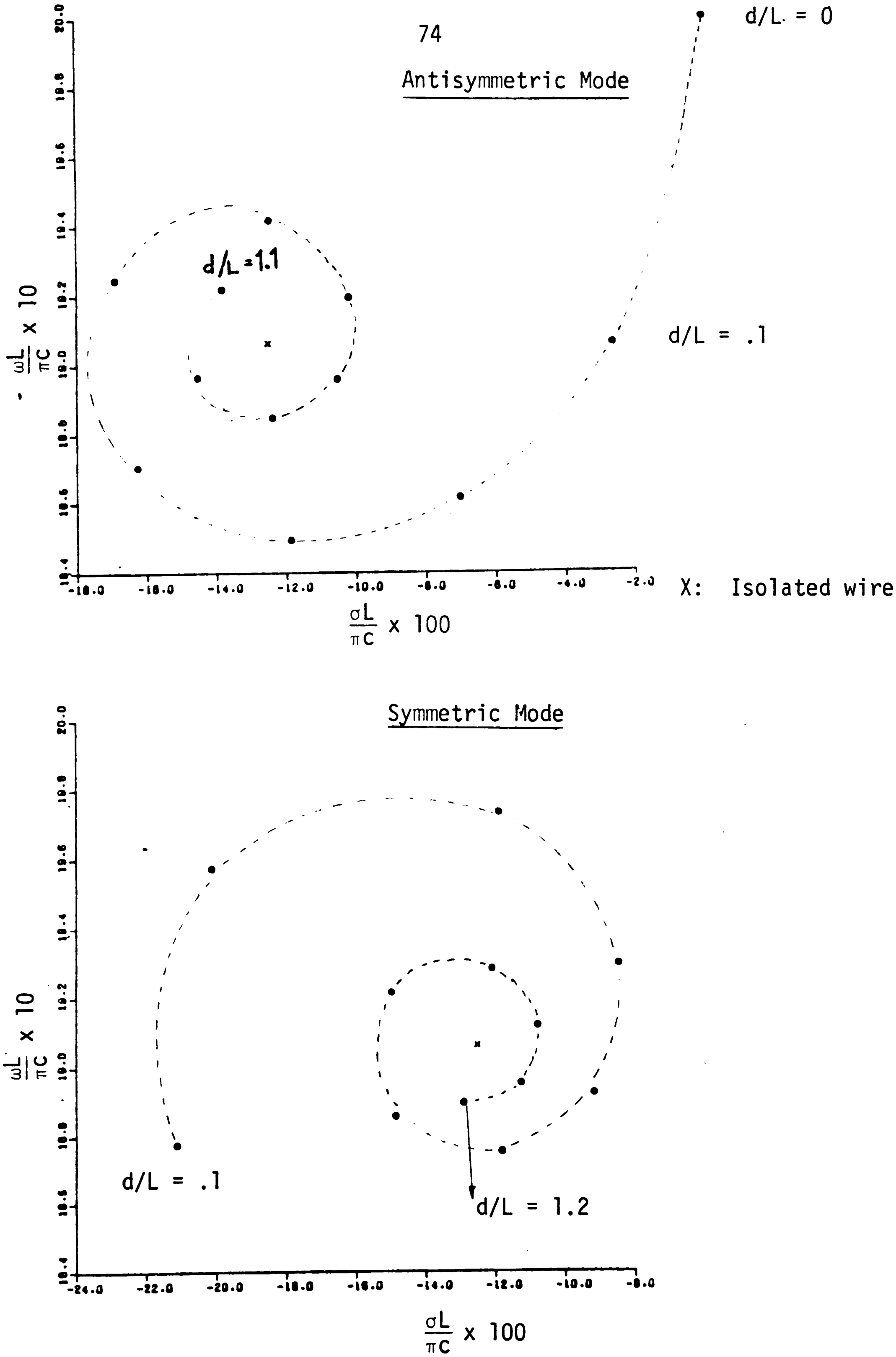

Figure 4.9. Locations of the second natural frequencies of antisymmetric mode vary as functions of d/L for $\alpha = 0^{o}$ and L/a = 200.

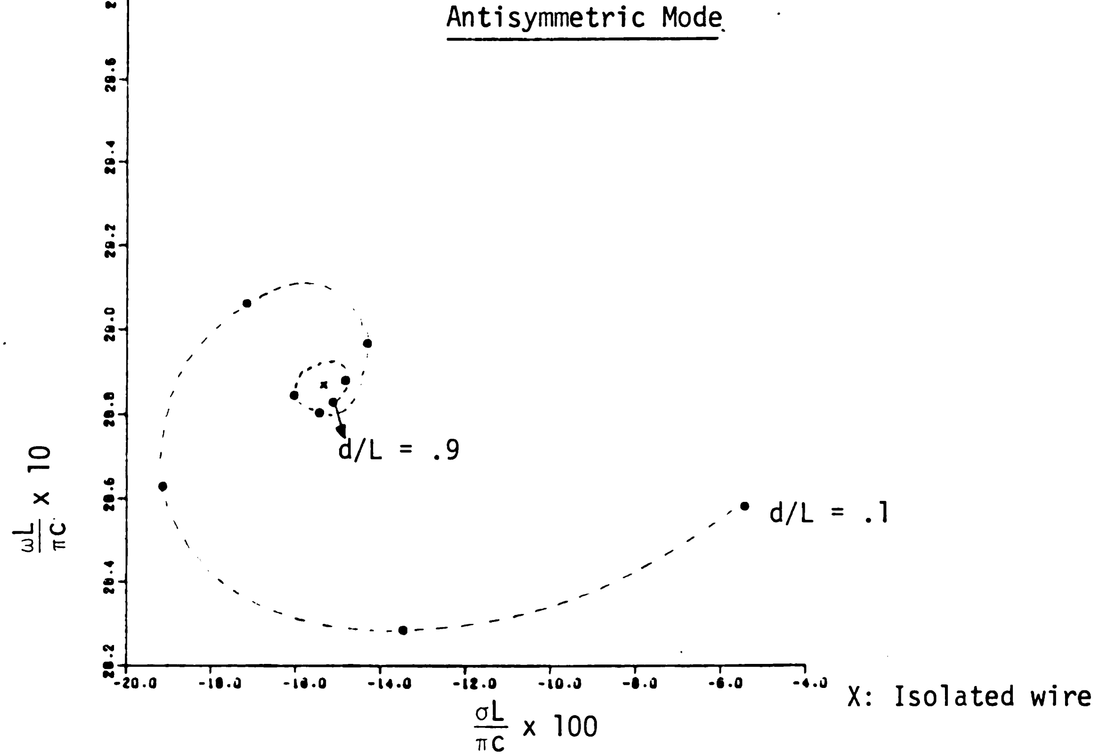

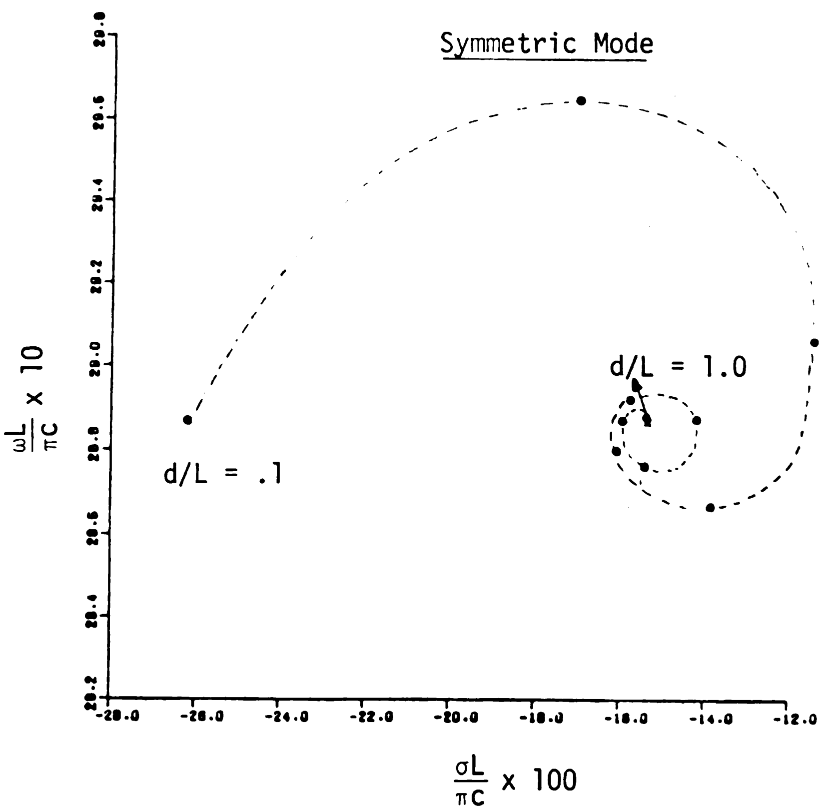

Figure 4.10. Locations of the third natural frequencies of antisymmetric mode and symmetric mode vary as functions of d/L for $\alpha = 0^{0}$ and L/a = 200.

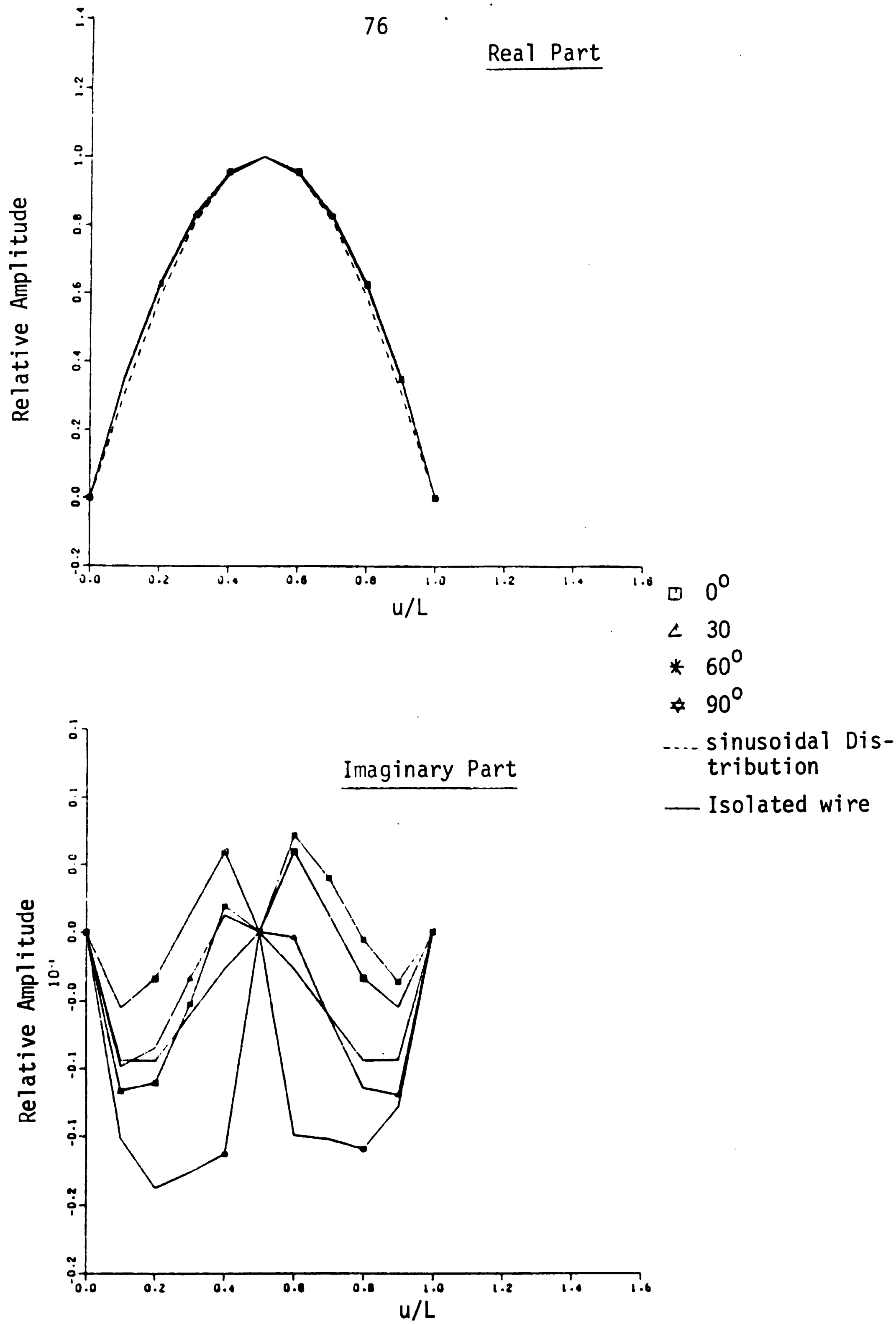

Figure 4.11. Real and imaginary parts of the first natural-mode current for $\alpha = 0^o$, 30^o, 60^o and 90^o with $L/a = 200$, $d/L = 0.5$ along with those for the isolated wire.

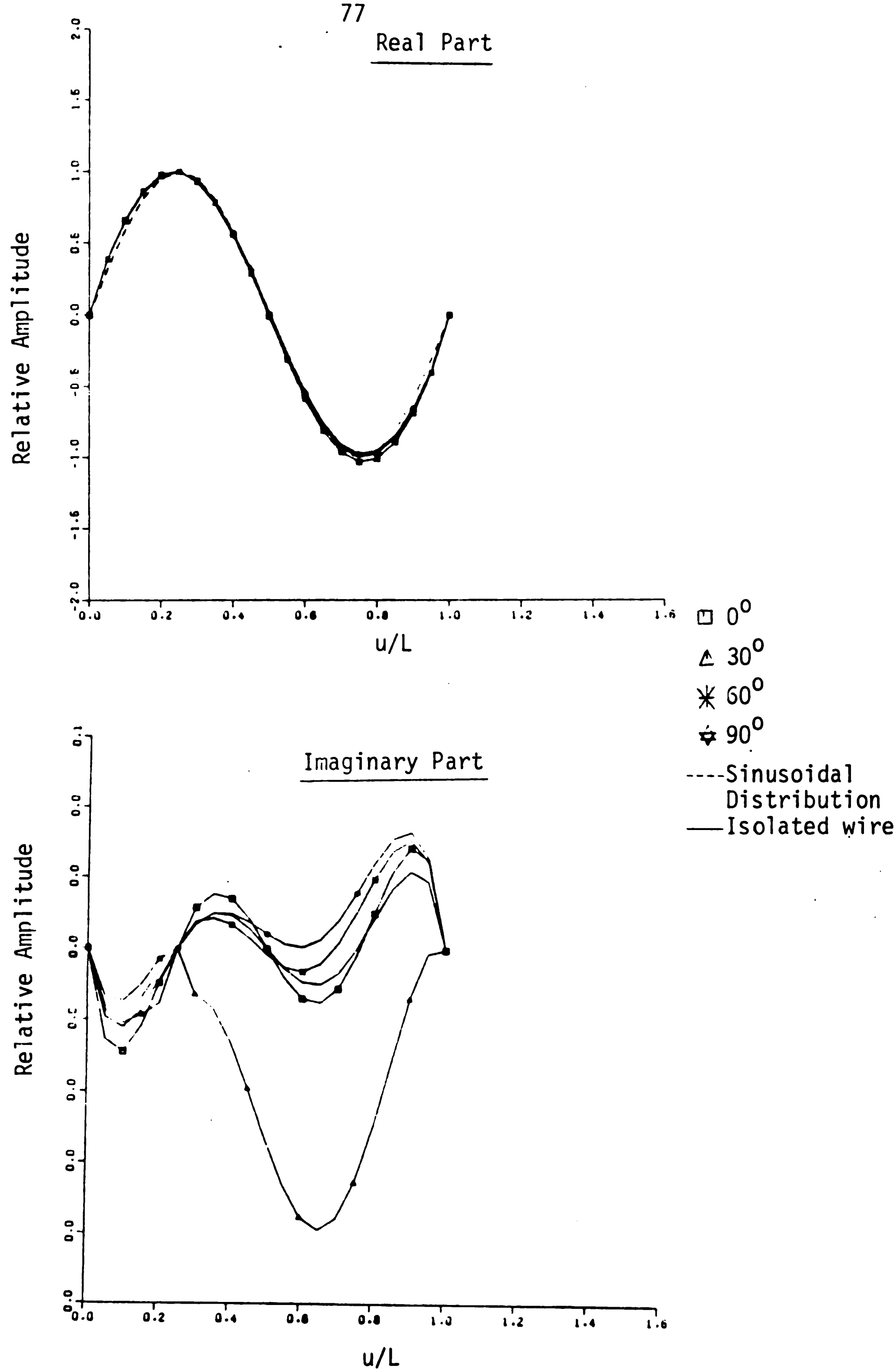

Figure 4.12. Real and imaginary parts of the second natural-mode current for $\alpha = 0^{\circ}, 30^{\circ}, 60^{\circ}$ and 90° with $L/a = 200$, $d/L = 0.5$ along with those for the isolated wire.

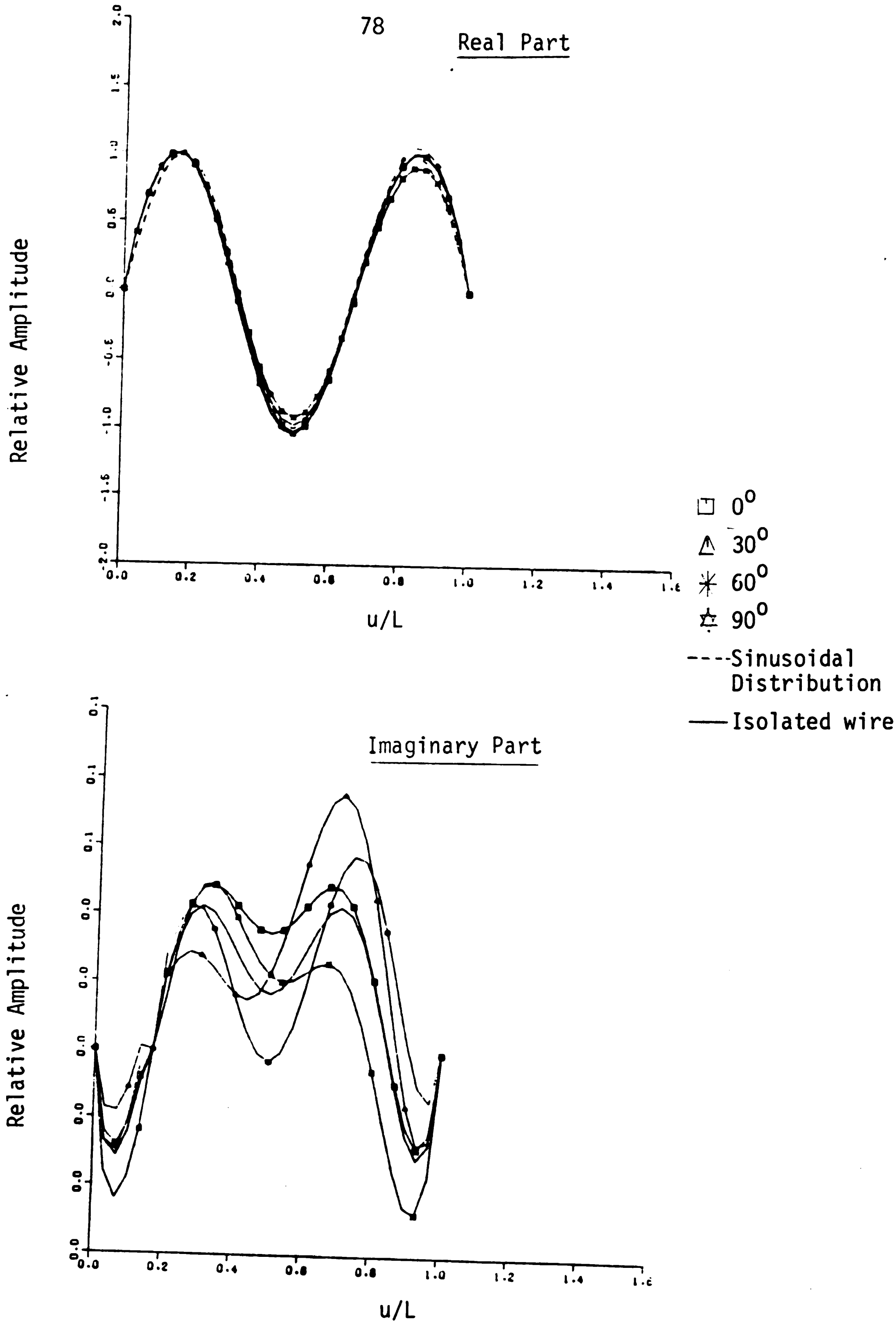

Figure 4.13. Real and imaginary parts of the third natural-mode current for $\alpha = 0^{o}$, 30^{o}, 60^{o} and 90^{o} with $L/a = 200$, $d/L = 0.5$ along with those for the isolated wire.

4.3.2 Coupling Coefficients

From SEM, the induced current can be expressed as

$$I(n,s) = \sum_{n=1}^{N} a_n(s)\, \nu_n(u)\, (s-s_n)^{-1}$$

Where $\nu_n(u)$ is the distribution of the nth mode current, $a_n(s)$ is the coupling coefficient corresponding to the spatial disbribution $\nu_n(u)$ and the temperal variation is controlled by $(s-s_n)^{-1}$ in the Laplace-transform domain.

The coupling coefficient is computed by using equation (2.37).

For this problem currents are decomposed into symmetric and antisymmetric components and expressed as

$$\left.\begin{aligned} I_s(u,s) &= \sum_{n=1}^{N_s} a_{sn}(s)\, \nu_{sn}(u)\, (s-s_{sn})^{-1} \\ I_a(u,s) &= \sum_{n=N_s+1}^{N} a_{an}(s)\, \nu_{an}(u)\, (s-s_{an})^{-1} \end{aligned}\right\} \tag{4.20}$$

where $N = N_s + N_a$ and N_s = number of symmetric modes used, and N_a = number of antisymmetric modes used. In the following computations $N_s = N_a = 10$ are used.

The coupling coefficients are computed by

$$\left.\begin{aligned} a_{sn}(s) &= \frac{\int_0^L S_s(u,s)\, \nu_{sn}(u)du}{\int_0^L\int_0^L \nu_{sn}(u)\nu_{sn}(u')\{\frac{\partial}{\partial s}[K_s(u|u',s)]\}_{s=s_{sn}}\, du'du} \\ a_{an}(s) &= \frac{\int_0^L S_a(u,s)\, \nu_{an}(u)du}{\int_0^L\int_0^L \nu_{an}(u)\, \nu_{an}(u')\{\frac{\partial}{\partial s}[K_a(u\ u',s)]\}_{s=s_{an}}\, du'du} \end{aligned}\right\} \tag{4.21}$$

Coupling coefficients in (4.21) are called "class-2" coupling coefficients which take into account of the causal property by different "turn-on" times for the contributions from different current segments. The "class-1" coupling coefficients are

$$\left.\begin{aligned} a_{sn} &= a_{sn}(s)|s=s_{sn} \\ a_{an} &= a_{an}(s)|s = s_{an} \end{aligned}\right\}. \qquad (4.22)$$

We'll see that this formula is indeed true only in the late-time since it does not take care of causality.

4.3.3 Computation of the Induced Currents

Referring again to Figure 4.2 with $NP = M_n = 10n$, the nth mode current can be expressed as

$$\nu_n(u) = \sum_{i=2}^{M_n} I_{ni}\, p_{ni}(u) \qquad (4.23)$$

Where $p_{ni}(u) = 1$ for $(i - \frac{3}{2})\Delta_n \leq u \leq (i - \frac{1}{2})\Delta_n$

$= 0$ elsewhere,

and $\Delta_n = \frac{L}{M_n}$, $I_{ni} = 0$ for $i = 1$ and $M_n + 1$.

Defining $u_{ni} = (i - 1)\Delta_n$ = center of the ith segment for the nth mode, we get, from equation (4.19),

$$a_n(s) = \frac{\displaystyle\sum_{i=2}^{M_n} I_{ni} \int_{(i-\frac{3}{2})\Delta_n}^{(i-\frac{1}{2})\Delta_n} S_n(u,s)du}{\displaystyle\sum_{i=2}^{M_n} \sum_{j=2}^{M_n} I_{ni}\, I_{nj} \int_{(i-\frac{3}{2})\Delta_n}^{(i-\frac{1}{2})\Delta_n} \int_{(j-\frac{3}{2})\Delta_n}^{(j-\frac{1}{2})\Delta_n} \left\{\frac{\partial}{\partial s}[K(u|u',s)]\right\}_{S=S_n} du'du} \qquad (4.24)$$

With $S_n(u,s)$ for symmetric modes and antisymmetric modes expressed in terms of equaitons (4.12), (4.6) and (4.2), $K(u|u',s)$ in terms of equations (4.11) and (4.8), we can carry out the integrations in (4.24) as

$$a_n(s) = \frac{G_n(s)}{D_n} = \frac{-\varepsilon_o s}{2}\tilde{F}(s)\frac{\sum_{i=2}^{M_n} I_{ni}g_{ni}(s)}{\sum_{i=2}^{M_n}\sum_{j=2}^{M_n} I_{ni}I_{nj}d_{nij}} = -\frac{c\tilde{F}(s)}{6o\Omega}\frac{\sum_{i=2}^{M_n} I_{ni}g'_{ni}(s)}{\sum_{i=2}^{M_n}\sum_{j=2}^{M_n} I_{ni}I_{nj}d'_{nij}} \tag{4.25}$$ [1]

where $g_{ni}'(s) = \gamma\, g_{ni}(s)$

$$= \frac{2(\zeta_y \mathrm{Cos}\alpha + \zeta_z \sin\alpha)}{(k_y\cos\alpha + k_z\sin\alpha)} \sinh\left[\gamma(k_y\cos\alpha + k_z\sin\alpha)\frac{\Delta_n}{2}\right]$$

$$\cdot \exp\{-\gamma[k_z d + (k_y\cos\alpha + k_z\sin\alpha)u_{ni}]\} \pm \frac{2(\zeta_y\cos\alpha - \zeta_z\sin\alpha)}{(k_y\cos\alpha - k_z\sin\alpha)}$$

$$\cdot \sinh\left[\gamma(k_y\cos\alpha - k_z\sin\alpha)\frac{\Delta_n}{2}\right]\exp\{\gamma[k_z d-(k_y\cos\alpha-k_z\sin\alpha)u_{ni}]\}, \tag{4.26}$$

$$d'_{nij}(s) = 4\pi c\; d_{nij}$$

$$= I_{nij} - 2\gamma_n J_{nij} + \gamma_n^2 K_{nij}, \tag{4.27}$$

with $I_{nij} = 2e^{-\gamma_n\sqrt{(i-j)^2\Delta_n^2+a^2}} - e^{-\gamma_n\sqrt{(i-j+1)^2\Delta_n^2+a^2}} - e^{-\gamma_n\sqrt{(i-j-1)^2\Delta_n^2+a^2}}$

---

[1] $\sqrt{\frac{\mu_o}{\varepsilon_o}} = 120\ \Omega$ is used.

$$\pm \{e^{-\gamma_n\sqrt{(i-j)^2\Delta_n^2\cos^2\alpha + [2d+(i+j-1)\Delta_n\sin\alpha]^2+a^2}}$$

$$+ e^{-\gamma_n\sqrt{(i-j)^2\Delta_n^2\cos^2\alpha + [2d+(i+j-3)\Delta_n\sin\alpha]^2+a^2}}$$

$$- e^{-\gamma_n\sqrt{(i-j+1)^2\Delta_n^2\cos^2\alpha + [2d+(i+j-2)\Delta_n\sin\alpha]^2+a^2}}$$

$$- e^{-\gamma_n\sqrt{(i-j-1)^2\Delta_n^2\cos^2\alpha + [2d+(i+j-2)\Delta_n\sin\alpha]^2+a^2}}, \quad (4.28)$$

$$J_{nij} = \Delta_n^2 \frac{e^{-\gamma R(u_{ni},u_{nj})}}{R(u_{ni},u_{nj})} \pm \frac{e^{-\gamma_n R_2(u_{ni},u_{nj})}}{R_2(u_{ni},u_{nj})} \operatorname{Cos} 2\alpha \quad \text{for } i \neq j$$

$$= \pm \Delta_n^2 \frac{e^{-\gamma R_2(u_{ni},u_{nj})}}{R_2(u_{ni},u_{nj})} \operatorname{Cos} 2\alpha - \gamma_n\Delta_n^2 + \mathcal{J}_n \quad \text{for } i = j, \quad (4.29)$$

$$\mathcal{J}_n = \Delta_n \ln \left(\frac{\Delta_n+\sqrt{\Delta_n^2+a^2}}{-\Delta_n+\sqrt{\Delta_n^2+a^2}}\right) -2\sqrt{\Delta_n^2 + a^2}, \quad (4.30)$$

$$K_{nij} = \Delta_n^2[e^{-\gamma_n R(u_{ni},u_{nj})} \pm e^{-\gamma_n R_2(u_{ni},u_{nj})} \operatorname{Cos} 2\alpha] \quad (4.31)$$

and $\gamma_n = \frac{S_n}{c}$.

The "$\pm$" sign from equation (4.26) to Equation (4.31):

"+" should be used for symmetric modes for $n \in [1,N_s]$

"-" should be used for antisymmetric modes for $n \in [N_s + 1,N]$.

It is obvious from the above definitions that both d'_{nij} and $g'_{ni}(s)$ are dimensionless.

Upon substitution of (4.23) and (4.25) into (4.20), we obtain symmetric and antisymmetric components of induced current as

$$I_s(u,s) = -\frac{c\tilde{F}(s)}{60\Omega} \sum_{n=1}^{N_s} \sum_{i=2}^{M_n} \sum_{k=2}^{M_n} D_n'^{-1}(s-s_n)^{-1} I_{ni} I_{nk}\, g'_{ni}(s) p_{nk}(u) \tag{4.32}$$

Where $D_n' = 4\pi c D_n = \sum_{j=2}^{M_n} \sum_{j=2}^{M_n} I_{ni} I_{nj} d'_{nij}$; (4.33)

and similarly,

$$I_a(u,s) = -\frac{c\tilde{F}(s)}{60\Omega} \sum_{n=N_{s+1}}^{N} \sum_{i=2}^{M_n} \sum_{k=2}^{M_n} D_n'^{-1}(s-s_n)^{-1} I_{ni} I_{nk} g'_{ni}(s) P_{nk}(u). \tag{4.34}$$

The induced currents on both wires are thus computed according to equations (4.3). The numerical result for the special case of $L/a = 200$, $d/L = 0.5$, $\alpha = 0^{0}$ and the wire over ground plane (therefore only anti-symmetric modes are considered) with a step-function input at $u = 0.5L$ as a function of time is shown in Figure 4.14. This result is compared with the result shown in an existing paper [33]. Using equation (4.34) with $L/a = 200$, $d/L = 0$, $\alpha = 90^{0}$ without computing the contribution from coupled wire, we can determine the current at $u = 0.5L$ due to the step-function input applied to an isolated wire. This result is shown in Figure 4.15 and compared well with the result shown in [10]. The impulse responses of induced current at $u = 0.5L$ are shown in Figure 4.16 and Figure 4.17 for a parallel wire over ground plane and the isolated wire. It is easy to see that the early time of the current for an aspect angle φ is just one-way transit time, $T_t = L \cos \varphi/c$, the time for all the current segments to be "turned on". The aspect angle used in Figures 4.14 - 4.17 is 30^{0}, which gives us $T_t = \sqrt{\frac{3}{2}}\, L/c$ as the early-time in which "class-1" and "class-2" impulse responses are different as shown in Figure 4.17.

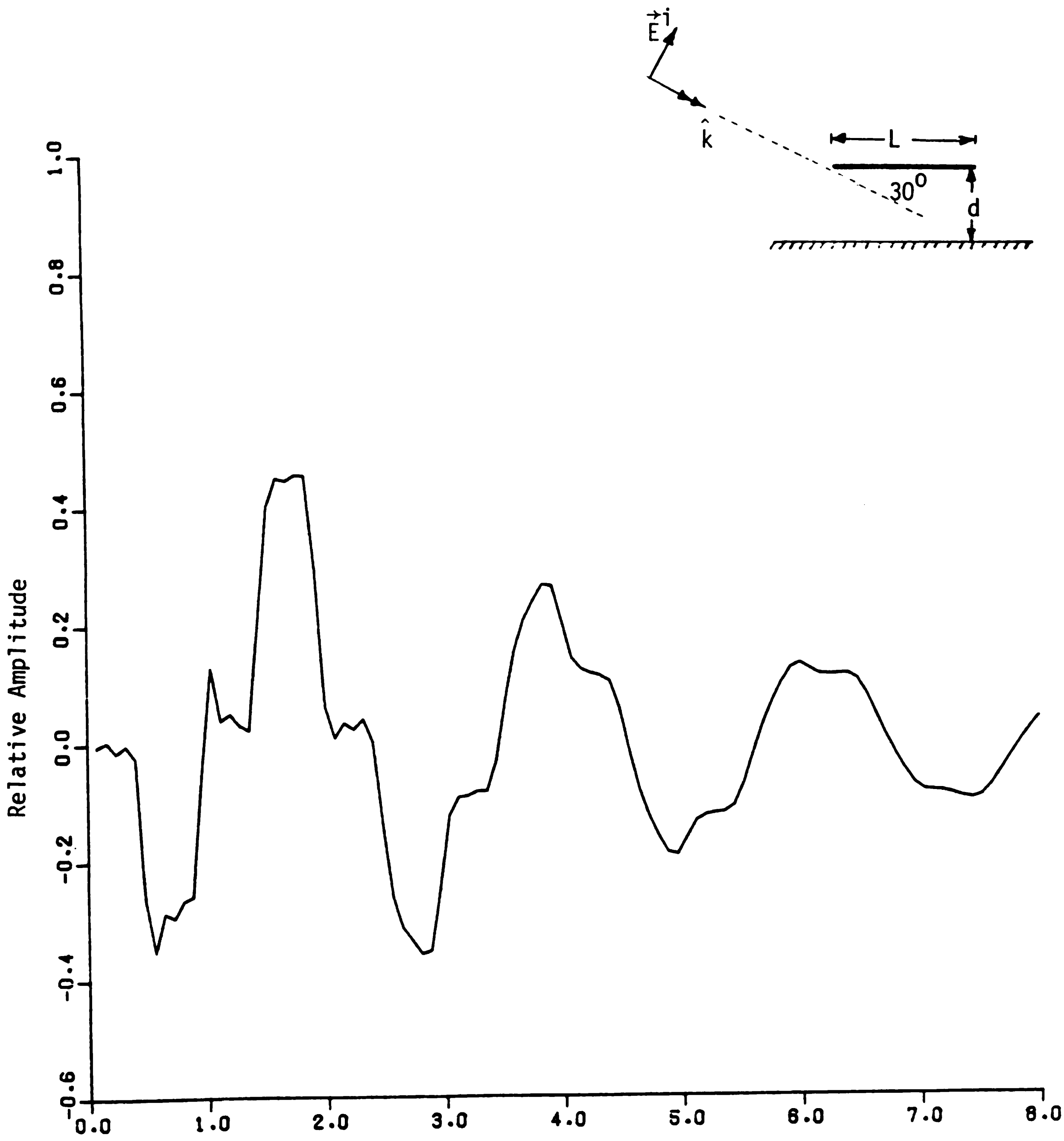

Figure 4.14. Step response of current at u = 0.5 L of a parallel wire over the ground plane with L/a = 200, d/L = 0.5 and aspect-angle 30^o.

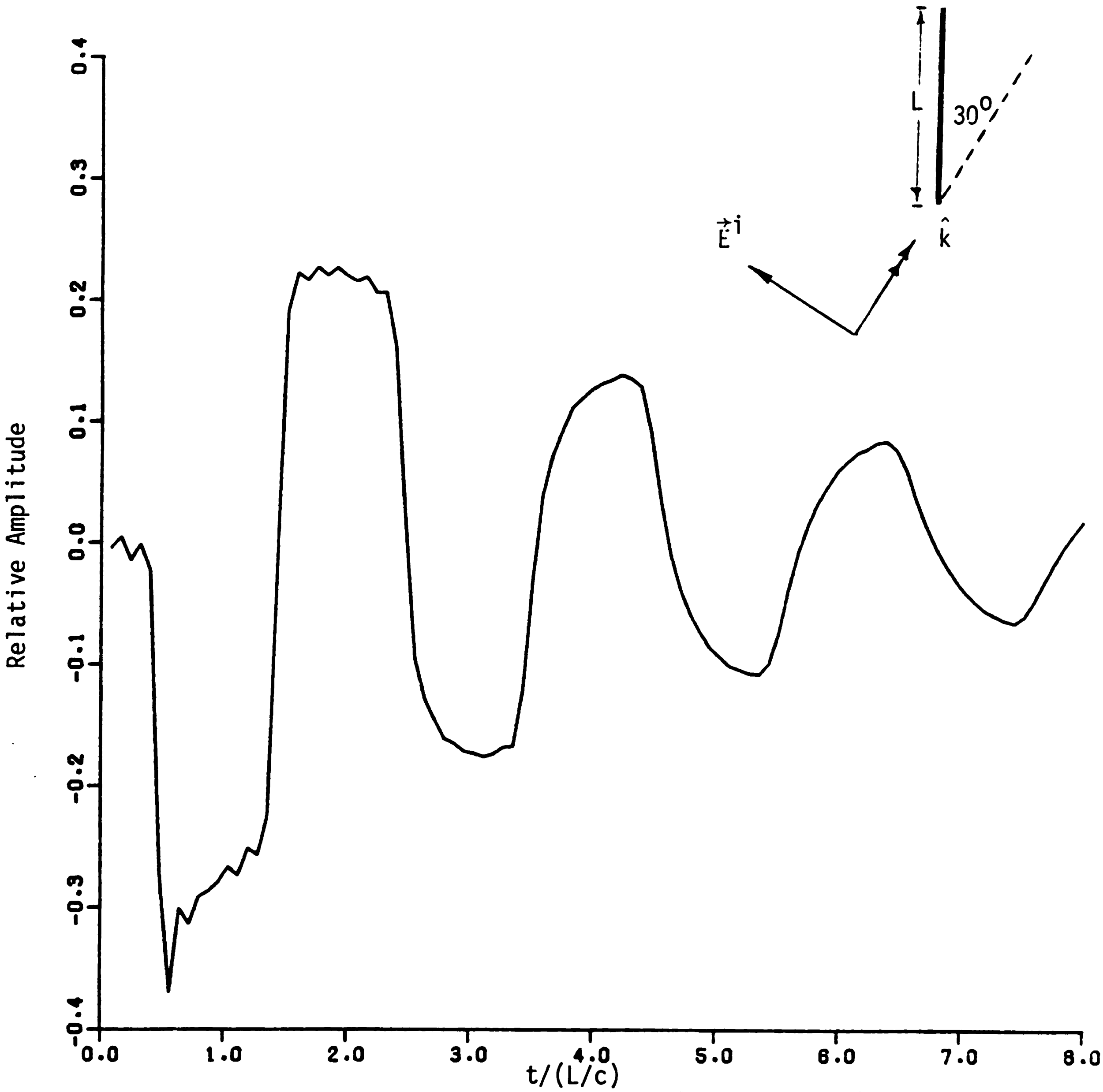

Figure 4.15. Step response of current at $u = 0.5_oL$ of an isolated wire with $L/a = 200$ and aspect-angle 30^o.

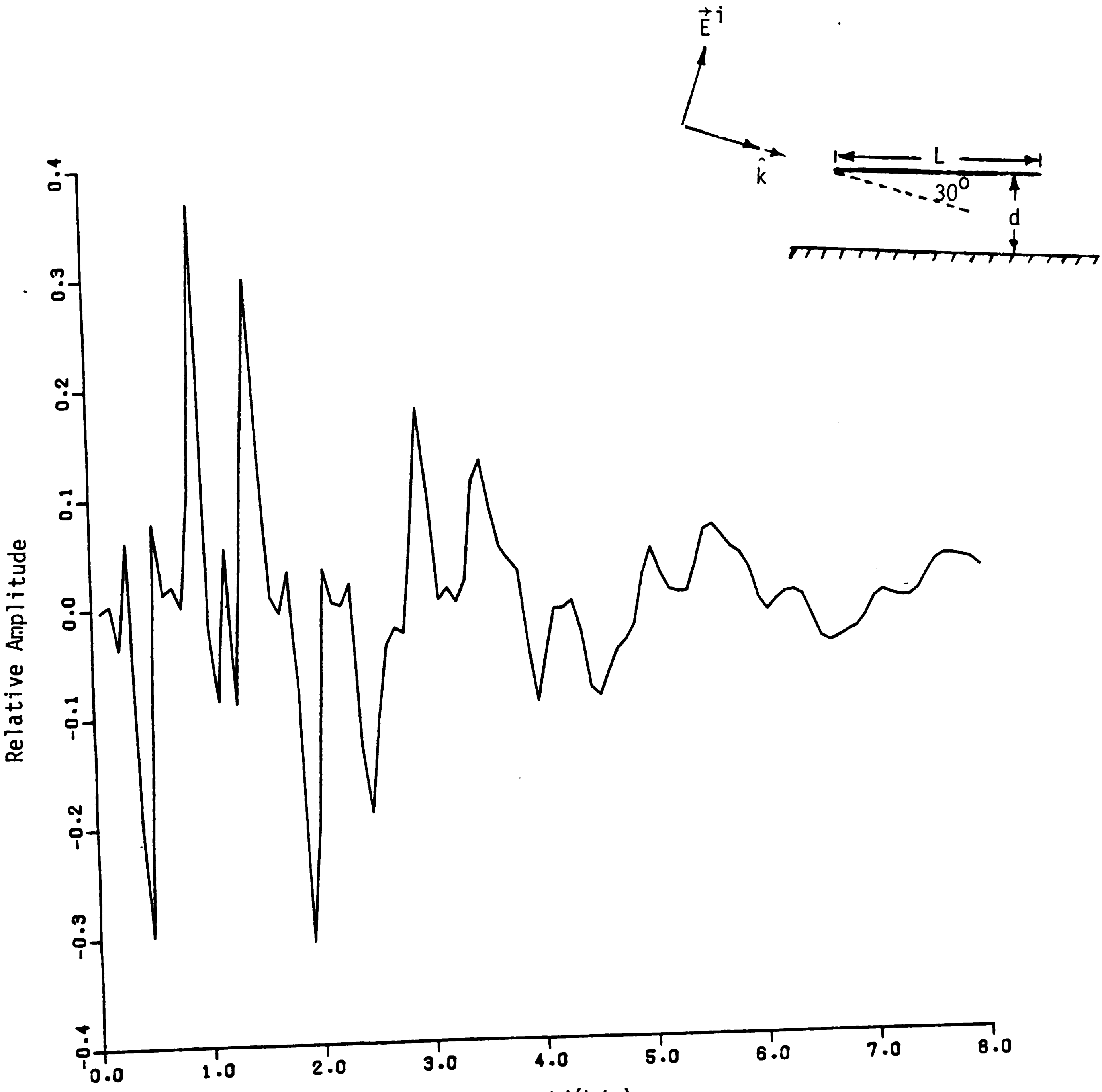

Figure 4.16. Impulse response of a parallel wire over the ground plane for current at $u = 0.5$ L with L/a = 200, d/L = 0.5 and aspect-angle 30^o.

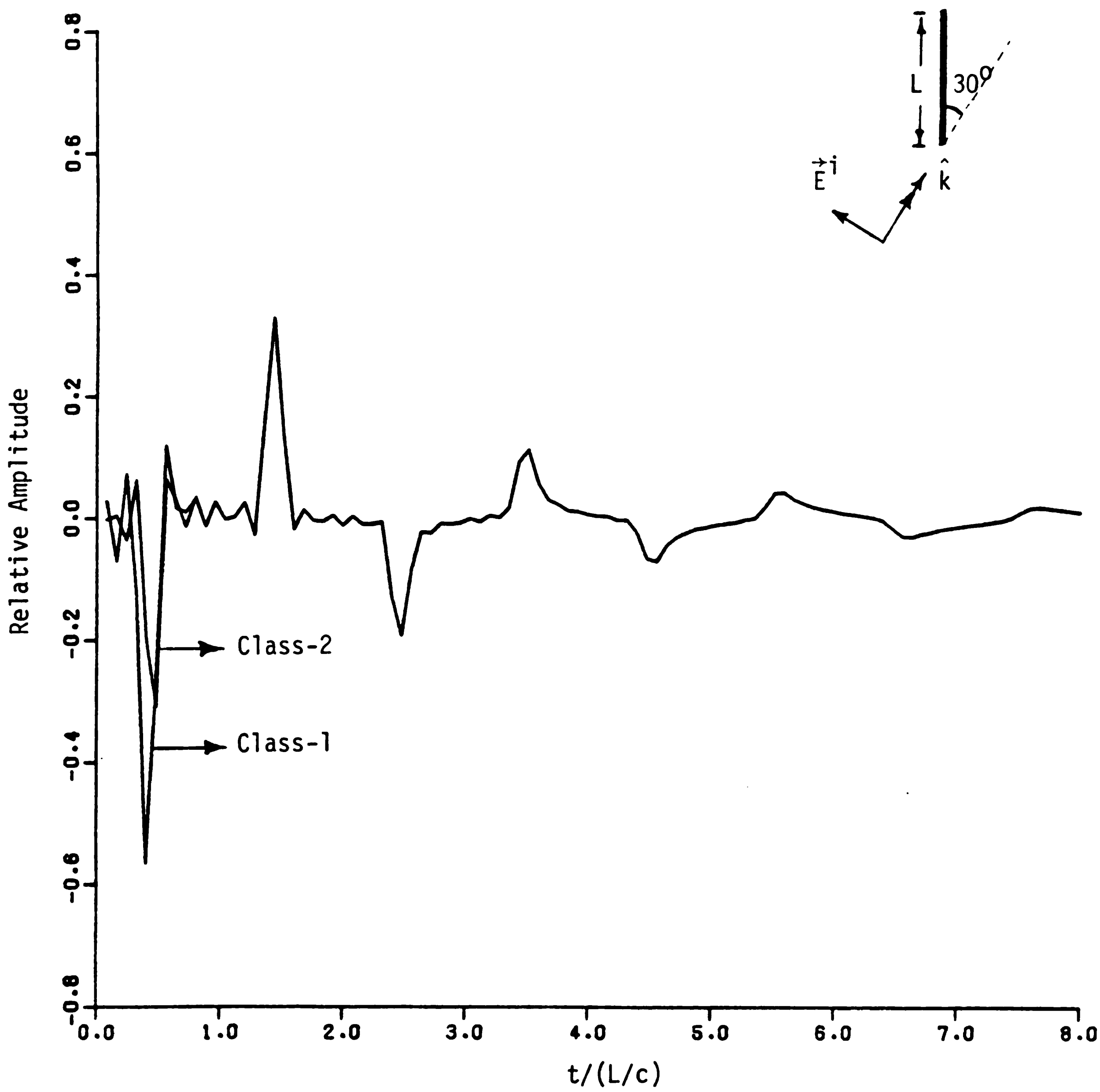

Figure 4.17. Impulse response of current at u = 0.5 L of an isolated wire with L/a = 200 and aspect-angle 30°, both class-1 and class-2 coupling coefficients are used.

4.4 Backscattered Field

The scattered electric field in the radiation-zone can be determined from the vector potentials maintained by induced currents on the two-wires. Consider first the scattered field maintained by the current on only one wire, as shown in Figure 4.18. It is easy to show that

$$\tilde{\vec{E}}^s(\vec{r},s) = \hat{\theta}\ s\ \tilde{A}^s(\vec{r},s)\sin\theta \tag{4.35}$$

where $$\tilde{A}^s = \frac{\mu_o}{4\pi}\ \frac{e^{-\gamma R_\infty}}{R_\infty} \int_o^L I(z',s)e^{\gamma z'\cos\theta}dz' . \tag{4.36}$$

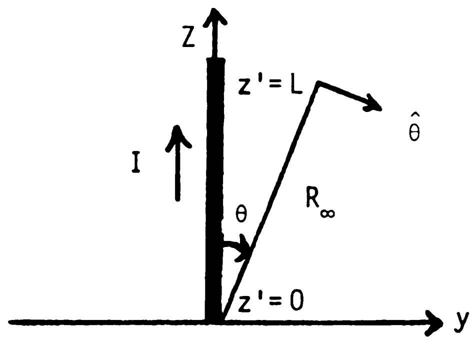

Figure 4.18. Geometry of equation (4.35) for radiation-zone field maintained by current in single wire.

R_∞ in (4.36) is the distance between the starting end of the wire and the observation point.

Using linear superposition, consider the current problem as shown in Figure 4.19, the scattered field can be expressed as

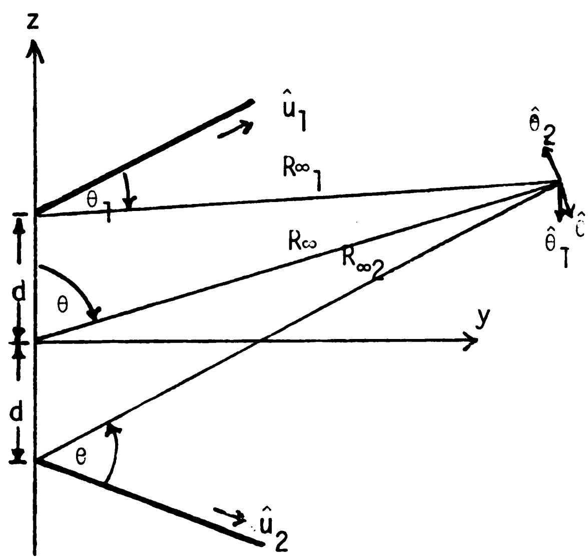

Figure 4.19. Geometry of Equation (4.37) for radiation-zone field maintained by currents in two wires.

$$\tilde{\vec{E}}^s(\vec{r},s) = \hat{\theta}_1\, s\tilde{A}_1^s \sin\theta_1 + \hat{\theta}_2\, s\tilde{A}_2^s \sin\theta_2 \tag{4.37}$$

where

$$\left.\begin{aligned} \tilde{A}_1^s &= \frac{\mu_o}{4\pi}\,\frac{e^{-\gamma R_{\infty 1}}}{R_{\infty 1}} \int_o^L I_1(u',s)\, e^{\gamma u' \cos\theta_1} du' \\ \tilde{A}_2^s &= \frac{\mu_o}{4\pi}\,\frac{e^{-\gamma R_{\infty 2}}}{R_{\infty 2}} \int_o^L I_2(u',s)\, e^{\gamma u' \cos\theta_2} du' \end{aligned}\right\}, \tag{4.38}$$

and

$$\begin{aligned} R_{\infty 1} &\approx R_\infty - d\cos\theta \\ R_{\infty 2} &\approx R_\infty + d\cos\theta\,. \end{aligned} \tag{4.39}$$

For radiation-zone backscattered electric field, $\hat{r}_1 \approx \hat{r}_2 \approx \hat{r} = -\hat{k}$, then

$$\left.\begin{aligned} \text{Cos}\ \theta &= [\hat{z}\cdot(-\hat{k})] = -k_z \\ \text{Cos}\ \theta_1 &= [\hat{u}_1\cdot(-\hat{k})] = -k_y\cos\alpha - k_z\sin\alpha \\ \text{Cos}\ \theta_2 &= [\hat{u}_2 - (-\hat{k})] = -k_y\cos\alpha + k_z\sin\alpha \end{aligned}\right\}. \tag{4.40}$$

Since in spherical coordinates $\hat{\theta}\sin\theta = (\hat{z}\times\hat{r})\times\hat{r}$, by the analogy of Figure 4.19 and the spherical coordinate, the following relations can easily be derived:

$$\hat{\theta}_1 \sin\theta_1 = [\hat{u}_1 \times (-\hat{k})]\times(-\hat{k}) = \hat{x}(k_xk_y\cos\alpha + k_zk_x\sin\alpha)$$

$$+\ \hat{y}(k_y^2\cos\alpha + k_yk_z\sin\alpha - \cos\alpha) + \hat{z}(k_yk_z\cos\alpha + k_z^2\sin\alpha - \sin\alpha)$$

$$\hat{\theta}_2 = [\hat{u}_2 \times(-\hat{k})]\times(-\hat{k})$$

$$= \hat{x}(k_xk_y\cos\alpha - k_zk_x\sin\alpha) + \hat{y}(k_y^2\cos\alpha - k_yk_z\sin\alpha - \cos\alpha)$$

$$+\ \hat{z}(k_yk_z\cos\alpha - k_z^2\sin\alpha + \sin\alpha)\,. \tag{4.41}$$

Substitution of Equations (4.39), (4.32) and (4.34) into Equation (4.38) leads to

$$\tilde{A}_1^s = \frac{\mu_o}{4\pi}\ \frac{e^{-\gamma R\infty+\gamma d\cos\theta}}{R\infty}\ \{-\ \frac{c\tilde{F}(s)}{60\Omega}\ \sum_{n=1}^{N}\sum_{i=2}^{M_n}\sum_{k=2}^{M_n} D_n'^{-1}(s-s_n)^{-1} I_{ni} I_{nk} g_{ni}'(s)$$

$$\int_{(k-\frac{3}{2})\Delta_n}^{(k-\frac{1}{2})\Delta_n} P_{nk}(u')\, e^{\gamma u'\cos\theta_1}\, du'\}$$

$$= -\ \frac{c\mu_o\tilde{F}(s)}{120\pi\Omega}\ \ \frac{1}{\gamma\text{Cos}\theta_1}\ \ \frac{e^{-\gamma R\infty+\gamma d\cos\theta}}{R\infty}\{\sum_{n=1}^{N}\sum_{i=2}^{M_n}\sum_{k=2}^{M_n} D_n'^{-1}(s-s_n)^{-1} I_{ni} I_{nk} g_{ni}'(s)$$

$$e^{\gamma u_{nk}\cos\theta_1}\ \sinh\left(\frac{\gamma\Delta_n\cos\theta_1}{2}\right)$$

$$= -\ \frac{\tilde{F}(s)}{\gamma\cos\theta_1}\ \ \frac{e^{-\gamma R\infty+\gamma d\cos\theta}}{R\infty}\ \sum_{n=1}^{N}\sum_{i=2}^{M_n}\sum_{k=2}^{M_n}\frac{I_{ni} I_{nk} g_{ni}'(s)}{D_n'(s-s_n)}\ e^{\gamma u_{nk}\cos\theta_1}\sin\left(\frac{\gamma\Delta_n\cos\theta_1}{2}\right); \tag{4.42}$$

similarly,

$$\tilde{A}_2^s = - \frac{\tilde{F}(s)}{\gamma\cos\theta_2} \frac{e^{-\gamma R\infty - \gamma d\cos\theta}}{R\infty} \left(\sum_{n=1}^{N_s} - \sum_{n=Ns+1}^{N} \right) \sum_{i=2}^{M_n} \sum_{k=2}^{M_n} \frac{I_{ni} I_{nk} g'_{ni}(s)}{D'_n(s-s_n)} e^{\gamma u_{nk}\cos\theta_2} \sinh\left(\frac{\gamma\Delta_n\cos\theta_2}{2}\right). \quad (4.43)$$

Substituting (4.42) and (4.43) into (4.37), we obtain the expression for $\tilde{\vec{E}}^{bs}(\vec{r},s)$ as

$$\tilde{\vec{E}}^{bs}(\vec{r},s) = -c\tilde{F}(s) \frac{e^{-\gamma R\infty}}{R\infty} \{\hat{\theta}_1 \tan\theta_1 e^{\gamma d\cos\theta} \sum_{n=1}^{N} \sum_{i=2}^{M_n} \sum_{k=2}^{M_n} [\frac{I_{ni} I_{nk} g'_{ni}(s)}{D'_n(s-s_n)}$$

$$e^{\gamma u_{nk}\cos\theta_1} \sinh(\frac{\gamma\Delta_n\cos\theta_1}{2})] + \hat{\theta}_2 \tan\theta_2 e^{-\gamma d\cos\theta} \left(\sum_{n=1}^{N_s} - \sum_{n=N_s+1}^{N} \right) \sum_{i=2}^{N_n} \sum_{k=2}^{N_n}$$

$$[\frac{I_{ni} I_{nk} g'_{ni}(s)}{D'_n(s-s_n)} e^{\gamma u_{nk}\cos\theta_2} \sinh(\frac{\gamma\Delta_n\cos\theta_2}{2})]\}. \quad (4.44)$$

Notice that $\left(\sum_{n=1}^{N_s} - \sum_{n=N_s+1}^{N} \right)$ in the latter part of Equation (4.44) takes care of symmetric and antisymmetric contributions in wire #2. It is easy to see that all the parameters in Equation (4.44) have been defined.

4.5 Impulse Response

To determine the impulse response, let's specify $\hat{k}$ and $\hat{\zeta}$ in terms of aspect-angel φ. It is easy to show from Figure 4.1 that

$$\left.\begin{aligned} \zeta_x &= o \\ \zeta_y &= \sin\varphi \\ \zeta_z &= \cos\varphi \end{aligned}\right\} \quad (4.45)$$

and

$$\left.\begin{aligned} k_x &= o \\ k_y &= \cos\varphi \\ k_z &= -\sin\varphi . \end{aligned}\right\} \tag{4.46}$$

Substitute the above two set of equations into Equation (4.26), we get

$$\begin{aligned} g'_{ni}(s) &= 2\tan(\varphi+\alpha)\sinh\left[\gamma\cos(\varphi+\alpha)\frac{\Delta_n}{2}\right]e^{-\gamma[u_{ni}\cos(\varphi+\alpha)-d\sin\varphi]} \\ &\pm 2\tan(\varphi-\alpha)\sinh\left[\gamma\cos(\varphi-\alpha)\frac{\Delta_n}{2}\right]e^{-\gamma[u_{ni}\cos(\varphi-\alpha)+d\sin\varphi]} \end{aligned} \tag{4.47}$$

Substitutions of (4.45) and (4.46) into (4.40) and (4.41) provide

$$\left.\begin{aligned} \hat{\theta}_1\sin\theta_1 &= -\hat{\zeta}\sin(\varphi+\alpha) \\ \hat{\theta}_2\sin\theta_2 &= -\hat{\zeta}\sin(\varphi-\alpha) \\ \mathrm{Cos}\,\theta_1 &= -\cos(\varphi+\alpha) \\ \mathrm{Cos}\,\theta_2 &= -\cos(\varphi-\alpha) \\ \mathrm{Cos}\,\theta &= \sin\varphi , \end{aligned}\right. \tag{4.48}$$

Equations (4.47) and (4.48) together with Equation (4.44) lead to

$$\begin{aligned} \tilde{\vec{E}}^{bs}(\vec{r},s) &= c\tilde{F}(s)\frac{e^{-\gamma R_\infty}}{R_\infty}\hat{\zeta}\{\tan(\varphi+\alpha)e^{\gamma d\sin\varphi}\sum_{n=1}^{N}\sum_{i=2}^{M_n}\sum_{k=2}^{M_n}\frac{I_{ni}I_{nk}g'_{ni}(s)}{D'_n(s-s_n)}e^{-\gamma u_{nk}\cos(\varphi+\alpha)} \\ &\sinh\left(\frac{\gamma\Delta_n\cos(\varphi+\alpha)}{2}\right)+\tan(\varphi-\alpha)e^{-\gamma d\sin\varphi}\left(\sum_{n=1}^{N_s}-\sum_{n=Ns+1}^{N}\right)\sum_{i=2}^{M_n}\sum_{k=2}^{M_n}\frac{I_{ni}I_{nk}g'_{ni}(s)}{D'_n(s-s_n)} \\ &e^{-\gamma u_{nk}\cos(\varphi-\alpha)}\sinh\left(\frac{\gamma\Delta_n\cos(\varphi-\alpha)}{2}\right)\} \\ &= \hat{\zeta}\,K'\tilde{F}(s)\frac{e^{-\gamma R_\infty}}{R_\infty}\,H'(s) \end{aligned} \tag{4.49}$$

where $$K' = 2c\,, \tag{4.50}$$

and

$$H'(s) = \tan^2(\varphi+\alpha)e^{2\gamma d}\sin\varphi \sum_{n=1}^{N}\sum_{i=2}^{M_n}\sum_{k=2}^{M_n}\frac{I_{ni}I_{nk}}{D_n'(s-s_n)}\,e^{-\gamma(u_{ni}+u_{nk})\cos(\varphi+\alpha)}\sinh^2\left[\frac{\gamma\Delta_n\cos(\varphi+\alpha)}{2}\right]$$
$$+\tan(\varphi+\alpha)\tan(\varphi-\alpha)\left(\sum_{n=1}^{N_s}-\sum_{n=N_s+1}^{N}\right)\sum_{i=2}^{M_n}\sum_{k=2}^{M_n}\frac{I_{ni}I_{nk}}{D_n'(s-s_n)}\{e^{-\gamma[u_{ni}\cos(\varphi+\alpha)+u_{nk}\cos(\varphi-\alpha)]}$$
$$+e^{-\gamma[u_{ni}\cos(\varphi-\alpha)+u_{nk}\cos(\varphi+\alpha)]}\}\sinh\left[\frac{\gamma\Delta_n\cos(\varphi+\alpha)}{2}\right]\sinh\left[\frac{\gamma\Delta_n\cos(\varphi-\alpha)}{2}\right]$$
$$+\tan^2(\varphi-\alpha)e^{-2\gamma d}\sin\varphi \sum_{n=1}^{N}\sum_{i=2}^{M_n}\sum_{k=2}^{M_n}\frac{I_{ni}I_{nk}}{D_n'(s-s_n)}e^{-\gamma(u_{ni}+u_{nk})\cos(\varphi-\alpha)}\sinh^2\left[\frac{\gamma\Delta_n\cos(\varphi-\alpha)}{2}\right]. \tag{4.51}$$

For experiments, as will be discussed in Chapter 6, $\varphi = 0^o$,

$$H'(s) = 4\tan^2\alpha \sum_{n=N_s+1}^{N}\sum_{i=2}^{M_n}\sum_{k=2}^{M_n}\frac{I_{ni}I_{nk}}{D_n'(s-s_n)}e^{-\gamma(u_{ni}+u_{nk})\cos\alpha}\sinh^2\left(\frac{\gamma\Delta_n\cos\alpha}{2}\right)$$
$$= \tan^2\alpha \sum_{n=N_s+1}^{N}\sum_{i=2}^{M_n}\sum_{k=2}^{M_n}\frac{I_{ni}I_{nk}}{D_n'(s-s_n)}e^{-\gamma(u_{ni}+u_{nk})\cos\alpha}\left[e^{\gamma\Delta_n\cos\alpha}-2+e^{-\gamma\Delta_n\cos\alpha}\right] \tag{4.52}$$

Notice that in computing $\tilde{\vec{E}}^{bs}(\vec{r},s)$, we should also add the complex-conjugate of (4.51) and finally

$$\tilde{\vec{E}}^{bs}(\vec{r},t) = \hat{\zeta}\ K\,\frac{e^{-\gamma R_\infty}}{R_\infty}\,F(t)*h(t) \tag{4.53}$$

where $$K = 2K'\tan^2\alpha = 4c\tan^2\alpha \tag{4.54}$$

and $h(t)$ = impulse response

$$= L^{-1}\left\{\frac{\mathrm{Re}H'(s)}{\tan^2\alpha}\right\}$$

$$= \mathrm{Re}\left\{\sum_{n=N_s+1}^{N}\sum_{i=2}^{M_n}\sum_{k=2}^{M_n}\frac{I_{ni}I_{nk}}{D'_n}\left[e^{s_n(t-\tau_1(n,i,k))}u[t-\tau_1(n,i,k)]\right.\right.$$

$$\left.\left.+ e^{s_n[t-\tau_2(n,i,k)]}u[t-\tau_2(n,i,k)]-2\,e^{s_n[t-\tau_3(n,i,k)]}u[t-\tau_3(n,i,k)]\right]\right\} \tag{4.55}$$

$$\left.\begin{aligned} \text{with}\quad \tau_1(n,i,k) &= (u_{ni}+u_{nk}-\Delta_n)\cos\alpha\ /c = \frac{i+k-3}{M_n}L\cos\alpha/c = \frac{i+k-3}{M_n}T_t \\ \tau_2(n,i,k) &= (u_{ni}+u_{nk}+\Delta_n)\cos\alpha\ /c = \frac{i+k-1}{M_n}L\cos\alpha/c = \frac{i+k-1}{M_n}T_t \\ \tau_3(n,i,k) &= (u_{ni}+u_{nk})\cos\alpha/c = \frac{i+k-2}{M_n}L\cos\alpha/c = \frac{i+k-2}{M_n}T_t\,. \end{aligned}\right\} \tag{4.56}$$

It is obvious from (4.55) and (4.56) that the late-time for the impulse response begins at $t = 2T_t = 2\,\frac{L\cos\alpha}{c}$ when all the unit step functions are turned on.

The impulse response of two parallel wires $(\alpha = 0^o)$ and $\varphi \neq 0^o$ is similar to Equation (4.55) with α replaced by φ and time-delay factor, $\pm 2\gamma d \sin\varphi$, included to account for different "turn-on" times for two wires, the late-time response is thus begins at $t = 2T_t = 2[L\cos\varphi/c + 2d\sin\varphi/c]$.

The numerical results of $h(t)$ are shown in Figure 4.20 - Figure 4.22 for $\alpha = 30^o$, 60^o and 90^o respectively with $\varphi = 0^o$, and in Figure 4.23 - Figure 4.24 for $\alpha = 0^o, \varphi = 30^o$ and 60^o respectively. Also shown in Figure 4.23 - Figure 4.24 are the special cases for the wire over ground plane and the isolated wire, which are compared well with results computed by using sinusoidal modal currents [13]. The comparison of the computed impulse responses with the experimental results will be

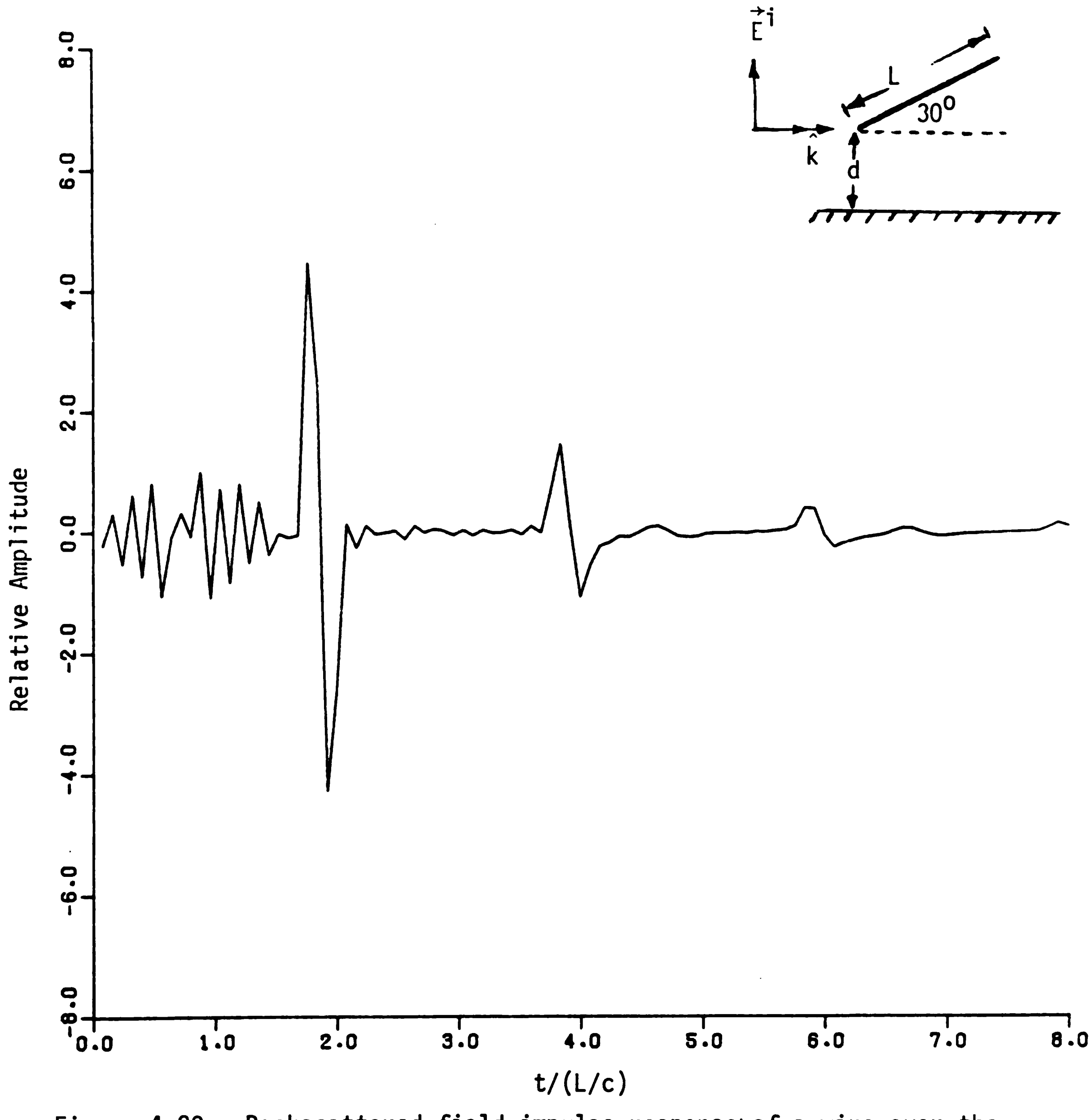

Figure 4.20. Backscattered-field impulse response of a wire over the ground plane with $L/a = 200$, $d/L = 0.5$, $\alpha = 30^o$ and aspect-angle 0^o.

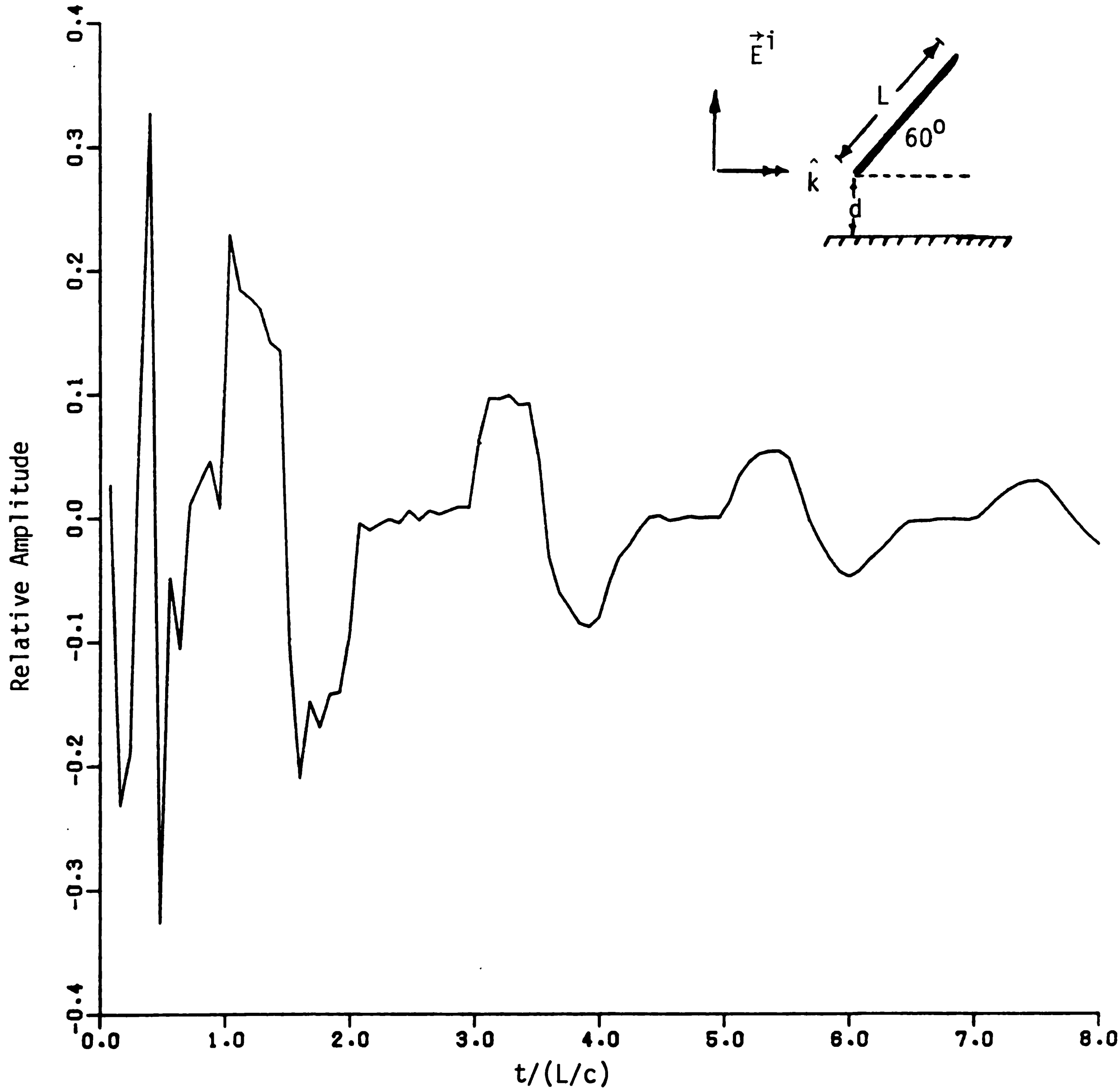

Figure 4.21. Backscattered-field impulse response of a wire over the ground plane with $L/a = 200$, $d/L = 0.5$, $\alpha = 60^\circ$ and aspect-angle 0°.

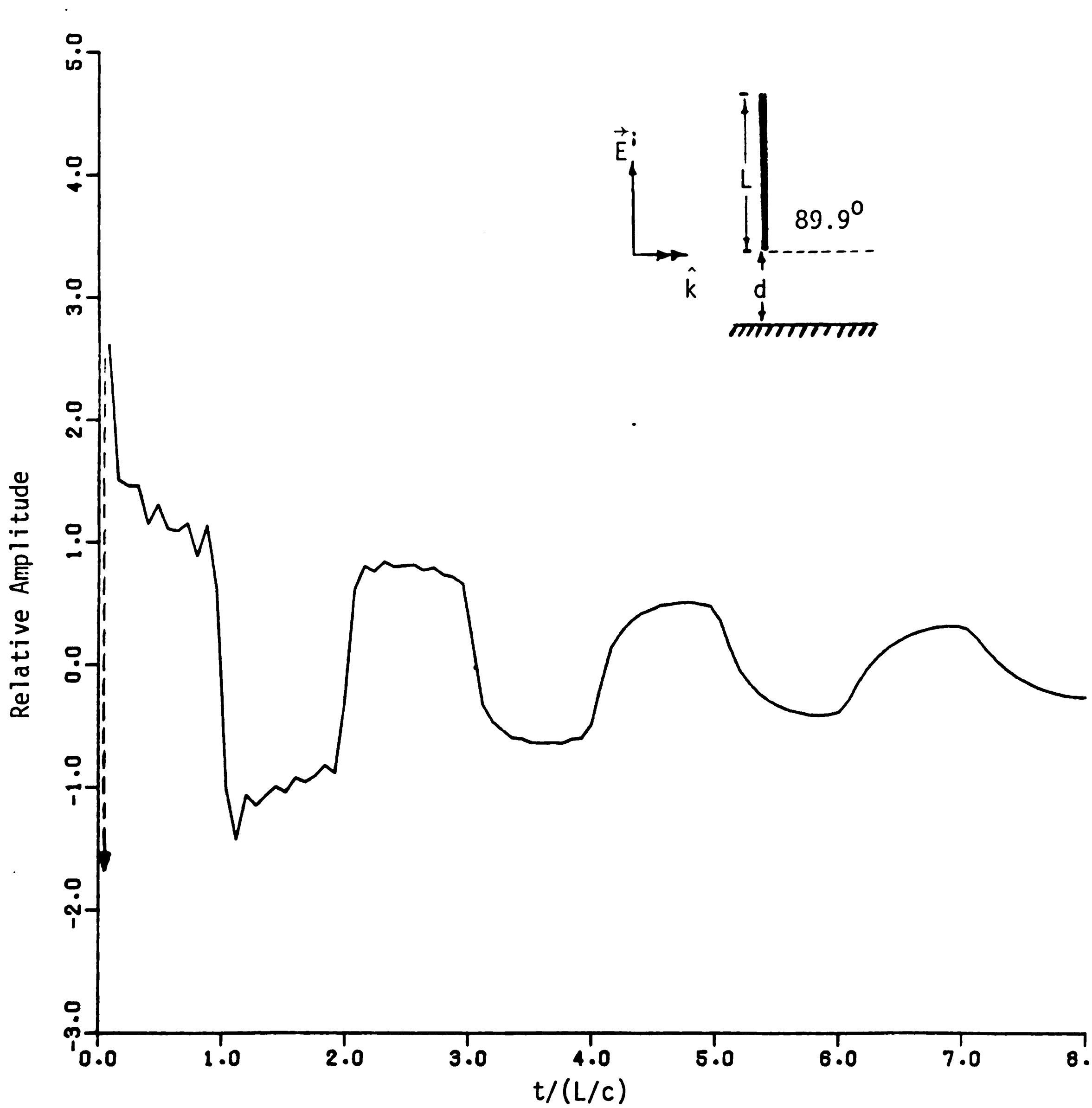

Figure 4.22. Backscattered-field impulse response of a wire over the ground plane with $L/a = 200$, $d/L = 0.5$, $\alpha = 89.9^o$ and aspect-angle 0^o. The dashed line at $t = 0$ shows the specular-reflection response for the normal incidence situation when $\alpha \to 90^o$ is considered.

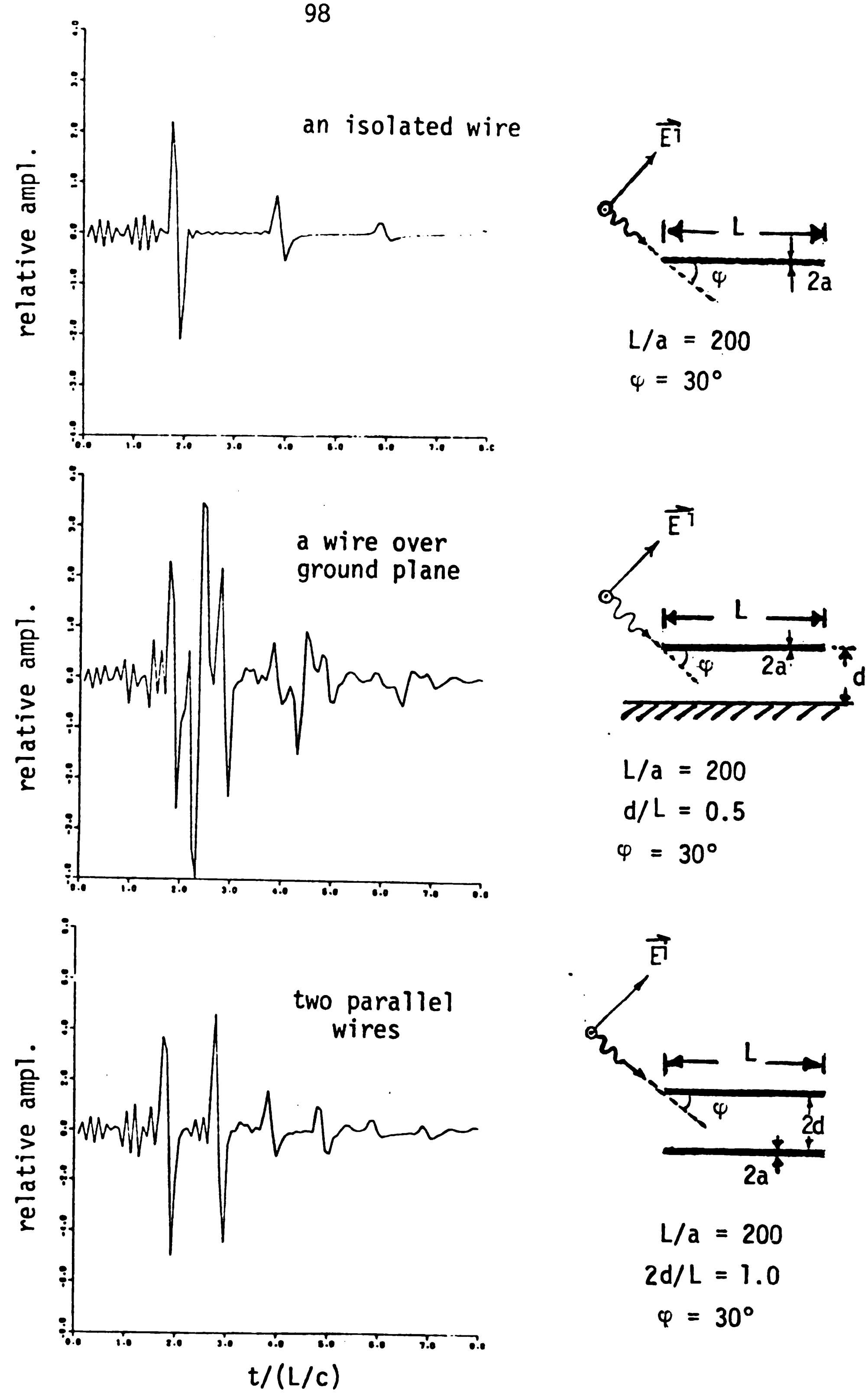

Figure 4.23. Impulse responses of an isolated wire, a wire over the ground plane and two parallel wires with an aspect angle of 30°.

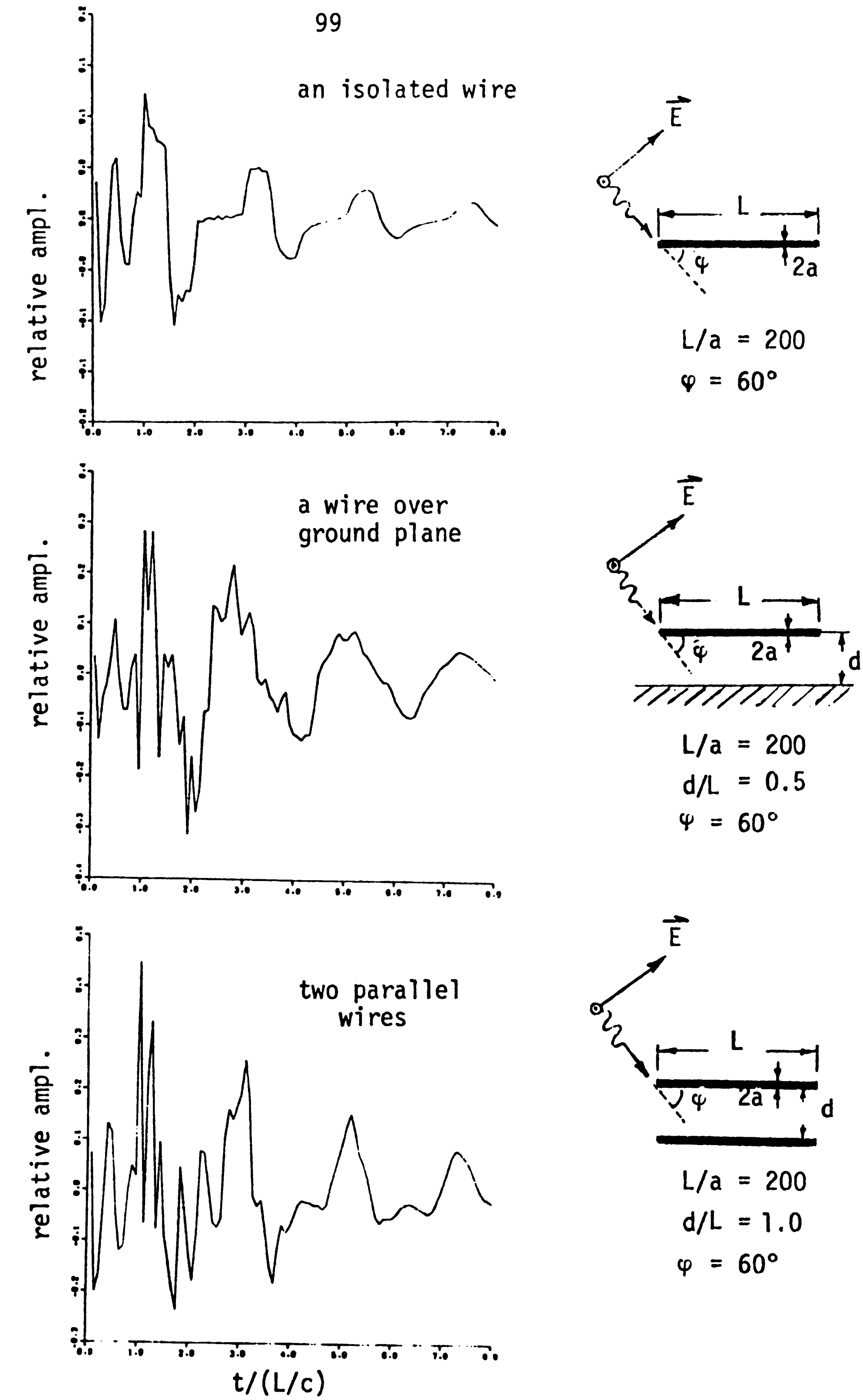

Figure 4.24. Impulse responses of an isolated wire, a wire over the ground plane and two parallel wires with an aspects angle of 60°.

shown in Chapter 6. Figure 4.25 indicates the difference between "class-1" and "class-2" responses for $\alpha = 0^{o}$ and $\varphi = 30^{o}$, it is clear that they differ from each other only in the early-time period.

4.6 Numerical Results for Incident-Waveform Synthesis and Target Discrimination.

Incident waveforms required to excit monomode backscatters consisting of purely the first and the second natural modes of the skew-coupled wires target are synthesized according to the procedure described in Chapter 2. The finite duration of the incident waveform is chosen based on the experience with thin-cylinder targets [13], as one (normalized) period of the first natural mode; this choice leads to, e.g., $Te = 1/f_1 = \frac{2\pi}{0.8888\pi c/L} = 2.2502(L/c)$ for the coupled wire over the ground plane with $\alpha = 0^{o}$, $d/L = 0.5$, $a/L = 0.005$. The late-time response, upon which the synthesis procedure was based, occurs during $t \geq T_e + 2T_t$ where $T_t = \frac{L\cos\varphi}{c} + \frac{2d\sin\varphi}{c}$ = one-way transit time for the incident waveform to sweep across the whole target in this particular case. Therefore, the late-time response begins at $t = 2(\cos 30^{o} + 2x0.5x\sin 30^{o})\, L/c + 2.2502\, L/c = 4.9822\, L/c$ for $\varphi = 30^{o}$ and begins also at $t = 2(\cos 60^{o} + 2x0.5\sin 60^{o})\, L/c + 2.2502\, L/c = 4.9822\, L/c$ for $\varphi = 60^{o}$; on the other hand $T_e = \frac{2\pi}{0.9201\pi c/L} = 2.1737(L/c)$ for case with $\alpha = 30^{o}$, $d/L = 0.5$, $a/L = 0.005$ and $T_t = \frac{L\cos\alpha}{c}$ for $\varphi = 0^{o}$. Therefore, the late-time response begins at $t = T_e + 2T_t = (2.1737 + 2x\cos 30^{o})\frac{L}{c} = 3.9057\,(\frac{L}{c})$ for this particular case upon which we have performed one of the experiments.

The incident signal required during $0 \leq t \leq 2.2502\,(\frac{L}{c})$ to excite a pure first-mode $[s_1 = (-0.0734 + j0.8888)\frac{\pi c}{L}]$ response is indicated

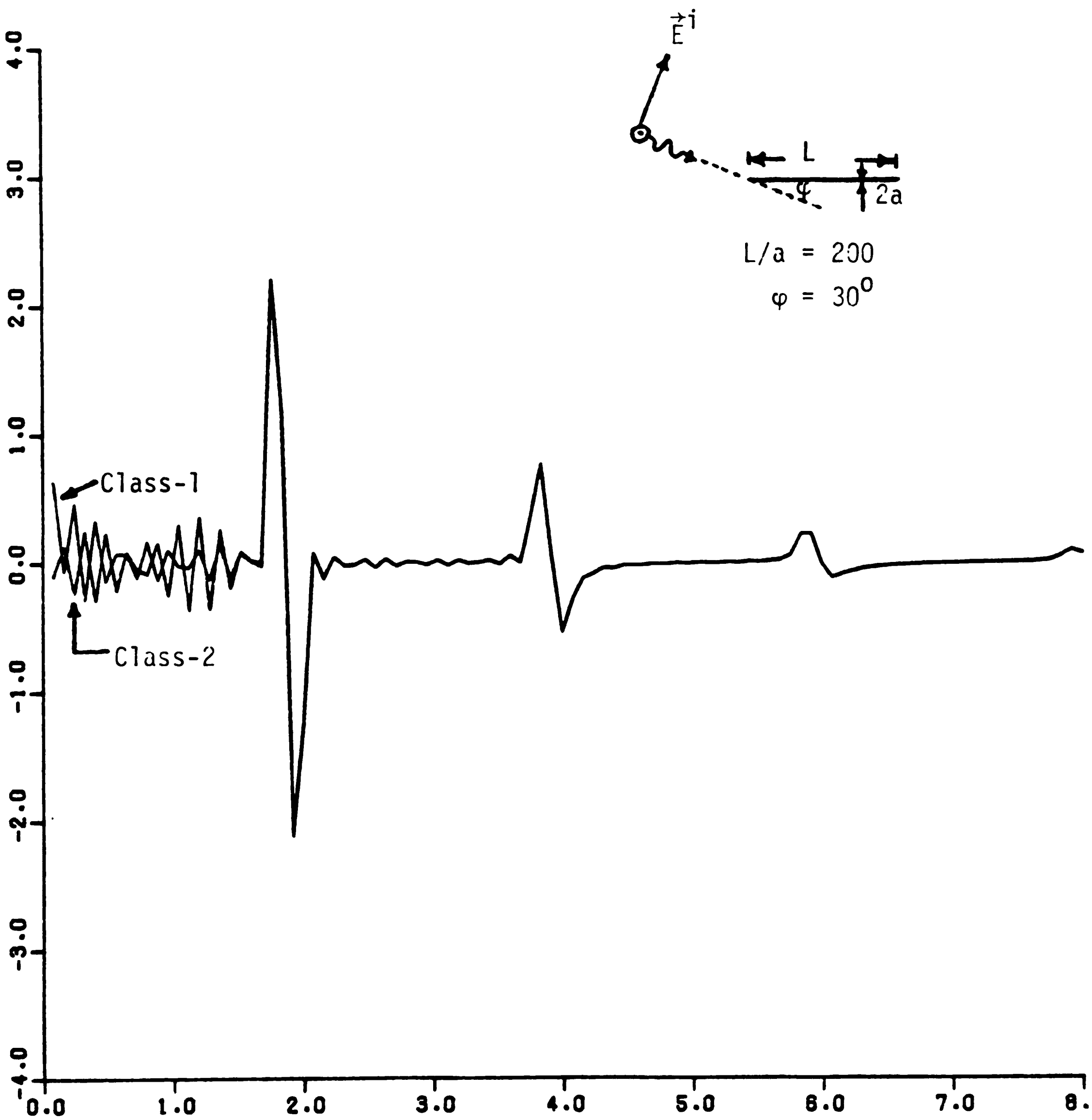

Figure 4.25: Impulse responses of an isolated wire with L/a = 200 and aspect-angle 30^0 computed by using "class-1 and "class-2" coupling coefficients.

in Figure 4.26. The return signal for aspect-angle $\varphi = 30^{o}$, which is obtained by convolving the synthesized waveform with the impulse reponse in Figure 4.23, is shown in Figure 4.28 along with the return signal from a target consisting of a parallel wire over the ground plane with 10% shorter length. It is seen that before the late-time response begins, i.e., $t \leq 4.9822$ L/c, the return signal exhibits an irregular waveform while for $t \geq 4.9822$ L/c the return signal indeed demonstrates the monomode behavior. The return signal from the shorter target can not be identified as a single natural mode of this target and it can therefore be discriminated from the preselected "right" target. Figure 4.29 shows only the late-time response part for better discrimination. The required signal to excite the second-mode [$s_2 = (-0.1691 + j\ 1.9248)\pi c/L$] backscattered field is shown in Figure 4.27. The return signals of aspect-angle $\varphi = 30^{o}$ for the right target and the wrong target with 10% shorter length are indicated in Figure 4.30. It is noted that the higher order mode displays a better target-discrimination ability. Figures 4.31 - 4.32 demonstrate the return signals of aspect-angle $\varphi = 60^{o}$, which is obtained by convolving required synthesized waveforms with the impulse response in Figure 4.24, for the right target and the wrong target with 20% longer length; Figure 4.31 is for the first-mode excitation while Figure 4.32 is for the second mode excitation. It is found that the target-discrimination ability is excellent in this case. For a skew-coupled wire over the ground plane with $\alpha = 30^{o}$, d/L = 0.5, a/L = 0.005, the incident signal during $0 \leq t \leq 2.1737$ (L/c) to excite a pure first-mode [$s_1 = (-0.1156 + j\ 0.9201)\pi c/L$] response is indicated in Figure 4.26 while that for the

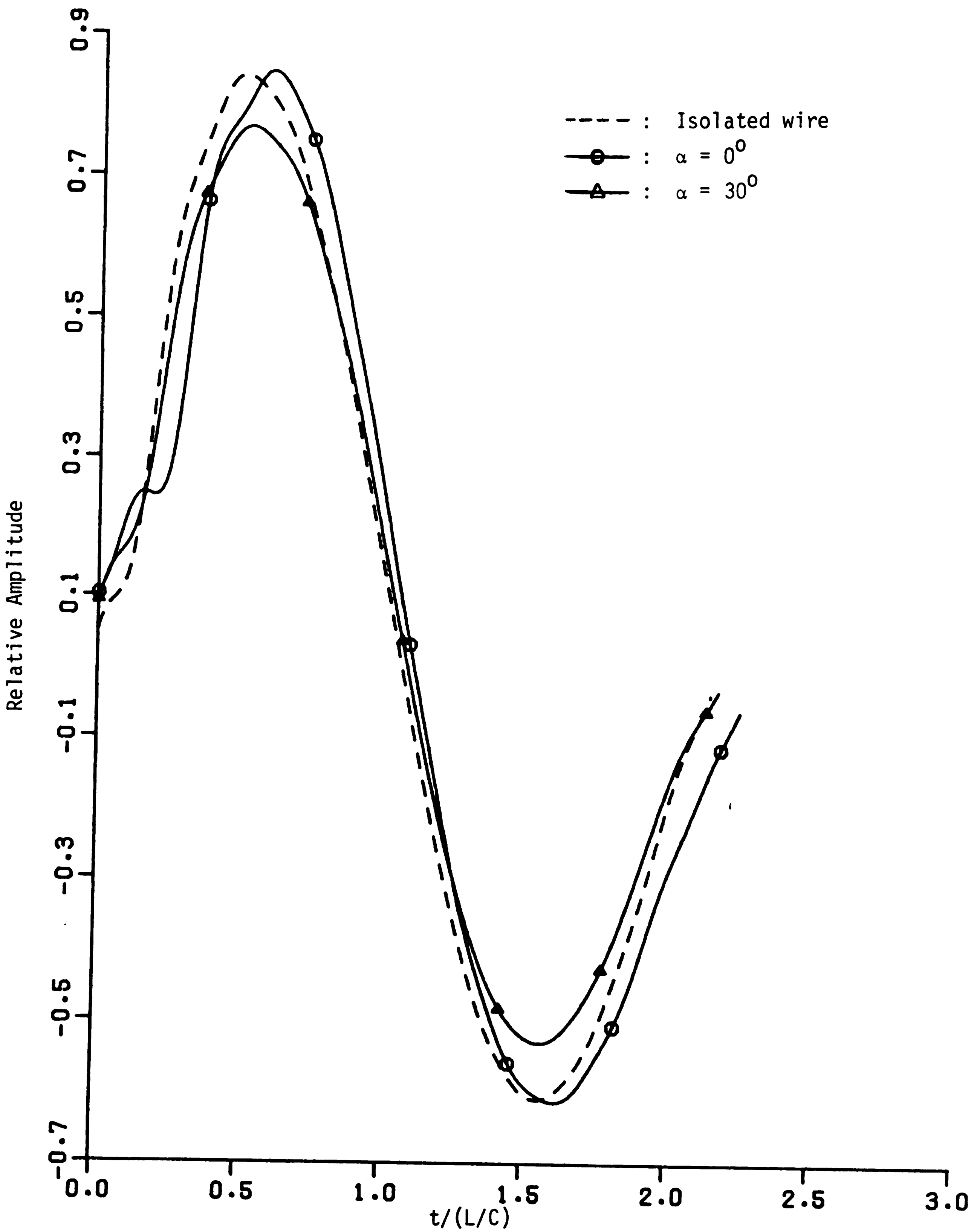

Figure 4.26. Required waveforms for the incident radar signals to excite the first mode from the wire over the ground plane with $a/L = 1/200$, $d/L = 0.5$ and for $\alpha = 0^{0}$ and 30^{0}. The required waveform for the isolated wire is also shown for comparison.

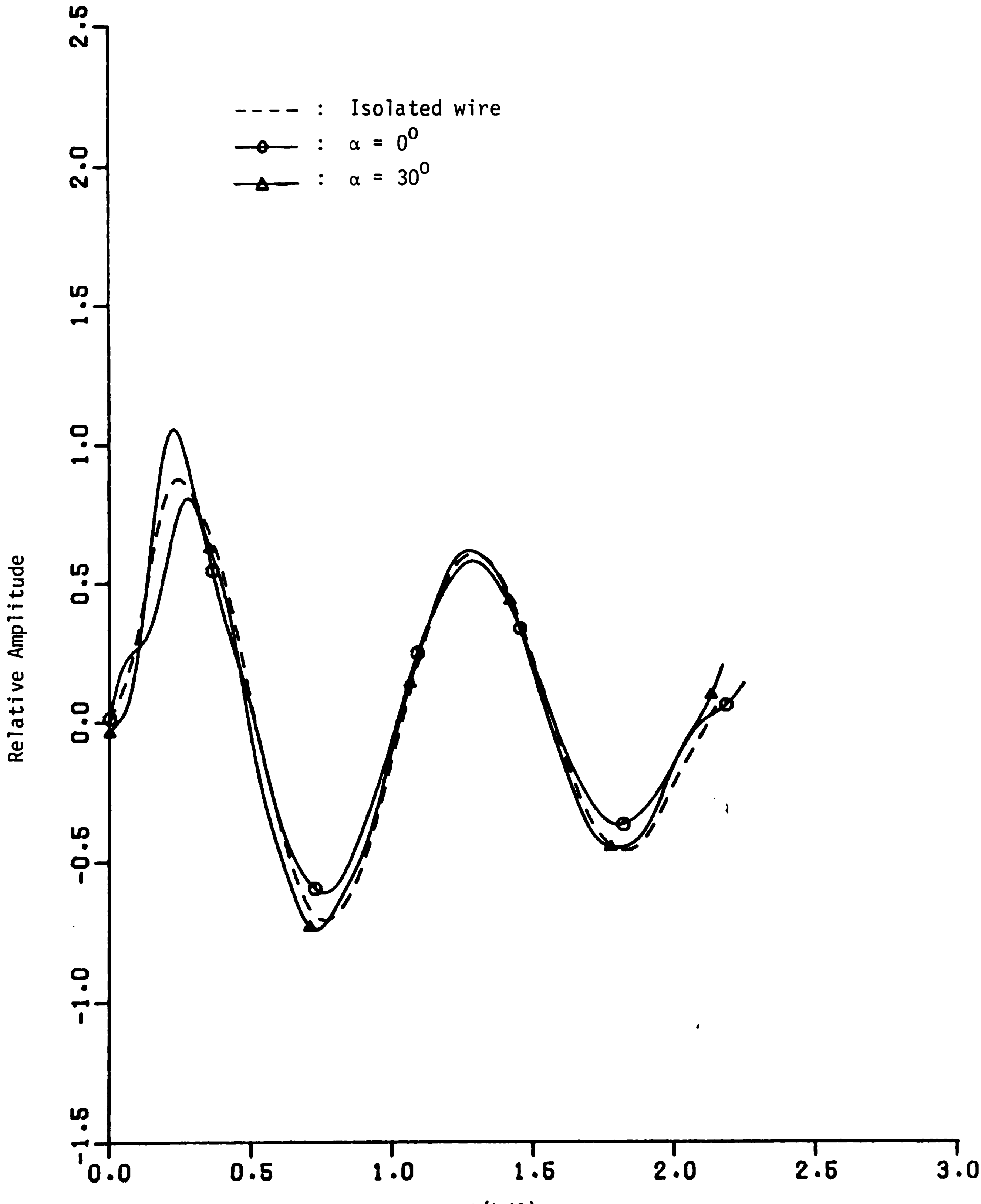

Figure 4.27. Required waveforms for the incident radar signals to excite the second mode from the wire over the ground plane with $a/L = 1/200$, $d/L = 0.5$ and for $\alpha = 0^{\circ}$ and 30°. The required waveform for the isolated wire is also shown for comparison.

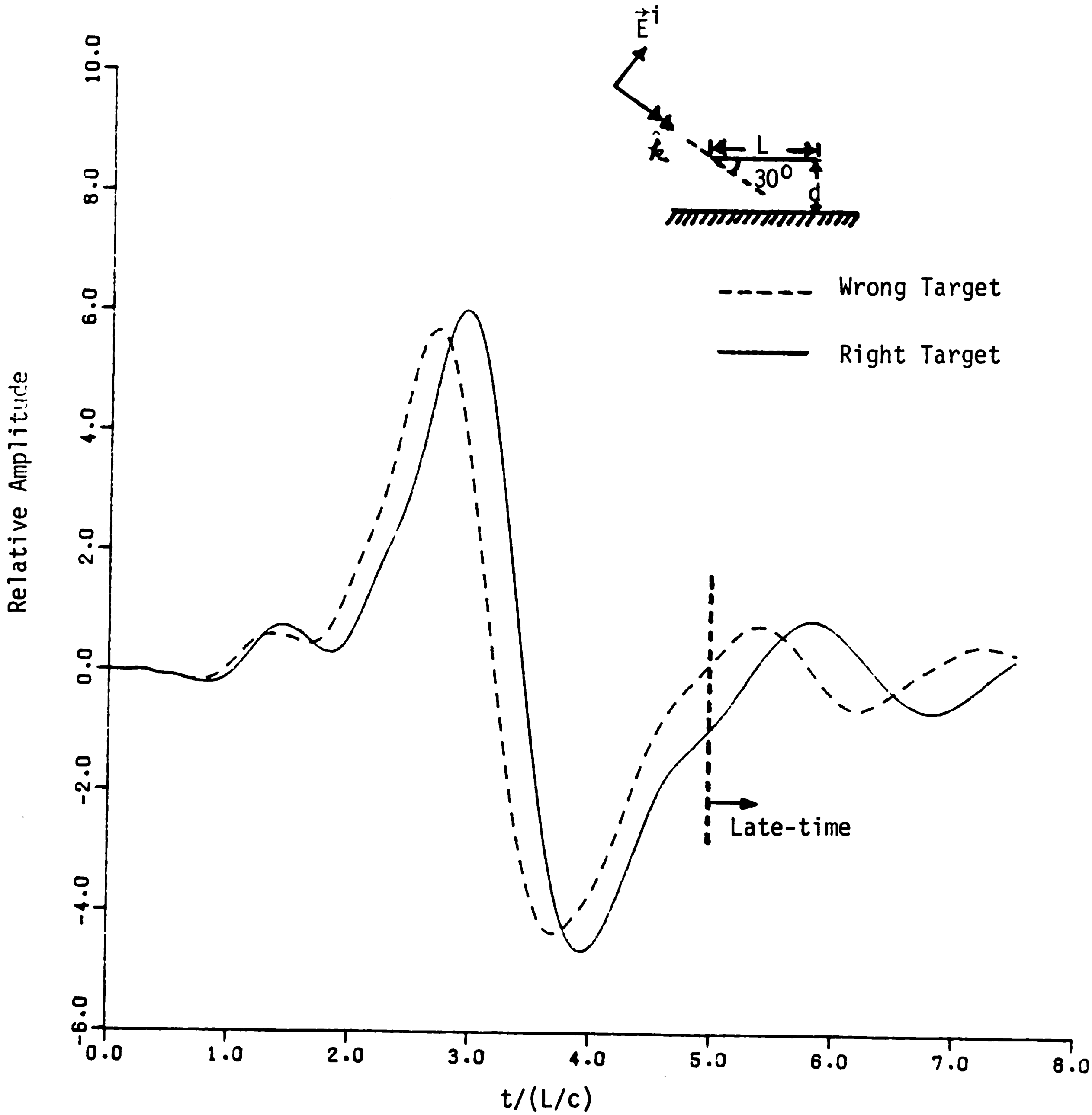

Figure 4.28. Return waveform from right target and target with 10% shorter length when the incident field is synthesized to excite the first mode of a paralled wire over the ground plane with $L/a = 200$ and $d/L = 0.5$. The aspect-angle $\varphi = 30^{o}$.

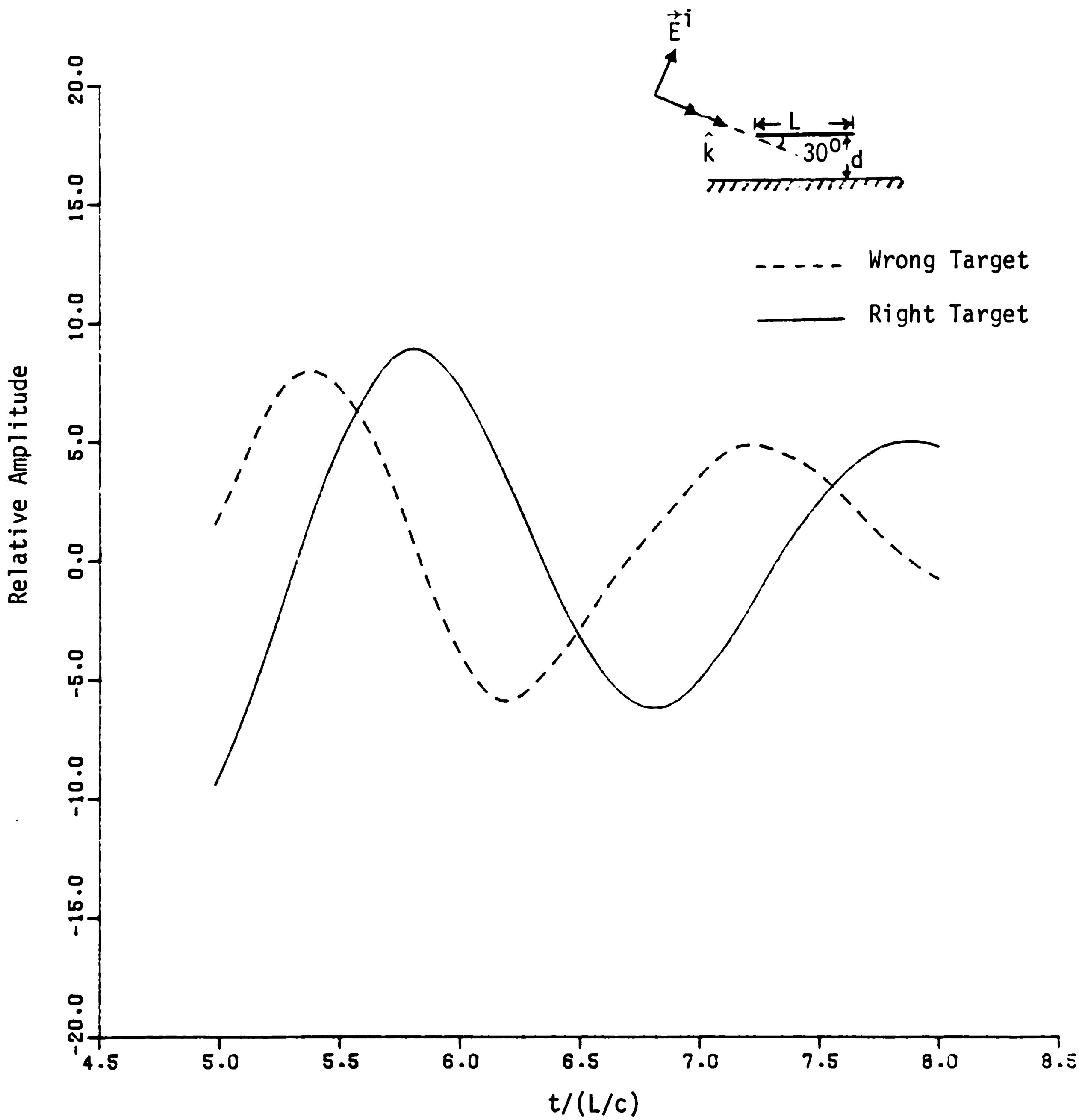

Figure 4.29. Late-time backscattered fields from right and wrong targets of the case shown in Figure 4.28.

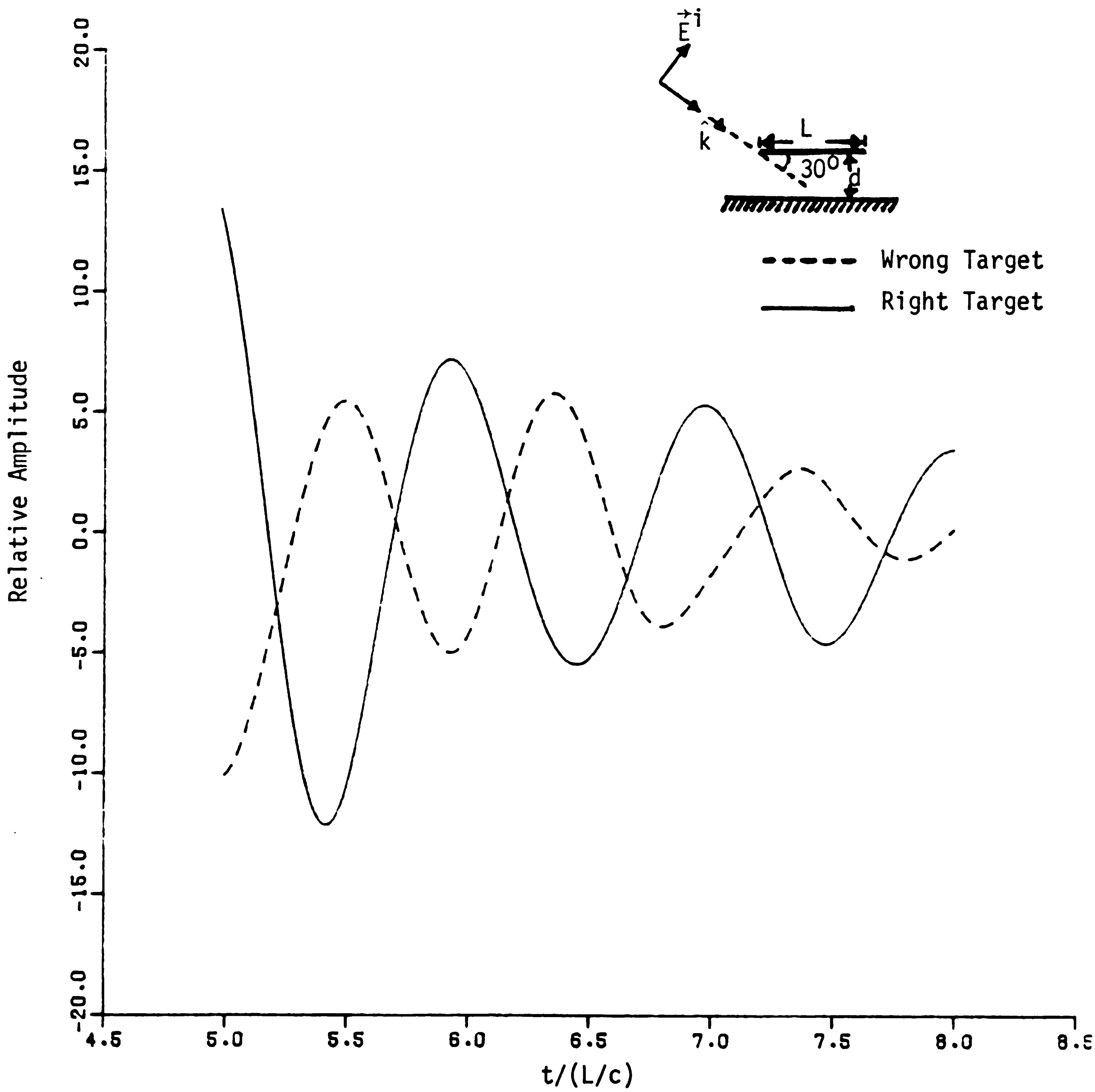

Figure 4.30. Late-time backscattered fields from right target and wrong target with 10% shorter length when the incident field is synthesized to excite the second mode of a paralled wire over the ground plane with $L/a = 200$, $d/L = 0.5$. The aspect-angle $\varphi = 30^o$.

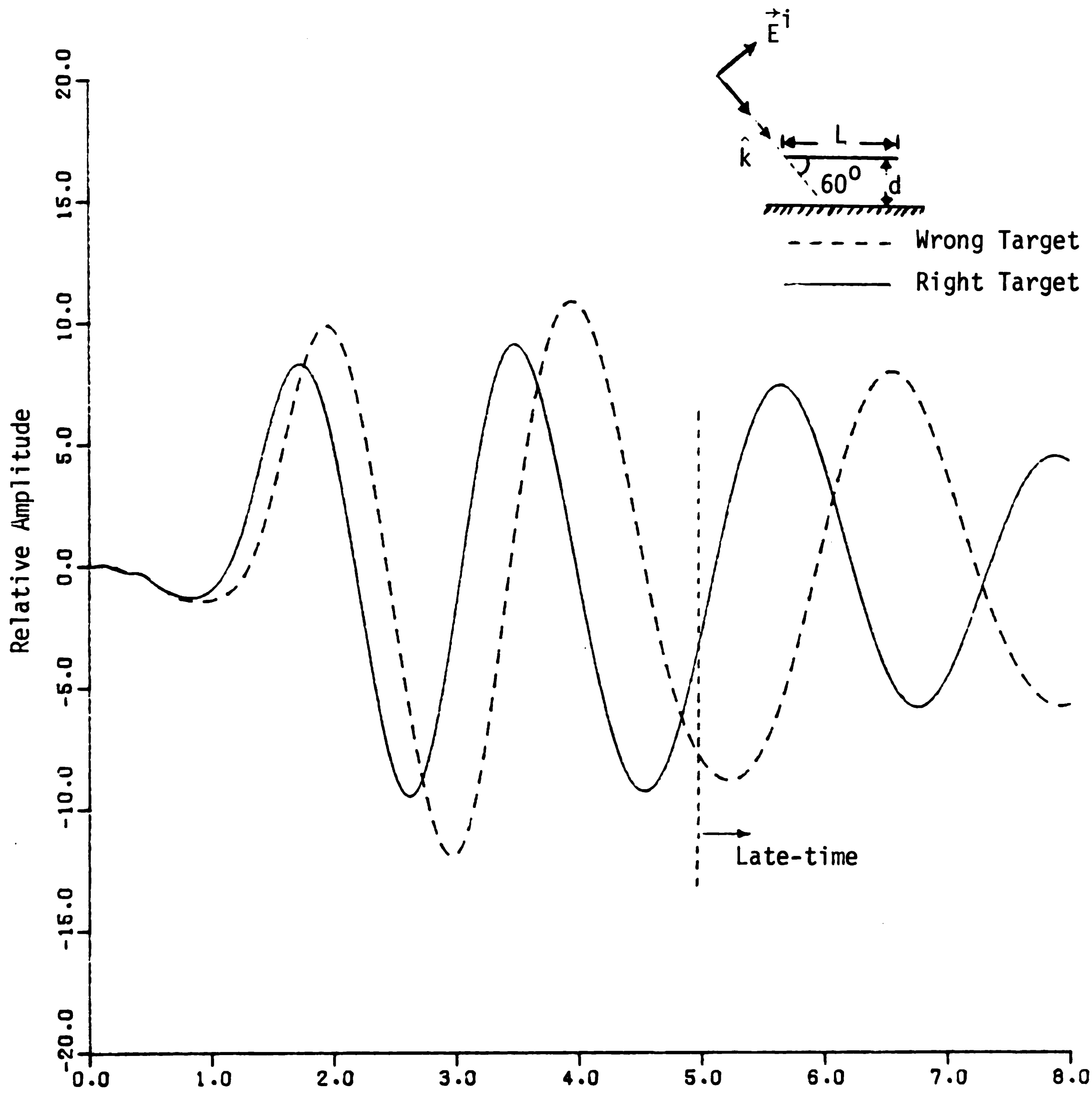

Figure 4.31. Return waveform from right target and target with 20% longer length for the first mode excitation of a parallel wire over the ground plane with L/a = 200, d/L = 0.5 and aspect-angle 60^o.

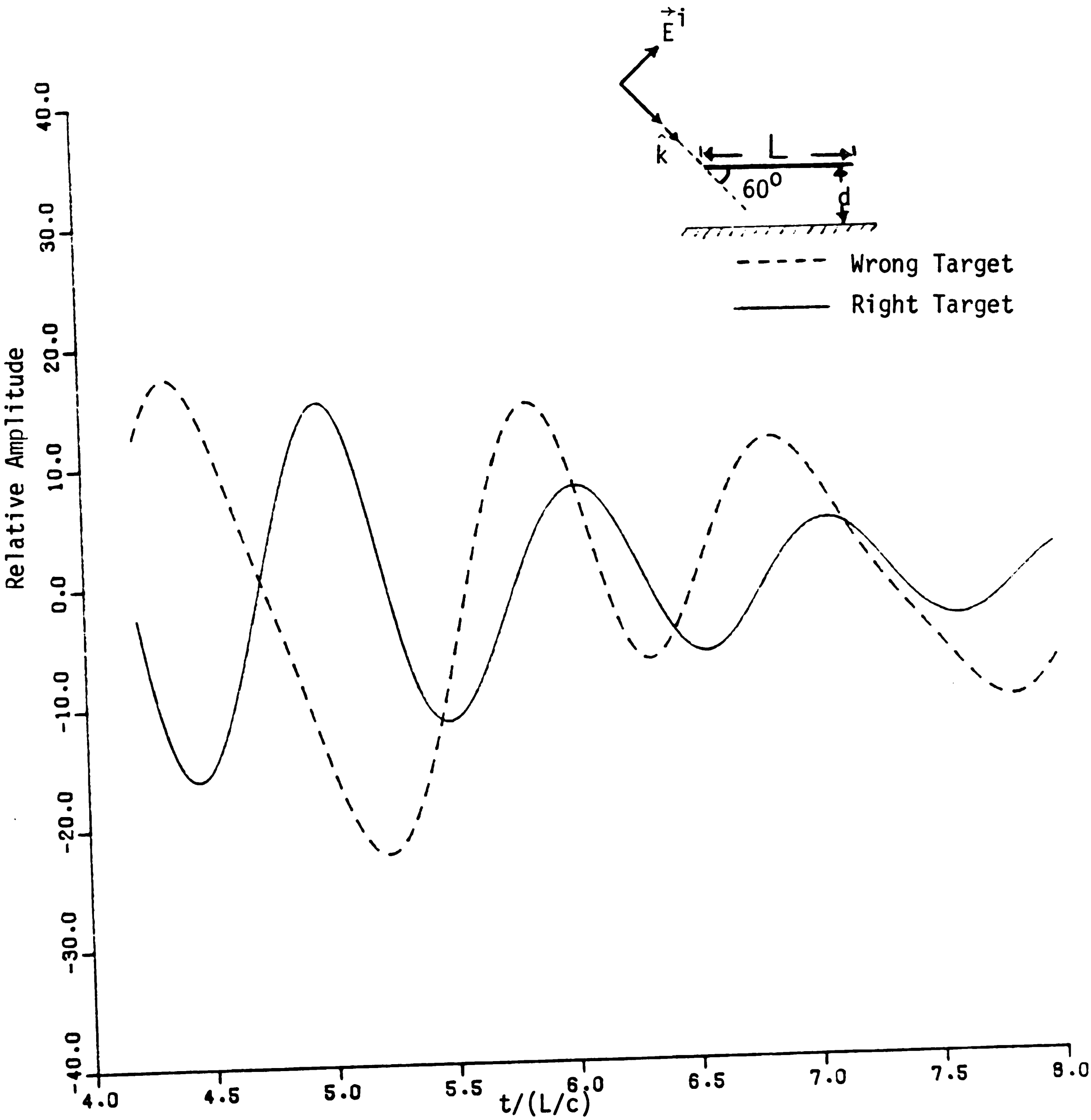

Figure 4.32. Late-time backscattered fields from right and wrong targets for the second mode excitation of the case shown in Figure 4.31.

second-mode $[s_2 = (-0.1215 + j\ 1.9400)\pi c/L]$ excitation is shown in Figure 4.27. The return signals for the right target and the wrong target (with 15% error in length) are shown in Figure 4.33 and Figure 4.34 for the first and the second modes, respectively.

The above numerical results are based upon synthesis using 10 natural-mode basis functions. It is found that the required waveforms for the isolated wire, the wire over ground plane (therefore only anti-symmetric modes are excitable) for $\alpha = 0^{\circ}$ and $\alpha = 30^{\circ}$ are roughly the same as can be easily seen form Figures 4.26 and 4.27. From the experience with the isolated wire [13], due to the fact that the natural modes are nearly orthogonal, the natural-mode basis functions can well span the 10-dimensional space; different choices of basis functions like δ-function basis and pulse-function basis lead to a unique required waveform. Therefore there is really no difference in using natural-mode basis or pulse-function basis. This is also true for the case in which the incident signal is symmetric with respect to two wires so that only the symmetric modes are excitable, since 10 symmetric modes are also nearly orthogonal and complete in 10-dimensional space. Figures 4.35 and 4.36 are some typical required waveforms for this case. For the general case in which both symmetric and antisymmetric modes are excitable, the matrix in (2.9) is somewhat ill-conditioned due to the fact that each symmetric natural frequency is quite close to its corresponding antisymmetric counterpart numerically. This leads to different synthesized waveforms for different basis functions. We will discuss more about the possibility of using different basis functions in Chapter 7. For the time being, only some results for waveform-synthesis using natural-mode basis set are shown in Figures 4.37 - 4.42.

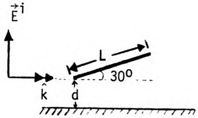

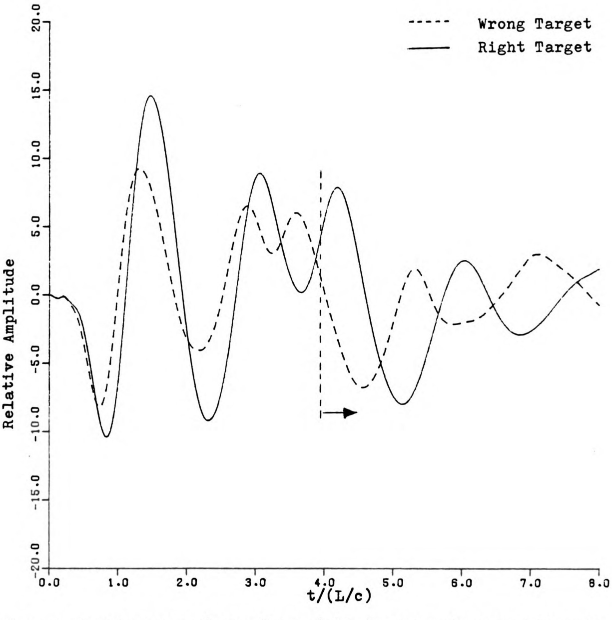

Figure 4.33 Return waveforms from right target and target with 15 % shorter length when the incident field is the synthesized waveform to excite the first mode of a wire over the ground plane with $L/a=200$, $d/L=0.5$ and $\alpha=30^\circ$. The aspect-angle $\varphi = 0^\circ$.

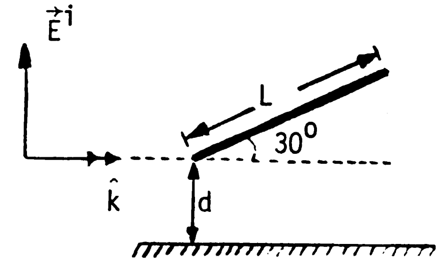

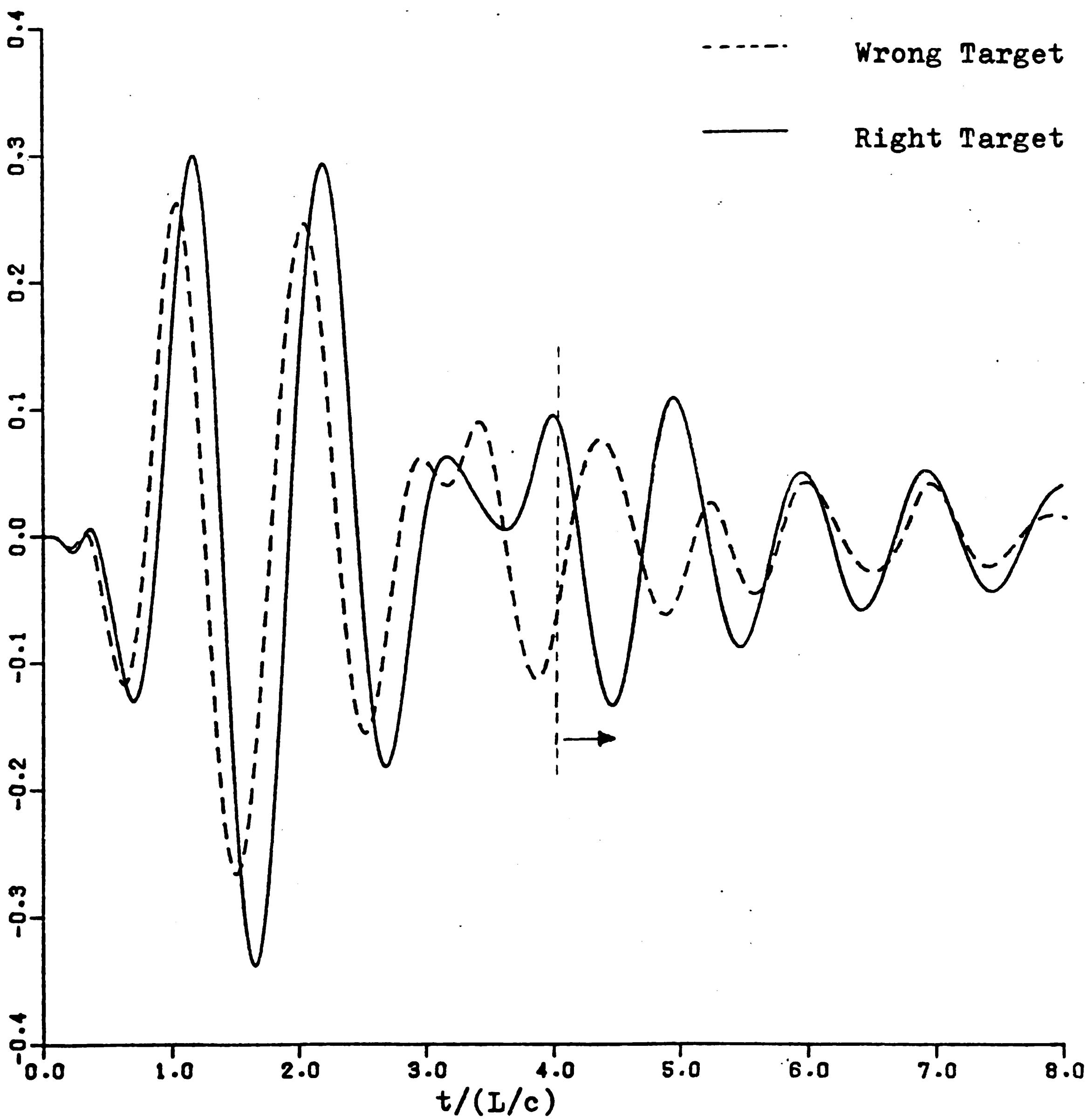

Figure 4.34. Return waveforms from right target and target with 15 % shorter length when the incident field is the synthesized waveform to excite the second mode of a wire over the ground plane with L/a=200, d/L=0.5 and α=30°. The aspect-angle φ =0°.

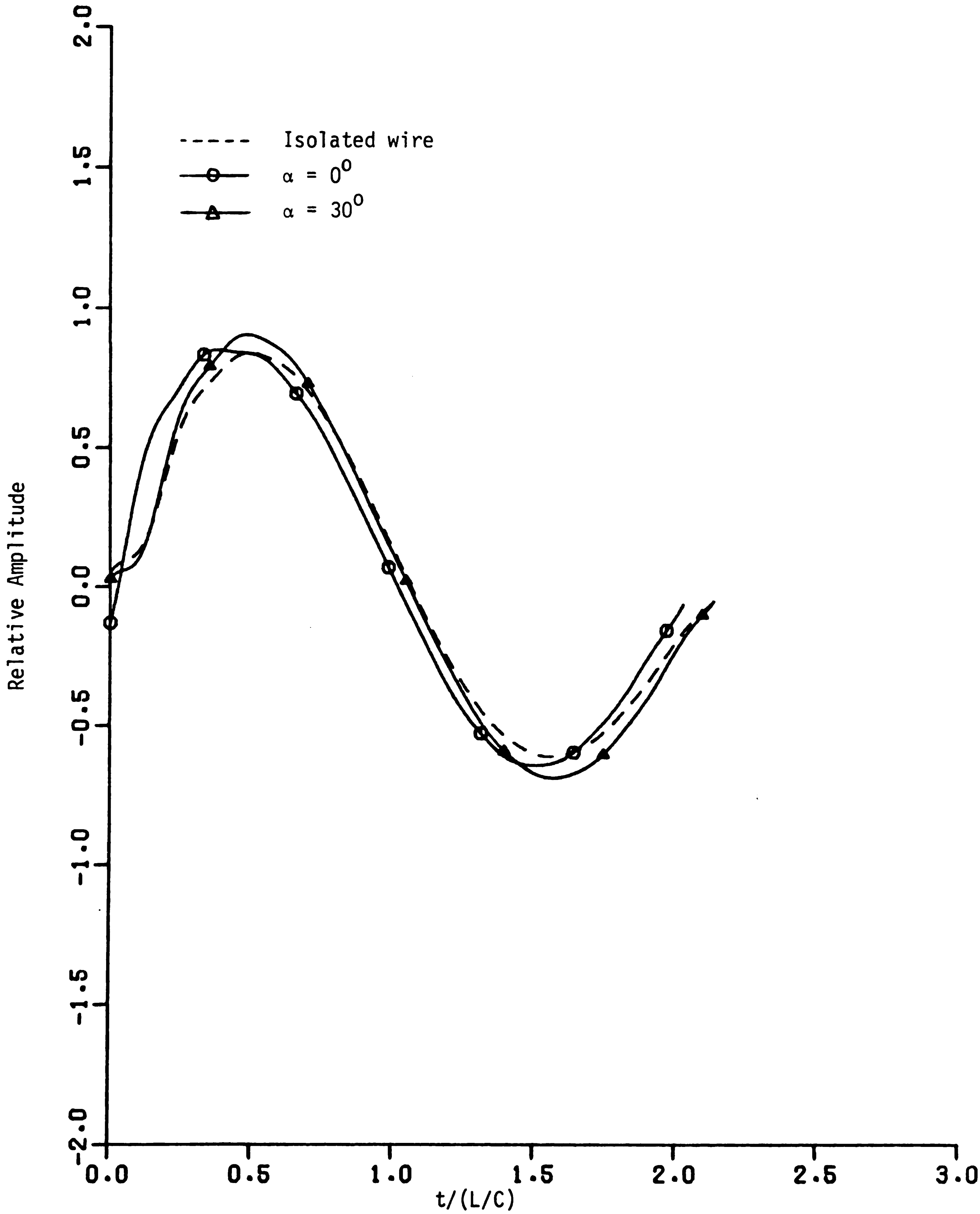

Figure 4.35. Required waveforms for the incident radar signals to excite the first modes from the two wires which are Symmetric with respect to the incident signal, $a/L = 1/200$, $d/L = 0.5$ and for $\alpha = 0^{\circ}$ and 30°. The required waveform for the isolated wire is also shown for comparison.

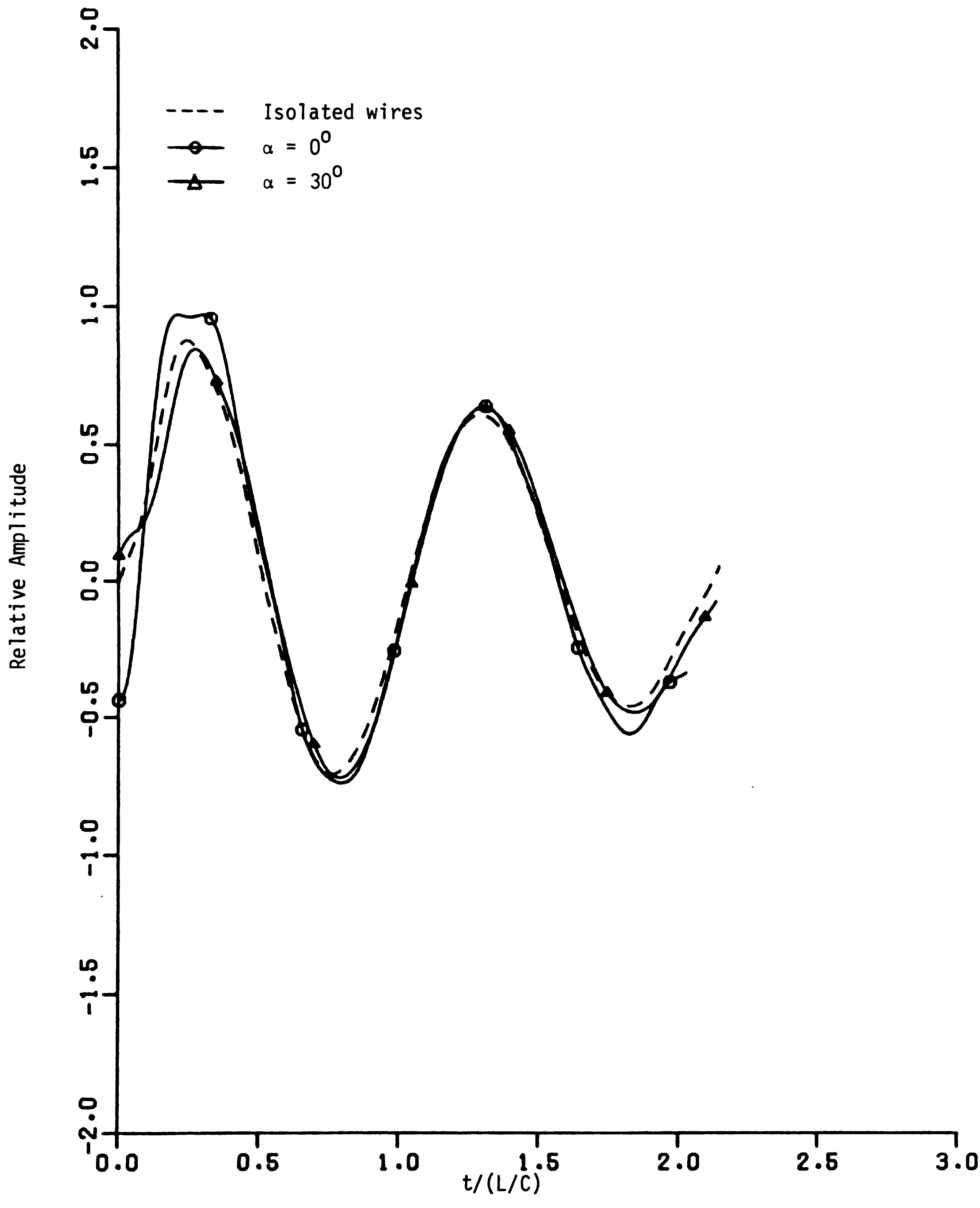

Figure 4.36. Required waveforms for the incident radar signals to excite the second modes from the two wires which are Symmetric with respect to the incident signal, $a/L = 1/200$, $d/L = 0.5$ and for $\alpha = 0^{0}$ and 30^{0}. The required waveform for the isolated wire is also shown for comparison.

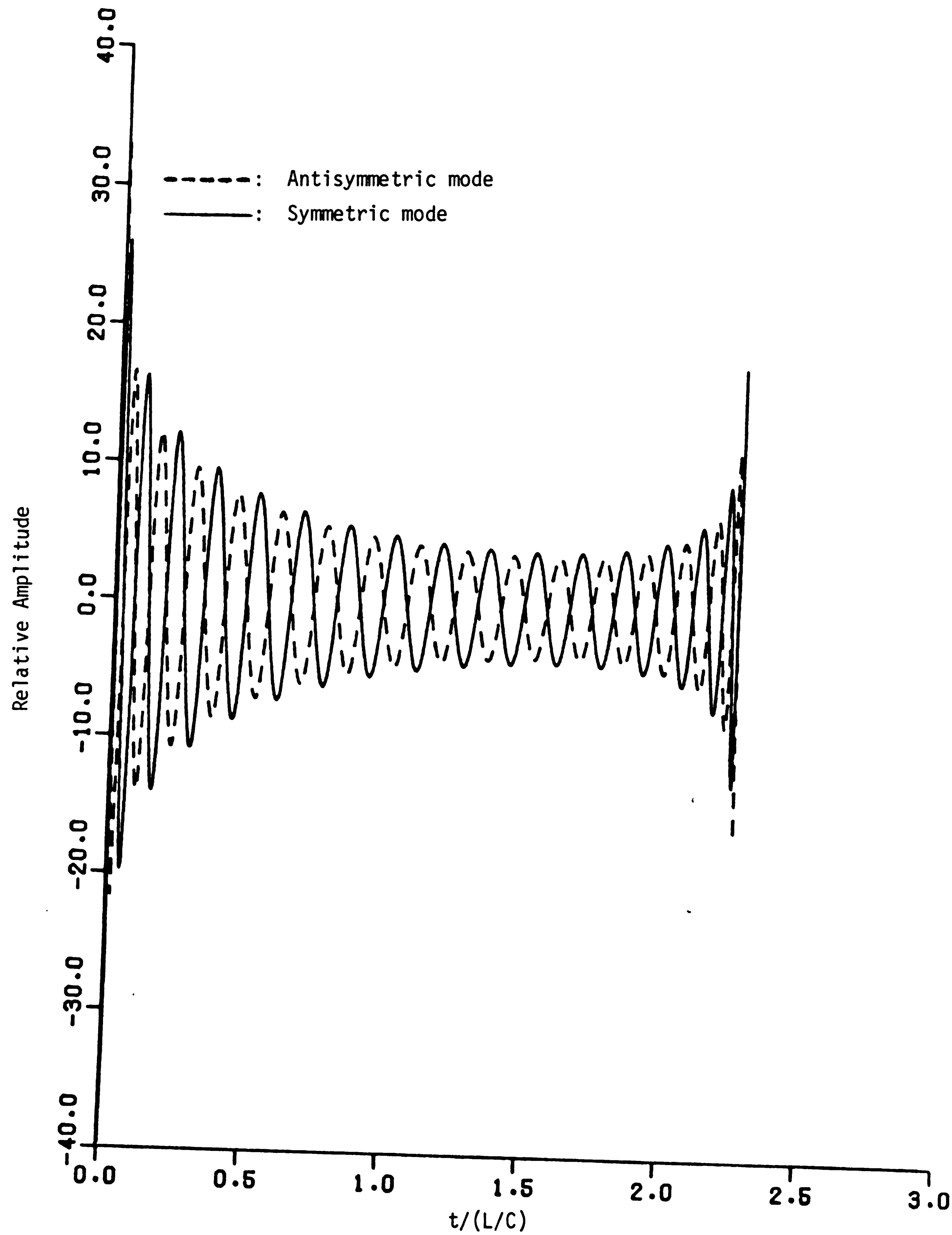

Figure 4.37. Required waveforms for the incident radar signals to excite the first modes from two parallel wires with a/L = 1/200 and d/L = 0.5, when both Symmetric and Antisymmetric modes are excitable.

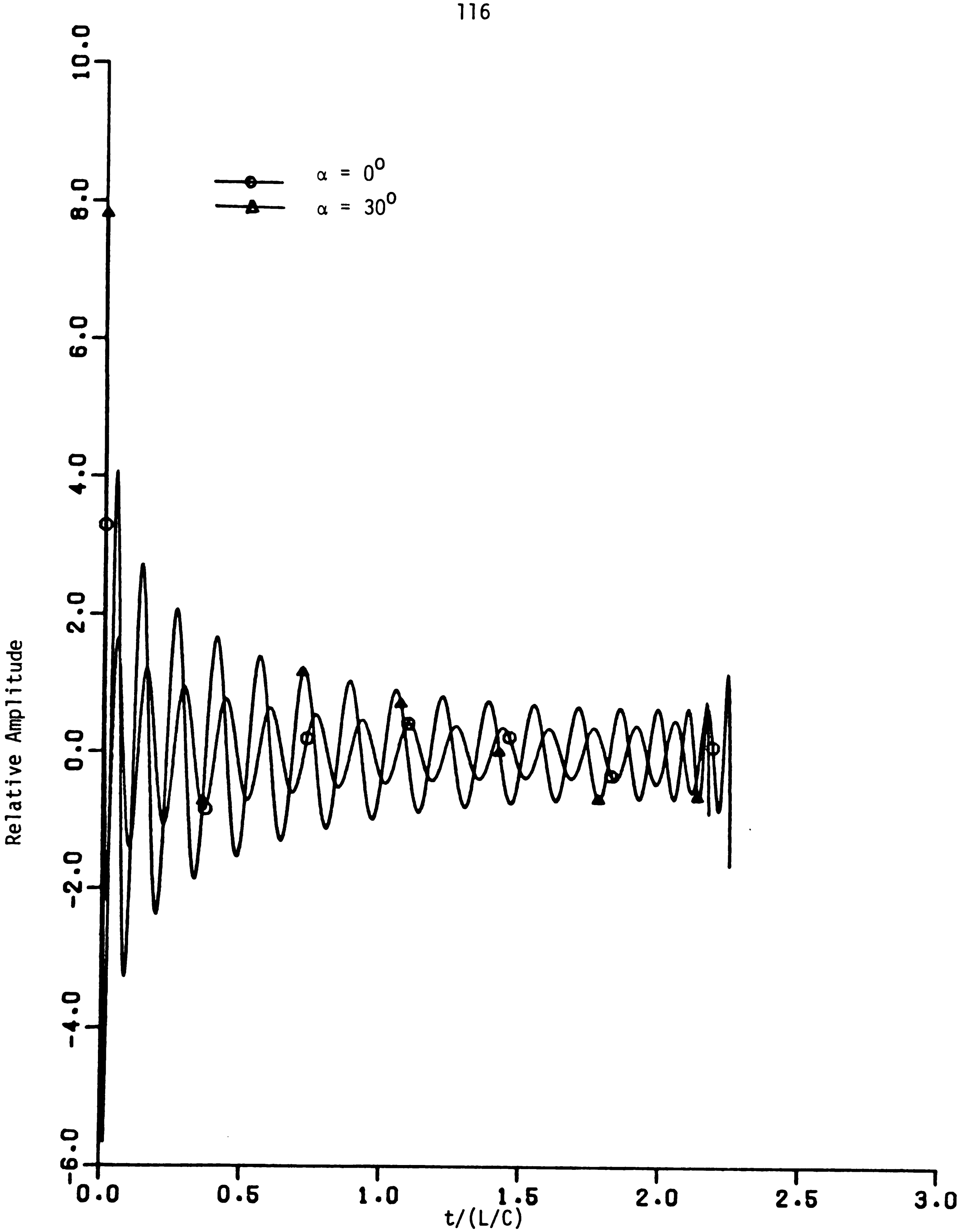

Figure 4.39. Required waveforms for the incident radar signals to excite the first Antisymmetric modes from two wires with a/L = 1/200, d/L = 0.5 and for $\alpha = 0^o$ and 30^o, when both Symmetric and Antisymmetric modes are excitable.

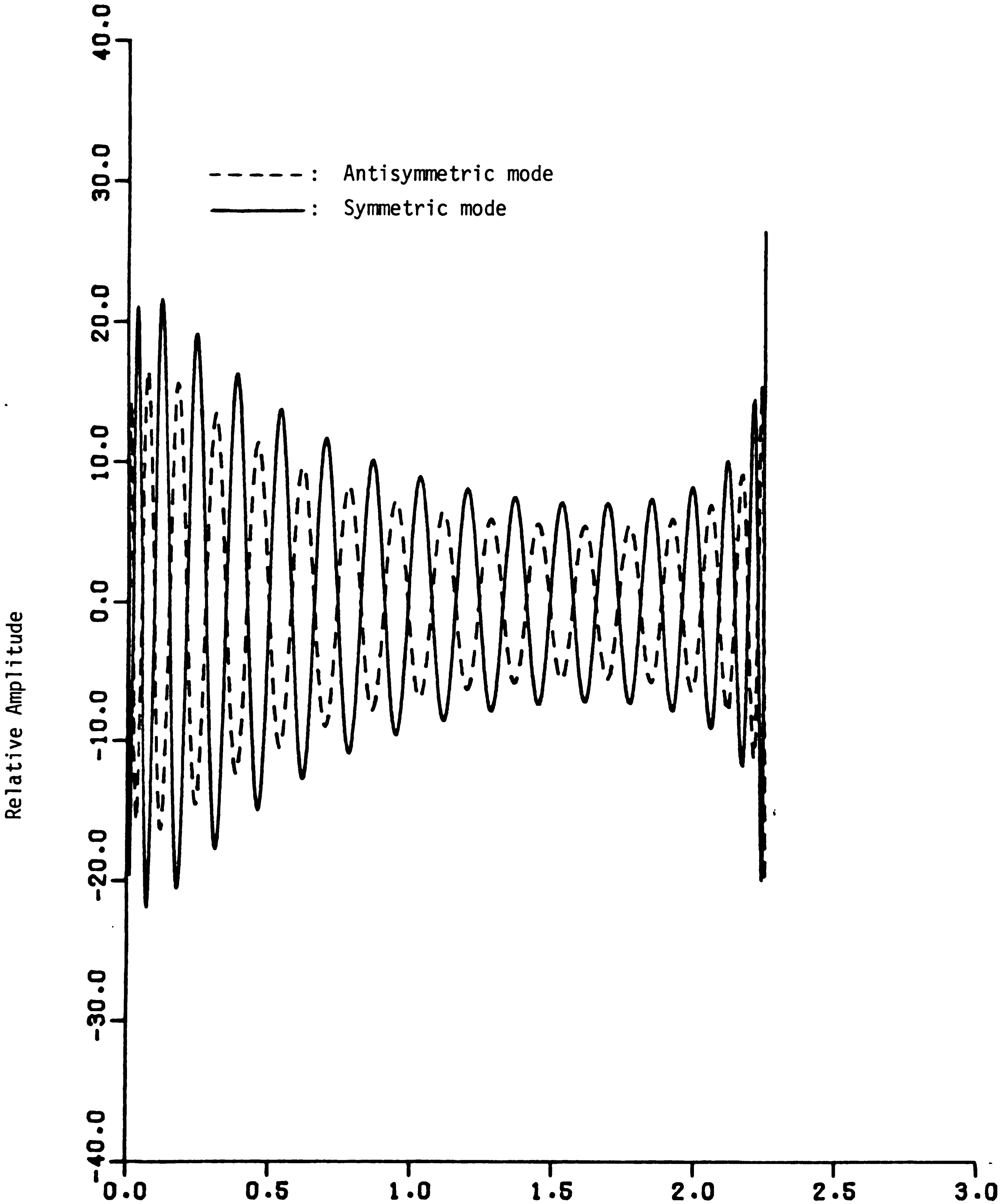

Figure 4.38. Required waveforms for the incident radar signals to excite the second modes from two parallel wires with a/L = 1/200 and d/L = 0.5, when both Symmetric and Antisymmetric modes are excitable.

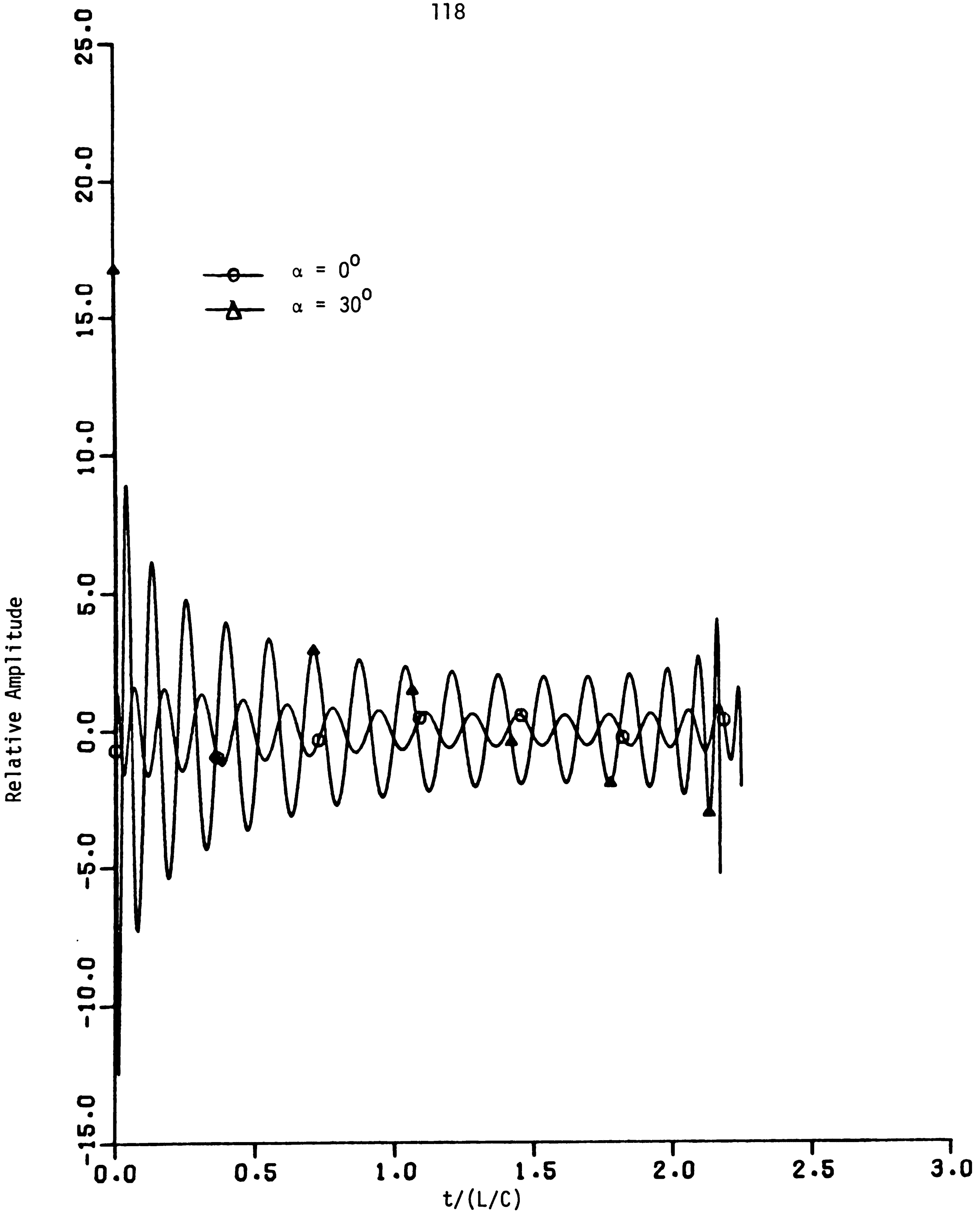

Figure 4.40. Required waveforms for the incident radar signals to excite the second Antisymmetric modes from two wires with $a/L = 1/200$, $d/L = 0.5$ and for $\alpha = 0^{\circ}$ and 30°, when both Symmetric and Antisymmetric modes are excitable.

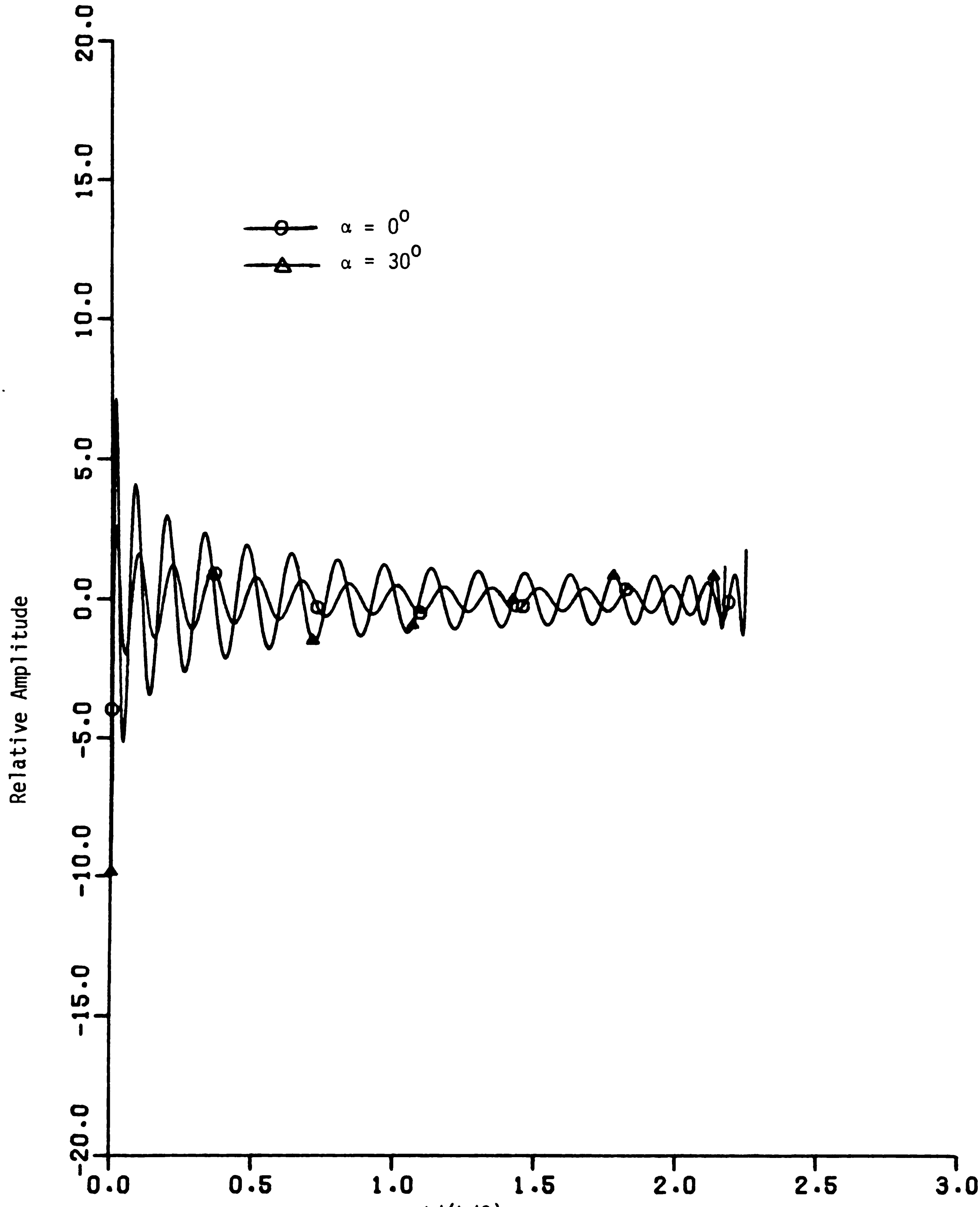

Figure 4.41. Required waveform for the incident radar signals to excite the first symmetric modes from two wires with a/L = 1/200, d/L = 0.5 and for $\alpha = 0^{\circ}$ and 30°, when both Symmetric and Antisymmetric modes are excitable.

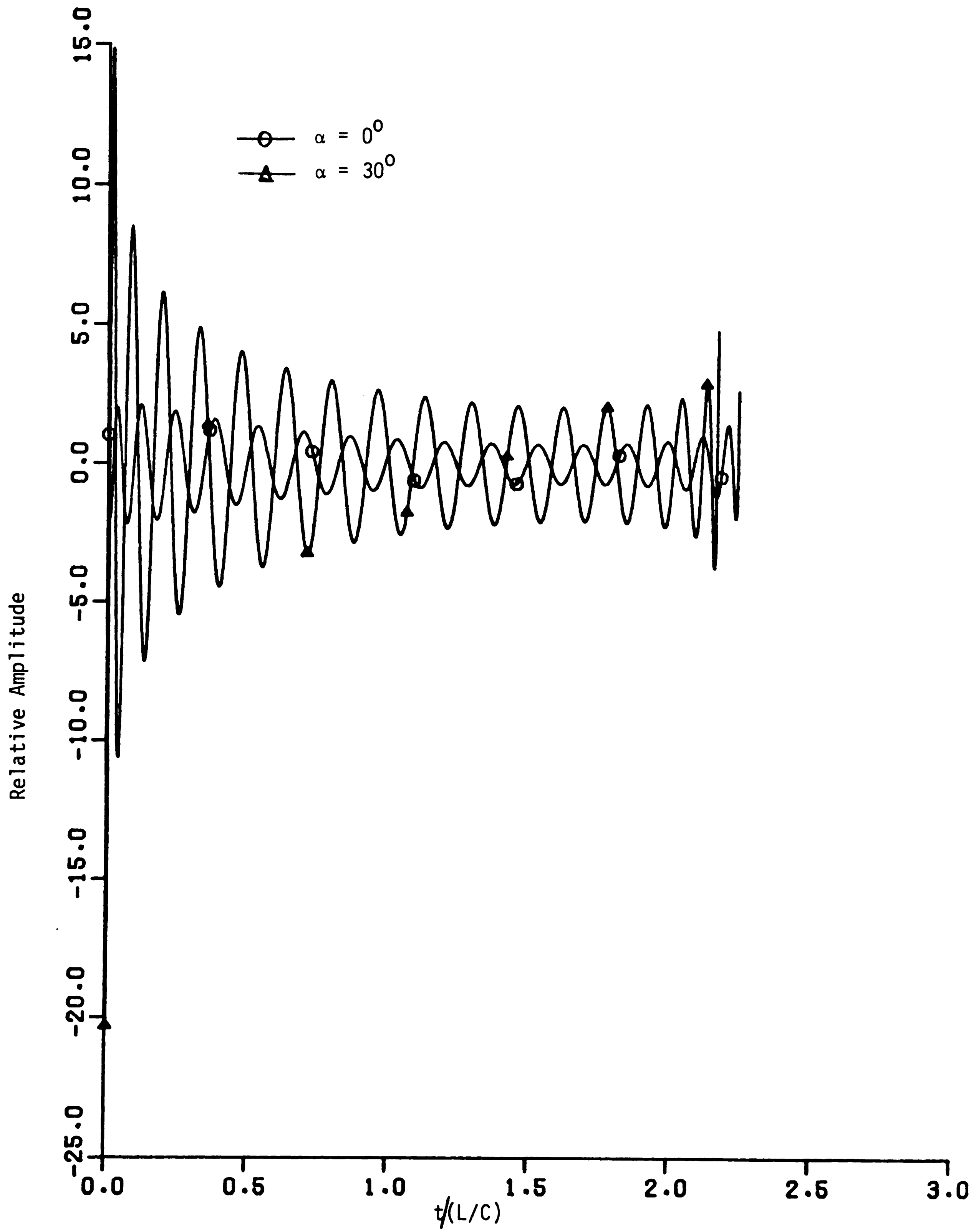

Figure 4.42. Required waveforms for the incident radar signals to excite the second Symmetric modes from two wires with $a/L = 1/200$, $d/L = 0.5$ and $\alpha = 0^{\circ}$ and 30°, when both Symmetric and Anti-symmetric modes are excitable.

CHAPTER 5

CROSSED WIRES

In this chapter, a crossed-wire system is used as a crude model of an airplane to investigate the applicability of the waveform-synthesis method. The geometry of this problem is described in Section 5.1. The results of Section 2.3.2 are applied to this target and symmetry is considered to obtain both EFIE and Hallen-type IE's in Section 5.2. As it turns out, only one integral equation is needed for the antisymmetric modes while a set of two couped integral equations are required to solve the symmetric modes. Section 5.3 is devoted to the solutions of the induced currents to both symmetric- and antisymmetric-excitations: Section 5.3.1 concerns mainly the natural modes; Section 5.3.2 discusses the coupling coefficients which are used in Sections 5.3.3 and 5.3.4 to compute the induced currents for the antisymmetric- and the symmetric-excitations, respectively. Section 5.4 applies the field-current relation derived in Section 4.4 to compute the backscattered fields for two types of excitations. Some numerical results are shown in Section 5.5 to demonstrate the impulse responses for different polarizations of the incident waveform. The waveform-synthesis method is used in Section 5.6 to discriminate the right and wrong targets.

5.1 Geometry of Problem

A crude model of an airplane consisting of a "fuselage" of length $L_1 + L_4$, two "wings" each with length L_2 oriented at an angle α with respect to the fuselage is indicated in Figure 5.1. The junction of this crossed wires system is L_1 from the "nose" and L_4 from the "tail". To simplify the problem, we assume that the fuselage and wings are constructed using thin wires with radii a_f and a_w, respectively. The incident field is expressed as

$$\vec{E}^i(\vec{r},t) = \hat{\zeta}\ F(t- \frac{\hat{k}\cdot\vec{r}}{c}) \tag{5.1}$$

where $\hat{\zeta}$, $\hat{k}$ and $\vec{r}$ are defined in the same way as in Section 4.1, and $F(t)$ is an unknown waveform fucntion to be synthesized to excite a single-mode scattered field in the late-time period. There are two types of polarizations to be considered in the latter sections:

(1) symmetric-mode excitation with

$$\hat{\zeta} = \hat{z}\sin\varphi + \hat{x}\cos\varphi \tag{5.2}$$

so that $I_2 = I_3$.

(2) Antisymmetric-mode excitation with

$$\hat{\zeta} = \hat{y} \tag{5.3}$$

so that $I_2 = -I_3$.

and $\hat{k} = -\hat{z}\cos\varphi + \hat{x}\sin\varphi$. (5.4)

Notice that $\hat{k}\cdot\hat{\zeta} = 0$ for this plane-wave incident transient field.

The tangential components of $\vec{E}^i(\vec{r},t)$ on the wires, in their Laplace-transform, are

$$\vec{E}^i_{\tan_k}(u_k,s) = (\hat{\zeta}\cdot\hat{u}_k)\hat{F}(s)e^{-\gamma(\hat{k}\cdot\vec{r})} \tag{5.5}$$

$$u_k \in [0,L_k],\ k = 1,2,3;\ u_4 \in [-L_4,0].$$

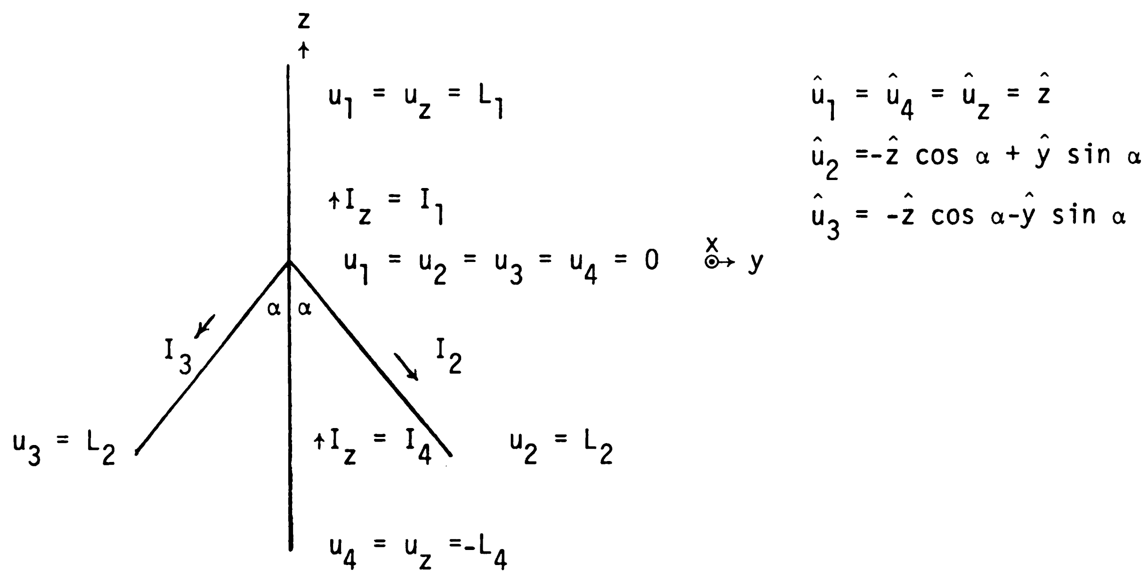

Figure 5.1. A crude model of an airplane consisting of a system of crossed wires.

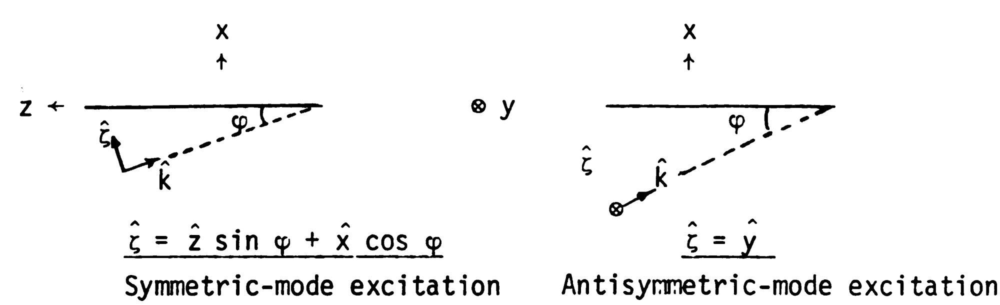

Figure 5.2. The side-view of the airplane along with the incident field with two types of polarizations.

These electric fields excite transient induced currents on the wires, and induced currents, in turn, generate transient backscattered electric field. Our objective is to synthesize an aspect-independnent waveform $F(t)$ for the monomode excitation.

5.2 Integral Equations

To simplify this problem, we decompose the induced currents on the wings into symmetric and antisymmetric components; i.e.,

$$\left.\begin{aligned} I_2 &= I_s + I_a \\ I_3 &= I_s - I_a \end{aligned}\right\} \tag{5.6}$$

where I_s is the symmetric-current component which is the same in both wings while I_a is the antisymmetric-current component which flows in opposite directions with equal amplitude in both wings. After this simplification, each mode needs only one integral equation to describe the wings instead of two coupled integral equations. However, the coupling between wings and fuselage still exists. The electric field integral equation can be obtained from Equation (2.16) as

$$\sum_{\ell=1}^{4} \{-\int_{0}^{L_\ell}{}^{1} I_\ell(u_\ell',s)[\frac{\partial^2}{\partial u_k \partial u_\ell'} + \gamma^2(\hat{u}_k\cdot\hat{u}_\ell)]\, \frac{e^{-\gamma R_{k\ell}}}{4\pi R_{k\ell}}\, du_\ell' + \frac{\partial W(u_k)}{\partial u_k}\}$$

$$= -\varepsilon_0 s\, \tilde{E}^i_{\tan_k}(u_k,s) \text{ --- for } u_k \in [0,L_k],\ k = 1,2,3;\ u_4 \in [-L_4,0] \tag{5.7}$$

---

[1] $\int_{-L_4}^{0}$ when $\ell = 4$

where
$$W_{k\ell}(u_k) \equiv I_\ell(L_\ell^-,s)\,\frac{e^{-\gamma R_{k\ell}(u_k,L_\ell)}}{4\pi R_{k\ell}(u_k,L_\ell)} - I_\ell(0^+,s)\,\frac{e^{-\gamma R_{k\ell}(u_k,0)}}{4\pi R_{k\ell}(u_k,0)} \quad \text{for } \ell = 1,2,3$$
$$\equiv I_4(0^-,s)\,\frac{e^{-\gamma R_{k4}(u_k,0)}}{4\pi R_{k4}(u_k,0)} - I_4[(-L_4)^+,s]\,\frac{e^{-\gamma R_{k4}(u_k,-L_4)}}{4\pi R_{k4}(u_k,-L_4)} \quad \text{for } \ell = 4. \tag{5.8}$$

Since $I_\ell(L_\ell^-,s) = 0$ for $\ell = 1,2,3$ and $I_4[(-L_4)^+,s] = 0$ for $\ell = 4$ at wire ends, $W_{k\ell}(u_k)$ can be rewritten as

$$\left.\begin{aligned} W_{k\ell}(u_k) &= -I_\ell(0^+,s)\,\frac{e^{-\gamma R_{k\ell}(u_k,0)}}{4\pi R_{k\ell}(u_k,0)} \quad \text{for } \ell = 1,2,3 \\ &= I_4(0^-,s)\,\frac{e^{-\gamma R_{k4}(u_k,0)}}{4\pi R_{k4}(u_k,0)} \quad \text{for } \ell = 4 \end{aligned}\right\}. \tag{5.9}$$

If we define
$$\left.\begin{aligned} I_z(u,s) &= I_1(u,s) \quad \text{for } u \in [0,L_1] \\ &= I_4(u,s) \quad \text{for } u \in [-L_4,0] \end{aligned}\right\} \tag{5.10}$$

as shown in Figure 5.1, then the fuselage can be described by the following integral equation by setting $k = z$ in Equation (5.7) and dropping the subscripts for u_k and u_ℓ',

$$-\int_{-L_4}^{L_1} I_z(u',s)\left[\frac{\gamma^2}{\partial u\partial u'} + \gamma^2\right]\frac{e^{-\gamma R_f}}{4\pi R_f}\,du' - \int_0^{L_2}[I_2(u',s) + I_3(u',s)]$$
$$\left[\frac{\partial^2}{\partial u\partial u'} - \gamma^2\cos\alpha\right]\frac{e^{-\gamma R_{1f}}}{4\pi R_{1f}}\,du' = S_z(u,s) + [I_z(0^+,s) - I_z(0^-,s)]\,\frac{\partial}{\partial u}\frac{e^{-\gamma R_f(u,0)}}{4\pi R_f(u,0)}$$
$$+ [I_2(0^+,s) + I_3(0^+,s)]\,\frac{\partial}{\partial u}\frac{e^{-\gamma R_{1f}(u,0)}}{4\pi R_{1f}(u,0)} \tag{5.11}$$

where
$$\left.\begin{aligned} R_f &= [(u-u')^2 + a_f^2]^{\frac{1}{2}} \\ R_{1f} &= [u^2 + u'^2 + 2uu' \cos\alpha + a_f^2]^{\frac{1}{2}} \end{aligned}\right\} \tag{5.12}$$

and $S_z(u,s) = -\epsilon_0 s\, \tilde{E}^i_{\tan_z}(u,s)$ = the forcing function on the fuselage.

(5.13)

Because $R_f(u,0) = (u^2 + a_f^2)^{\frac{1}{2}} = R_{1f}(u,0)$ from Equation (5.12), the last two terms on the right hand side of Equation (5.11) become

$$\frac{\partial}{\partial u} \frac{e^{-\gamma R_f(u,0)}}{4\pi R_f(u,0)} [I_2(0^+,s) + I_3(0^+,s) + I_z(0^+,s) - I_z(0^-,s)] = 0,$$ due to

KCL: $I_z(0^-,s) = I_z(0^+,s) + I_2(0^+,s) + I_3(0^+,s)$.

By defining
$$\left.\begin{aligned} K_f(u|u',s) &= -[\frac{\partial^2}{\partial u \partial u'} + \gamma^2] \frac{e^{-\gamma R_f}}{4\pi R_f} = \text{self kernel for fuselage} \\ K_{1f}(u|u',s) &= -[\frac{\partial^2}{\partial u \partial u'} - \gamma^2 \cos\alpha] \frac{e^{-\gamma R_{1f}}}{4\pi R_{1f}} = \alpha\text{-coupling kernel} \end{aligned}\right\}$$

for fuselage (5.14)

and using definitions in (5.6), the integral equation in (5.11) can be rewritten as

$$\int_{-L_4}^{L_1} I_z(u',s) K_f(u|u',s) du' + 2\int_0^{L_2} I_s(u',s) K_{1f}(u|u',s) du' = S_z(u,s) \tag{5.15}$$

$$u \in [-L_1, L_4].$$

Similarly, the integral equations associated with the wings can be obtained from Equation (5.7) as

$$-\int_{-L_4}^{L_1} I_z(u',s)[\frac{\partial^2}{\partial u \partial u'} - \gamma^2 \cos\alpha] \frac{e^{-\gamma R_{1W}}}{4\pi R_{1W}} du' - \int_0^{L_2} I_2(u',s)[\frac{\partial^2}{\partial u \partial u'} + \gamma^2] \frac{e^{-\gamma R_W}}{4\pi R_W} du'$$

$$-\int_0^{L_2} I_3(u',s)\left[\frac{\partial^2}{\partial u\partial u'} + \gamma^2 \cos 2\alpha\right]\frac{e^{-\gamma R_{2w}}}{4\pi R_{2w}}\,du' = S_2(u,s) + [I_z(0^+,s)- I_z(0^-,s)]$$

$$\frac{\partial}{\partial u}\frac{e^{-\gamma R_{1w}(u,0)}}{4\pi R_{1w}(u,0)} + I_2(0^+,s)\frac{\partial}{\partial u}\frac{e^{-\gamma R_w(u,0)}}{4\pi R_w(u,0)} + I_3(0^+,s)\frac{\partial}{\partial u}\frac{e^{-\gamma R_{2w}(u,0)}}{4\pi R_{2w}(u,0)} \quad (5.16)$$

and

$$-\int_{-L_4}^{L_1} I_z(u',s)\left[\frac{\partial^2}{\partial u\partial u'} - \gamma^2 \cos \alpha\right]\frac{e^{-\gamma R_{1w}}}{4\pi R_{1w}}\,du' - \int_0^{L_2} I_2(u',s)\left[\frac{\partial^2}{\partial u\partial u'} + \gamma^2 \cos 2\alpha\right]\frac{e^{-\gamma R_{2w}}}{4\pi R_{2w}}\,du'$$

$$-\int_0^{L_2} I_3(u',s)\left[\frac{\partial^2}{\partial u\partial u'} + \gamma^2\right]\frac{e^{-\gamma R_w}}{4\pi R_w}\,du' = S_3(u,s) + [I_z(0^+,s)-I_z(0^-,s)]$$

$$\frac{\partial}{\partial u}\frac{e^{-\gamma R_{1w}(u,0)}}{4\pi R_{1w}(u,0)} + I_2(0^+,s)\frac{\partial}{\partial u}\frac{e^{-\gamma R_{2w}(u,0)}}{4\pi R_{2w}(u,0)} + I_3(0^+,s)\frac{\partial}{\partial u}\frac{e^{-\gamma R_w(u,0)}}{4\pi R_w(u,0)} \quad (5.17)$$

where

$$\left.\begin{aligned} R_w &= [(u-u')^2 + a_w^2]^{1/2} \\ R_{1w} &= [u^2 + u'^2 + 2uu' \cos \alpha + a_w^2]^{1/2} \\ R_{2w} &= [u^2 + u'^2 - 2uu' \cos 2\alpha + a_w^2]^{1/2} \end{aligned}\right\}, \quad (5.18)$$

and

$$\left.\begin{aligned} S_2(u,s) &= -\varepsilon_0 s\, \tilde{E}^i_{tan_2}(u,s) \\ S_3(u,s) &= -\varepsilon_0 s\, \tilde{E}^i_{tan_3}(u,s) \end{aligned}\right\}. \quad (5.19)$$

The fact that $R_w(u,0) = R_{1w}(u,0) = R_{2w}(u,0) = [u^2 + a_w^2]^{1/2}$ and KCL lead to the vanishing of the right hand side of Equations (5.16) and (5.17) except $S_2(u,s)$ and $S_3(u,s)$.

If we define

$$\left.\begin{aligned} K_w(u|u',s) &= -[\frac{\partial^2}{\partial u \partial u'} + \gamma^2]\,\frac{e^{-\gamma R_w}}{4\pi R_w} = \text{self kernel for wing} \\ K_{1w}(u|u',s) &= -[\frac{\partial^2}{\partial u \partial u'} - \gamma^2 \cos\alpha]\,\frac{e^{-\gamma R_{1w}}}{4\pi R_{1w}} = \alpha\text{-coupling kernel for wing,} \\ K_{2w}(u|u',s) &= -[\frac{\partial^2}{\partial u \partial u'} + \gamma^2 \cos 2\alpha]\,\frac{e^{-\gamma R_{2w}}}{4\pi R_{2w}} = 2\alpha\text{-coupling kernel for wing} \end{aligned}\right\}, \tag{5.20}$$

Equations (5.16) and (5.17) can be rewritten as

$$\int_{-L_4}^{L_1} I_z(u',s)K_{1w}(u\ u',s)du' + \int_0^{L_2} I_2(u',s)K_w(u|u',s)du' + $$

$$+ \int_0^{L_2} I_3(u',s)K_{2w}(u|u',s)du' = S_2(u,s), \tag{5.21}$$

and

$$\int_{-L_4}^{L_1} I_z(u',s)K_{1w}(u|u',s)du' + \int_0^{L_2} I_2(u',s)K_{2w}(u|u',s)du'$$

$$+ \int_0^{L_2} I_3(u',s)K_w(u|u',s)du' = S_3(u,s). \tag{5.22}$$

Both Equations (5.21) and (5.22) have the domain $u \in [0,L_2]$, therefore they can be added and subtracted with each other as [by using the definitions in Equation (5.6)],

$$\int_{-L_4}^{L_1} I_z(u',s)K_{1w}(u|u',s)du' + \int_0^{L_2} I_s(u',s)K_s(u|u',s)du' = S_s(u,s)\ u\in[0,L_2]$$

for the symmetric modes, (5.23)

and

$$\int_0^{L_2} I_a(u',s)K_a(u|u',s)du' = S_a(u,s)\ u \in [0,L_2] \text{ for the antisymmetric modes.} \tag{5.24}$$

where
$$\left.\begin{aligned} K_s(u|u',s) &= K_w(u|u',s) + K_{2w}(u|u',s) \\ K_a(u|u',s) &= K_w(u|u',s) - K_{2w}(u|u',s) \end{aligned}\right\} , \tag{5.25}$$

and
$$\left.\begin{aligned} S_s(u,s) &= \tfrac{1}{2}[S_2(u,s) + S_3(u,s)] \\ S_a(u,s) &= \tfrac{1}{2}[S_2(u,s) - S_3(u,s)] \end{aligned}\right\} . \tag{5.26}$$

It is important to notice that the symmetric modes can be solved by using the coupled integral Equations (5.15) and (5.23) while the antisymmetric modes can be solved by using only a decoupled integral Equation (5.24). This is because whenever we are dealing with the anitsymmetric modes. due to the cancellations from two wings, the forcing function on the fuselage, $S_z(u,0)$, is zero and $I_z(u,0)$ is thus vanishing. In other words, if $I_z \neq 0$ for the antisymmetric modes, then the coupling between wings and fuselage will result in non-zero symmetric current which should be zero under the requirement for the existence of only the antisymmetric modes. Therefore, antisymmetric modes can be solved much more easily. Equations (5.15), (5.23) and (5.24) are the EFIE's to be used for computing the coupling coefficients.

To compute the natural modes, Hallen-type integral equations will be used due to the reasons discussed in Chapter 2. They are obtained from Equation (2.35) as

$$\int_{-L_4}^{L_1} I_z(u',s)K_{hf}(u|u',s)du' + \int_0^{L_2}[I_2(u',s) + I_3(u',s)]K_{h1f}(u|u',s)du'$$

$$= C_1 \cosh \gamma u + C_{21} \sinh \gamma u + \frac{1}{\gamma}\int_0^u S_z(\xi,s)\sinh \gamma(u-\xi)d\xi \tag{5.27}$$

for fuselage[1] $-L_4 \le u \le L_1$,

and

$$\int_{-L_4}^{L_1} I_z(u',s)K_{h1w}(u|u',s)du' + \int_0^{L_2} I_2(u',s)K_{hw}(u|u',s)du' + \int_0^{L_2} I_3(u',s)K_{h2w}(u|u',s)du'$$

$$= C_{12}\cosh\gamma u + C_{22}\sinh\gamma u + \frac{1}{\gamma}\int_0^u S_2(\xi,s)\sinh\gamma(u-\xi)d\xi\,, \tag{5.28}$$

$$\int_{-L_4}^{L_1} I_z(u',s)K_{h1w}(u|u',s)du' + \int_0^{L_2} I_2(u',s)K_{h2w}(u|u',s)du' + \int_0^{L_2} I_3(u',s)K_{hw}(u|u',s)du'$$

$$= C_{13}\cosh\gamma u + C_{23}\sinh\gamma u + \frac{1}{\gamma}\int_0^u S_3(\xi,s)\sinh\gamma(u-\xi)d\xi \tag{5.29}$$

for wings $0 \le u \le L_2$,

where
$$\left.\begin{aligned}
K_{hf}(u|u',s) &= \frac{e^{-\gamma R_f}}{4\pi R_f} = \text{Hallen-type self kernel for fuselage,}\\
K_{hw}(u|u',s) &= \frac{e^{-\gamma R_w}}{4\pi R_w} = \text{Hallen-type self kernel for wing,}\\
K_{h1f}(u|u',s) &\equiv \frac{e^{-\gamma R_f}}{4\pi R_{1f}}\cos\alpha - \int_0^u g_{1f}(\xi,u',s)\cosh\gamma(u-\xi)d\xi\\
&= \text{Hallen-type }\alpha\text{-coupling kernel for fuselage,}\\
K_{h1w}(u|u',s) &\equiv \frac{e^{-\gamma R_{1w}}}{4\pi R_{1w}}\cos\alpha - \int_0^u g_{1w}(\xi,u',s)\cosh\gamma(u-\xi)d\xi\\
&= \text{Hallen-type }\alpha\text{-coupling kernel for wing,}
\end{aligned}\right\} \tag{5.30}$$

---

[1] Due to continuity of vector potential in the z direction across this junction [20], $C_{11} = C_{14} \equiv C_1$ and IE's for wires #1 and #4 can therefore be combined as a single integral equation.

$$K_{h2w}(u|u',s) = \frac{e^{-\gamma R_{2w}}}{4\pi R_{2w}} \cos 2\alpha - \int_0^u g_{2w}(\xi,u',s) \cosh \gamma (u-\xi) d\xi$$

= Hallen-type 2α-coupling kernel for wing.

and

$$\left.\begin{aligned} g_{1f}(u,u',s) &= \left[\frac{d}{dR_{1f}} \left(\frac{e^{-\gamma R_{1f}}}{4\pi R_{1f}}\right)\right] \frac{u' \sin^2\alpha}{R_{1f}} \\ g_{1w}(u,u',s) &= \left[\frac{d}{dR_{1w}} \left(\frac{e^{-\gamma R_{1w}}}{4\pi R_{1w}}\right)\right] \frac{u' \sin^2\alpha}{R_{1w}} \\ g_{2w}(u,u',s) &= \left[\frac{d}{dR_{2w}} \left(\frac{e^{-\gamma R_{2w}}}{4\pi R_{2w}}\right)\right] \frac{u' \sin^2 2\alpha}{R_{2w}} \end{aligned}\right\} . \qquad (5.31)$$

Continuity of scalar potential across the juction [20] leads to

$C_{2k} \equiv C_2$, $k = 1,2,3,4$.

Addition and subtraction of Equation (5.28) and (5.29) thus provide

$$\int_{-L_4}^{L_1} I_z(u',s) K_{h1w}(u|u',s) du' + \int_0^{L_2} I_s(u',s) K_{hs}(u|u',s) du'$$

$$= C_s \cosh \gamma u + C_2 \sinh \gamma u + \frac{1}{\gamma} \int_0^u S_s(\xi,s) \sinh \gamma(u-\xi) d\xi \qquad (5.32)$$

for the symmetric modes, $u \in [0,L_2]$;

and

$$\int_0^{L_2} I_a(u',s) K_{ha}(u,u',s) du' = C_a \cosh \gamma u + \frac{1}{\gamma} \int_0^u S_a(\xi,s) \sinh \gamma(u-\xi) d\xi \qquad (5.33)$$

for the antisymmetric modes, $u \in [0,L_2]$

where

$$\left.\begin{aligned} C_s &= \frac{C_{12} + C_{13}}{2} \\ C_a &= \frac{C_{12} - C_{13}}{2} \end{aligned}\right\} \qquad (5.34)$$

and
$$
\left.\begin{aligned}
K_{hs}(u|u',s) &= K_{hw}(u|u',s) + K_{h2w}(u|u',s) \\
K_{ha}(u|u',s) &= K_{hw}(u|u',s) - K_{h2w}(u|u',s)
\end{aligned}\right\}. \tag{5.35}
$$

Using the definition of symmetric-mode current, Equation (5.27) is re-written as

$$
\begin{aligned}
\int_{-L_4}^{L_1} I_z(u',s)K_{hf}(u|u',s)du' + 2\int_0^{L_2} I_s(u',s)K_{h1f}(u|u',s)du' &= C_1 \cosh \gamma u \\
+ C_2 \sinh \gamma u + \frac{1}{\gamma}\int_0^u S_z(\xi,s)\sinh \gamma(u-\xi)d\xi
\end{aligned} \tag{5.36}
$$

for $u \in [-L_4, L_1]$.

Equations (5.32), (5.33) and (5.36) are used to search for the natural modes by setting all forcing functions zero.

5.3 Induced Currents

5.3.1 Natural Modes

Natural modes are those solutions which exist when all the forcing functions are zero. We apply moment method to this problem by the partitioning as shown in Figure 5.3. Note that only one wing is needed due to symmetry.

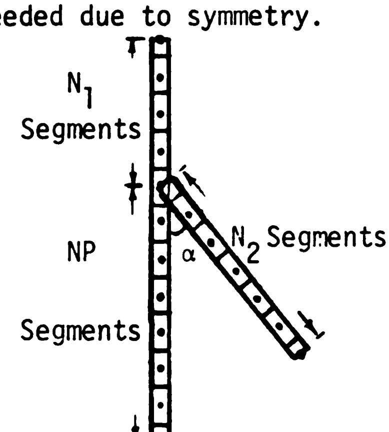

Figure 5.3. Partitioning of the crossed wires for moment method, only one wing is used due to symmetry.

For the antisymmetric modes only one wing is considered and only (5.33) is used. By applying moment method, Equation (5.33) becomes

$$A_a(s)I_a = 0 \tag{5.37}$$

where

$$I_a = \begin{bmatrix} I_1 \\ I_2 \\ \cdot \\ \cdot \\ \cdot \\ I_{N_2} \\ C_a \end{bmatrix}. \tag{5.38}$$

C_a is included as unknown while I_{N_2+1} is zero at wire end and thus dropped.

For the symmetric modes, both (5.32) and (5.36) are sloved. This is a system of coupled integral equations, moment method can still be used to solve the problem, however, much more effort should be taken with extreme care. The matrix form of Equations (5.32) and (5.36) is

$$A_s(s)I_s = 0 \tag{5.39}$$

where

$$I_s = \left[\begin{array}{l} \left.\begin{array}{l} C_1 \\ I_2 \\ \vdots \\ I_{Np+1} \end{array}\right\} \text{Wire \#4} \\ \left.\begin{array}{l} I_{Np+2} \\ \vdots \\ I_{NZ} \\ C_2 \end{array}\right\} \text{Wire \#1} \\ \left.\begin{array}{l} I_{NZ+2} \\ \vdots \\ I_{NT+1} \\ C_s \end{array}\right\} \text{Wire \#2} \\ I_{NT+3} \end{array}\right] \tag{5.40}$$

$NZ = Np+N_1$, $NT = Np+N_1+N_2$;

$I_1 = I_z(-L_4) = 0$, $I_{NZ+1} = I_z(L_1) = 0$ and $I_{NT+2} = I_2(L_2) = 0$

are replaced by the unknown constants;

$I_{Np+1} = I_z(0^-)$ while $I_{NT+3} = I_z(0^+)$.

The last row of $A_s(s)$ is to apply the boundary condition by using KCL at $u_z = 0$: $I_{Np+1} = I_{NT+3} + 2\, I_{NZ+2}$ since

$I_z(0^-) = I_z(0^+) + I_2(0^+) + I_3(0^+) = I_z(0^+) + 2I_2(0^+)$

for symmetric modes.

The boundary condition for the antisymmetric modes is automatically satisfied because $I_z(0^-) = I_z(0^+) + I_2(0^+) + I_3(0^+) = I_z(0^+)$ for antisymmetric modes and we don't have to apply KCL explicitly in $A_a(s)$.

The natural frequencies are those roots of $\det[A_s(s)] = 0$ and $\det[A_a(s)] = 0$ which yield the nontrivial solutions for Equations (5.37) and (5.39).

The roots are computed as in Chapter 4 by Newton's method. We first search for the roots of antisymmetric modes, because it is almost the same as those of the skew-coupled wires except that $d = 0$ and $I_2(u = 0) \neq 0$. For the testing purpose, $\frac{a_w}{L_2} = 0.01$, $\alpha = 90^o$ with $N_2 = 5n$ for the nth mode are used in the root-searching subroutine. As expected, the roots found are exactly the same as those of an isolated wire with $\frac{a}{L} = 0.005$ and number of partitions 10n for the nth mode except that only the first, third, fifth,---modes are found since these modes have the current distributions which are antisymmetric modes by our definition. We therefore use the roots just found as initial guesses and $N_2 = 5n$ for the nth mode to search for the roots of the special case with $\frac{a_w}{L_2} = 0.01$, $\alpha = 45^o$, $\frac{L_2}{L_4} = 0.8$ $\frac{L_1}{L_4} = 0.6$, $a_w = a_f$. If we define $L = L_4 + L_1 = 2L_2$ then the roots are:

$$S_1 = (-.0606 + j.9743)\,\frac{\pi c}{L}$$

$$S_2 = (-.2051 + j2.9720)\,\frac{\pi c}{L}$$

$$S_3 = (-.2974 + j4.9039)\,\frac{\pi c}{L}$$

$$S_4 = (-.3202 + j6.8690)\,\frac{\pi c}{L}$$

$$S_5 = (-.3719 + j8.8708)\,\frac{\pi c}{L} \quad .$$

We next search for the roots of symmetric mode. To compare with roots found in the existing literature [34] using EFIE and piecewise sinusoidal expansion, we computed the roots for cases with $L_4 + L_1 = L = 2L_2$, $a_w = a_f = a$, $\frac{a}{L} = 0.05$, $\alpha = 90^o$, and $\frac{L_1}{L_4} = 0.5, 0.6, \frac{2}{3}, 1.0$

with $N_2 = 8$ (in [34], $N_2 = 9$) and found that the comparison is very good. We then use the results of $\alpha = 90^o$ as initial guesses to search for the roots of $\alpha = 45^o$, $L_1 + L_4 = L = 2L_2$, $\frac{L_1}{L_4} = 0.8$, $a_w = a_f = a$, $\frac{a}{L_2} = 0.01$. Here are the roots:

$$S_1 = (-.0469 + j\ 0.9315)\ \pi c/L$$
$$S_2 = (-.0769 + j\ 1.0418)\ \pi c/L$$
$$S_3 = (-.1358 + j\ 2.6620)\ \pi c/L$$
$$S_4 = (-.1444 + j\ 3.3028)\ \pi c/L$$
$$S_5 = (-.1738 + j\ 3.9582)\ \pi c/L$$
$$S_6 = (-.2039 + j\ 4.7351)\ \pi c/L$$
$$S_7 = (-.2315 + j\ 5.3609)\ \pi c/L$$
$$S_8 = (-.2503 + j\ 6.8961)\ \pi c/L$$
$$S_9 = (-.2253 + j\ 7.1328)\ \pi c/L$$
$$S_{10} = (-.2915 + j\ 8.0685)\ \pi c/L\ .$$

Due to the tremendous computing cost, we use $N_2 = 8$ for the first five roots and $N_2 = 12$ for the rest (in [34], $N_2 = 9$ for all the roots). We tested with $N_2 = 20$ for S_6 and found that only 1.35% difference exists between $N_2 = 12$ and $N_2 = 20$. Therefore, the convergence of Hallen-type IE using pulse expansion is reasonably good and comparable to EFIE using piecewise sinusoidal expansion.

Natural mode currents are found by solving the homogeneous equation by the procedure as described in Section 4.3.1. Natural-mode current distributions for the first three antisymmetric modes are shown in Figures 5.4 and 5.5 for the real and imaginary parts respectively while Figures 5.6 and 5.7 show the symmetric modes. It should be noted

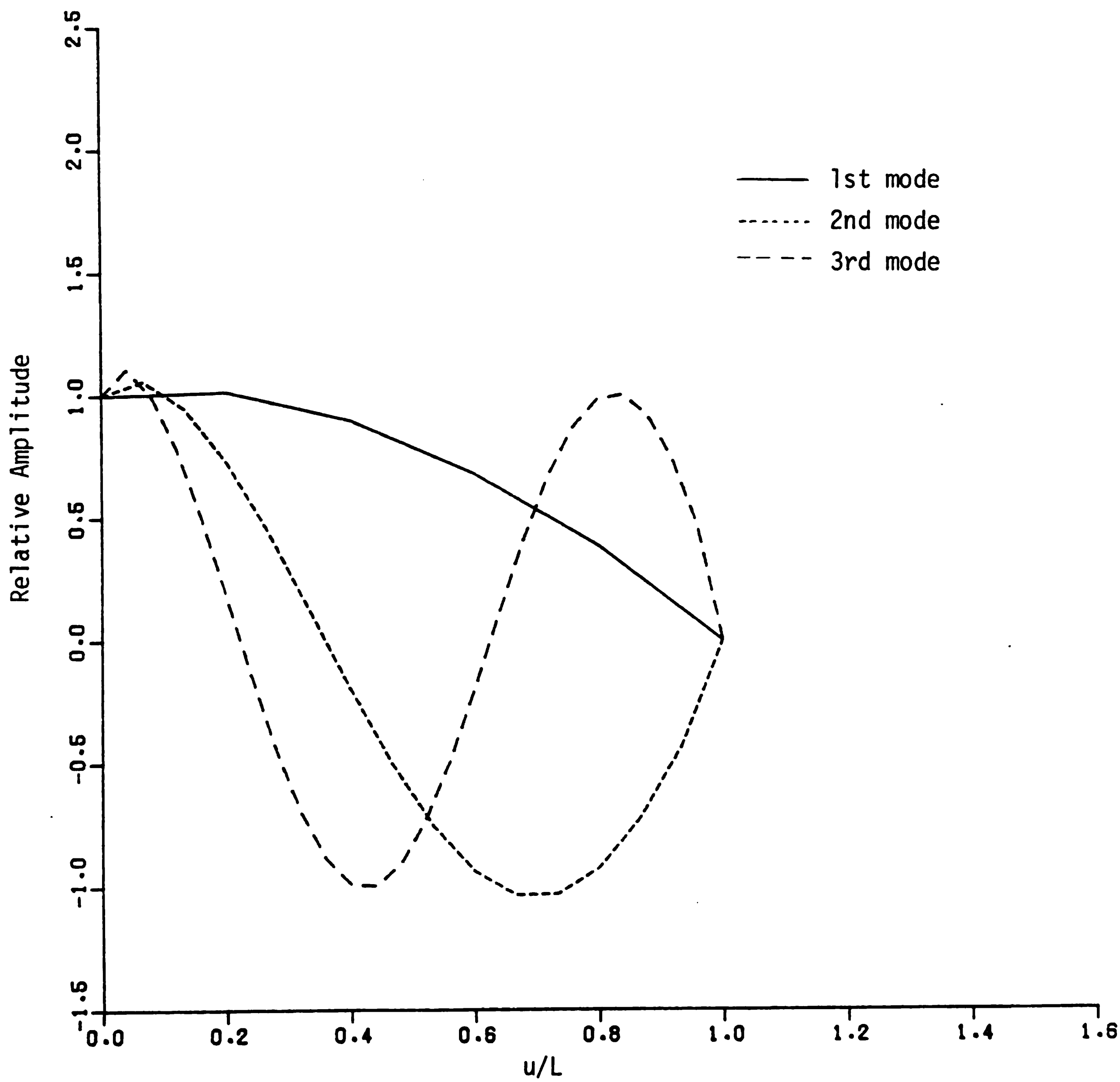

Figure 5.4. Real parts of the first three antisymmetric model currents on the wings.

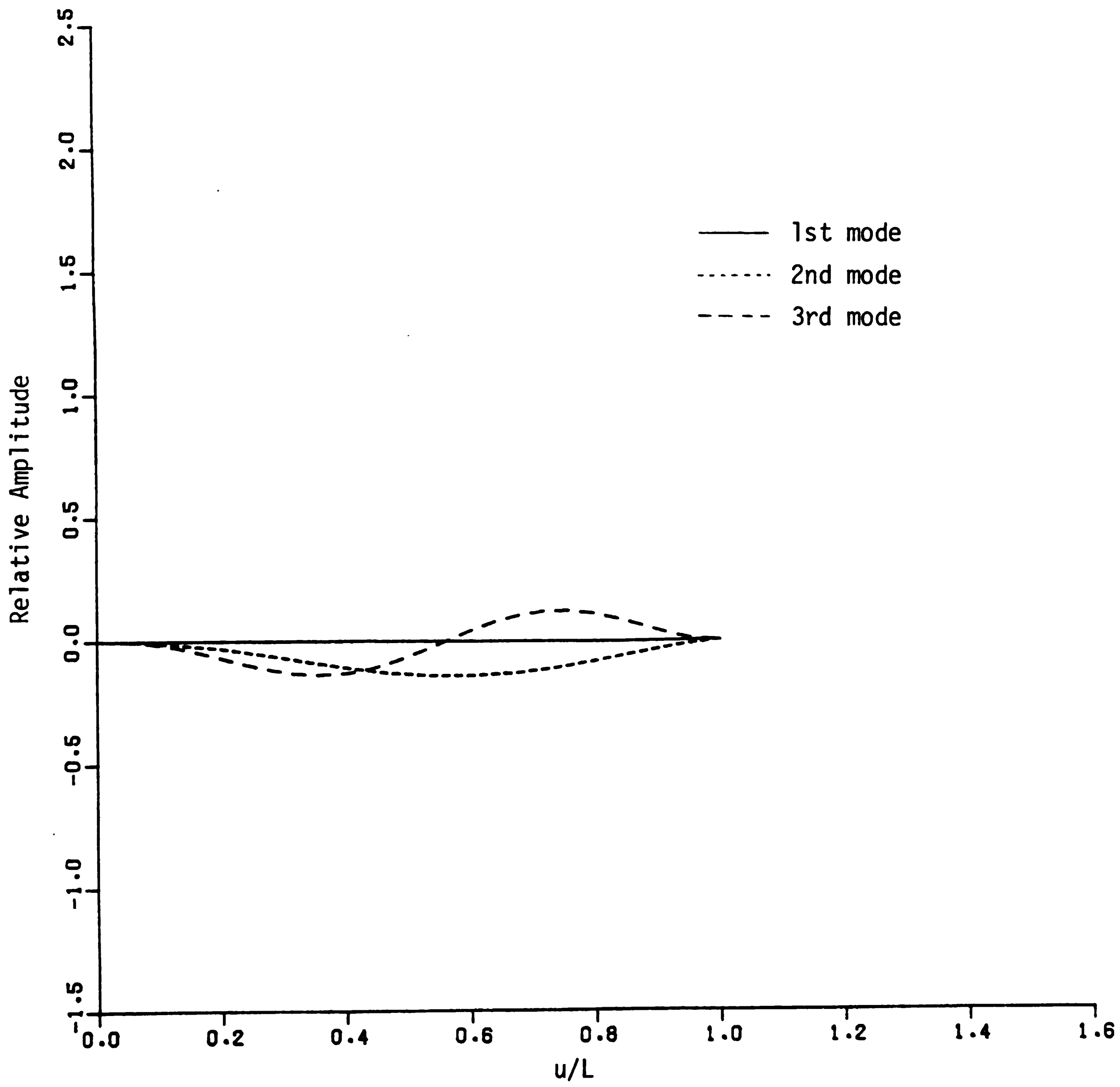

Figure 5.5. Imaginary parts of the first three antisymmetric modal currents on the wings.

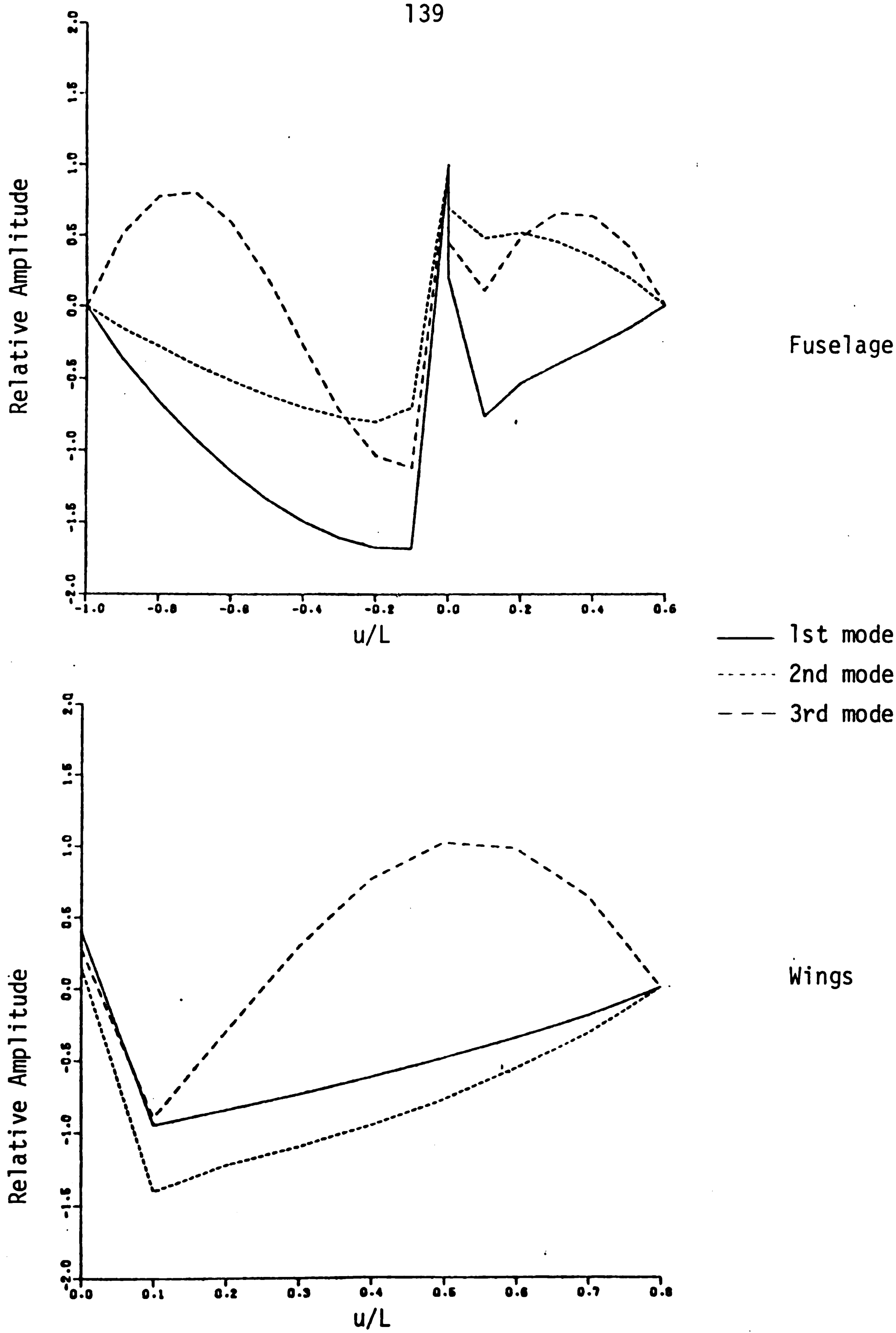

Figure 5.6. Real parts of the first three symmetric modal currents.

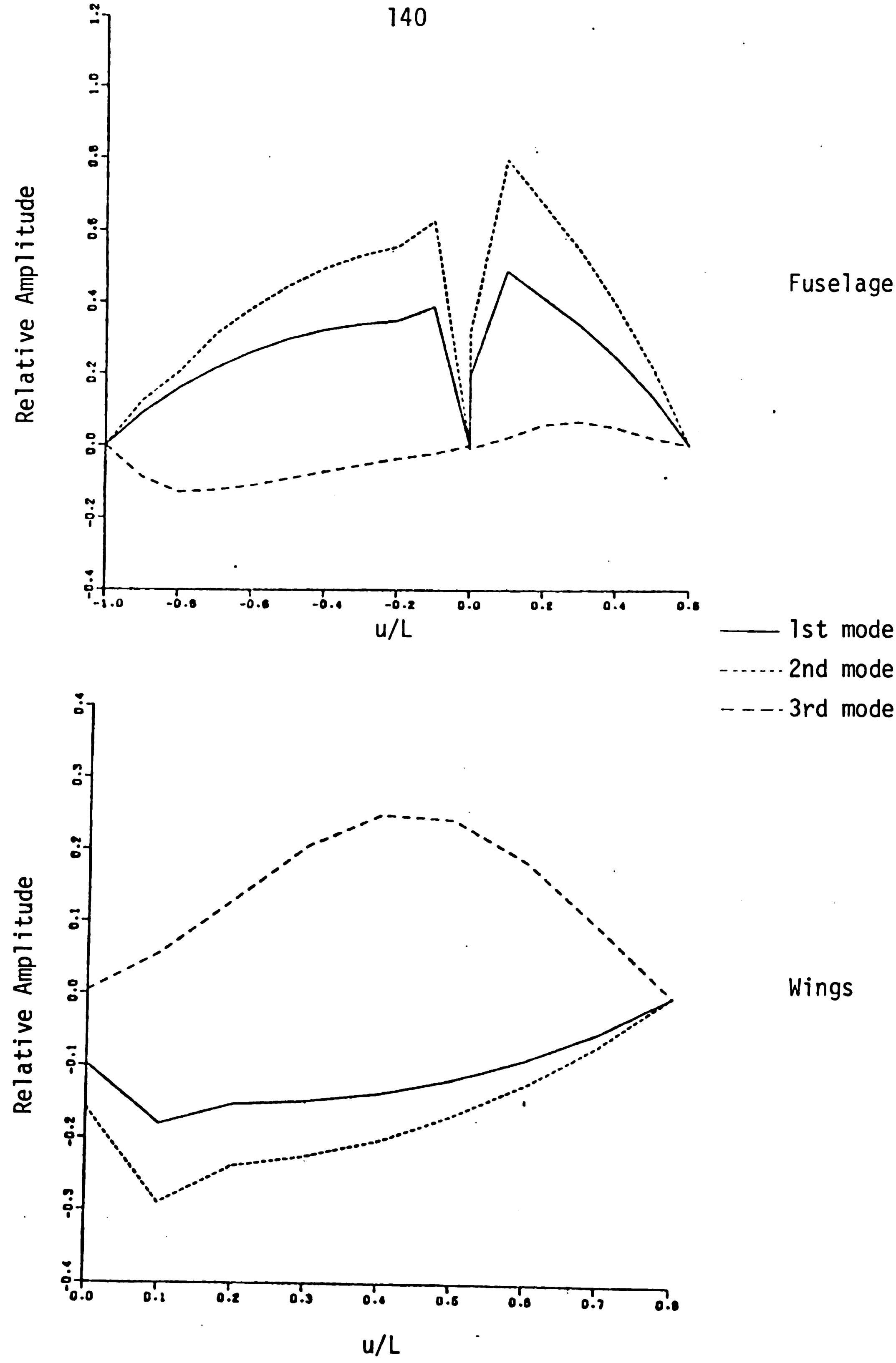

Figure 5.7. Imaginary parts of the first three symmetric modal currents.

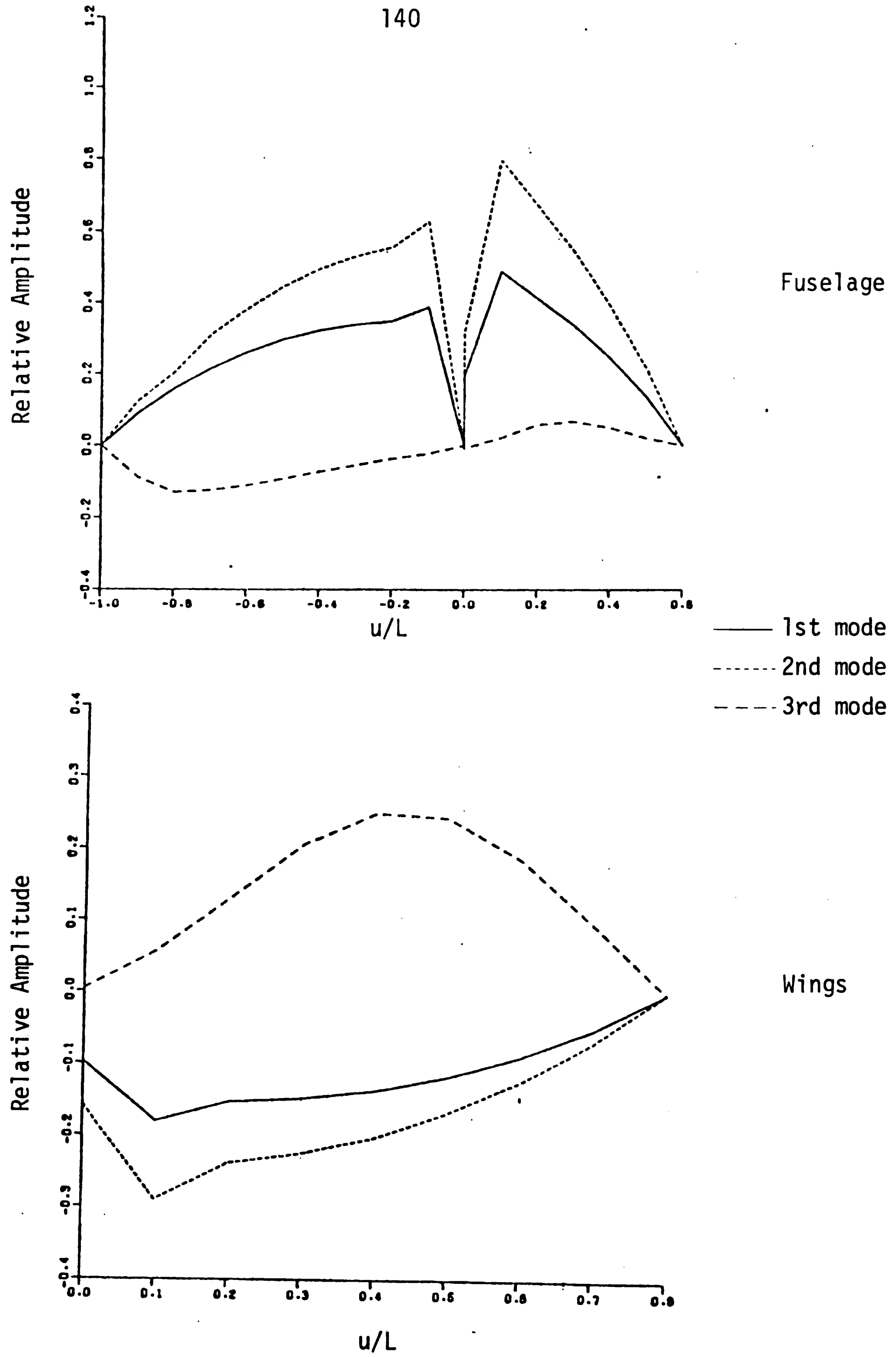

Figure 5.7. Imaginary parts of the first three symmetric modal currents.

that junction condition on KCL is satisfied.

5.3.2 Coupling Coefficients

The induced current as expressed in terms of SEM is

$$I(u,s) = \sum_{n=1}^{N} a_n(s)\nu_n(u)(s-s_n)^{-1} \tag{5.41}$$

where $\nu_n(u)$ is the distribution of the nth natural-mode current, and $a_n(s)$ is the coupling coefficient associated with the nth mode.

The coupling coefficient can be computed by using (2.37) with the integration performed over all the wires involved. Using the short hand notation introduced by Baum [9], Equation (2.37) can be rewritten as

$$a_n(s) = \frac{\langle S(u,s);\nu_n(u)\rangle}{\langle \nu_n(u);\ \frac{d}{ds}[K(u|u',s)];\ \nu_n(u')\rangle} \tag{5.42}$$

Where $<\ ,\ >$ is the inner product of functions seperated by the comma with integration over the common spatial coordinates; a symbol (dot product in (5.42)) above this comma indicates the type of multiplication used and the integration limit is over the object of interest. With this notation, we can always use Equation (5.42) to compute the coupling coefficients for both symmetric and antisymmetric modes without any confusion by knowing that for antisymmetric modes the domain is $u \in [0,L_2]$ while for symmetric modes the domain is over $u \in [0,L_2]$ for the wing and $u \in [-L_4,L_1]$ for the fuselage. In the following sections, we will consider symmetric and antisymmetric modes seperately. The kernel function in Equation (5.42) is the kernel function for the electric field integral equation.

5.3.3 Computation of Induced Currents for Antisymmetric-mode Excitation

For the antisymmetric-mode excitation as shown in Figure 5.2, the forcing functions are computed from Equations (5.5), (5.13) and (5.19) as

$$S_a(u,s) = \frac{1}{2}[S_2(u,s) - S_3(u,s)]$$

$$= - \epsilon os \sin\alpha\, e^{\gamma z \cos\varphi}\, \tilde{F}(s)$$

$$= - \epsilon os \sin\alpha\, e^{-\gamma u \cos\alpha \cos\varphi}\, \tilde{F}(s) \quad \text{for } 0 \leq u \leq L_2,$$

$$S_s(u,s) = 0 \qquad \text{for } 0 \leq u \leq L_2, \tag{5.43}$$

and $$S_z(u,s) = 0 \qquad \text{for } -L_4 \leq u \leq L_1 .$$

The kernel function for Equation (5.42) is

$$K_a(u|u',s) = - [\frac{\partial^2}{\partial u \partial u'} + \gamma^2]\frac{e^{-\gamma R_w}}{4\pi R_w} + [\frac{\partial^2}{\partial u \partial u'} + \gamma^2 \cos 2\alpha]\frac{e^{-\gamma R_{2w}}}{4\pi R_{2w}} . \tag{5.44}$$

Since (5.24) is the only equation we need to use [(5.15),(5.23) give us $I_z = I_s = 0$], the integration limits in (5.42) are therefore 0 and L_2.

The detailed computation of induced currents for this particular case is very similar to that for the coupled wires as shown in Chapter 4 except that the current at $u = 0$ is not necessarily zero any more. If we adopt the same notations and definitions used in Section 4.3.3, the only difference is that instead of $\sum_{2}^{M_n}(\ )$, we have $\sum_{2}^{M_n}(\ )$ + (half-segment contribution from I_{n1} at $u_2 = 0$) now.

The coupling coefficient can therefore expressed as

$$a_n(s) = \frac{N_n(s)}{D_n} \qquad (5.45)$$

where

$$N_n(s) = \sum_{i=2}^{M_n} I_{ni} \int_{(i-\frac{3}{2})\Delta_n}^{(i-\frac{1}{2})\Delta_n} [-\epsilon os \sin\alpha\, e^{-\gamma u \cos\alpha\cos\varphi}\, \tilde{F}(s)]du$$

$$+ I_{n1} \int_0^{\frac{\Delta_n}{2}} [-\epsilon os \sin\alpha\, e^{-\gamma u \cos\alpha\cos\varphi}\, \tilde{F}(s)]du$$

$$= -\frac{2\epsilon_o c\tan\alpha}{\cos\varphi}\tilde{F}(s) \sum_{i=1}^{M_n} I_{ni}\, e^{-\gamma u_{ni}\cos\alpha\cos\varphi} \sinh[\frac{\gamma\Delta_n}{2}\cos\alpha\cos\varphi]$$

$$-\frac{\epsilon_o c\tan\alpha}{\cos\varphi}\tilde{F}(s)\, I_{n1}(1-e^{-\gamma\frac{\Delta_n}{2}\cos\alpha\cos\varphi}) \qquad (5.46),$$

$$D_n = \sum_{t=1}^{M_n}\sum_{j=1}^{M_n} I_{ni}I_{nj}d_{nij} \equiv \frac{D'_n}{4\pi c} \qquad (5.47);$$

with $$d_{nij} = \int_{(i-\frac{3}{2})\Delta_n}^{(i-\frac{1}{2})\Delta_n}\int_{(j-\frac{3}{2})\Delta_n}^{(j-\frac{1}{2})\Delta_n} \frac{\partial}{\partial s}[K_a(u|u',s)]\Big|_{s=s_n} du'du \quad \text{for } i \neq 1 \text{ and } j \neq 1$$

$$\equiv (\frac{1}{4\pi c})d'_{nij}$$

and $d'_{nij} = I_{nij} - 2\gamma_n J_{nij} + \gamma_n^2 K_{nij}$ as defined in equations (4.28) - (4.31) by taking "-" sign for the antisymmetric mode. We consider only the half-segment contribution from current at junction for $i = 1$ or $j = 1$. Induced currents are thus expressed as

$$I_z(u,s) = 0$$
$$I_3(u,s) = -I_2(u,s), \qquad (5.48)$$

and $I_2(u,s) = \sum_{n=1}^{N} \frac{N_n(s)}{D_n} \nu_n(u)(s-s_n)^{-1}$.

5.3.4 Computation of Induced Currents for Symmetric-mode Excitation

For the symmetric-mode exciation as shown in Figure 5.2, the forcing functions are computed from Equations (5.5), (5.13) and (5.19) as

$$S_z(u,s) = -\epsilon os \sin\varphi\, \tilde{F}(s)\, e^{\gamma z \cos\varphi} = -\epsilon os \sin\varphi\, \tilde{F}(s)\, e^{\gamma u \cos\varphi}$$

$$\text{for} \quad u \in [-L_4, L_1],$$

$$S_s(u,s) = \tfrac{1}{2}[S_2(u,s) + S_3(u,s)]$$

$$= \epsilon os \sin\varphi \cos\alpha\, \tilde{F}(s)\, e^{\gamma z \cos\varphi} \tag{5.49}$$

$$= \epsilon os \sin\varphi \cos\alpha\, \tilde{F}(s)\, e^{-\gamma u \cos\alpha \cos\varphi}$$

$$\text{for} \quad u \in [0, L_2],$$

$$S_a(u,s) = 0 \qquad \text{for} \quad u \in [0, L_2].$$

The computation of coupling coefficients is now very complicated because there are two Equations, (5.15) and (5.23), with nontrivial currents, I_z and I_s, coupled together although Equation (5.24) can be dropped and $I_a = 0$ due to the vanishing of $S_a(u,s)$.

To simplify conceptually the complicated computation, let's rewrite the EFIE's (assuming $a_w = a_f = a$, therefore subscripts f and w are dropped) by some convenient notations as follows:

$$\left.\begin{aligned}
&<I_z,K>_z + <I_2,K_1>_2 + <I_3,K_1>_2 = S_z(u,s) \quad u\in[-L_1,L_4] \\
&<I_z,K_1>_z + <I_2,K>_2 + <I_3,K_2>_2 = S_2(u,s) \quad u\in[0,L_2] \\
&<I_z,K_1>_z + <I_2,K_2>_2 + <I_3,K>_2 = S_3(u,s) \quad u\in[0,L_2]
\end{aligned}\right\} \tag{5.50}$$

where $< >_z$ stands for the integration with respect to u' form $-L_4$ to L_1 while $< >_2$ is the integration form 0 to L_2.

The reason for showing all three EFIE's without considering the symmetry at this point is that Equations (5.50) can be considered as a single EFIE which is symmetric:

$$<\underline{I}, \underline{K}> = \underline{S} \tag{5.51}$$

where $\underline{I} = \begin{bmatrix} I_z \\ \hline I_2 \\ \hline I_3 \end{bmatrix}$ $\underline{S} = \begin{bmatrix} S_z \\ \hline S_2 \\ \hline S_3 \end{bmatrix}$ and $\underline{K} = \left[\begin{array}{c:c:c} k & K_1 & K_1 \\ \hdashline K_1 & K & K_2 \\ \hdashline K_1 & K_2 & K \end{array}\right]$.

Because $\underline{K}$ is, as a whole, a symmetric kernel, $\mu_n = \nu_n$ [definition of μ_n is illustrated in the footnote of Equation (2.37)], and (5.42) can therefore be used without changing the denominator to $<\mu_n(u); \frac{d}{ds}[K(u|u',s)]; \nu_n(u')>$.

The computation of Equation (5.42) is now conceptually easy. It can be reduced to the following form: (note that $I_2 = I_3$ and $S_2 = S_3$ for symmetric modes and $K_s = K + K_2$)

$$a_n(s) = \frac{<S_z;\nu_{zn}> + 2\ <S_2;\nu_{2n}>}{<\nu_{zn};\ \frac{d}{ds}\ K;\ \nu_{zn}> + 4<\nu_{zn};\ \frac{d}{ds}\ K_1;\ \nu_{2n}> + 2<\nu_2,\ \frac{d}{ds}\ K_s,\nu_2>} \tag{5.52}$$

where $\nu_n = \begin{bmatrix} \nu_{zn} \\ --- \\ \nu_{2n} \\ --- \\ \nu_{3n} \end{bmatrix}$ and $\nu_{2n} = \nu_{3n}$ for symmetric modes.

It should be noted that

$$<\nu_{zn};\ \frac{d}{ds}K_1;\ \nu_{2n}> = \int_{-L_4}^{L_1}\int_0^{L_2} \nu_{zn}(u)\nu_{2n}(u')\frac{d}{ds}K_1(u|u',s)du'du.$$

Equation (5.52) can be rewritten as (refer to Figure 5.3 with $NP = M_{4n}$, $N_1 = M_{1n}$ and $N_2 = M_{2n}$ for the nth mode)

$$a_n(s) = \frac{N_n(s)}{D_n} \tag{5.53}$$

where $$N_n(s) = N_{zn}(s) + N_{2n}(s) = N_{4n}(s) + N_{1n}(s) + N_{2n}(s) \tag{5.54}$$

$$N_{4n}(s) \equiv <S_z;\ \nu_{zn}> \quad \text{for} \quad u \in [-L_4,0]$$

$$\equiv <S_z;\ \nu_{4n}>$$

$$= -\epsilon os \sin\varphi\ \tilde{F}(s)\{\sum_{i=2}^{M_{4n}} I_{4ni}\int_{(i-M_{4n}-\frac{3}{2})\Delta_n}^{(i-M_{4n}-\frac{1}{2})\Delta_n} e^{\gamma u\cos\varphi}\,du$$

$$+ I_{4n(M_{4n}+1)}\int_{-\frac{\Delta_n}{2}}^{0} e^{\gamma u\cos\varphi}\,du\} \tag{5.55}$$

$$N_{1n}(s) \equiv \langle S_z; \nu_{zn}\rangle \quad \text{for} \quad u \in [0,L_1]$$

$$\equiv \langle S_z; \nu_{1n}\rangle$$

$$= -\epsilon os \sin\varphi\, \tilde{F}(s)\, \{ \sum_{i=2}^{M_{1n}} I_{1ni} \int_{(i-\frac{3}{2})\Delta_n}^{(i-\frac{1}{2})\Delta_n} e^{\gamma u \cos\varphi}\, du$$

$$+ I_{1n1} \int_0^{\frac{\Delta_n}{2}} e^{\gamma u \cos\varphi}\, du\} \tag{5.56}$$

and

$$N_{2n}(s) \equiv 2\langle S_s; \nu_{2n}\rangle$$

$$= 2\, \epsilon os \sin\varphi \cos\alpha\, \tilde{F}(s)\{ \sum_{i=2}^{M_{2n}} I_{2ni} \int_{(i-\frac{3}{2})\Delta_n}^{(i-\frac{1}{2})\Delta_n} e^{-\gamma u \cos\alpha\cos\varphi}\, du$$

$$+ I_{2n1} \int_0^{\frac{\Delta_n}{2}} e^{-\gamma u \cos\alpha\cos\varphi}\, du\} \tag{5.57};$$

D_n is defined similar to Equation (5.47) with three terms involved.

Induced currents can now be expressed as

$$\left.\begin{aligned} I_z(u,s) &= \sum_{n=1}^{N} \frac{N_n(s)}{D_n}\, \nu_{zn}(u)\, (s-s_n)^{-1} \\ I_2(u,s) = I_3(u,s) &= \sum_{n=1}^{N} \frac{N_n(s)}{D_n}\, \nu_{2n}(u)\, (s-s_n)^{-1} \end{aligned}\right\}. \tag{5.58}$$

5.4 Backscattered Field

The scattered field in the radiation-zone can be determined from the method discussed in Section 4.4 by linear superposition. It is therefore obvious that

$$\tilde{\vec{E}}^s(\vec{r},s) = \hat{\theta}\, s\, \tilde{A}_z^s \sin\theta + \hat{\theta}_2\, s\, \tilde{A}_2^s \sin\theta_2 + \hat{\theta}_3\, s\, \tilde{A}_3^s \sin\theta_3 \tag{5.59}$$

where $(\hat{\theta}_1,\hat{\theta}_2,\hat{\theta}_3)$ and $(\theta_1,\theta_2,\theta_3)$ are defined in the same way as indicated in Figure 4.19.

In the following two sections we will discuss the backscattered fields of symmetric- and antisymmetric-mode excitations separately.

5.4.1 Backscattered Field from the Antisymmetric-mode Excitation

This case is very similar to that of the skew-coupled wires in Chapter 4 except $d = 0$ and $I_2 = -I_3 \neq 0$ at $u = 0$.

The vector potentials are expressed as [refer to (4.38) and (4.39)]

$$\left.\begin{aligned}
\tilde{A}_2^s &= \frac{\mu_o}{4\pi}\,\frac{e^{-\gamma R_\infty}}{R_\infty}\int_0^{L_2} I_2(u',s)e^{\gamma u' \cos\theta_2}\,du' \\
\tilde{A}_3^s &= -\frac{\mu_o}{4\pi}\,\frac{e^{-\gamma R_\infty}}{R_\infty}\int_0^{L_2} I_2(u',s)e^{\gamma u' \cos\theta_3}\,du' \\
\tilde{A}_z^s &= 0
\end{aligned}\right\} , \tag{5.60}$$

where

$$\left.\begin{aligned}
\cos\theta_2 &= [\hat{u}_2\cdot(-\hat{k})] = -\cos\varphi\cos\alpha \\
\cos\theta_3 &= [\hat{u}_3\cdot(-\hat{k})] = -\cos\varphi\cos\alpha
\end{aligned}\right\} . \tag{5.61}$$

And from Equation (4.41),

$$\left.\begin{aligned}
\hat{\theta}_2\sin\theta_2 &= [\hat{u}_2 \times (-\hat{k})]\times(-\hat{k}) = \hat{x}\sin\varphi\cos\varphi\cos\alpha - \hat{y}\sin\alpha + \hat{z}\sin^2\varphi\cos\alpha \\
\hat{\theta}_3\sin\theta_3 &= [\hat{u}_3 \times (-\hat{k})]\times(-\hat{k}) = \hat{x}\sin\varphi\cos\varphi\cos\alpha + \hat{y}\sin\alpha + \hat{z}\sin^2\varphi\cos\alpha
\end{aligned}\right\} \tag{5.62}$$

Substitutions of Equations (5.60)-(5.62) into Equation (5.59) yield

$$\begin{aligned}\tilde{\vec{E}}^{bs}(\vec{r},s) &= -2s\ \tilde{A}_2^s(\vec{r},s)\sin\alpha\ \hat{y} \\ &= -2\sin\alpha\ s\ \tilde{A}_2^s(\vec{r},s)\hat{\zeta}.\end{aligned} \tag{5.63}$$

5.4.2 Backscattered Field from the Symmetric-mode Excitation

All three wires contribute to the scattered field, this is a much more complicated case although conceptually easy.

The vector potentials are expressed as [refer to Equations (4.38) and (4.39)]

$$\left.\begin{aligned}\tilde{A}_z^s &= \frac{\mu_o}{4\pi}\frac{e^{-\gamma R_\infty}}{R_\infty}\int_{-L_4}^{L_1} I_z(u',s)e^{\gamma u'\cos\theta}\,du' \\ \tilde{A}_2^s &= \frac{\mu_o}{4\pi}\frac{e^{-\gamma R_\infty}}{R_\infty}\int_0^{L_2} I_2(u',s)e^{\gamma u'\cos\theta_2}\,du' \\ \tilde{A}_3^s &= \frac{\mu_o}{4\pi}\frac{e^{-\gamma R_\infty}}{R_\infty}\int_0^{L_2} I_2(u',s)e^{\gamma u'\cos\theta_3}\,du'\end{aligned}\right\} \tag{5.64}$$

where

$$\left.\begin{aligned}\text{Cos}\ \theta &= [\hat{u}_z\cdot(-\hat{k})] = \cos\varphi \\ \text{Cos}\ \theta_2 &= \cos\theta_3 = -\cos\varphi\cos\alpha\end{aligned}\right\} \tag{5.65}$$

Equation (4.41) yields

$$\left.\begin{aligned}\hat{\theta}\sin\theta &= [\hat{u}_z x(-\hat{k})]x(-\hat{k}) = -\hat{x}\cos\varphi\sin\varphi - \hat{z}\sin^2\varphi \\ \hat{\theta}_2\sin\theta_2 &= \hat{x}\sin\varphi\cos\varphi\cos\alpha - \hat{y}\sin\alpha + \hat{z}\sin^2\varphi\cos\alpha \\ \hat{\theta}_3\sin\theta_3 &= \hat{x}\sin\varphi\cos\varphi\cos\alpha + \hat{y}\sin\alpha + \hat{z}\sin^2\varphi\cos\alpha\end{aligned}\right\} \tag{5.66}$$

Substitute Equations (5.64)-(5.66) into Equation (5.59), we can obtain the following result:

$$\tilde{\vec{E}}^{bs}(\vec{r},s) = [-\hat{x}\cos\varphi\sin\varphi - \hat{z}\sin^2\varphi]s\,\tilde{A}_z^s(\vec{r},s) + 2[\hat{x}\sin\varphi\cos\varphi\cos\alpha$$

$$+ \hat{z}\sin^2\varphi\cos\alpha]s\,\tilde{A}_2^s(\vec{r},s)$$

$$= s\sin\varphi\,[\hat{x}\cos\varphi + \hat{z}\sin\varphi][2\cos\alpha\,\tilde{A}_2^s(\vec{r},s) - \tilde{A}_z^s(\vec{r},s)]$$

$$= s\sin\varphi\,[2\,\tilde{A}_2^s(\vec{r},s)\cos\alpha - \tilde{A}_z^s(\vec{r},s)]\hat{\zeta}. \qquad (5.67)$$

It is obvious that when α equals 90^o, the only contribution comes from fuselage, and zero-angle incidence results in zero response for the symmetric-mode exictation.

5.5 Impulse Responses

By setting $\tilde{F}(s) = 1$ in Equations (5.63) and (5.67), we can compute the impulse responses of the backscattered fields for both symmetric- and antisymmetric-mode excitations. In the following sections, $\alpha = \varphi = 45^o$, $a_w = a_f = a$, $L_1 + L_4 = L = 2L_2$, $a/L_2 = 0.01$, $\frac{L_1}{L_4} = 0.6$ and $\frac{L_2}{L_4} = 0.8$ are assumed.

5.5.1 Impulse Response to the Antisymmetric-mode Excitation

By working out the detail of Section 5.4.1, the backscattered field due to the antisymmetric-mode excitation can be expressed as

$$\tilde{\vec{E}}^{bs}(\vec{r},s) = \hat{\zeta}\,A\,\frac{e^{-\gamma R_\infty}}{R_\infty}\,F(t)*h(t) \qquad (5.68)$$

where

$$A = 4c\,\frac{\tan^2\alpha}{\cos^2\varphi} = 8c\ , \qquad (5.69)$$

and $$h(t) = \text{Impulse response}$$

$$= L^{-1}\{\mathrm{Re}[H_c(s)]\} \quad ;$$

with $$H_c(s) = \sum_{n=1}^{N} \frac{1}{D_n'(s-s_n)} [4 \sum_{i=2}^{M_n} \sum_{k=2}^{M_n} I_{ni} I_{nk}\, e^{-\gamma(u_{ni}+u_{nk})/2} \sinh^2(\frac{\gamma\Delta_n}{4})$$

$$+ 4I_{n1}\sinh(\frac{\gamma\Delta_n}{4})(1-e^{-\gamma\Delta_n/4})(\sum_{i=2}^{M_n} I_{ni}\, e^{-\gamma u_{ni}/2}) + I_{n1}^2(1-e^{-\gamma\Delta_n/4})^2] \quad (5.70)$$

It is easy to see from the first term in the bracket of (5.70) that the early-time period of $h(t)$ is $t \leq \frac{L_2}{c}$ which is the two-way transit time. From now on we would like to concentrate on the late-time response upon which the waveform-synthesis method is based, the "Class-1" coupling coefficients are therefore applied with all γ's replaced by γ_n for the nth mode. Physically, this means that all sources corresponding to different segments are "turned on" and the bracket quantity becomes a constant coefficient. The impulse response is thus expressed as

$$h(t) = \{\mathrm{Re} \sum_{n=1}^{N} C_n e^{s_n t}\} \text{---for } t \geq \frac{L_2}{c} \quad (5.71)$$

where $$C_n = \frac{1}{D_n'} [4 \sum_{i=2}^{M_n} \sum_{k=2}^{M_n} I_{ni} I_{nk} e^{-\gamma_n(u_{ni}+u_{nk})/2} \sinh^2(\frac{\gamma_n\Delta_n}{4})$$

$$+ 4I_{n1}\sinh(\frac{\gamma_n\Delta_n}{4})(1-e^{-\gamma_n\Delta_n/4})(\sum_{i=2}^{M_n} I_{ni} e^{-\gamma_n u_{ni}/2})$$

$$+ I_{n1}^2(1-e^{-\gamma_n\Delta_n/4})^2]$$

$$= \frac{1}{D_n'} [2 \sinh (\frac{\gamma_n\Delta_n}{4}) \sum_{i=2}^{M_n} I_{ni} e^{-\gamma_n u_{ni}/2} + I_{n1}(1-e^{-\gamma_n\Delta_n/4})]^2 . \quad (5.72)$$

With the natural modes computed in Section 5.3.1, the impulse response of Equation 5.71 is shown in Figure 5.8.

5.5.2 Impulse Response to the Symmetric-mode Excitation

The backscattered field due to the symmetric-mode excitation in Section 5.4.2 can be expressed as

$$\tilde{E}^{bs}(\vec{r},s) = \hat{\zeta}\, B\, \frac{e^{-\gamma R_\infty}}{R_\infty}\, F(t)*h(t) \tag{5.73}$$

where
$$B = 8\, c \tan^2 \varphi = 8c \tag{5.74}$$

and
$$h(t) = \text{Impulse response}$$
$$= L^{-1}\{\mathrm{Re}[H_c(s)]\}$$

with
$$H_c(s) = \sum_{n=1}^{N} \frac{1}{D_n'(s-s_n)} \Big[2 \sum_{i=2}^{M_{2n}} I_{2ni}\, e^{-\gamma u_{2ni}/2} \sinh\!\left(\frac{\gamma\Delta_n}{4}\right)$$
$$+ I_{2n1}\left(1-e^{-\frac{\gamma\Delta_n}{4}}\right) - \sum_{i=2}^{M_{1n}} I_{1ni}\, e^{\gamma u_{1ni}/\sqrt{2}} \sinh\!\left(\frac{\gamma\Delta_n}{2\sqrt{2}}\right)$$
$$- \frac{I_{1n1}}{2}\left(e^{\frac{\gamma\Delta_n}{2\sqrt{2}}} - 1\right) - \sum_{i=2}^{M_{4n}} I_{4ni}\, e^{\gamma u_{4ni}/\sqrt{2}} \sinh\left(\frac{\gamma\Delta_n}{2\sqrt{2}}\right)$$
$$- \frac{I_{4n(M_{4n}+1)}}{2}\left(1-e^{-\frac{\gamma\Delta_n}{2\sqrt{2}}}\right)\Big]^2 \equiv \sum_{n=1}^{N} \frac{C_n'(s)}{D_n'(s-s_n)} \tag{5.75}$$

where
$$\left.\begin{aligned} u_{2ni} &= (i-1)\Delta_n \\ u_{1ni} &= (i-1)\Delta_n \\ u_{4ni} &= (i-M_{4n}-1)\Delta_n . \end{aligned}\right\} \tag{5.76}$$

The fact that $C_n'(s)$ in (5.75) is square of the bracket quantity is not a coincidence, as a matter of fact, $C_n'(s) \propto N_n^2(s)$: this is true for all wire targets discussed in Chapter 4 and this chapter. This is

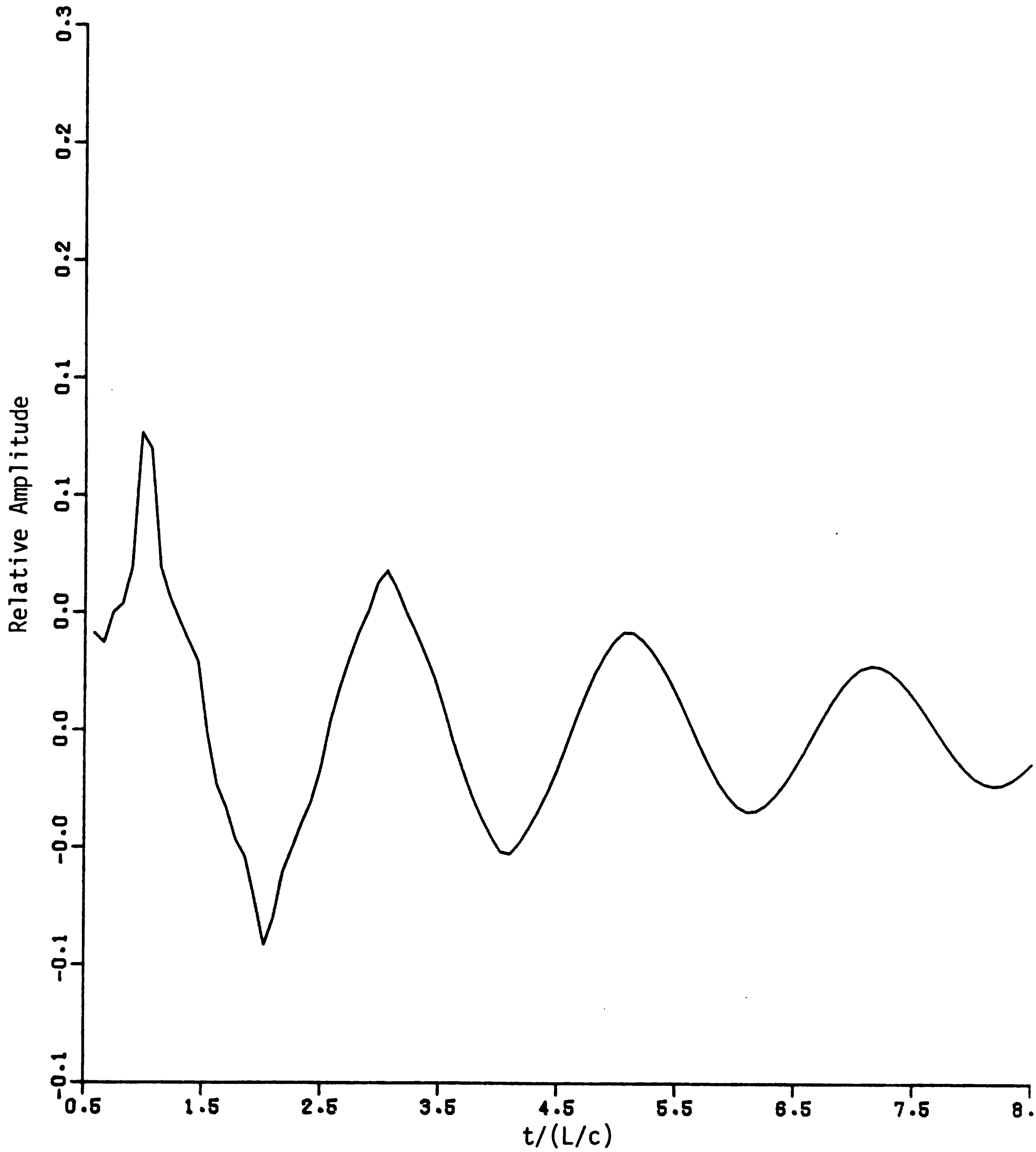

Figure 5.8. Backscattered-field impulse response of a cross-wire target with $a/L_2 = 0.01$, $\alpha = 45^o$, $a_w = a_f = a$, $L_1 + L_4 = L = 2L_2$ and $\frac{L_1}{L_4} = 0.6$ due to the antisymmetric-mode excitation with aspect-angle $\varphi = 45^o$.

because $N_n(s) = \langle S(u,s); \nu_n(u)\rangle$ and

$$\tilde{E}^{bs}(\vec{r},s) \propto \tilde{A}(\vec{r},s) \propto \int I(u',s)e^{\gamma u' \cos\theta} du'$$

$$= \sum_{n=1}^{N} \int \frac{N_n(s)}{D_n'(s-s_n)} \nu_n(u')e^{\gamma u'[\hat{u}\cdot(-\hat{k})]} du'$$

$$= \sum_{n=1}^{N} \frac{N_n(s)}{D_n'(s-s_n)} \int \nu_n(u')e^{-\gamma(\vec{r}'\cdot\hat{k})} du'$$

$$\propto \sum_{n=1}^{N} \frac{N_n(s)}{D_n'(s-s_n)} \int \nu_n(u')S(u',s)du'$$

$$= \sum_{n=1}^{N} \frac{N_n^2(s)}{D_n'(s-s_n)} \propto \sum_{n=1}^{N} \frac{C_n'(s)}{D_n'(s-s_n)}$$

Notice that $S(u',s) \propto \tilde{E}^{i}_{tan}(u',s) \propto e^{-\gamma(\vec{r}'\cdot\hat{k})}$ is used to show the above interesting relation and this is ture only when we consider the backscattered field for which $\cos\theta = [\hat{u}\cdot(-\hat{k})]$ in the vector potential integration (for any direction scattered field $-\hat{k}$ should be replaced by the appropriate unit vector).

From Equation (5.75) it is easy to see that the early-time period is $t \leq 2\,T_t$, T_t = two-way transit time = $\max\{\frac{L_2}{c}, \sqrt{2}\,\frac{L_1+L_4}{c}\} = \sqrt{2}\,\frac{L_1+L_4}{c} = \sqrt{2}\,\frac{L}{c}$ this is twice the time for the incident waveform to sweep across the fuselage: during this period it also sweeps across the wing because it only takes $\frac{1}{2}\frac{L_2}{c}$ to pass the wings (this is the one-way transit time for the antisymmetric-excitation in which only the wings are involved). The late-time impulse response can therefore be expressed as

$$h(t) = \mathrm{Re}\{\sum_{n=1}^{N} c_n\, e^{s_n t}\} \text{---} \quad \text{for } t \geq \sqrt{2}\,\frac{L}{c} \tag{5.77}$$

where $$c_n = \frac{C_n(s_n)}{D_n'} . \tag{5.78}$$

The numerical result as computed by Equation (5.77) and the natural modes in Section 5.3.2 is plotted in Figure 5.9.

5.6 Incident-Waveform Synthesis for Single-Mode Excitation and its Application to Target Discrimination

Incident waveform required to excite single-mode backscatter consisting of purely the first or the second natural modes of the crossed wires target are synthesized according to the procedure described in Chapter 2. The finite duration is chosen as one period of the first antisymmetric mode, i.e., $T_e = 1/f_1 = \frac{2\pi}{0.9743\pi c/L} = 2.0528\frac{L}{c}$. The required waveform to excite the first antisymmetric mode is shown in Figure 5.10. The return backscattered waveform can be computed as the convolution of waveforms in Figures 5.8 and 5.10. Figure 5.11 is the result of this convolution along with the return waveform from the wrong target with 10% shorter wings. It is easy to see that the return from the right target displays single-mode response after the late-time begins at $t = 2T_t + T_e = (0.5 + 2.0528)\frac{L}{c}$. However, the return from the wrong target can not be identified as the single-mode.

For the symmetric-mode excitation, the required waveform to excite the first mode is shown in Figure 5.12, and Figure 5.13 is the returns from right and wrong targets. This time the late-time begins at $t = 2T_t + T_e = (\sqrt{2} + \frac{2\pi}{0.9315\pi})\frac{L}{c}$. Similar results of required waveform for the second symmetric mode and its radar returns from right and wrong targets are shown in Figures 5.14 and 5.15.

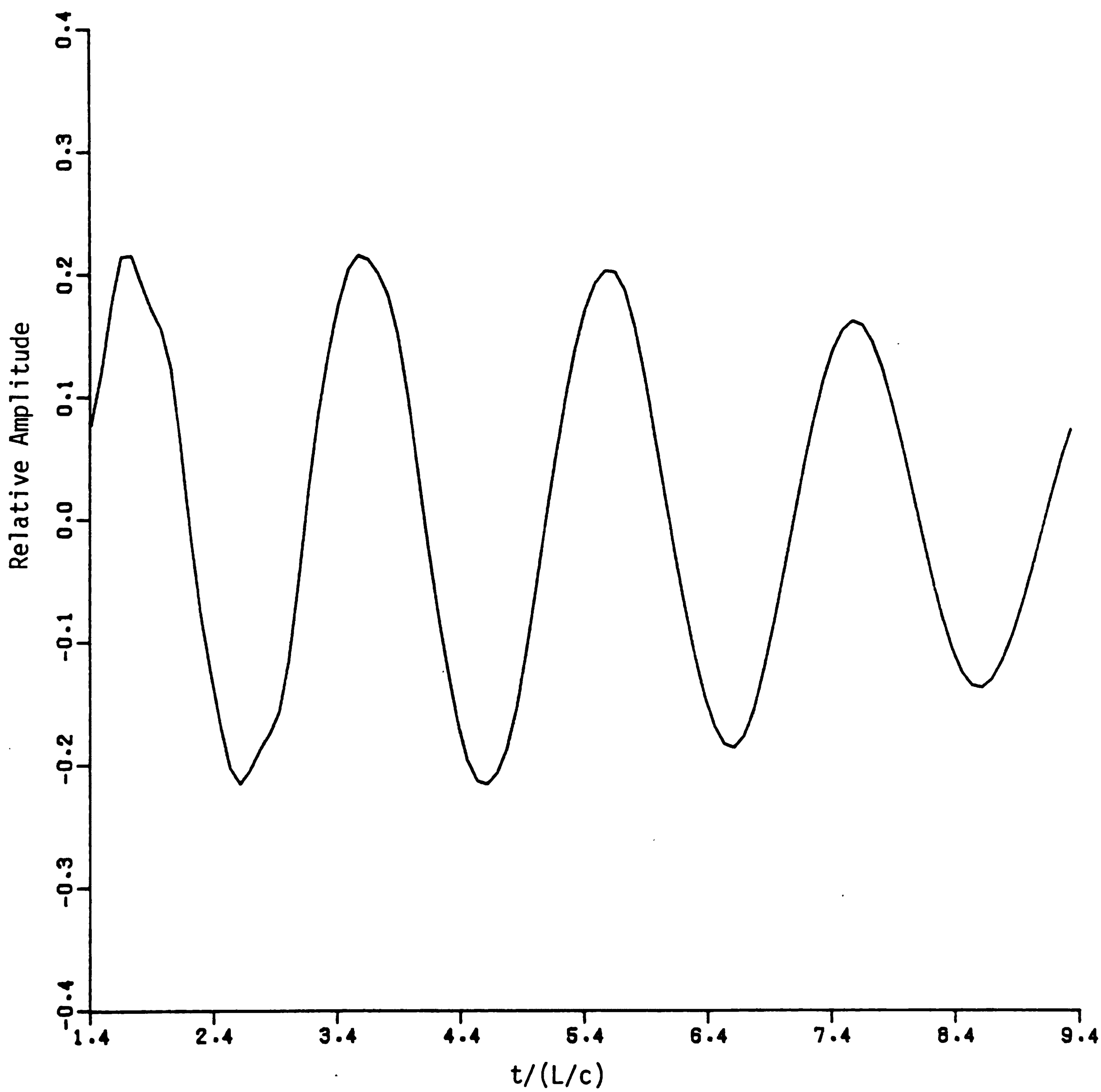

Figure 5.9. Backscattered-field impulse response of a cross-wire target with $a/L_2 = 0.01$, $\alpha = 45^o$, $a_w = a_f = a$, $L_1 + L_4 = L = 2L_2$ and $\frac{L_1}{L_4} = 0.6$ due to the symmetric-mode excitation with aspect-angle $\varphi = 45^o$.

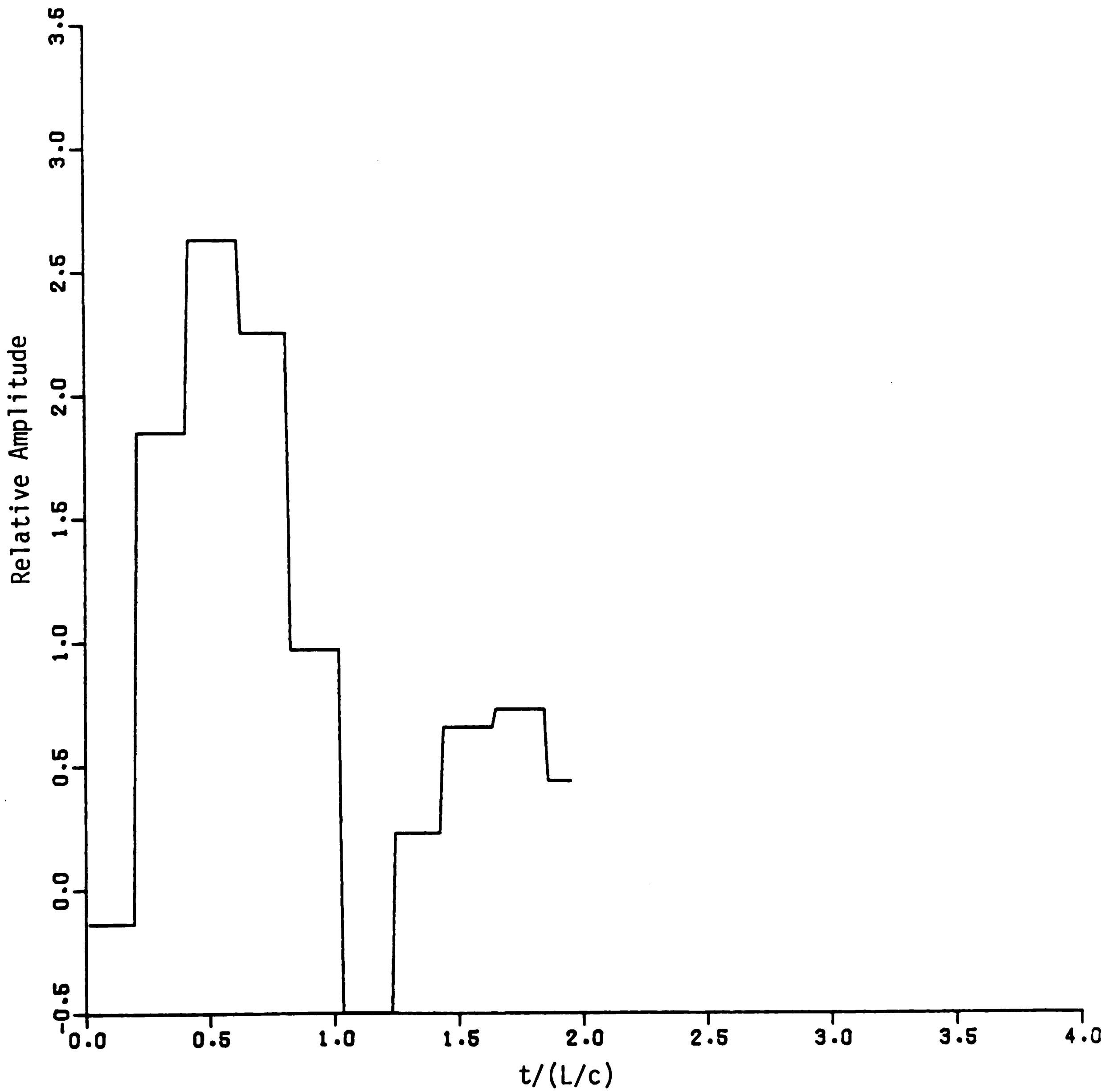

Figure 5.10. The required incident waveform to excite the first anti-symmetric mode of the target described in Section 5.5.

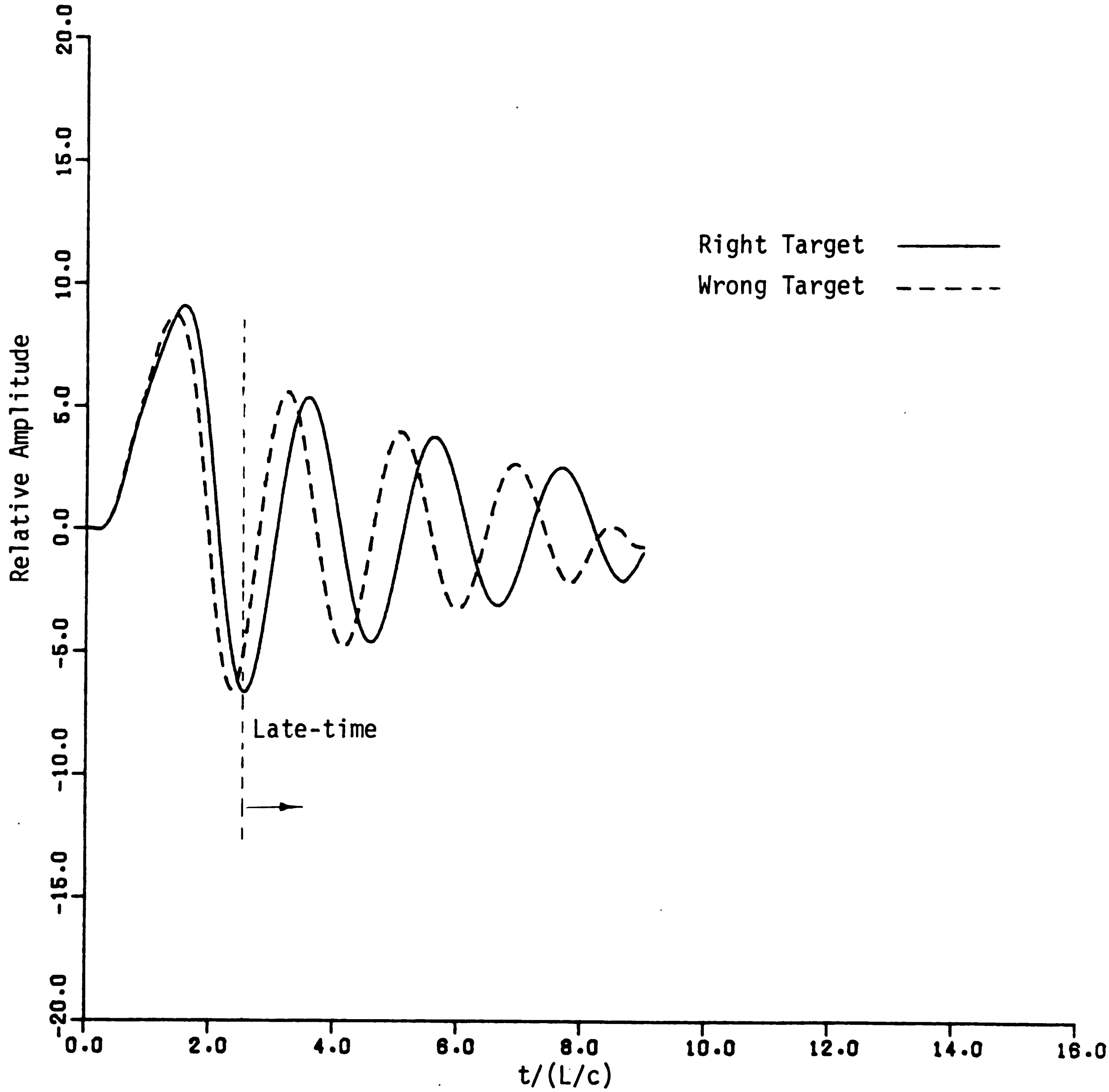

Figure 5.11. Return waveforms from right target and target with 10% shorter length when these targets are illuminated by the synthesized waveform of Figure 5.10 with antisymmetric excitation.

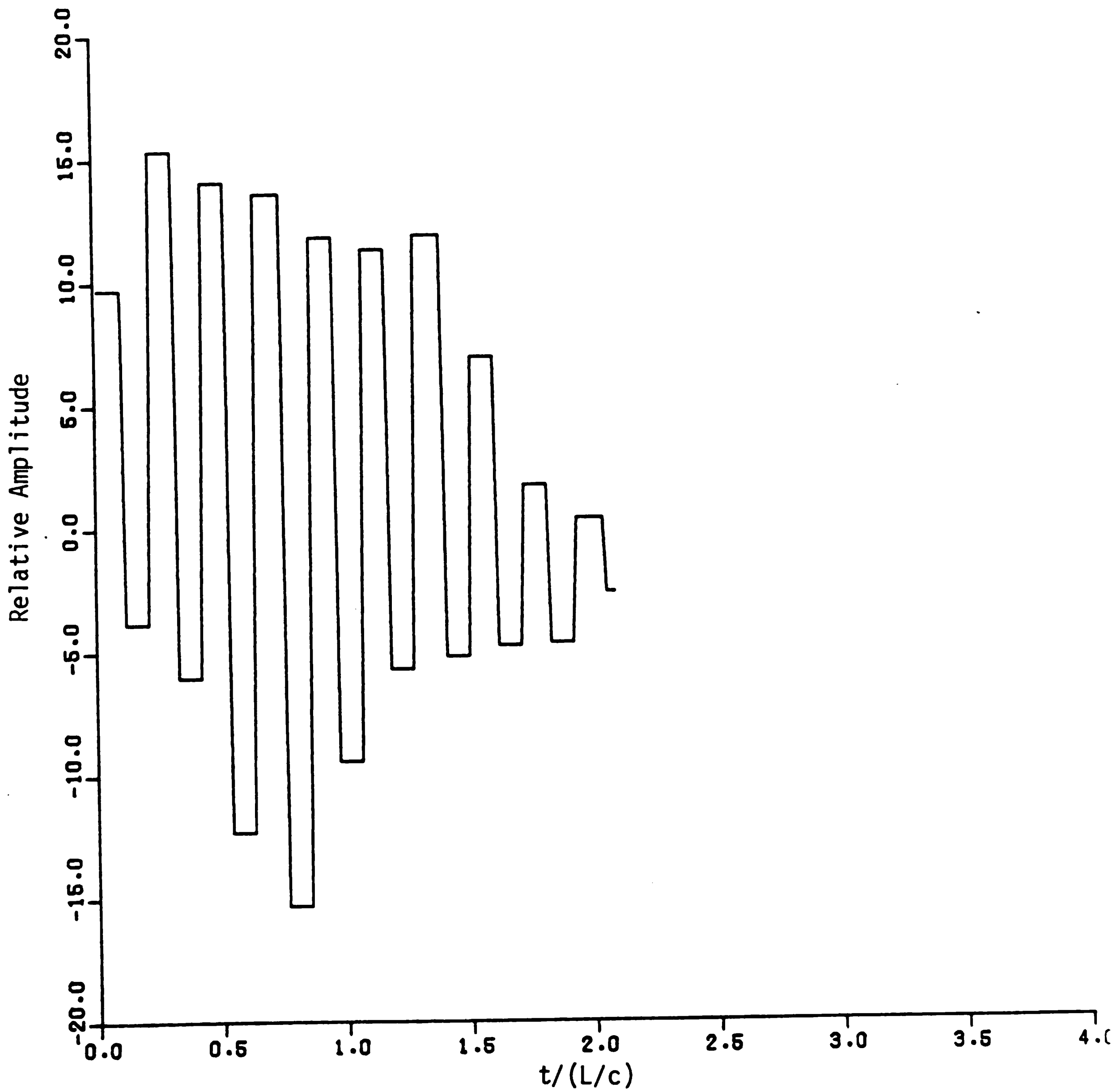

Figure 5.12. The required incident waveform to excite the first symmetric mode of target described in Section 5.5.

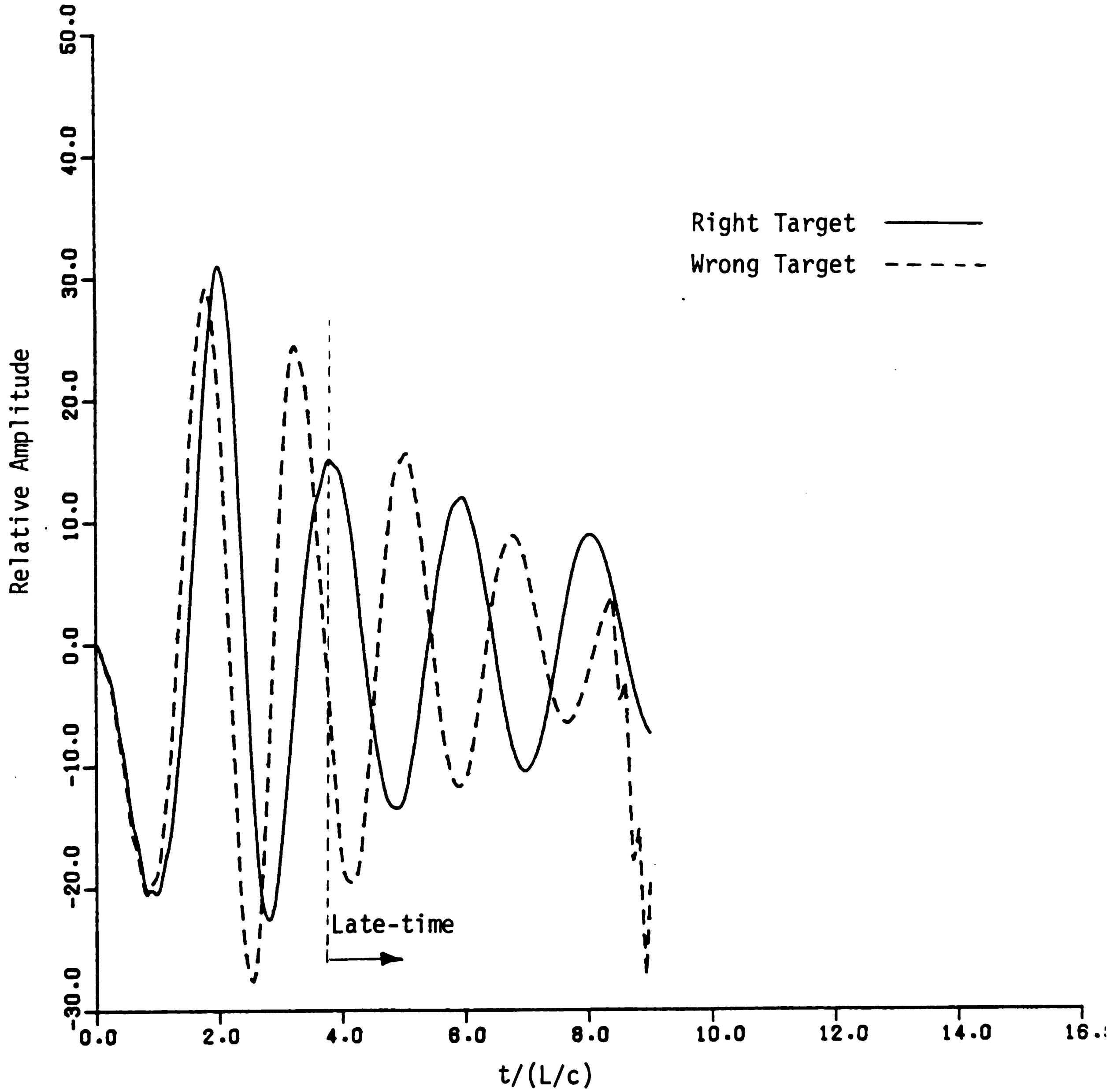

Figure 5.13. Return waveforms from right target and target with 10% shorter length when these targets are illuminated by the synthesized waveform of Figure 5.12 with symmetric excitation.

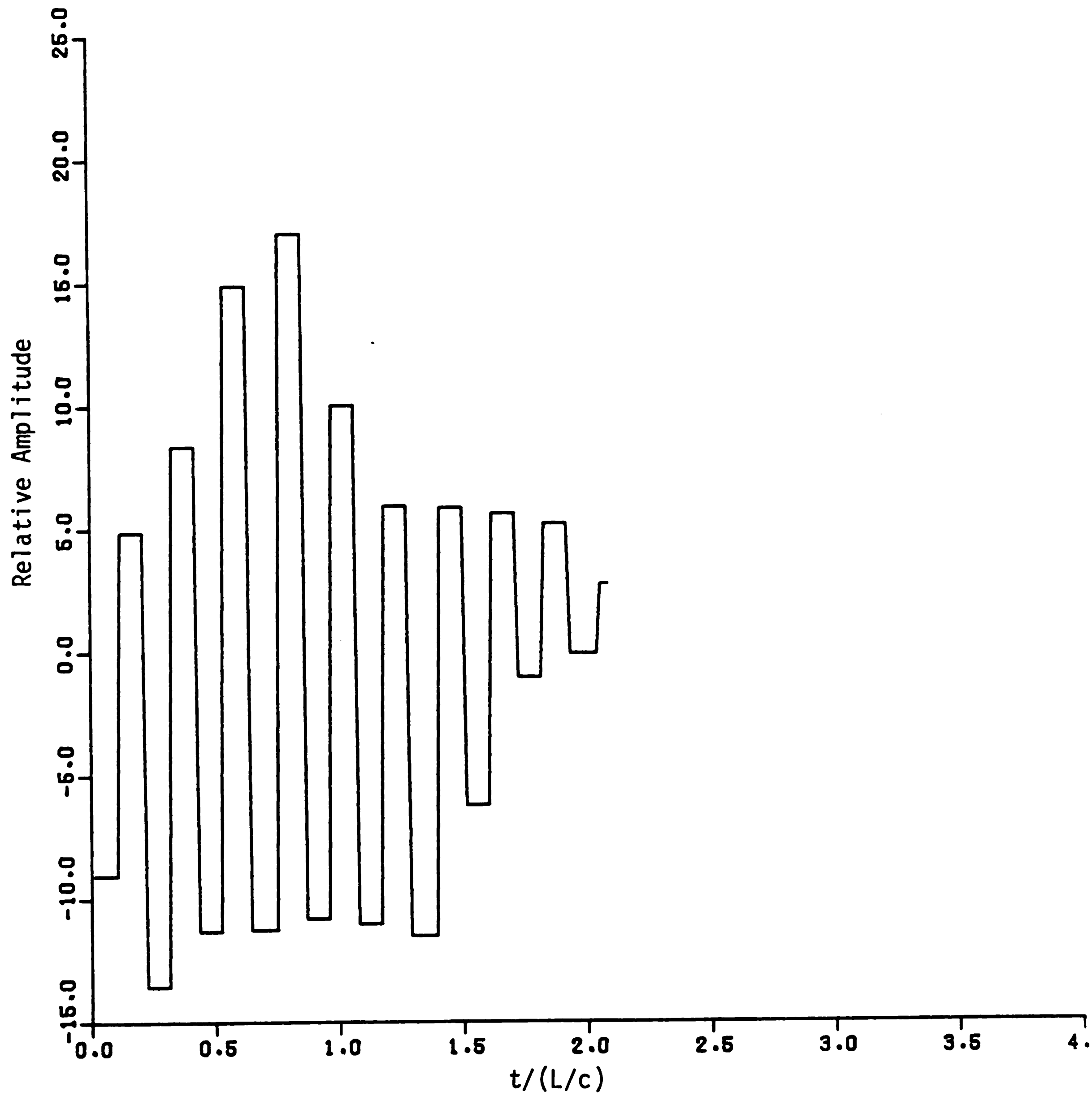

Figure 5.14. The required incident waveform to excite the second symmetric mode of the target described in Section 5.5.

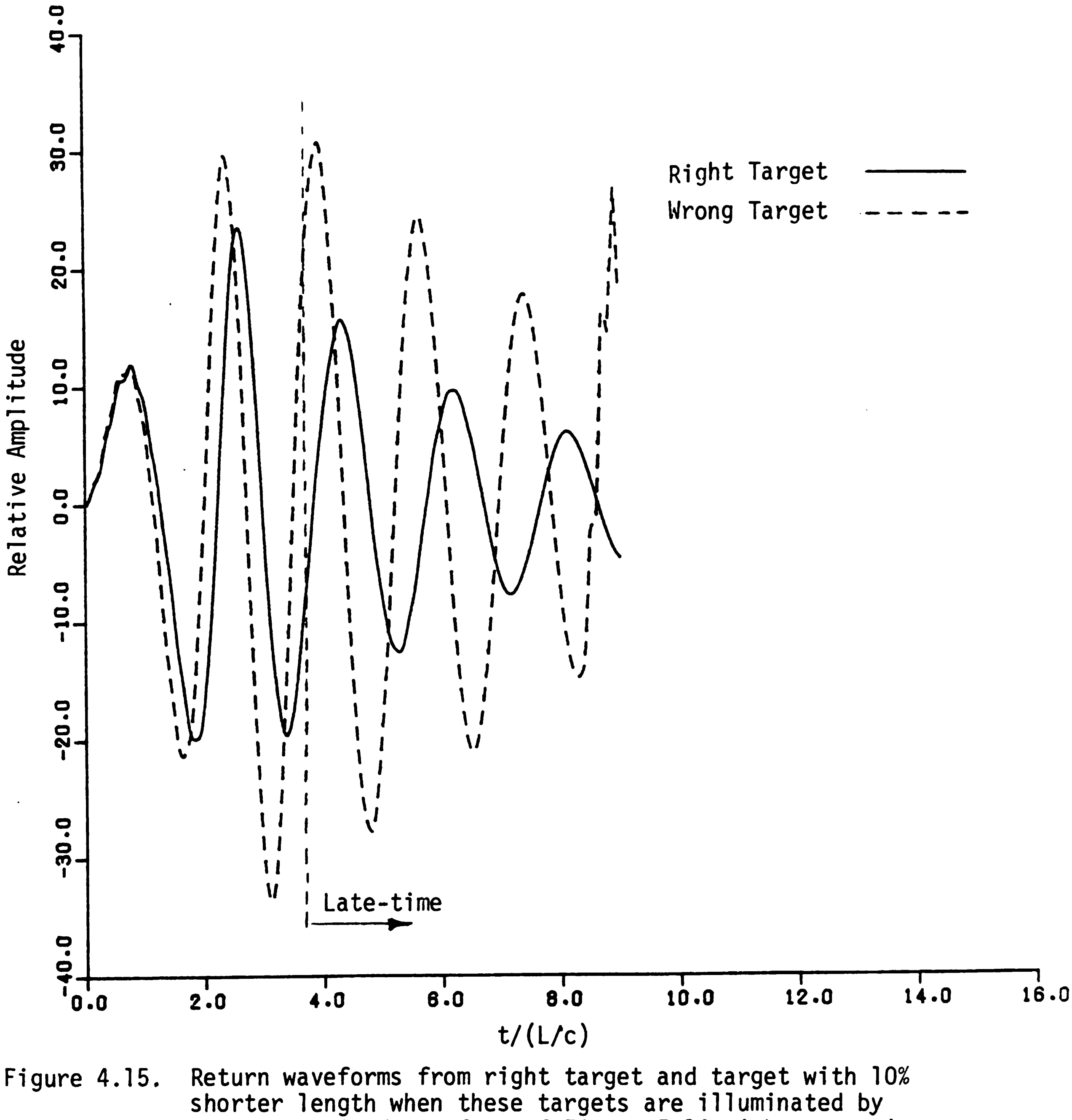

Figure 4.15. Return waveforms from right target and target with 10% shorter length when these targets are illuminated by the synthesized waveform of Figure 5.14 with symmetric excitation.

CHAPTER 6

EXPERIMENTS

An experimental facility, the time-domain scattering range, has been constructed for the measurement of time-domain, transient, scattered fields excited by radar targets which are illuminated by short-pulse incident fields. This chapter is dovoted to the description of the experimental setup, its operating principle, the experimental procedure and the data-processing along with the experimental results. Section 6.1 describes the setup of this time-domain scattering range. Section 6.2 discusses the operating principle upon which the range functions. The experimental procedure is described in detail in Section 6.3. Then, in Section 6.4, we develop a software package for processing the irregular raw data into the useful information. In the end, we conclude this chapter by showing the neumerical results from different targets including sphere, isolated wire and skew-coupled wires in comparison with the theoretical results.

6.1 Experimental Setup

A large ground plane composed of nine 4' x 8' modules has been constructed. A biconical transmitting antenna (monocone over ground plane) with a length of 8 feet and a half-angle of 8^{o} is fabricated. A short monopole (1.6 cm) is used as the receiving probe. The setup is shown in Figure 6.1. The basic experimental arrangement including

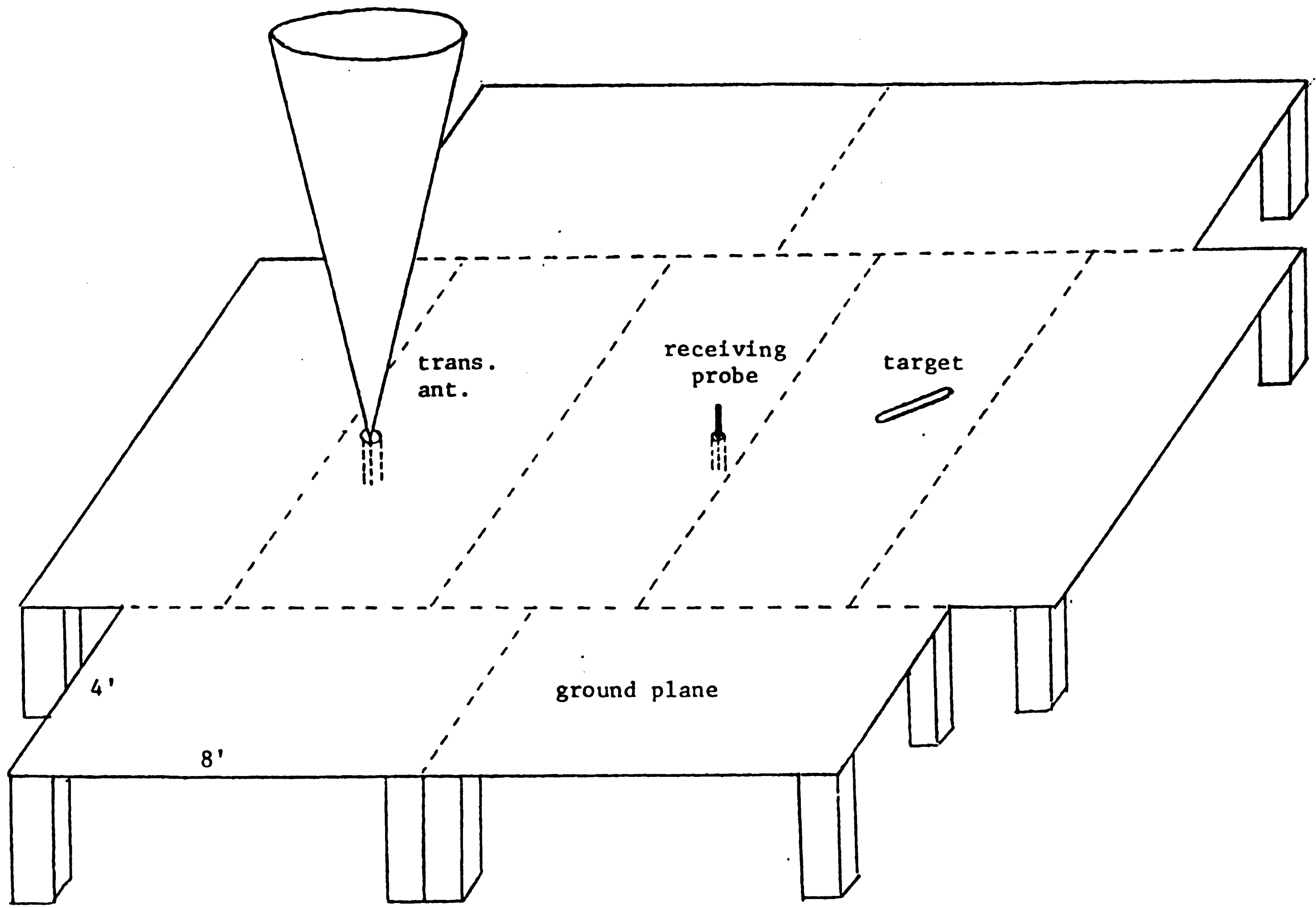

Figure 6.1. Experimental setup for measuring return signals from the target

relevant pieces of equipment is shown in Figure 6.2. Nanosecond pulses of 400 V amplitude excite the TEM biconical-horn transmitting antenna and are displayed on a sampling oscilloscope which is triggered by those same pulses. The incident field E^i illuminates both the receiving probe and test target. The backscattered field E^s from the target subsequently excites the receiving probe, and can be separated from E^i due to its additional propogation time. The output signal from the short receiving probe is processed through the sampling oscilloscope.

Both the horizontal sweep voltage and the sampled receiving probe signal outputs from the oscilloscope are analog-to-digital converted by an A-D converter which is controlled by a microcomputer. Both the time-base and receiving-probe data are stored in computer memory (RAM). The data can then be recorded on the cassette tape or the floppy disk and subsequently transferred, via telephone modem, to the MSU CYBER 750 computer system where they are placed in permanent disk-file storage. All data processings are then accomplished on the CYBER.

6.2 Operating Principle

Since the impedance of the biconical horn is essentially frequency-independent, then the transmitted incident wave field nearly replicates the pulse generator output.

The operating principle of the sampling oscilloscope can be easily demonstrated in Figure 6.3. The sample density determines the horizontal display rate since one sample is taken for each repetition of the 1KHz pulse generator.

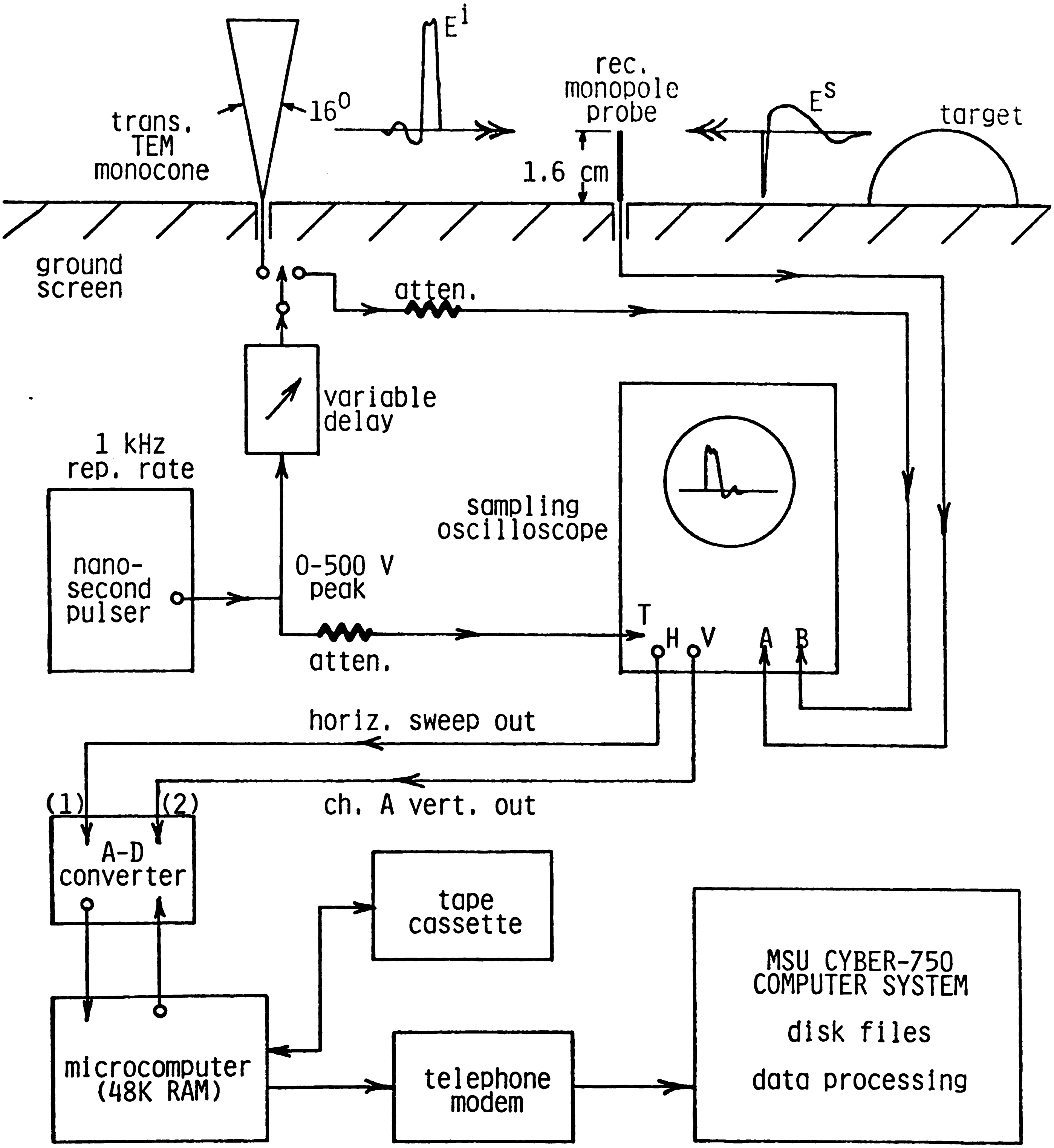

Figure 6.2 Experimental arrangement for measurement of transient scattered EM waveforms.

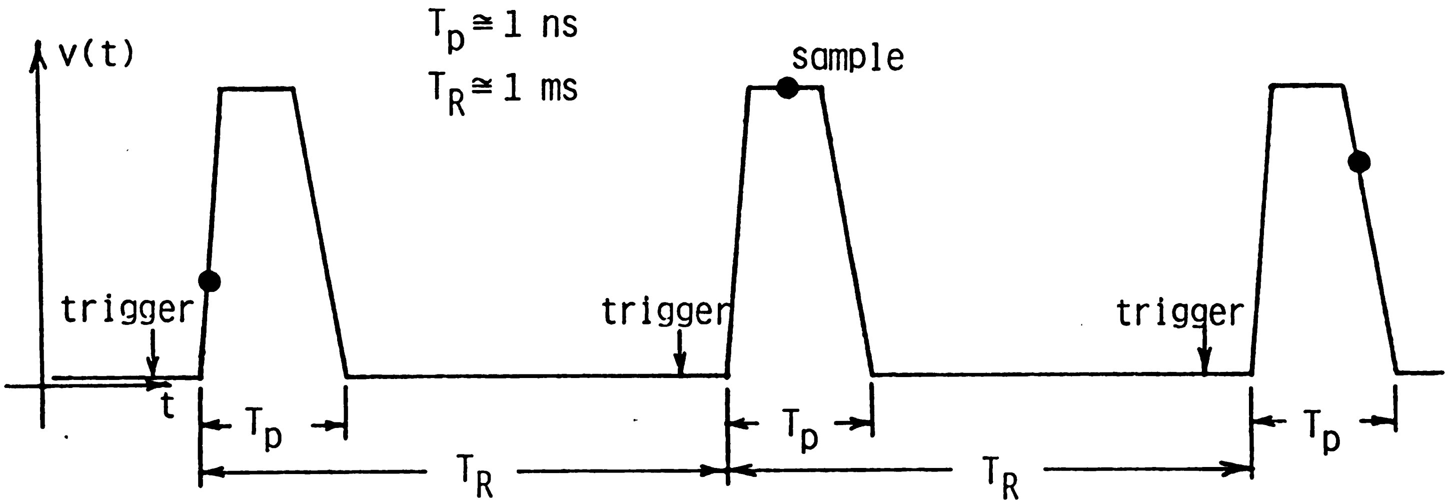

Repetitive waveform to be sampled

1. Input to sampling scope must be perfectly repetitive at a low repetition rate (usually 1-10 kHz).

2. Sampling system acquires samples at fixed time intervals (incremented delays) following arrival of a trigger signal.

3. One sample is taken from each repetition of the waveform being sampled.

4. Total number of samples taken from measured waveform depends upon variable sample density (samples/div.).

5. Horizontal data display rate depends upon sample density and signal repetition rate.

Figure 6.3. Illustration of the operating principle of the sampling oscilloscope.

The equivalent circuit of the receiving probe is shown in Figure 6.4. The voltage source, V_s, is proportional to the electric field which illuminates the probe and therefore equals to $E^S h$, where h is the effective length of the antenna, Z_A is the probe impedance when it is used as a transmitting antenna, and R_L is the load resistance. The voltage received by sampling scope, V_R, is therefore

$$V_R = \frac{V_s R_L}{Z_A + R_L} = \frac{E^S h R_L}{Z_A + R_L} \tag{6.1}$$

from the theory of linear antenna [35]. For the short probe,

$$Z_A(s) = \frac{1}{SC_A} + r_A \tag{6.2}$$

where C_A is the capacitance and r_A is the resistance of the antenna acting as a transimitting element, with $\frac{1}{SC_A} >> r_A$ over the main part of the frequency range of this experiment ($f \leq 3$ GHz).

Equation (6.1) can be rewritten as

$$V_R(s) = sE^S h R_L C_A / [1 + s(r_A + R_L) C_A]. \tag{6.3}$$

In this experiment $R_L = 50\Omega$ for the coaxial cable and therefore

$$\left.\begin{aligned} \frac{1}{SC_A} &>> R_L \\ R_L &>> r_A \end{aligned}\right\} \tag{6.4}$$

over the main part of the frequency range of this experiment. Based on equation (6.4), equation (6.3) now becomes

$$V_R(s) \approx sE^S h\, R_L C_A. \tag{6.5}$$

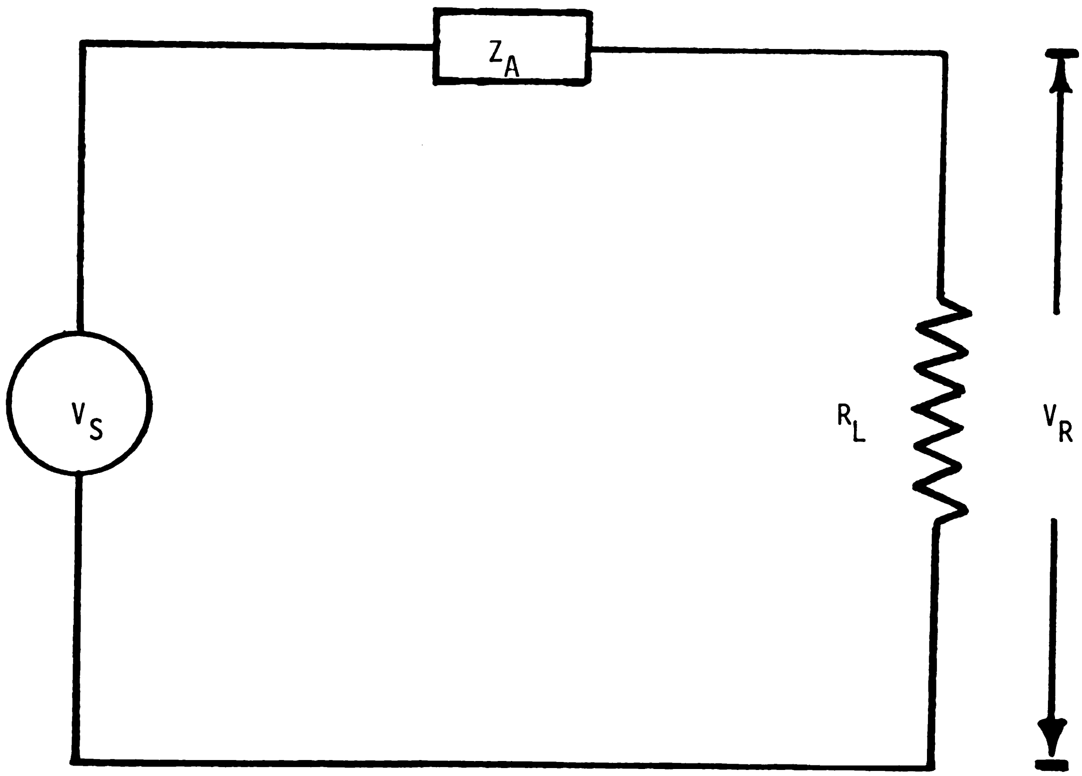

Figure 6.4. Equivalent circuit of the receiving probe.

This implies that

$$V_R(t) \propto \frac{dE^s(t)}{dt} . \tag{6.6}$$

We used (6.6) as the approximation to perform our data-processing, and obtained satisfactory results.

6.3 Experimental Procedure

To start an experimental run, the operator first enters the number of data points to be A-D converted for the entire horizontal display, and the computer then directs the A-D converter to begin sampling the horizontal sweep output. The operator then actuates the single-sweep mode of the scope; when the converted horizontal sweep signal exceeds a preset threshold, the microcomputer commands the A-D converter to begin taking probe data samples at a fixed rate until the previously specified number of data points have been acquired. Both the time-base and receiving-probe data are stored in RAM and later recorded on the cassette-tape.

It is important to make sure that the sample density is adjusted to yield an accurate reproduction of the measured waveform. Another parameter which must be preset before any experimental run is the time per division of the experimental waveform, t_{pd}, which controls the total time interval of valid data. It is necessary that E^s be measured during the time interval which precedes the arrival of clutter return from edges of the ground screen, etc. at the receiving probe.

Since the A-D converter of this particular system can only record the positive voltage accurately, any negative voltage will be recorded as zero voltage, we should add a DC offset, through the use of an oscilloscope, to all the output signals to the A-D converter. This DC voltage should be adjusted so that the minimum voltage to the A-D converter is positive and yet the maximum voltage does not exceed the saturation voltage of the oscilloscope. It is therefore necessary to evaluate this DC voltage in the data-processing. For this purpose, the time axis should be adjusted so that we have enough points (10-20 points) which precede the incident waveform as the basis for evaluating the DC level. Usually, there will be a DC-level drifting during the experimental interval, and it may be necessary to make another 10 to 20 points after the retrace of the scope available. If we want to get these several points after the retrace for the evaluation of the DC level near the end of experimental time interval, it is desirable to actuate the sweeping of time base by first setting scope in the single-sweep mode and then switching to the normal mode when the experimental run begins. By doing so,data points after the retrace are recorded until we switch to the single-sweep mode again.

In any scatter-field measurement, the receiving probe response is sampled, A-D converted, and stored both with and without the target present. Those responses are subsequently numerically integrated during CYBER processing to annul the differentiation introduced by the receiving probe. Finally, the reference signal (target absent) is subtracted from the total probe response to isolate the desired backscattered field.

During the entire experiment, the key controller is a cassette-tape recorder: it not only records the experimental data, but also is responsible for loading the program which controls the sampling and the

A-D conversion of the data. To transfer the data from microcomputer to CYBER, we also need this recorder to control the action.

6.4 Data Processing

The FORTRAN program for processing the experimental data is stored in a CYBER permanent file named EXPDPEW as listed in Appendix .

Before using this program, it is necessary to attach four input data files which are transferred from microcomputer to CYBER:

TAPE 1 = horizontal sweep out (time base) raw data for the experimental run without target present

TAPE 2 = vertical out raw data for the experimental run without target

TAPE 5 = horizontal sweep out raw data for the experimental run with target

TAPE 6 = vertical out raw data for the experimental run with target

The objective of this program is to create five output data files:

TAPE 3 = Data in TAPE 1 and TAPE 2 are combined together to display the measured response in volts as a function of real time in nanoseconds. This file shows all the data points before the retrace and subtracts the DC offset which appears in TAPE 1 and TAPE 2. This file has three columns; the first is the real time in ns, the second is the raw data of real voltage and the third is the data after integration.

TAPE 7 = Same as TAPE 3 except that this file is for the raw data of the experimental run with target present.

TAPE 4 = Data in TAPE 3 are splined using a IMSL subroutine "ICSSCU" so that the response as a continuous function of any particular time becomes available. This enables us to subtract the response without target from the response with target.

TAPE 8 = Same as TAPE 4 for the splined data with target.

TAPE 9 = Data in TAPE 4 is subtracted from data in TAPE 8, so that we have the target response along with the result after integration. Therefore, the integrated data in this file is supposed to be the backscattered field.

There are four options for evaluating the DC offset:

Option 1 - DC is the average of the first 10 points which precede this incident waveform.

Option 2 - DC is the average of 10 points right after the retrace.

Option 3 - With DC1 = DC from Option 1 and DC2 = DC from Option 2, DC value is assumed to be drifting linearly from DC1 in the beginning to DC2 in the end.

Option 4 - Based upon the assumption that the transmitting antenna does not transmit DC component, $\int_0^\infty f(t)dt = 0$ should be satisfied; therefore, $\int_0^t (f(t)+V_{DC})dt \doteq V_{DC}t$ if t is properly chosen. This option is very sensitive to the choice of upper integral limit t.

Usually, the DC level drifts a great deal during the experiment and it is not necessarily a linear drift. If the DC level is not evaluated accuralely, there will be an accumulated error present after integration, i.e., an error estimation of DC results in a ramp-function type of error. It is therefore desirable to use Option 1 or Option 2 and then change the slope of the response using a plotter and the plotting software package like SPOCS [36].

Two experimental runs (with and without target) sometimes display the incident waveforms with shifted time and drifted voltage. We handle this problem by adding another option with an index IY: if IY = 1, we shift time axis and rescale the vertical axis so that the maxima of the incident waveforms appear at the same time with the same amplitude.

6.5 Experimental Results

Typical scattered field measurements are indicated in Figures 6.5 - 6.8. Figure 6.5 is the measured waveform of the incident pulse transmitted by the biconical antenna. It is clear from this result that E^i maintained by the transmitting bicone is an approximate replication of the pulse generator output. The measured scattered field response of a sphere with 11" diameter illiminated normally by this incident pulse is indicated in Figure 6.6, which displays the right creeping-wave and the specular reflection behavior [28]. The response of an isolated wire with $L/a = 200$, and $L/c = 2.116$ ns due to normal incidence is indicated in Figure 6.7. This latter smoothed impulse response (target impulse response to a short incident pulse) compares very well with the result obtained when the measured incident pulse of Figure 6.5 is convolved with the known theoretical impulse response. Figure 6.8 is the backscattered field response of an isolated wire with $L/c = 200$

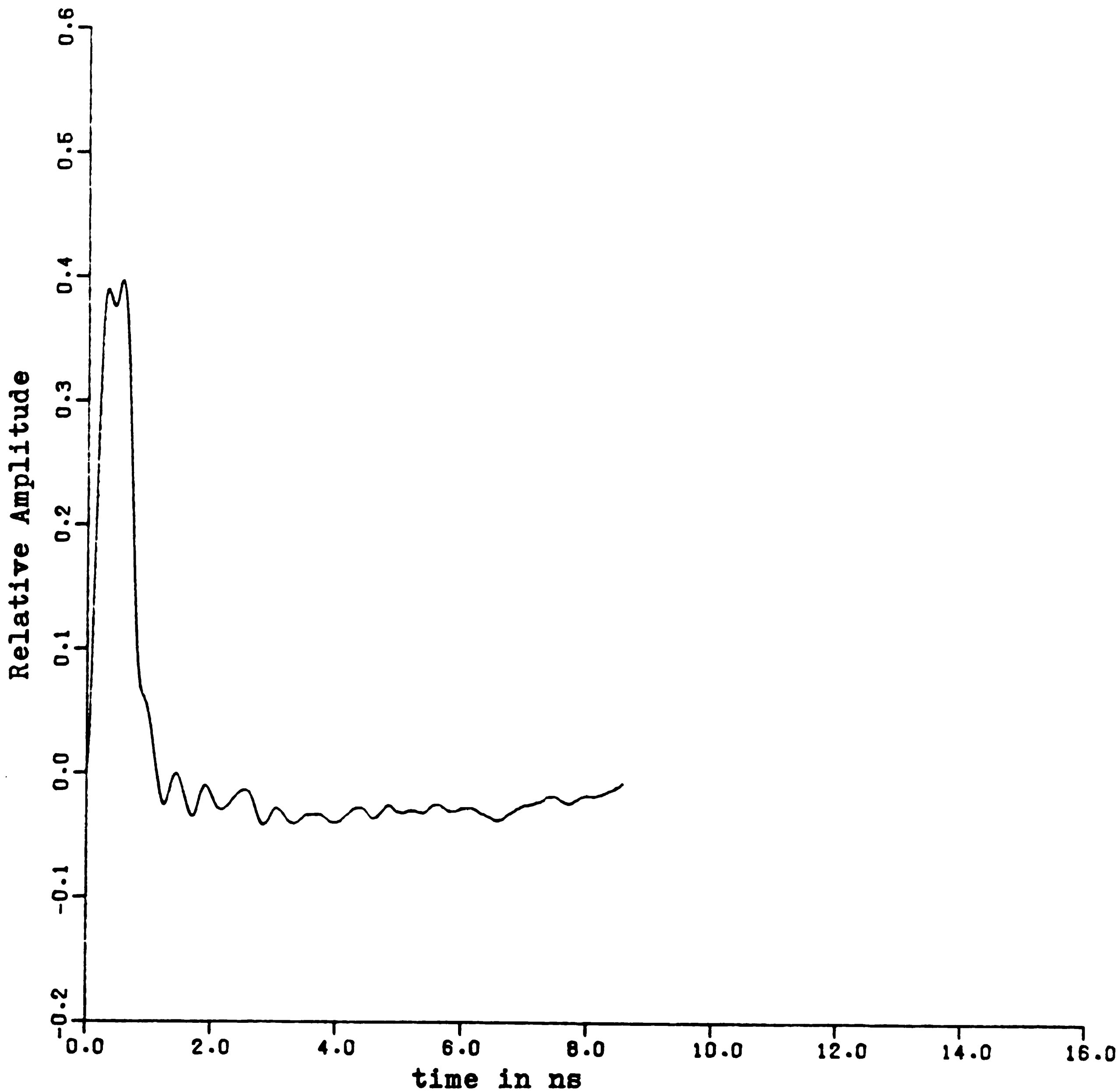

Figure 6.5. Measured waveform of incident pulse transmitted by biconical antenna.

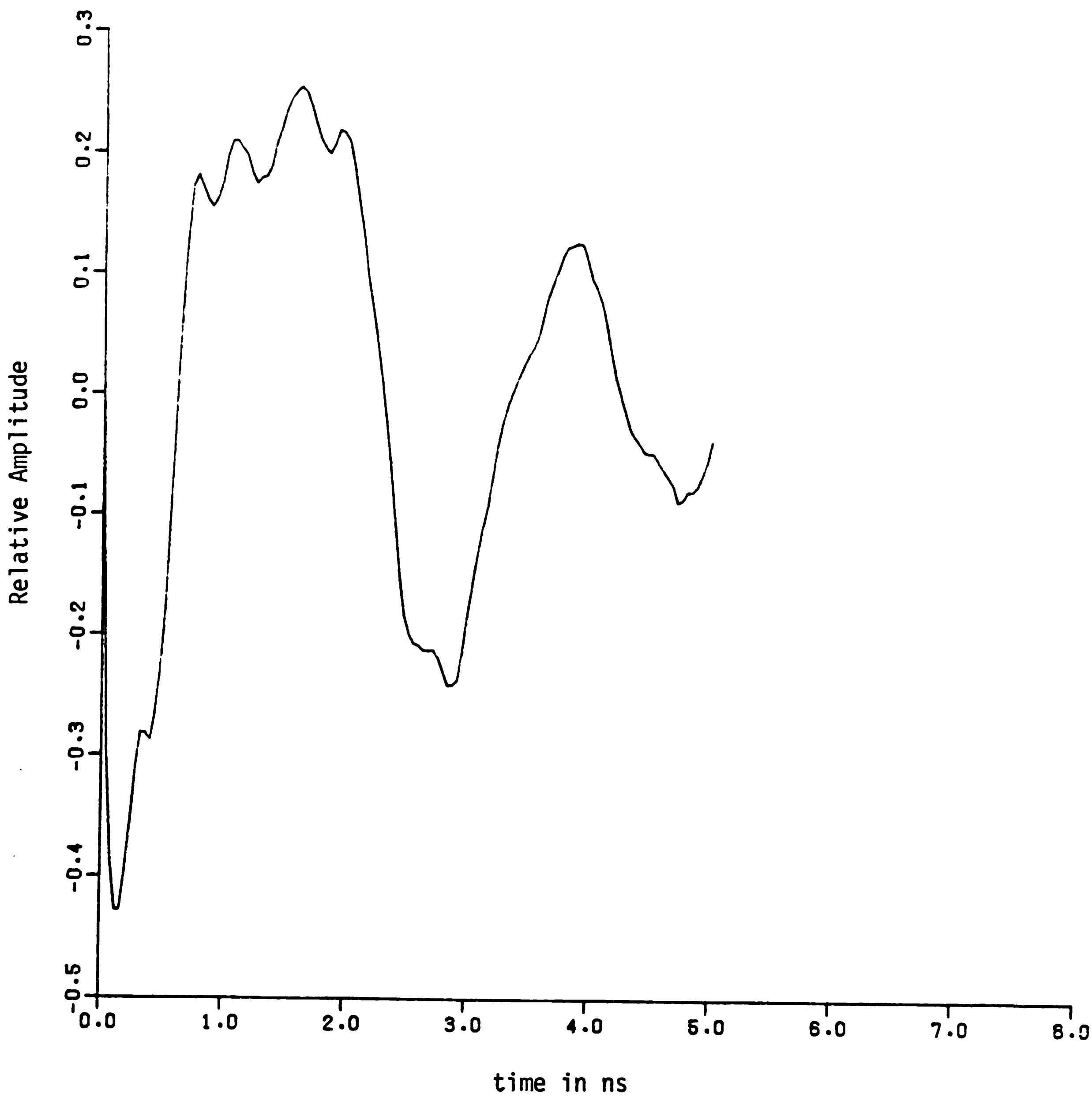

Figure 6.6. Measured nanosecond-pulse backscatter field response of a sphere with 11" diameter to normally incident illumination.

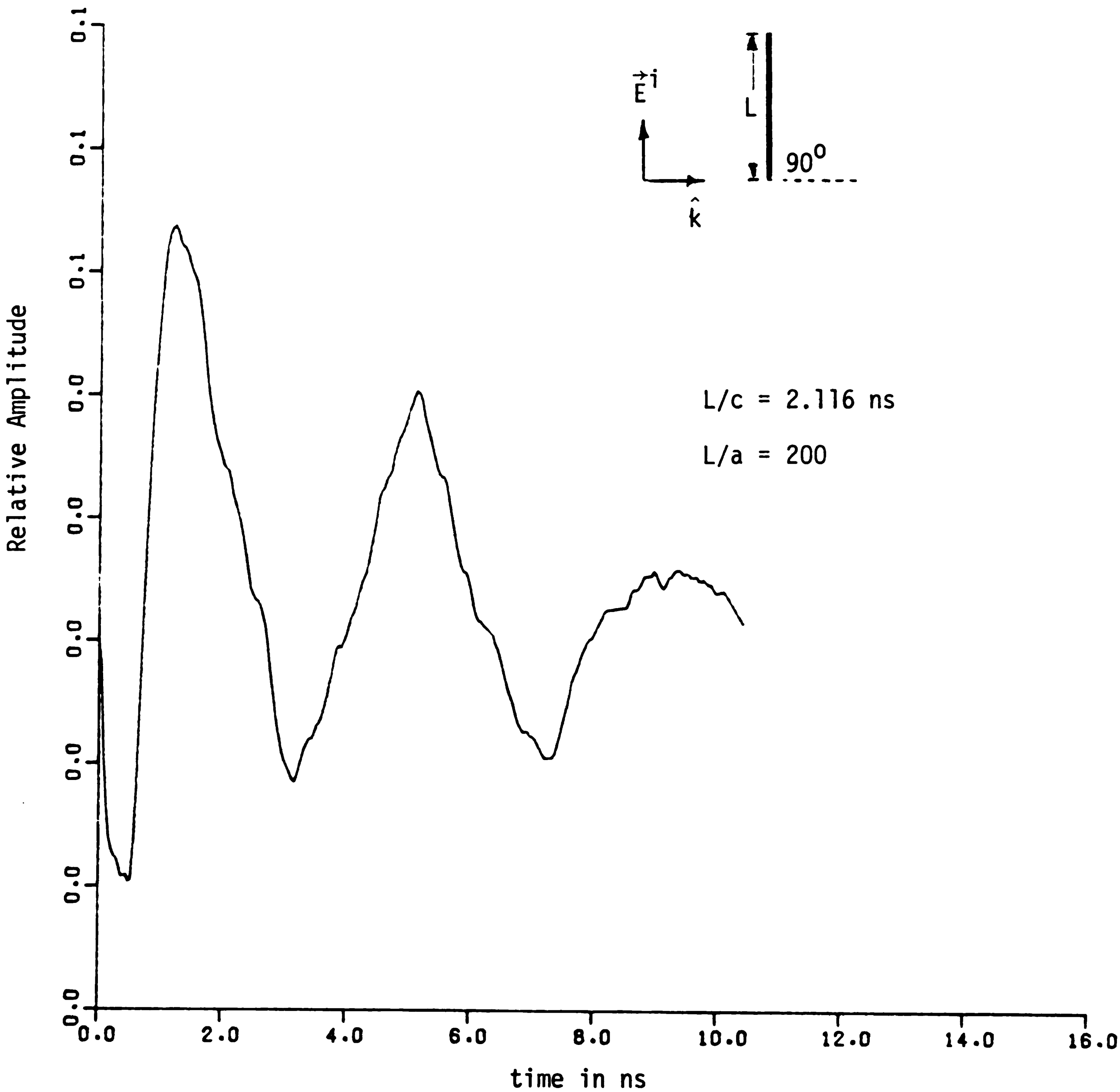

Figure 6.7. Measured nanosecond-pulse backscatter field response of a thin, conducting cylinder to normally incident illumination.

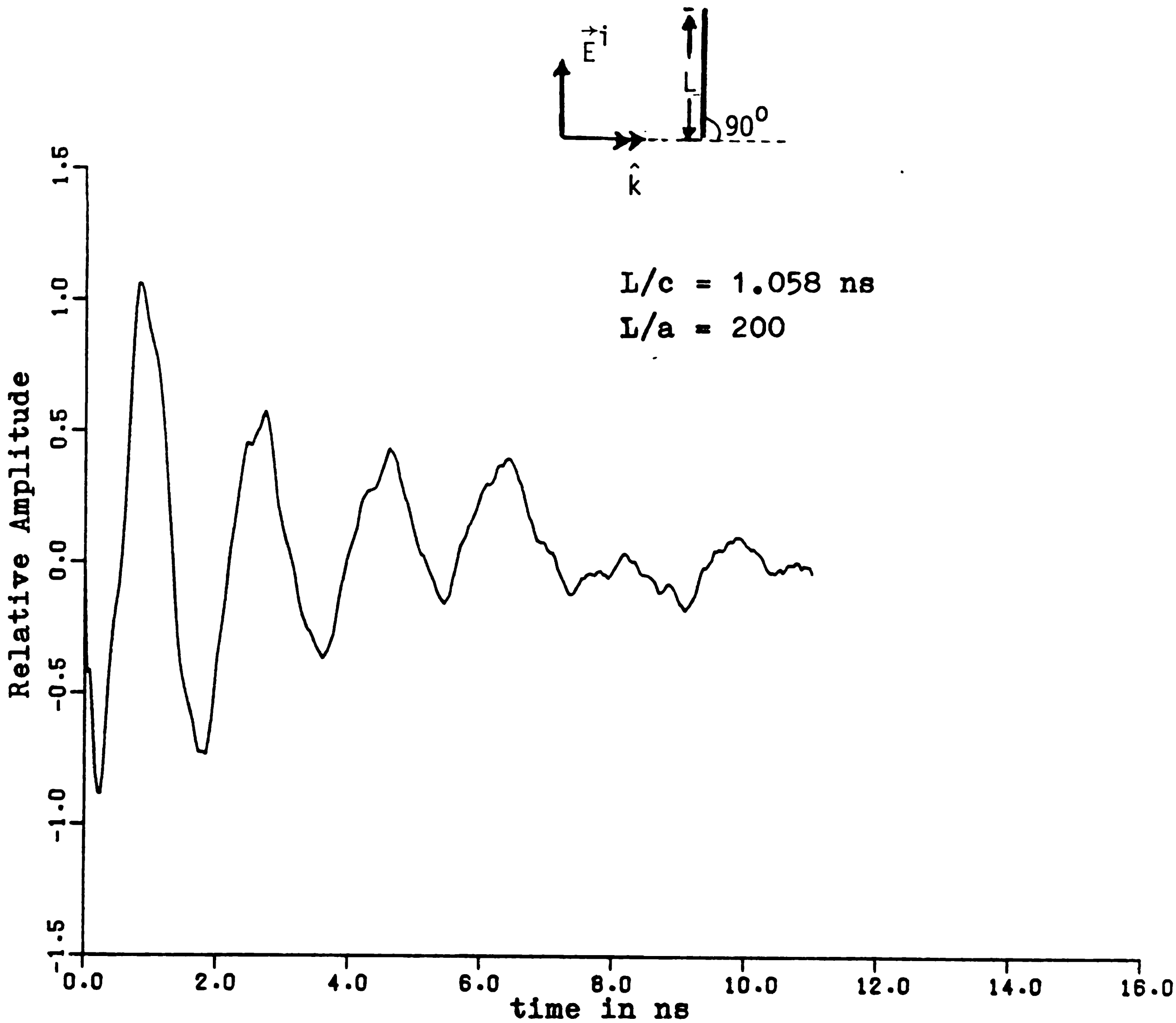

Figure 6.8. Measured nanosecond-pulse backscatter field response of a thin, conducting cylinder to normally incident illumination.

and $L/C = 1.058$ ns. In this figure, more "ringings" are seen because the length of the wire is one half of the previous one.

The response of the skew-coupled wires with different angles are indicated in Figures 6.9, 6.11 and 6.13. Figure 6.9 is the experimental result for the case of $L/a = 200$, $L/c = 1.058$ ns, $d/L = 0.5$ and $\alpha = 90^0$; this is very similar to those in Figures 6.7 and 6.8. Figure 6.9 compares very well with Figure 6.10 which is the convolved result of the incident waveform of Figure 6.5 and the impulse response of Figure 4.22. Figure 6.11 and Figure 6.12 are the similar results for the case of $\alpha = 60^0$; the comparision is not as good as the case of $\alpha = 90^0$. This is because the "ringings" of $\alpha = 60^0$ case is not as strong as that of $\alpha = 90^0$ case and, therefore, the signal-to-noise ratio is not as good. Results for $\alpha = 30^0$ case are shown in Figure 6.13 and Figure 6.14. The signal-to-noise ratio in this case is even worse and, therefore, a poor agreement between these two figures is observed.

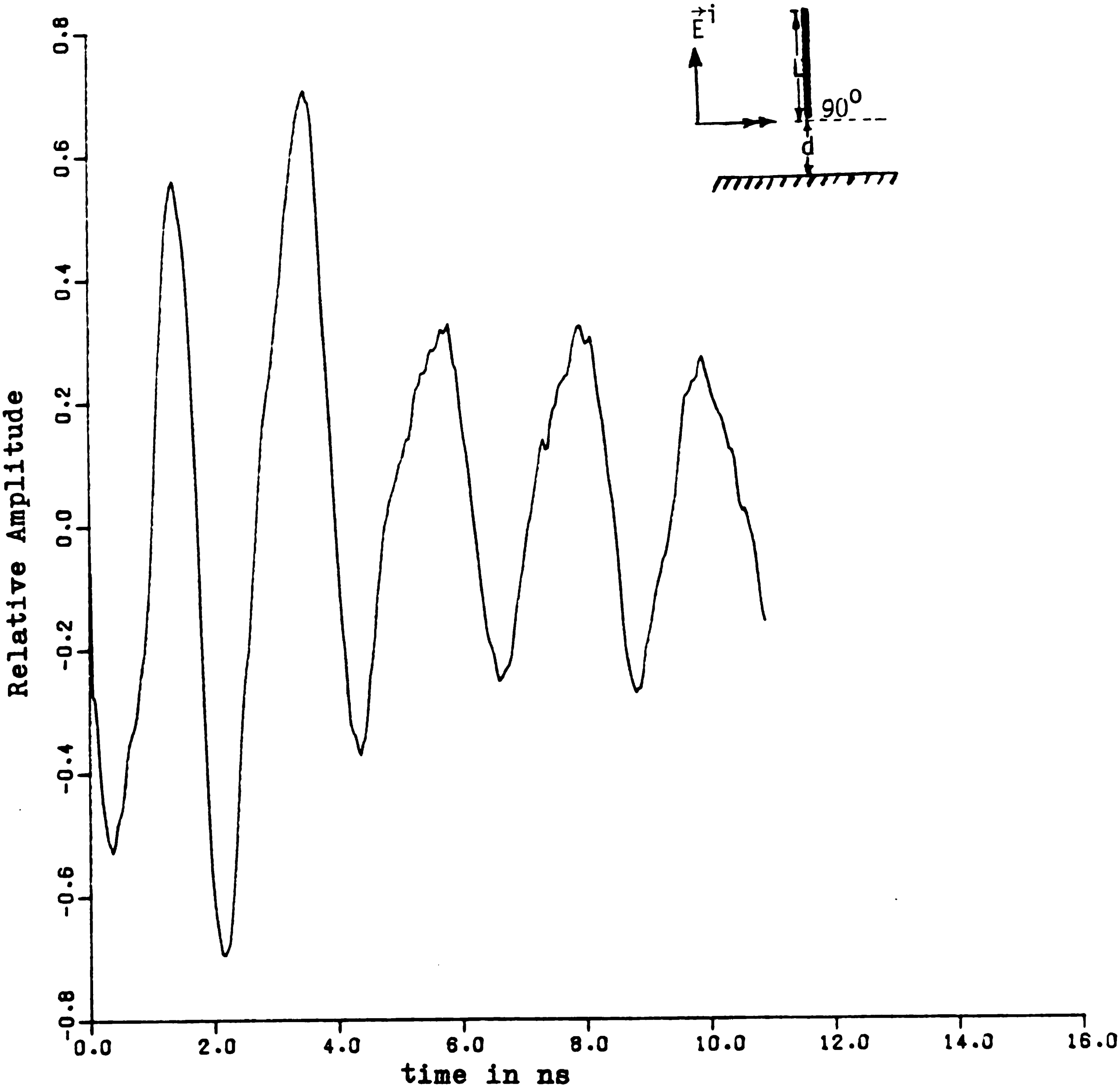

Figure 6.9. **Measured nanosecond-pulse backscatter field response of a** wire over the ground plane **with α=90°, L/a=200, L/c=1.058 ns, d/L=0.5 to normally incident illumination.**

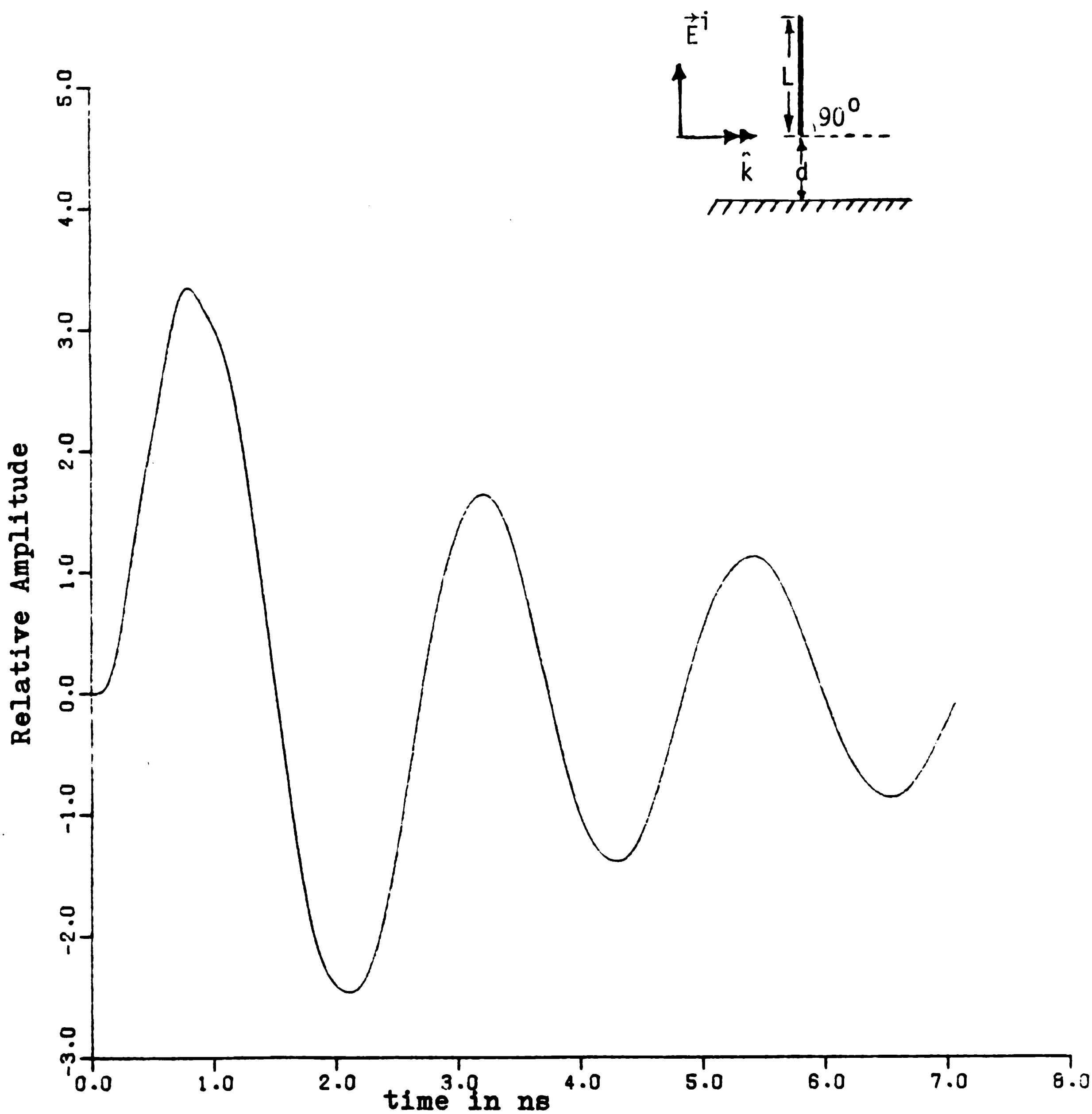

Figure 6.10. **Result of convolution between** nanosecond-pulse and **impulse response** of a wire over ground plane with $\alpha = 89.9^0$ **L/a=200, d/L=0.5, L/c=1.058 ns and aspect-angle 0°. Notice that the specular reflection is not seen because a negative impulse is not shown in the impulse response.**

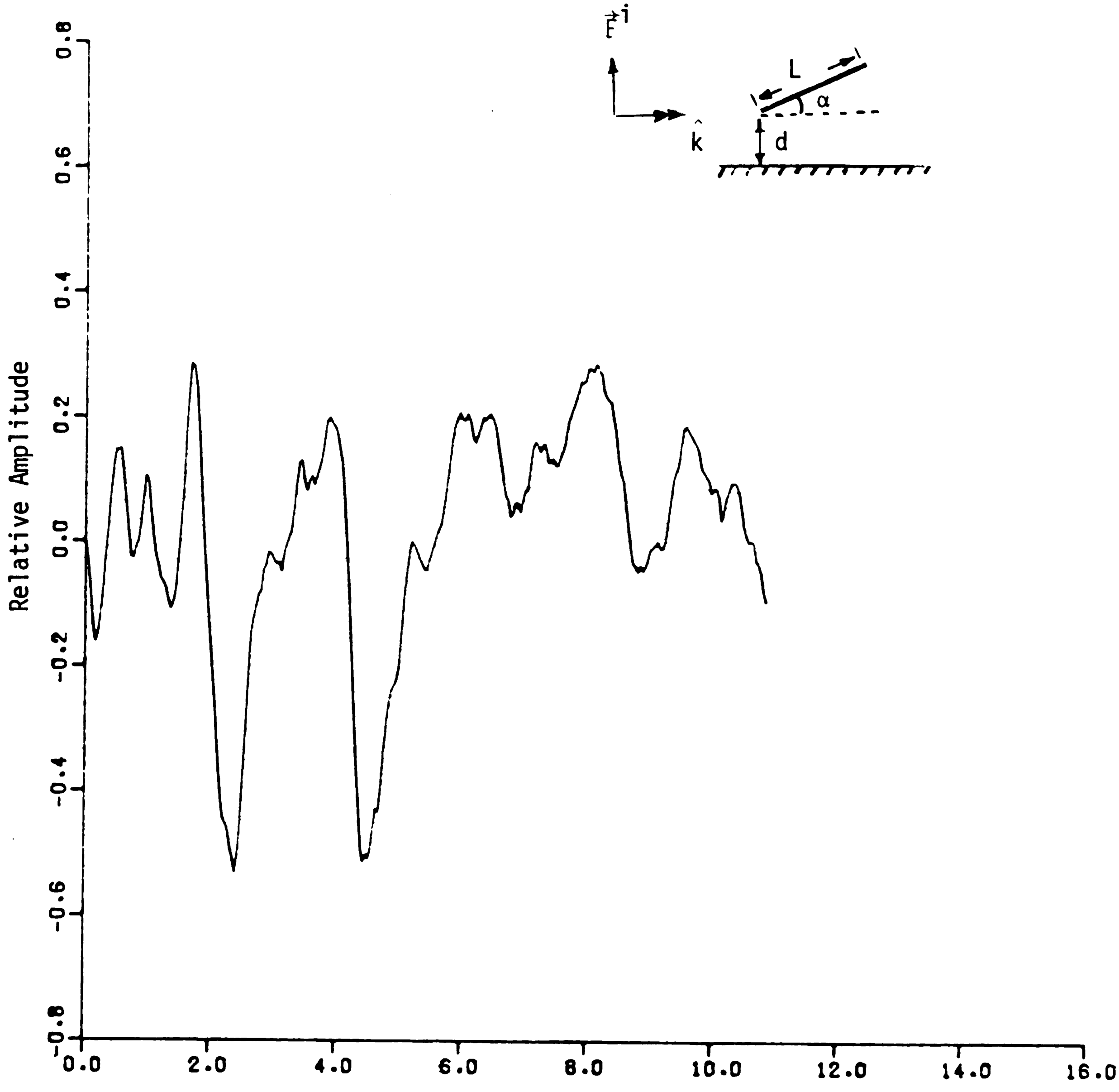

Figure 6.11. Measured nanosecond-pulse backscatter field response of a wire over the ground plane with $\alpha = 60^o$, L/a = 200, L/c = 1.058 ns, d/L = 0.5 to normally incident illumination.

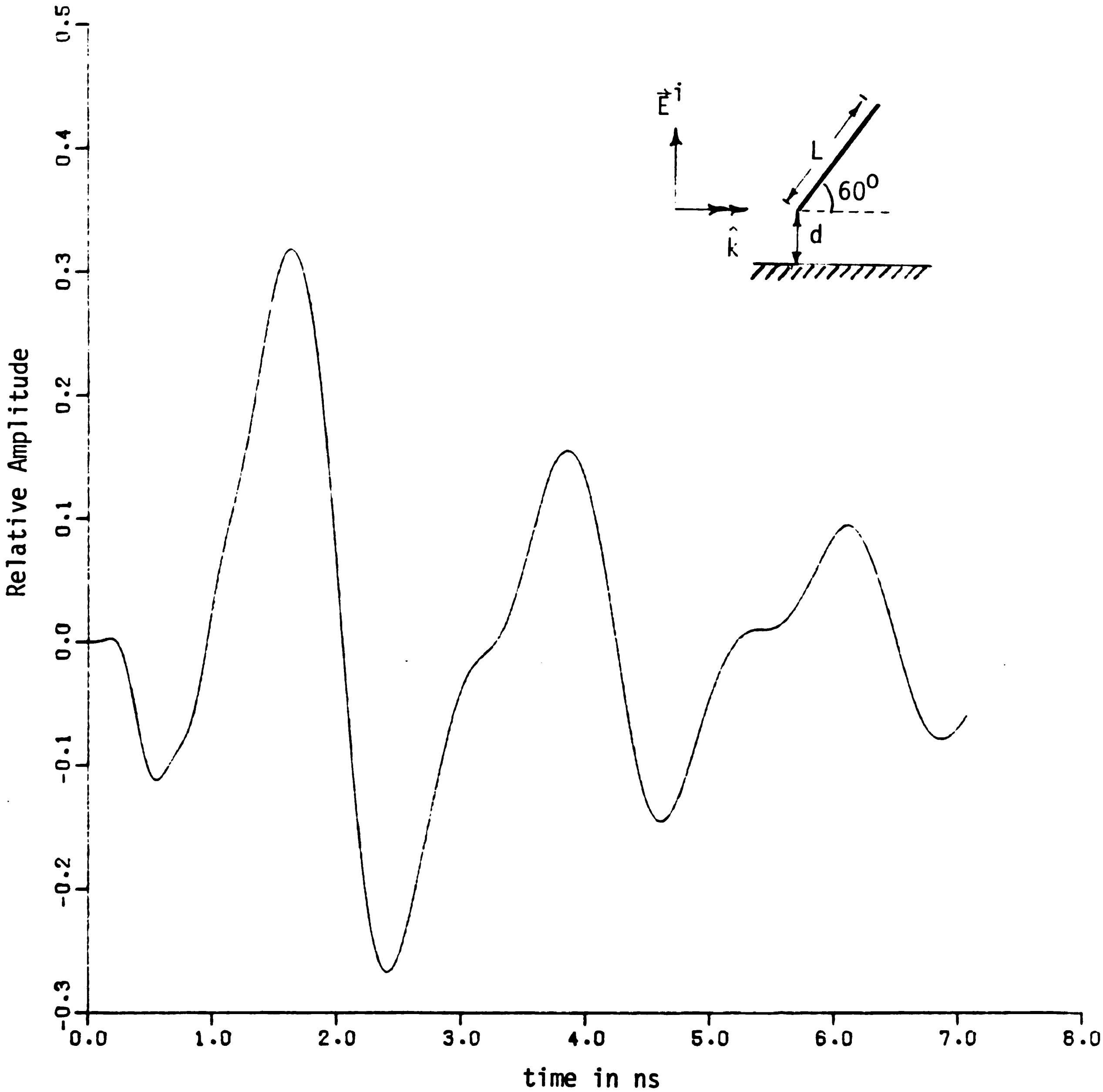

Figure 6.12. Result of convolution between nanosecond-pulse and impulse response of a wire over ground plane with $\alpha = 60^o$, $L/a = 200$ $d/L = 0.5$, $L/c = 1.058$ ns and aspect-angle 0^o.

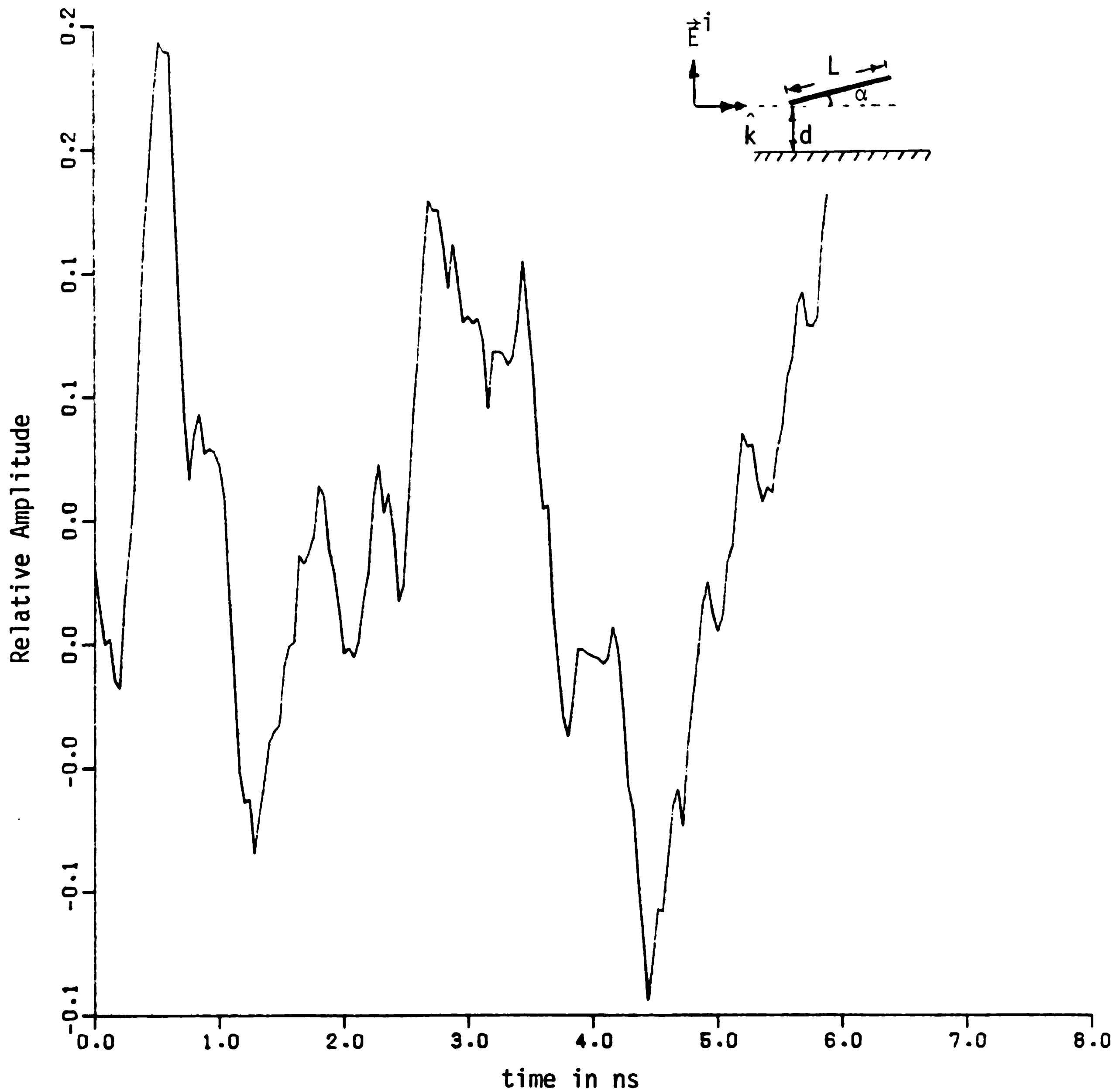

Figure 6.13. Measured nanosecond-pulse backscatter field response of a wire over the ground plane with $\alpha = 30^o$, $L/a = 200$ $L/c = 1.058$ ns, $d/L = 0.5$ to normally incident illumination.

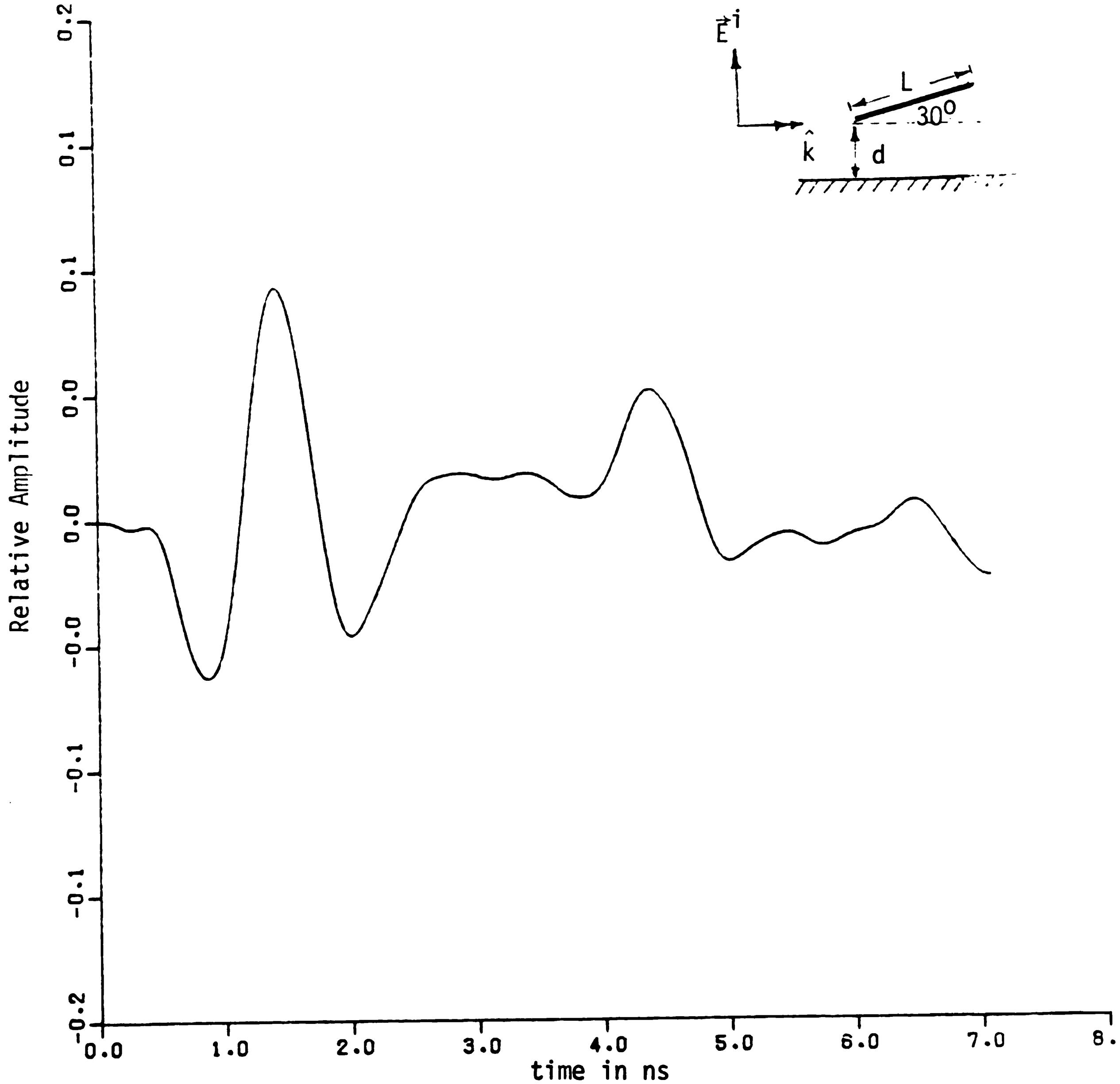

Figure 6.14. Result of convolution between nanosecond-pulse and impulse response of a wire over ground plane with $\alpha = 30^{\circ}$, $L/a = 200$, $d/L = 0.5$, $L/c = 1.058$ ns and aspect-angle 0°.

CHAPTER 7

CONCLUSION

It has been demonstrated that an aspect-independent, optimal incident radar waveform of finite duration T_e can be synthesized to excite a target in such a way that in the late-time period of $t > T_e + 2T_t$ (T_t = target one-way transit time) its backscattered field consists of a single natural mode which can be used to identify and discriminate the target. By constraining only the late-time target response, a time-domain synthesis technique was developed which does not require the knowledge of the forced, early-time impulse response. Three types of targets are presented not only to confirm the applicability of this scheme but also to study the transient electromagnetic behaviors of the three targets. A time-domain scattering range has also been constructed to perform the transient electromagnetic experiments. In this chapter, we will conclude this study by summarizing the waveform-synthesis method from the system point of view and discussing some potential problems associated with this method for the future investigation.

7.1 A Target-Discrimination System Employing Waveform-Synthesis Method

Depicted in Figure 7.1 is a potential target-discrimination system employing the waveform-synthesis method. In this system, all the required waveforms to excite the single-mode responses of the "friendly" targets are stored in a large computer system, one "channel" for each target. Each "channel" is a subsystem of the large computer

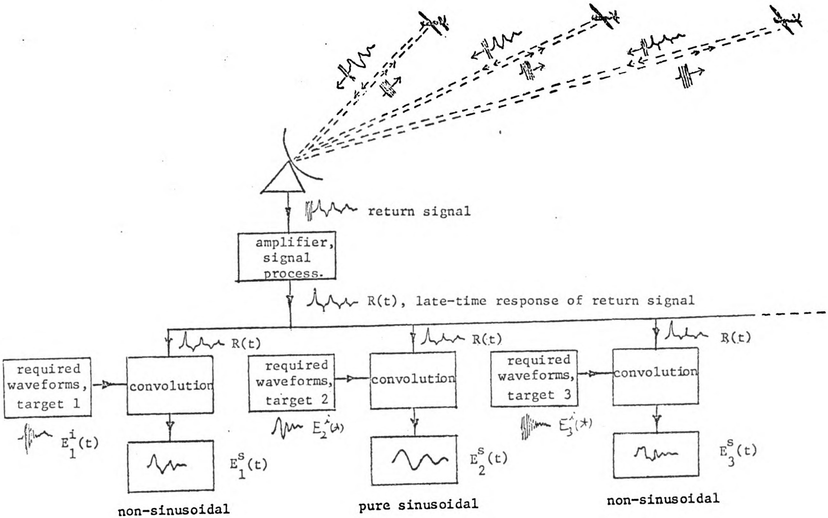

$$E_n^s(t) = \int_o^{\tau_e} E_n^i(t')\, R(t-t')dt'$$

Figure 7.1. A proposed target discrimination system

system and can be represented by the linear-system model on the right side of Figure 2.2. An incident radar signal with some convenient waveform (provided it possesses the frequency components of the natural modes to be excited) excites the target, which yields a return signal with an irregular waveform. The return signal is subsequently convolved numerically with this stored, required incident signal in each channel using the real-time, on-line computer system. For the example shown in Figure 7.1, only channel 2 displays a single-mode return and therefore the interrogated target can be concluded as the friendly target which is stored in channel 2. If all channels "reject" any identification of this target, it can be regarded as a possible "unfriendly" target and precaution can be taken. Sometimes unfriendly targets may possess natural modes which are quite close to the natural modes of certain friendly targets, therefore we need to check different modes if there is an indication of "match" for some modes. This is a very flexible and quick decision procedure if a reliable computer system is available. Advantage of this system is that this doesn't really change the current radar system; what is needed is only to implement some natural-mode information and a fast and reliable software in addition to the current system. Therefore it is compatible with the current radar system. Moreover, this system is aspect-independent so that no additional information related to the aspect angle is needed. One of the challenges, however, is to choose a reasonable "convenient" incident waveform which covers the spectra of interest so that the receiving antenna can receive the return signal without missing any natural-mode information in that frequency range.

A precise way to synthesize the required waveform from the experimental results is also necessary because it is very difficult to solve the transient electromagnatic problem related to a complicated target like a bomber.

7.2 Some Potential Problems for Future Study

7.2.1 Synthesis of required waveforms using different basis functions

As we mentioned in the preceding chapters, as long as the basis functions are complete as $N \to \infty$, the required incident waveform should converge to a unique waveform no matter what kind of basis functions are used. This is true for thin-wire targets for which the natural modes are near orthogonal and only one type of mode (either antisymmetric or symmetric mode) is considered. This is, however, not quite true for the thick target like an infinite cylinder or when we consider both types of modes for the coupled wires. Theoretically, as long as we can synthesize a certain waveform which excites the target with single-mode response, it is not important for this particular waveform to be unicue. But there may be some serious problems: First, there might be a conditioning problem associated with the waveform-synthesis procedure, and the synthesized waveform could be a wrong numerical solution resulting from the computing error. Take Chapter 4 as an example. Let's consider both symmetric- and antisymmetric-modes. Since the corresponding natural frequencies for both modes are quite close, if we use pulse expansion, the matrix elements of the "M-matrix" in Equation (2.8) are the integrations over only a small segment and will be about the same for two modes with nearly identical natural frequencies. This results in a "M-matrix" which is almost singular and the condition number of the matrix is huge so that the synthesized waveform is possibly in the range of computing error and it doesn't make any sense even though the convolution of this waveform with the impulse response yields a monomode response. Under these circumstances a natural-mode basis may be more reasonable, because the integration of matrix elements are over the whole T_e duration now and if the damping constants are different for two modes, then after evaluting the upper and lower limits the matrix elements can be quite different and "M-matrix" will not be nearly singular any more. The condition number of the matrix then becomes acceptable. This was the reason why we displayed the required E-field using natural-mode basis in Chapter 4. Secondly, in some cases like the infinite cylinder in Chapter 3, the higher-order modes are quite important and natural modes are not orthogonal. Using natural-mode basis functions results in a required waveform which has strong higher-order-mode contribution and thus displays rapid-oscillatory characteristics like those shown in [37] for sphere. This kind of waveform will cause us difficulty in the convolution process when a quick decision is needed in the target-discrimination system. We therefore used pulse-basis in this problem and obtained much nicer waveforms.

From the study of the infinite-cylinder target, it was found that when both pulse-basis and Fourier-cosine-basis were used, the required waveforms converged to a unique result when $\tau_e = 0.594 \frac{1}{f_1}$ and condition numbers were small. For $\tau_e = \frac{1}{f_1}$, convergence was bad and condition numbers were large. This may be an indication that condition number is an important consideration in the waveform-synthesis process.

The other important aspect about the waveform-synthesis method is that when a waveform is synthesized, it should be made sure that this waveform should not be sensitive to the number of modes used. Because we retain a finite number of modes in the SEM series of the late-time response, this number is somewhat arbitrary and a small perturbation of it should not affect the final result. If the required waveform is sensitive to the number of modes used, we can not guarantee the single-mode return when it is used for target-discrimination.

Summing up the above discussion, three things warrant further study: (1) How to synthesize the required waveform for coupled wires when both antisymmetric and symmetric modes are excitable (and later for any complicated target of which natural frequencies may be closely distributed)? (2) How to use the condition number of the matrix as a means for determining the validity of the required waveform? (3) More study on the relation between the number of modes used and waveforms using different basis functions.

7.2.2 Improvements on Experiments

We have indicated in Chapter 6 that the most difficult part of our experiment is the accumulated error due to integration. This problem comes from the fact that we didn't have a probe which is distortionless. As a matter of fact, our probe approximates a differentiator by not with great precision. The fact that it approximates a differentiator forces us to perform the integration which accumulates the error; that it is an imperfect differentiator adds yet another theorectical error. This is not a serious problem when we are considering the case with a strong signal-to-noise ratio like the wire with 90° orientation angle. But it is almost impossible to obtain an accurate waveform for case of $\alpha = 30^{\circ}$ where the signal-to-noise ratio is poor. Thus, the most important task is to improve the receiving probe so that the integration becomes unnecessary.

The second thing which should be improved is the pulse generator The incident pulse as shown in Figure 6.5 is not clean at all; there are a number of small oscillations after the main pulse. To make things worse, the drift of signal and DC level is quite serious. We need a generator which can generate steady and clean pulses.

7.2.3 Further Study on Crossed Wires

There are serveral points worthy of further investigation concerning this problem:

(1) How can we make sure we don't miss any lower-order natural modes when target is complicated?

(2) How to get the early-time response correctly?
How good are the "class-2" coupling coefficients for the early-time response?

If the "class-2" coupling coefficients are correct, then how many modes are needed to guarantee the accuracy of the early-time response?

(3) How to simplify the problem so that the computer program for a general excitation may be executed by a computer efficiently?

(4) Is it necessary to subdivide the segment which contains the junction?

(5) Are there any more boundary conditions which will simplify the computation so that a target with any number of junctions can be solved practically?

7.2.4 More basic questions on SEM

Many unresolved questions on SEM are discussed in [10] and [38]. Here only one question will be raised because it relates to the validity of this thesis.

Do poles of order greater than one occur for the cases in Chapters 4 and 5? If they do occur, can the late-time response still be approximated as a sum of damped sinusoids just like the case of Chapter 3 where branch-cut singularity was approximated by exponentially-decaying functions?

APPENDICES

APPENDIX A

PROGRAM FOR MODIFIED BESSEL FUNCTIONS

```
C****************************************************************************
C THIS IS A UTILITY PROGRAM  TO GENERATE MODIFIED BESSEL FUNCTIONS BY CD RFP
C   I(Z)=MOBEI(Z), I'(Z)=DMOBEI(Z)
C    K(Z)=MOBEKI(Z), K'(Z)=DMOBEK(Z)
C****************************************************************************
      COMPLEX FUNCTION MOBEI(Z)
      COMPLEX Z,CO
      DIMENSION BJRE(100),BJIM(100),YRE(50),YIM(50)
      COMMON N
      M=IABS(N)+1
      CO=CMPLX(0.,-1.)
      A=REAL(Z)
      B=AIMAG(Z)
      CALL COMBES(-B,A,0.,0.,N,BJRE,BJIM,YRE,YIM)
      MOBEI=CMPLX(BJRE(M),BJIM(M))
      MOBEI=MOBEI*(CO**N)
      RETURN
      END
      COMPLEX FUNCTION DMOBEI(Z)
      EXTERNAL MOBEI
      COMPLEX Z,Z1,Z2,MOBEI
      COMMON N
      N=N-1
      Z1=MOBEI(Z)
      N=N+2
      Z2=MOBEI(Z)
      DMOBEI=(Z1+Z2)/2.
      N=N-1
      RETURN
      END
      COMPLEX FUNCTION MOBEKI(Z)
      COMMON N
      COMPLEX Z
      A=REAL(Z)
      B=AIMAG(Z)
      CALL MOBEK(A,B,N,BRK,BIK)
      MOBEKI=CMPLX(BRK,BIK)
      RETURN
      END
      COMPLEX FUNCTION DMOBEK(Z)
      COMPLEX Z,Y1,Y2
      COMMON NI
      A1=REAL(Z)
      B1=AIMAG(Z)
      N1=NI-1 $N2=NI+1
      CALL MOBEK(A1,B1,N1,BRK1,BIK1)
      Y1=CMPLX(BRK1,BIK1)
      CALL MOBEK(A1,B1,N2 ,BRK1,BIK1)
      Y2=CMPLX(BRK1,BIK1)
      DMOBEK=-(Y1+Y2)/2.
      RETURN
      END
      SUBROUTINE MOBEK(A,B,N,BRK,BIK)
      DIMENSION BRJ(100),BIJ(100),RY(50),YI(50)
      PI=2.*ASIN(1.)
      NK=N/2*2
      M=IABS(N)+1
      IF(A.GT.0.) GO TO 14
      IF(B.LT.0.) GO TO 14
      CALL COMBES(B,-A,0.,0.,N,BRJ,BIJ,RY,YI)
      IF(N.EQ.NK) GO TO 1
      NK=NK/2
      NL=NK/2*2
      IF(N.LT.0) GO TO 88
      IF(NK.EQ.NL) GO TO 11
      GO TO 55
   88 IF(NK.NE.NL) GO TO 11
   55 BRK= PI/2*(BRJ(M)+YI(M))
      BIK= PI/2*(BIJ(M)-RY(M))
      GO TO 15
   11 BRK=-PI/2*(BRJ(M)+YI(M))
      BIK=-PI/2*(BIJ(M)-RY(M))
      GO TO 15
    1 NL=N/4*4
      IF(N.LT.0) GO TO 34
      IF(NK.EQ.NL) GO TO 12
      GO TO 51
   34 IF(NK.NE.NL) GO TO 12
   51 BRK=-PI/2*(BIJ(M)-RY(M))
      BIK= PI/2*(BRJ(M)+YI(M))
      GO TO 15
   12 BRK= PI/2*(BIJ(M)-RY(M))
      BIK=-PI/2*(BRJ(M)+YI(M))
```

```
      GO TO 16
   14 CALL COMBES(-B,A,0.,0.,N,BRJ,BIJ,RY,YI)
      IF(N.EQ.NK) GO TO 3
      NK=NK/2
      NL=NK/2*2
      IF(N.LT.0) GO TO 98
      IF(NK.EQ.NL) GO TO 13
      GO TO 54
   98 IF(NK.NE.NL) GO TO 13
   54 BRK= PI/2*(BRJ(M)-YI(M))
      BIK= PI/2*(BIJ6M)+RY(M))
      GO TO 16
   13 BRK=-PI/2*(BRJ(M)-YI(M))
      BIK=-PI/2*(BIJ(M)+RY(M))
      GO TO 16
    3 NL=N/4*4
      IF(N.LT.0) GO TO 97
      IF(NK.EQ.NL) GO TO 15
      GO TO 52
   97 IF(NK.NE.NL) GO TO 15
   52 BRK= PI/2*(BIJ(M)+RY(M))
      BIK=-PI/2*(BRJ(M)-YI(M))
      GO TO 16
   15 BRK=-PI/2*(BIJ(M)+RY(M))
      BIK= PI/2*(BRJ(M)-YI(M))
   16 RETURN
      END
C***********************************************************************
C SUBROUTINE COMBES FOR BESSEL FUNCTIONS OF COMPLEX ORDER AND ARGUMENT
C    CHECK REFERENCE FOR DETAILS.
C***********************************************************************
      SUBROUTINE COMBES(X,Y,ALPHA,BETA,N,BJRE,BJIM,YRE,YIM)
      DIMENSION BJRE(100),BJIM(100),YRE(50),YIM(50)
      CALL BEGIN(X,Y,N,K,R)
      CALL JRECUR(X,Y,ALPHA,BETA,K,R,BJRE,BJIM)
      CALL JSUM(ALPHA,BETA,K,BJRE,BJIM,SUMRA,SUMIA)
      CALL FACTOR(X,Y,ALPHA,BETA,Q,K)
      CALL JNORM(K,Q,R,SUMRA,SUMIA,BJRE,BJIM)
 7    CALL YSUM (X,Y,ALPHA,BETA,K,BJRE,BJIM,ASUMR,ASUMI)
 8    CALL YSNU (X,Y,ALPHA,BETA,Q,R,ASUMR,ASUMI,BJRE,BJIM,YRE,YIM)
 9    CALL WRONSK (X,Y,BJRE,BJIM,YRE,YIM)
       BJSQ=BJRE(1)**2+BJIM(1)**2
       IF(BJSQ-.0000000005) 14,14,15
 14   CALL YSUMP(X,Y,ALPHA,BETA,K,BJRE,BJIM,ASUMR,ASUMI)
      CALL YSNUP(X,Y,ALPHA,BETA,Q,R,ASUMR,ASUMI,BJRE,BJIM,YRE,YIM)
 15   IF (N-1)16,12,11
 16   IF (N)13,12,12
 13   CALL NEGN (X,Y,ALPHA,BETA,N,BJRE,BJIM,YRE,YIM)
      GO TO 12
   11 CALL YRECUR(X,Y,N,BJRE,BJIM,YRE,YIM)
 12   RETURN
      END
CBES402  BEGIN SUBROUTINE                           PART 2 OF 15
      SUBROUTINE BEGIN(X,Y,N,K,R)
      SSQ=X**2+Y**2
      KTEN=SQRT(SSQ)+20.0
      NTEN=IABS(N)+10
      M=MAX0(KTEN,NTEN) /2
      K=2*M+1
        R = K + 1
      RETURN
      END
CBES403  JRECUR SUBROUTINE                          PART 3 OF 15
      SUBROUTINE JRECUR(X,Y,ALPHA,BETA,K,R,BJRE,BJIM)
      DIMENSION BJRE(100),BJIM(100)
      RALPHA=R+ALPHA
      SSQ=X**2+Y**2
      BJRE(K+2)=0
      BJIM(K+2)=0
      BJRE(K+1)=1.0E-37
      BJIM(K+1)=0.0
      DO4I=1,K
      L1=K+1-I
      RALPHA=RALPHA-1.0
      A=((2.0*X*RALPHA)+(2.0*BETA*Y))/SSQ
      B=((-2.0*Y*RALPHA)+(2.0*BETA*X))/SSQ
      BJRE(L1)=(A*BJRE(L1+1))-(B*BJIM(L1+1))-BJRE(L1+2)
 4    BJIM(L1)=(B*BJRE(L1+1))+(A*BJIM(L1+1))-BJIM(L1+2)
      RETURN
      END
CBES404  JSUM SUBROUTINE                            PART 4 OF 15
      SUBROUTINE JSUM(ALPHA,BETA,K,BJRE,BJIM,SUMRA,SUMIA)
      DIMENSION BJRE(100),BJIM(100)
 901  SUMRA=(BJRE(3)*(ALPHA+2.0))-(BJIM(3)*BETA)
      SUMIA=(BETA*BJRE(3))+((ALPA+2.0)*BJIM(3))
      GRE=1.0
      GIM=0
      S=1.0
```

```
      DO6I=3,K,2
      S=S+1.0
      GREN=((GRE*(ALPHA+S-1.0))-(BETA*GIM))/S
      GIM=((GIM*(ALPHA+S-1.0))+(BETA*GRE))/S
      GRE=GREN
      ALPTS=ALPHA+2.0*S
      GJR=GRE*BURE(I)
      GJI=GIM*BUIM(I)
      GJRI=GRE*BUIM(I)
      GJIR=GIM*BURE(I)
      SUMRB=ALPTS*(GJR-GJI)-BETA*(GJIR+GJRI)+SUMRA
      SUMIB=ALPTS*(GJIR+GJRI)-BETA*(GJI-GJR)+SUMIA
      IF(SUMRA)15,21,15
   15 IF(ABS((SUMRB/SUMRA)-1.0)-.00000005)21,21,10
   21 IF(SUMIA)20,11,20
   20 IF(ABS((SUMIB/SUMIA)-1.0)-.00000005)11,11,10
   10 SUMRA=SUMRB
    6 SUMIA=SUMIB
   11 RETURN
      END
CBES405  FACTOR SUBROUTINE                              PART 5 OF 15
      SUBROUTINE FACTOR(X,Y,ALPHA,BETA,Q,R)
      CALL LOGGAM(ALPHA+1.0,BETA,U,V)
      CALL COMLOG(X,Y,A1,B1)
      A2=ALPHA*A1-BETA*B1
      B2=BETA*A1+ALPHA*B1
      A2=-A2
      B2=-B2
      CALL COMEXP(A2,B2,A3,B3)
      A4=.6931471806*ALPHA
      B4=.6931471806*BETA
      CALL COMEXP(A4,B4,A5,B5)
      A6=A3*A5-B3*B5
      B6=B3*A5+A3*B5
      CALL COMEXP(U,V,A7,B7)
      Q=A6*A7-B6*B7
      R=B6*A7+A6*B7
      RETURN
      END
CBES406  COMLOG SUBROUTINE                              PART 6 OF 15
C     COMPLEX LOGARITHM - BRANCH CUT ON NEGATIVE REAL AXIS
      SUBROUTINE COMLOG(X,Y,A,B)
      PI=3.141592654
      A=.5*ALOG(X*X+Y*Y)
      IF(X)3,1,4
    1 B=.5*PI
      IF(Y)2,3,8
    2 B=-B
      GO TO 8
    3 B=0.
      GO TO 8
    4 B=ATAN(Y/X)
      GO TO 8
    5 B=ATAN(Y/X)
      IF(Y)6,7,7
    6 B=B-PI
      GO TO 8
    7 B=B+PI
    8 RETURN
      END
CBES407  COMEXP SUBROUTINE                              PART 7 OF 15
      SUBROUTINE COMEXP(X,Y,A,B)
      C=EXP(X)
      A=C*COS(Y)
      B=C*SIN(Y)
      RETURN
      END
CBES408  UNORM SUBROUTINE                               PART 8 OF 15
      SUBROUTINE UNORM(K,Q,R,SUMRA,SUMIA,BURE,BUIM)
      DIMENSION BURE(100),BUIM(100)
      S=((SUMRA+BURE(1))*Q)-((SUMIA+BUIM(1))*R)
      T=((SUMIA+BUIM(1))*Q)+((SUMRA+BURE(1))*R)
      IF(ABS(S)-ABS(T))100,101,101
  101 TS=T/S
      TSSQ=S*(1.0+(TS**2))
   12 DO13I=1,K
      BUREN=(BURE(I)+BUIM(I)*TS)/TSSQ
      BUIM(I)=(BUIM(I)-BURE(I)*TS)/TSSQ
   13 BURE(I)=BUREN
      GO  TO  14
  100 ST=S/T
      STSQ=T*((ST**2)+1.0)
  102 DO103I=1,K
      BUREN=(BURE(I)*ST+BUIM(I))/STSQ
      BUIM(I)=(BUIM(I)*ST-BURE(I))/STSQ
  103 BURE(I)=BUREN
   14 RETURN
      END
```

```
CBES409   YSUM SUBROUTINE                                      PART 9 OF 15
      SUBROUTINE YSUM (X,Y,ALPHA,BETA,K,BJRE,BJIM,ASUMR,ASUMI)
      DIMENSION BJRE(100),BJIM(100)
      A1=ALPHA-1.0
      A2=A1-1.0
      A3=A1+ALPHA
      A4=BETA**2
      A5=2.0*A4
      ABSQ=(-A1)**2+A4
      GAMRE=((2.0+ALPHA)*(-A1)-A4)/ABSQ
      GAMIM=(BETA*3.0)/ABSQ
      ASUMR=GAMRE*BJRE(3)-GAMIM*BJIM(3)
      ASUMI=GAMIM*BJRE(3)+GAMRE*BJIM(3)
      T=1.0
      DO 500 I=5,K,2
      T=T+1.0
      B1=2.0*T
      F1=B1+ALPHA
      F2=A3+T
      F3=A1+T
      F5=T-ALPHA
      F6=A2+B1
      G1=F1*F2-A5
      G2=(F2+2.0*F1)*BETA
      H1=G1*F3-G2*BETA
      H2=G2*F3+G1*BETA
      P1=F5*F6+A4
      P2=(F5-F6)*BETA
      P3=P1**2+P2**2
      CRE=((H1*P1+H2*P2)/P3)/T
      CIM=((H2*P1-H1*P2)/P3)/T
      TEMP=-(CRE*GAMRE-CIM*GAMIM)
      GAMIM=-(CIM*GAMRE+CRE*GAMIM)
      GAMRE=TEMP
      BSUMR=GAMRE*BJRE(I)-GAMIM*BJIM(I)+ASUMR
      BSUMI=GAMIM*BJRE(I)+GAMRE*BJIM(I)+ASUMI
      IF(ABS((BSUMR/ASUMR)-1.0)-.00000005)521,521,510
  521 IF(ASUMI)520,511,520
  520 IF(ABS((BSUMI/ASUMI)-1.0)-.00000005)511,511,510
  510 ASUMR=BSUMR
  500 ASUMI=BSUMI
  511 RETURN
      END
CBES410   YSMU SUBROUTINE                                      PART 10 OF 15
      SUBROUTINE YSMU(X,Y,ALPHA,BETA,Q,R,ASUMR,ASUMI,BJRE,BJIM,YRE,YIM)
      DIMENSION BJRE(100),BJIM(100),YRE(50),YIM(50)
      PI=3.141592654
      TPI=2.0/PI
      GRE=TPI*(Q**2-R**2)
      GIM=TPI*2.0*Q*R
      QRE=GRE*ASUMR-GIM*ASUMI
      QIM=GIM*ASUMR+GRE*ASUMI
      IF(ALPHA)1,2,1
    2 IF(BETA)1,3,1
    3 CALL YZERO(X,Y,ALPRE,ALPIM)
      GO TO 720
    1 PALPHA=PI*ALPHA
      COX=COS(PALPHA)
      SIX=SIN(PALPHA)
      EXY=EXP(PI*BETA)
      EXY1=1.0/EXY
      COSH=.5*(EXY+EXY1)
      SINH=.5*(EXY-EXY1)
      DEN=(SIX*COSH)**2+(COX*SINH)**2
      ERE=(SIX*COX)/DEN
      EIM=(-COSH*SINH)/DEN
      ABSQ3=2.0*(ALPHA**2+BETA**2)
      ALPRE=ERE-((QRE*ALPHA+BETA*QIM)/ABSQ3)
      ALPIM=EIM-((QIM*ALPHA-BETA*QRE)/ABSQ3)
  720 YRE(1)=ALPRE*BJRE(1)-ALPIM*BJIM(1)+QRE
      YIM(1)=ALPIM*BJRE(1)+ALPRE*BJIM(1)+QIM
      RETURN
      END
CBES411   YZERO SUBROUTINE                                     PART 11 OF 15
      SUBROUTINE YZERO(X,Y,ALPRE,ALPIM)
      TPI=2.0/3.141592654
      CALL COMLOG(X,Y,A,B)
      ALPRE=TPI*(-.1159315157+A)
      ALPIM=TPI*B
      RETURN
      END
CBES412   WRONSK SUBROUTINE                                    PART 12 OF 15
      SUBROUTINE WRONSK(X,Y,BJRE,BJIM,YRE,YIM)
      DIMENSION BJRE(100),BJIM(100),YRE(50),YIM(50)
      SSQ=X**2+Y**2
      TPI=2.0/3.141592654
      AZRE=TPI*X/SSQ
      AZIM=-TPI*Y/SSQ
```

```
      ZRE=BJRE(2)*YRE(1)-BJIM(2)*YIM(1)
      ZIM=BJIM(2)*YRE(1)+BJRE(2)*YIM(1)
      BZRE=ZRE-AZRE
      BZIM=ZIM-AZIM
      BJSQ=BJRE(1)**2+BJIM(1)**2
      CZRE=BJRE(1)/BJSQ
      CZIM=(-BJIM(1))/BJSQ
      YRE(2)=BZRE*CZRE-BZIM*CZIM
      YIM(2)=BZIM*CZRE+BZRE*CZIM
      RETURN
      END
CBES413  NEGN SUBROUTINE                                PART 13 OF 15
      SUBROUTINE NEGN(X,Y,ALPHA,BETA,N,BJRE,BJIM,YRE,YIM)
      DIMENSION BJRE(100),BJIM(100),YRE(50),YIM(50)
      L=IABS(N)+1
      SSQ=X**2+Y**2
      TX=2.0*X
      TY=2.0*Y
      RALPHA=ALPHA
      A=(TX*RALPHA+TY*BETA)/SSQ
      B=(-TY*RALPHA+TX*BETA)/SSQ
      BJRE(2)=A*BJRE(1)-B*BJIM(1)-BJRE(2)
      BJIM(2)=B*BJRE(1)+A*BJIM(1)-BJIM(2)
      YRE(2)=A*YRE(1)-B*YIM(1)-YRE(2)
      YIM(2)=B*YRE(1)+A*YIM(1)-YIM(2)
      IF(L-3)3,2,2
    2 DO 1 I=3,L
      RALPHA=RALPHA-1.0
      A=(TX*RALPHA+TY*BETA)/SSQ
      B=(-TY*RALPHA+TX*BETA)/SSQ
      BJRE(I)=A*BJRE(I-1)-B*BJIM(I-1)-BJRE(I-2)
      BJIM(I)=B*BJRE(I-1)+A*BJIM(I-1)-BJIM(I-2)
      YRE(I)=A*YRE(I-1)-B*YIM(I-1)-YRE(I-2)
    1 YIM(I)=B*YRE(I-1)+A*YIM(I-1)-YIM(I-2)
    3 CONTINUE
      RETURN
      END
CBES414  YRECUR SUBROUTINE                              PART 14 OF 15
      SUBROUTINE YRECUR(X,Y,N,BJRE,BJIM,YRE,YIM)
      DIMENSION BJRE(100),BJIM(100),YRE(50),YIM(50)
      SSQ=X**2+Y**2
      TPI=2.0/3.141592654
      AZRE=TPI*X/SSQ
      AZIM=-TPI*Y/SSQ
      L=N+1
      IF(L-3)3,2,2
    2 DO 1 I=3,L
      ZRE=BJRE(I)*YRE(I-1)-BJIM(I)*YIM(I-1)
      ZIM=BJIM(I)*YRE(I-1)+BJRE(I)*YIM(I-1)
      BZRE=ZRE-AZRE
      BZIM=ZIM-AZIM
      BJSQ=BJRE(I-1)**2+BJIM(I-1)**2
      CZRE=BJRE(I-1)/BJSQ
      CZIM=(-BJIM(I-1))/BJSQ
      YRE(I)=BZRE*CZRE-BZIM*CZIM
    1 YIM(I)=BZIM*CZRE+BZRE*CZIM
    3 CONTINUE
      RETURN
      END
CBES415  YGNUP SUBROUTINE                               PART 15 OF 15
      SUBROUTINE YGNUP(X,Y,ALPHA,BETA,Q,R,ASUMR,ASUMI,BJRE,BJIM,YRE,YIM)
      DIMENSION BJRE(100),BJIM(100),YRE(50),YIM(50)
      PI=3.141592654
      TPI=2.0/PI
      GRE=TPI*(Q**2-R**2)
      GIM=TPI*2.0*Q*R
      DRE=GRE*ASUMR-GIM*ASUMI
      DIM=GIM*ASUMR+GRE*ASUMI
      IF(ALPHA)1,2,1
    2 IF(BETA)1,3,1
    3 CALL YZERO(X,Y,ALPRE,ALPIM)
      GO TO 72
    1 RALPHA=PI*ALPHA
      COX=COS(RALPHA)
      SIX=SIN(RALPHA)
      EXY=EXP(PI*BETA)
      EXY1=1.0/EXY
      COSH=.5*(EXY+EXY1)
      SINH=.5*(EXY-EXY1)
      DEN=(SIX*COSH)**2+(COX*SINH)**2
      ERE=(SIX*COX)/DEN
      EIM=(-COSH*SINH)/DEN
      ABSQ3=2.0*(ALPHA**2+BETA**2)
      ALPRE=ERE-((GRE*ALPHA+BETA*GIM)/ABSQ3)
      ALPIM=EIM-((GIM*ALPHA-BETA*GRE)/ABSQ3)
   72 TRE=ALPRE*BJRE(2)-ALPIM*BJIM(2)+DRE
      TIM=ALPIM*BJRE(2)+ALPRE*BJIM(2)+DIM
      ALPRE=-(Q*X+R*Y)/(X**2+Y**2)
```

```
      ALPIM=-(X*R-G*Y)/(X**2+Y**2)
      YRE(2)=ALPRE*BJRE(1)-ALPIM*BJIM(1)+TRE
      YIM(2)=ALPIM*BJRE(1)+ALPRE*BJIM(1)+TIM
      RETURN
       END
CBES416  YSUMP SUBROUTINE                              PART 16 OF 16
      SUBROUTINE YSUMP(X,Y,ALPHA,BETA,K,BJRE,BJIM,ASUMR,ASUMI)
      DIMENSION BJRE(100),BJIM(100)
      A1=ALPHA-1.0
      A2=A1-1.0
      A3=A1+ALPHA
      A4=BETA**2
      A5=2.0*A4
      ABSQ=(-A1)**2+A4
      ROLDRE=((2.0+ALPHA)*(-A1)-A4)/ABSQ
      ROLDIM=(BETA*3.0)/ABSQ
      RES1=-ROLDRE/2.0
      VMS1=-ROLDIM/2.0
      STORE=3.*(ALPHA*X+BETA*Y)/(X**2+Y**2)
      STOIM=3.*(X*BETA-ALPHA*Y)/(X**2+Y**2)
      RES2=(ROLDRE*STORE-ROLDIM*STOIM)
      VMS2=(ROLDRE*STOIM+ROLDIM*STORE)
      ASUMR=RES1*BJRE(2)-VMS1*BJIM(2)
      ASUMR=ASUMR+RES2*BJRE(3)-VMS2*BJIM(3)
      ASUMI=VMS1*BJRE(2)+RES1*BJIM(2)
      ASUMI=ASUMI+VMS2*BJRE(3)+RES2*BJIM(3)
      T=1.0
      DO 500 I=3,K,2
      T=T+1.0
      B1=2.0*T
      F1=B1+ALPHA
      F2=A3+T
      F3=A1+T
      F5=T-ALPHA
      F6=A2+B1
      G1=F1*F2-A5
      G2=(F2+2.0*F1)*BETA
      H1=G1*F3-G2*BETA
      H2=G2*F3+G1*BETA
      P1=F5*F6+A4
      P2=(F5-F6)*BETA
      P3=P1**2+P2**2
      CRE=((H1*P1+H2*P2)/P3)/T
      CIM=((H2*P1-H1*P2)/P3)/T
      TEMP=-(CRE*ROLDRE-CIM*ROLDIM)
      RNEWIM=-(CIM*ROLDRE+CRE*ROLDIM)
      RNEWRE=TEMP
      RES1=(ROLDRE-RNEWRE)/2.0
      VMS1=(ROLDIM-RNEWIM)/2.0
      RES2=(RNEWRE*STORE-RNEWIM*STOIM)
      VMS2=(RNEWRE*STOIM+RNEWIM*STORE)
      BSUMR=RES1*BJRE(I+1)-VMS1*BJIM(I+1)+ASUMR
      BSUMI=VMS1*BJRE(I+1)+RES1*BJIM(I+1)+ASUMI
      BSUMR=RES2*BJRE(I+2)-VMS2*BJIM(I+2)+BSUMR
      BSUMI=VMS2*BJRE(I+2)+RES2*BJIM(I+2)+BSUMI
      IF(ABS((BSUMR/ASUMR)-1.0)-.00000005)521,521,510
  521 IF(ASUMI)520,511,520
  520 IF(ABS((BSUMI/ASUMI)-1.0)-.00000005)511,511,510
  510 ASUMR=BSUMR
      ASUMI=BSUMI
      ROLDIM=RNEWIM
  500 ROLDRE=RNEWRE
  511 RETURN
       END
      SUBROUTINE LOGGAM(X,Y,U,V)
CLOGGAM  LOG OF THE GAMMA FUNCTION OF COMPLEX ARGUMENTS  FORTRAN II
C THIS SUBROUTINE COMPUTES THE NATURAL LOG OF THE GAMMA FUNCTION FOR
C COMPLEX ARGUMENTS.  THE ROUTINE IS ENTERED BY THE STATEMENT
C       CALL LOGGAM(X,Y,U,V)
C WHERE    X IS THE REAL PART OF THE ARGUMENT
C          Y IS THE IMAGINARY PART OF THE ARGUMENT
C          U IS THE REAL PART OF THE RESULT
C          V IS THE IMAGINARY PART OF THE RESULT
      DIMENSION H(7)
      H(1)=2.269488974
      H(2)=1.517473649
      H(3)=1.011523068
      H(4)=5.256064690E-1
      H(5)=2.523809524E-1
      H(6)=3.333333333E-2
      H(7)=8.333333333E-2
      E2=1.57079632679
      PI=3.14159265359
      B1=0.0
      B2=0.0
      J=2
      Y2=Y
    4 IF(Y)1,2,3
```

```
    3 B6=ATAN(Y/X)
      T=Y**2
    5 B7=Y**2+T
C   REAL PART OF LOG
      T1=.5*ALOG(B7)
      IF(X-2.0)7,7,6
    7 B1=B1+B6
      B2=B2+T1
      X=X+1.0
      J=1
      GO TO 4
    6 T3=-Y*B6+(T1*(X-.5)-X+9.1893853320E-1)
      T2=B6*(X-.5)+Y*T1-Y
      T4=X
      T5=-Y
      T1=B7
      DO 8 I=1,7
      T=H(I)/T1
      T4=T*T4+X
      T5=-(T*T5+Y)
    8 T1=T4**2+T5**2
      T3=T4-X+T3
      T2=-T5-Y+T2
      GO TO (9,10),J
    9 T3=T3-B2
      T2=T2-B1
   10 IF(Y2)11,12,12
   12 U=T3
      V=T2
      X=X2
      RETURN
   11 U=T3-E4
      V=T2-E5
      X=X2
      RETURN
C     X IS ZERO
    2 T=0.0
      IF(Y)13,14,15
   13 B6=-E2
      GO TO 5
   15 B6=E2
      GO TO 5
C     X IS NEGATIVE
    1 E4=0.0
      E5=0.0
      IE6=0
   16 E4=E4+.5*(ALOG(X**2+Y**2))
      E5=E5+ATAN(Y/X)
      IE6=IE6+1
      X=X+1.0
      IF(X)16,17,17
   17 IF(MOD(IE6,2))18,4,18
   18 E5=E5+E9
      GO TO 4
   14 PRINT 19,X2,Y
   19 FORMAT(29H ATTEMPTED TO TAKE LOGGAM OF 3HX=F6.0,1X2HY=F6.0)
      CALL EXIT
      END
```

APPENDIX B

PROGRAMS FOR NATURAL MODES

```
C**********************************************************************
C THIS PROGRAM COMPUTES NATURAL FREQS AND MODAL CURRENTS
C FOR COUPLED WIRES
C IT IS CATALOGED AS CHUANGEW
C THERE ARE TWO MODES OF OPRATIONS:
C  FOR MODAL CURRENTS(INTERCHANGE MAIN AND DET WITH MMODE & CURMODE):
C     TAPE1=ROOTS; TAPE2=REAL PART OF CURRENT; TAPE3=IMAG PART OF CU
C     TAPE4=COMPLEX CU
C      ATTACH,A,SIMAT152. FOR CMATPAC. LOAD,A. LGO. TO EXECUTE
C  FOR NATURAL FREQS( AS IT IS NOW ):
C     TAPE1=ROOTS
C      ATTACH,A,SIMAT152. FOR CMATPAC; ATTACH,B,NEWTONLGO. FOR NEWTON'S
C       METHOD
C      LOAD,A,B. LGO. TO EXECUTE
C**********************************************************************
       PROGRAM MAIN(INPUT,OUTPUT,TAPE1)
C**********************************************************************
C TO FIND THE NATURAL FREQUENCIES BY USING NEWTON'S METHOD.
C**********************************************************************
       COMPLEX ROOT(1), DET,H
       DIMENSION A(11),B(11)
       EXTERNAL DET
       COMMON/NUMBER/NP
       COMMON/AN/AN
       COMMON/DN/DN
       COMMON/ALPHA/ALPHA
       COMMON/ISO/ISO
       COMMON/INDEX/INDEX
       PI=4.*ATAN(1.)
       A(1)=-.0624 $ B(1)=.9251
       A(2)=-.1212 $ B(2)=1.9117
       A(3)=-.1491 $ B(3)=2.8835
       A(4)=-.1713 $ B(4)=3.8741
       A(5)=-.1909 $B(5)=4.8535
       A(6)=-.2080 $ B(6)=5.8453
       A(7)=-.2240 $ B(7)=6.8286
       A(8)=-.2383 $ B(8)=7.8212
       A(9)=-.2522 $ B(9)=8.8066
       A(10)=-.2648 $ B(10)=9.8001
       A(11)=2.*A(10)-A(9) $ B(11)=2.*B(10)-B(9)
       N=10 $ NR=10 $ AN=.0025 $ DN=.5 $ ALPHA=PI/6. $ INDEX=1
C INDEX=1 FOR SYM; -1 FOR ANTISYM
C AN=A/L; DN=D/L; NR=# OF ROOTS TO BE FOUND; NP=N*I=# OF PARTI FOR ITH
       ISO=1
C ISO=1 FOR ISOLATED WIRE; 0 FOR COUPLED WIRES
       DO 10 I=1,NR
       NP=N*I
       ROOT(1)=CMPLX(A(I),B(I))
       H=CMPLX(1.E-5,1.E-5)
       CALL NEWTON(DET,1.E-5,1.E-4,ROOT(1),H,500,500)
       PRINT 20,I,ROOT(1)
       WRITE(1,*) ROOT(1)
20     FORMAT(7H  ROOT(,I2,3H)=(,F10.4,1H,,F10.4,1H))
10     CONTINUE
       END
       COMPLEX FUNCTION DET(S)
C**********************************************************************
C TO EVALUATE DET(S) BY CALLING MET TO FIND THE MATRIX ELEMENTS
C AND CALLING CMATPAC TO FIND THE DETERMINANT.
C**********************************************************************
       COMPLEX A(152,1),S
       COMMON/NUMBER/NP
       COMMON A
       NPP1=NP+1
       NPP2=NP+2
       CALL SETFL(A(NPP2,NPP2))
C NOTE: ALWAYS DECLARE MORE DIMENSION THAN NECESSARY
       CALL MET(S)
       CALL CMATPAC(1,A,NPP1,0,DET,1.E-200)
       RETURN
       END
       SUBROUTINE MET(S)
C**********************************************************************
C GENERATING THE MATRIX ELEMENTS. (HALLEN'IE)
C**********************************************************************
       COMPLEX A(152,1),S,FACT,A2,Z,A1
       COMPLEX DET
       COMMON/NUMBER/NP
       COMMON A
       COMMON/AN/AN
       COMMON/DN/DN
       COMMON/ALPHA/ALPHA
       COMMON/Z/Z
```

```
      COMMON/INDEX/INDEX
      COMMON/N/N
      COMMON/ISO/ISO
      Z=S
      ALPHA2=2.*ALPHA
      PI=4.*ATAN(1.)
      A2=2./PI*ALOG(SQRT(1+(1./AN/2./NP)**2)+1./AN/2./NP)-S/NP
       NPP1=NP+1
       DO 5 M=1,NPP1
       N=2
       DMN=M-N $ SMN=M+N-2
       R=PI*SQRT((DMN/NP)**2+AN**2)
       IF(M.NE.N) A(M,N)=CEXP(-S*R)/R/NP
       IF(M.EQ.N) A(M,N)=A2
       A(M,N)=-A(M,N)*INDEX
       IF(ISO.EQ.1) GO TO 5
       IF(ALPHA.NE.0.) GO TO 5
       RI=PI*SQRT((DMN/NP*COS(ALPHA))**2+(2*DN+SMN/NP*SIN(ALPHA))**2
      ++AN**2)
       A(M,N)=A(M,N)-COS(ALPHA2)*CEXP(-S*RI)/RI/NP
     5 CONTINUE
       DO 15 M=1,NPP1
       DO 15 N=3,NP
       IDMN=IABS(M-N)
       K=2+IDMN
       A(M,N)=A(K,2)
    15 CONTINUE
       IF(ISO.EQ.1) GO TO 11
       IF(ALPHA.EQ.0.) GO TO 11
       IF(ALPHA.EQ.PI/2.) GO TO 21
C*******INTEGRATION TERMS; SEGMENT-BY-SEGMENT AND ACCUMULATE*********
       DO 10 N=2,NP
       A1=CMPLX(0.,0.) $ A2=A1
       XL=1. $ XU=2.
       DO 10 M=1,NPP1
       IF(M.EQ.1) GO TO 10
       CALL CIMCON(1,XL,XU,.01,100,FACT,NOI,ERR)
       A1=A1+FACT
       CALL CIMCON(2,XL,XU,.01,100,FACT,NOI,ERR)
       A2=A2+FACT
       XL=XU $ XU=XU+1.
       FACT=.5*(CEXP(S*M*PI/NP)+CEXP(-S*M*PI/NP))*A1-.5*(CEXP(S*M*PI/NP)
      +-CEXP(-S*M*PI/NP))*A2
       A(M,N)=A(M,N)-FACT*((N-1.)/NP*SIN(ALPHA2)**2+2*DN*SIN(ALPHA)*(1+
      +COS(ALPHA2)))
10     CONTINUE
21     CONTINUE
       DO 25 M=1,NPP1
       DO 25 N=1,M
       DMN=M-N $ SMN=M+N-2
       RI=PI*SQRT((DMN/NP*COS(ALPHA))**2+(2*DN+SMN/NP*SIN(ALPHA))**2
      ++AN**2)
       A2=COS(ALPHA2)*CEXP(-S*RI)/RI/NP
       IF(N.EQ.1.OR.N.EQ.NPP1) GO TO 26
       A(M,N)=A(M,N)-A2
26     IF(M.EQ.1.OR.M.EQ.NPP1) GO TO 25
       IF(M.NE.N) A(N,M)=A(N,M)-A2
25     CONTINUE
C***********MET RELATED TO CONSTS**********
11     DO 30 M=1,NPP1
       A(M,1)=CEXP(S*PI*(M-1.)/NP)+CEXP(-S*PI*(M-1.)/NP)
       A(M,NPP1)=CEXP(S*PI*(M-1.)/NP)-CEXP(-S*PI*(M-1.)/NP)
30     CONTINUE
       FACT=A(3,3)
C***********NORMALIZATION**********
       DO 50 M=1,NPP1
       DO 50 N=1,NPP1
50     A(M,N)=A(M,N)/FACT
       RETURN
       END
C*****************************************************************
C FUNCTION TO COMPUTE THE INTEGRAND
C*****************************************************************
       COMPLEX FUNCTION F(INDEX,X)
       COMPLEX S
       COMMON/DN/DN
       COMMON/AN/AN
       COMMON/NUMBER/NP
       COMMON/ALPHA/ALPHA
       COMMON/Z/S
       COMMON/N/N
       PI=ATAN(1.)*4.
       DXN=N-X $ SXN=N+X-2.
       RI=PI*SQRT((DXN/NP*COS(ALPHA))**2+(2*DN+SXN/NP*SIN(ALPHA))**2
      ++AN**2)
       IF(INDEX.EQ.2) GO TO 3
       F=(PI/NP)**2*(CEXP(S*PI*X/NP)+CEXP(-S*PI*X
      +/NP))/2.*(1+S*RI)/PI/PI/RI*CEXP(-S*RI)
```

```
      RETURN
3     CONTINUE
      F=(PI/NP)**2*(CEXP(S*PI*X/NP)-CEXP(-S*PI*X
     +/NP))/2.*(1+S*RI)/RI/RI/RI*CEXP(-S*RI)
      RETURN
      END
*EOS
C*****************************************************************
C SUBROUTINE TO FIND THE MODAL CURRENT
C S=ROOT; M=ROW TO BE DELETED; N=COLUMN TO BE MOVED TO RIGHT SIDE
C NN: I(NN) IS SET TO 1
C*****************************************************************
      SUBROUTINE CURMODE(S,M,N,NN)
      COMPLEX S,I(152),A(152,1),B(152),IN
      COMMON/NUMBER/NP
      COMMON A
      COMMON/CURRENT/I
      NPP2=NP+2 $ND=NP+1
      CALL SETFL(A(NPP2,NPP2))
      CALL MET(S)
      NDM1=ND-1
      NM1=N-1
      DO 10 J=1,ND
      B(J)=A(J,N)
10    CONTINUE
      DO 20 J=1,ND
      DO 21 K=N,NDM1
      KP1=K+1
      A(J,K)=A(J,KP1)
21    CONTINUE
      A(J,ND)=-B(J)
20    CONTINUE
      DO 30 J=M,NDM1
      DO 30 K=1,ND
      JP1=J+1
      A(J,K)=A(JP1,K)
30    CONTINUE
      CALL CMATRAC(-1,A,NDM1,1,DET,1.E-200)
      I(1)=CMPLX(0.,0.)
      DO 40 J=2,NM1
      I(J)=A(J,ND)
40    CONTINUE
      I(N)=CMPLX(1.,0.)
      NDM2=ND-2
      DO 50 J=N,NDM2
      JP1=J+1
      I(JP1)=A(J,ND)
50    CONTINUE
      I(ND)=CMPLX(0.,0.)
      IN=I(NN)
      DO 70 J=1,ND
      I(J)=I(J)/IN
70    CONTINUE
      RETURN
      END
C*****************************************************************
C SUBROUTINE OF NEWTON'S METHOD FOR ROOT-SEARCHING,
C NOT NECESSARY WHEN A COMPILED FILE NEWTON.LGO IS ATTACHED
C*****************************************************************
      SUBROUTINE NEWTON(F,EPS1,EPS2,S,H,IT1,IT2)
      COMPLEX S,F,G1,G2,G3,H1
      EXTERNAL F
      DO 20 J=1,IT2
      H1=H
      G1=F(S+H1)
      G2=F(S-H1)
      DO 10 I=1,IT1
      A=CABS(G1-G2)
      IF(A.LE.EPS1) GO TO 10
      H1=H1*.1
      G1=F(S+H1)
      G2=F(S-H1)
      IF(I.EQ.IT1) PRINT 1
1     FORMAT(2X,"DIFF ERR")
10    CONTINUE
      G3=(G1+G2)/2.
      G2=(G1-G2)/H1/2.
      IF(G2.EQ.CMPLX(0.,0.)) GO TO 5
      G3=G3/G2
      B=CABS(G3)
4     FORMAT(2X,E20.10)
      IF(B.LE.EPS2) RETURN
      S=S-G3
3     FORMAT(2X,E20.10,2X,E20.10)
      GO TO 15
5     S=S+H
15    IF(J.EQ.IT2) PRINT 2
2     FORMAT(2X,"FAIL TO CONV")
```

```
20      CONTINUE
        RETURN
        END
        PROGRAM NMODE(INPUT,OUTPUT,TAPE1,TAPE2,TAPE3,TAPE4)
        COMPLEX ROOT(20),CU(152),Y
        COMMON/NUMBER/NP
        COMMON/AN/AN
        COMMON/DN/DN
        COMMON/ALPHA/ALPHA
        COMMON/INDEX/INDEX
        COMMON/CURRENT/CU
        COMMON/ISO/ISO
        REWIND 1
        REWIND 2
        REWIND 3
        REWIND 4
        PI=4.*ATAN(1.)
        NF=10 $ NM=10
C NP=NF*I FOR ITH MODE; NM=# OF MODES WANTED
        AN=.005 $ DN=0.5 $ ALPHA=PI/2.
        ISO=0

        DO 10 I=1,NM
        INDEX=-1
        IF(I.GT.10) INDEX=1
        READ(1,20) ROOT(I)
        PRINT 20,ROOT(I)
        NP=NF*I
        IF(I.GT.10) NP=NF*(I-10)
        NPP1=NP+1
        CALL CURMODE(ROOT(I),6,6,6)
        DO 30 J=1,NPP1
        X=(J-1.)/NP

        WRITE(2,50) X,REAL(CU(J))
        WRITE(3,50) X,AIMAG(CU(J))
        WRITE(4,50) CU(J)
30      CONTINUE
20      FORMAT(F10.4,5X,F10.4)
40      FORMAT(2X,"I AT U=",F5.4,"L IS  (",F10.4,",",F10.4,")")
50      FORMAT(10X,E11.5,10X,F11.5)
10      CONTINUE
        END
01.04.31.  00033 PAGES 002460 LINES PRINTED AT SITE
```

```
C*****************************************************************
C THIS PROGRAM SEARCHES FOR NATURAL FREQS AND MODAL CURRENTS
C FOR CROSS
C IT IS CATALOGED AS CROSSEW
C THERE ARE TWO MODES OF OPERATIONS:
C    FOR MODAL CURRENTS( AS IT IS NOW ):TAPE1=ROOTS; TAPE2=REAL PART
C      OF CURRENT; TAPE3=IAMG PART OF CURRENT; TAPE4=COMPLEX CURRENT
C      ATTACH,A,SIMAT152. FOR CMATPAC; LOAD,A. LGO. TO EXECUTE
C    FOR NATURAL FREQ(INTERCHANGE PROGRAM AFTER *EOS WITH NMODE
C      AND MOVE *EOS IN FRONT OF CURMODE):
C         TAPE1=NATURAL FREQS
C      ATTACH,A,SIMAT152. FOR CMATPAC;
C      ATTACH,B,NEWTONLGO. FOR NEWTON'S METHOD;
C      LOAD,A,B. LGO. TO EXECUTE
C*****************************************************************
      PROGRAM NMODE(INPUT,OUTPUT,TAPE1,TAPE2,TAPE3,TAPE4)
      COMPLEX ROOT(20),CU(152),Y
      COMMON/NUMBER/NP
      COMMON/MODE/MODE
      COMMON/AN/AN
      COMMON/R/R
      COMMON/RW/RW
      COMMON/ALPHA/ALPHA
      COMMON/CURRENT/CU
      REWIND 1
      REWIND 2
      REWIND 3
      REWIND 4
C*****************************************************************
C INPUT PARAMETERS AND ROOTS
C AN=A/L; ALPHA=PI/NALPHA; R=L1/L4; RW=L3/L4; N DECIDES # OF PARTI.
C*****************************************************************
      PI=4.*ATAN(1.)
      PRINT*,"ENTER MODE TYPE: 1 FOR ANTI; 2 FOR SYM-"
      READ*,MODE
      PRINT*,"ENTER NR. # OF ROOTS-"
      READ*,NR
      PRINT*,"ENTER AN-"
      READ*,AN
      PRINT*,"ENTER NALPHA-"
      READ*,NALPHA
      ALPHA=PI/NALPHA
      PRINT*,"ENTER R-"
      READ*,R
      PRINT*,"ENTER RW-"
      READ*,RW
      PRINT*,"ENTER N-"
      READ*,N
      IF(MODE.EQ.2) NP=N
      DO 10 I=1,NR
      IF(MODE.EQ.1) NP=N*(2*I-1)
      IF(MODE.EQ.2.AND.I.GT.5) NP=N+3
      IF(MODE.EQ.2) NN=NP+1
      IF(MODE.EQ.1) ND=NP+1
      N1=NP*R $ N2=NP*RW
      IF(MODE.EQ.2) ND=NP+N1+N2+3
      IF(MODE.EQ.1) NN=1
      NZPP2=NP+N1+2 $ NPP2=NP+2
      PRINT*,"N1=",N1
      PRINT*,"N2=",N2
      READ(1,*) ROOT(I)
      PRINT *,ROOT(I)
C*****************************************************************
C FIND THE MODAL CURRENTS BY CALLING CURMODE
C AND OUTPUT CURRENTS FOUND
C*****************************************************************
      CALL CURMODE(ROOT(I),NE,3,3,NN)
      DO 30 J=1,ND
      IF(MODE.EQ.1) X=(J-1.)/(NP-1.)
      IF(MODE.EQ.2) X=1./NP*(J-NP-1)
      IF(MODE.EQ.2.AND.J.GE.NPP2) X=1./NP*(J-NPP2)
      IF(MODE.EQ.2.AND.J.GT.NZP2) X=1./NP*(J-NZPP2-1)
      IF(MODE.EQ.2) GO TO 38
      WRITE(2,50) X,REAL(CU(J))
      WRITE(3,50) X,AIMAG(CU(J))
      WRITE(4,50) CU(J)
      GO TO 30
38    CONTINUE
      IF(J.LT.NPP2) JJ=J
      IF(J.EQ.NPP2) JJ=ND
      IF(J.GT.NPP2)JJ=J-1
      WRITE(2,50) Y,REAL(CU(JJ))
      WRITE(3,50) Y,AIMAG(CU(JJ))
```

```
      WRITE(4,50) CU(JJ)
30    CONTINUE
40    FORMAT(2X,"I AT U=",F5.4,"L IS  (",F10.4,",",F10.4,")")
50    FORMAT(10X,E11.5,10X,E11.5)
10    CONTINUE
      END
      SUBROUTINE MET(S)
C*****************************************************************************
C GENERATING THE MATRIX ELEMENTS. (HALLEN'IE FOR ANTISYM MODE)
C*****************************************************************************
       COMPLEX A(152,1),S,FACT,A2,Z,A1
       COMMON/NUMBER/NP
       COMMON A
       COMMON/AN/AN
       COMMON/ALPHA/ALPHA
       COMMON/Z/Z
       COMMON/N/N
       Z=S
       ALPHA2=2.*ALPHA
       PI=4.*ATAN(1.)
       A2=2./PI*ALOG(SQRT(1+(1./AN/2./NP)**2)+1./AN/2./NP)-S/NP
       NPP1=NP+1
       DO 5 M=1,NPP1
       N=1
       DMN=M-N $ SMN=M+N-2
       R=PI*SQRT((DMN/NP)**2+AN**2)
       IF(M.NE.N) A(M,N)=CEXP(-S*R)/R/NP
       IF(M.EQ.N) A(M,N)=A2
     5 CONTINUE
       DO 15 M=1,NPP1
       DO 15 N=2,NP
       IDMN=IABS(M-N)
       K=1+IDMN
       A(M,N)=A(K,1)
    15 CONTINUE
       IF(ALPHA.EQ.PI/2.) GO TO 21
       DO 10 N=1,NP
       A1=CMPLX(0.,0.) $ A2=A1
       XL=1. $ XU=2.
       DO 10 M=1,NPP1
       IF(M.EQ.1) GO TO 10
       CALL CIMCON(1,XL,XU,.01,100,FACT,NCI,ERR)
       A1=A1+FACT
       CALL CIMCON(2,XL,XU,.01,100,FACT,NCI,ERR)
       A2=A2+FACT
       XL=XU $ XU=XU+1.
       FACT=.5*(CEXP(S*M*PI/NP)+CEXP(-S*M*PI/NP))*A1-.5*(CEXP(S*M*PI/NP)
      +-CEXP(-S*M*PI/NP))*A2
       A(M,N)=A(M,N)-FACT*(N-1.)/NP*SIN(ALPHA2)**2
10     CONTINUE
21     CONTINUE
       DO 25 M=1,NPP1
       DO 25 N=1,M
       DMN=M-N $ SMN=M+N-2
       R2=PI*SQRT((DMN/NP*COS(ALPHA))**2+(SMN/NP*SIN(ALPHA))**2+AN**2)
       A2=COS(ALPHA2)*CEXP(-S*R2)/R2/NP
       IF(N.EQ.NPP1) GO TO 25
       A(M,N)=A(M,N)-A2
25     IF(M.EQ.NPP1) GO TO 25
       IF(M.NE.N) A(N,M)=A(N,M)-A2
25     CONTINUE
       DO 30 M=1,NPP1
       A(M,NPP1)=CEXP(S*PI*(M-1.)/NP)+CEXP(-S*PI*(M-1.)/NP)
30     CONTINUE
       FACT=A(1,1)
       DO 50 M=1,NPP1
       DO 50 N=1,NPP1
50     A(M,N)=A(M,N)/FACT
       RETURN
       END
       SUBROUTINE METS(S)
C*****************************************************************************
C GENERATING THE MATRIX ELEMENTS. (HALLEN'IE FOR SYM MODE)
C*****************************************************************************
       COMPLEX A(152,1),S,FACT,A2,Z,A1
       COMPLEX C(152)
       COMPLEX B(152)
       COMMON/NUMBER/NP
       COMMON/R/RATIO
       COMMON/RW/RW
       COMMON A
       COMMON/AN/AN
       COMMON/ALPHA/ALPHA
       COMMON/Z/Z
       COMMON/N/N
       Z=S
       ALPHA2=2.*ALPHA
       NI=NP*RATIO
```

```
      NZ=N1+NP
      N2=NP*RW
      NT=NZ+N2
      ALPHAH=ALPHA/2.
      PI=4.*ATAN(1.)
      A2=2./PI*ALOG(SQRT(1+(1./AN/2./NP)**2)+1./AN/2./NP)-S/NP
      NPP1=NP+1
      NZP2=NZ+2
      NPP2=NP+2
      N2P1=N2+1
      NZP1=NZ+1
      NTP2=NT+2
      NTP3=NT+3
      MAX=NZP1
      IF(NZ.LT.N2) MAX=N2P1
      DO 9 I=1,MAX
      R=PI*SQRT(((I-1.)/NP)**2+AN**2)
      IF(I.EQ.1) C(I)=A2
      IF(I.NE.1) C(I)=CEXP(-S*R)/R/NP
9     CONTINUE
      DO 12 M=1,NZP1
      DO 12 N=2,NZ
      I=IABS(M-N)+1
      A(M,N)=C(I)
12    CONTINUE
      DO 13 M=1,N2P1
      DO 13 N=1,N2
      I=IABS(M-N)+1
      A(M+NZP1,N+NZP1)=C(I)
13    CONTINUE
      DO 23 M=1,NZP1
      DO 23 N=1,N2
      A(M,N+NZP1)=CMPLX(0.,0.)
23    CONTINUE
      DO 24 M=1,N2P1
      DO 24 N=2,NZ
      A(M+NZP1,N)=CMPLX(0.,0.)
24    CONTINUE
      IF(ALPHA.EQ.PI/2.) GO TO 17
      DO 14 M=1,N2P1
      DO 14 N=1,N2
      R1=PI*SQRT((1./NP*(M-N-NP)*SIN(ALPHAH))**2+(1./NP*(M+N-NPP2)*
     +COS(ALPHAH))**2+AN**2)
      A(M,N+NZP1)=-2.*CEXP(-S*R1)/R1/NP*COS(ALPHA)
14    CONTINUE
      DO 15 M=1,N2P1
      DO 15 N=2,NZ
      R1=PI*SQRT((1./NP*(M-N+NP)*SIN(ALPHAH))**2+(1./NP*(M+N-NPP2)*
     +COS(ALPHAH))**2+AN**2)
      A(M+NZP1,N)=-CEXP(-S*R1)/R1/NP*COS(ALPHA)
15    CONTINUE
17    CONTINUE
      IF(ALPHA.EQ.PI/4.) GO TO 11
      DO 16 M=1,N2P1
      DO 16 N=1,N2
      R2=PI*SQRT((1./NP*(M-N)*COS(ALPHA))**2+(1./NP*(M+N-2)*
     +SIN(ALPHA))**2+AN**2)
      A(M+NZP1,N+NZP1)=A(M+NZP1,N+NZP1)+CEXP(-S*R2)/R2/NP*COS(ALPHA)
16    CONTINUE
11    CONTINUE
      IF(ALPHA.EQ.PI/2.) GO TO 21
      DO 10 N=1,N2
      A1=CMPLX(0.,0.) $ A2=A1
      XL=1. $ XU=2.
      DO 10 M=1,N2P1
      IF(M.EQ.1) GO TO 10
      CALL CIMCON(1,XL,XU,.01,100,FACT,NOI,ERR)
      A1=A1+FACT
      CALL CIMCON(2,XL,XU,.01,100,FACT,NOI,ERR)
      A2=A2+FACT
      XL=XU $ XU=XU+1.
      FACT=.5*(CEXP(S*M*PI/NP)+CEXP(-S*M*PI/NP))*A1-.5*(CEXP(S*M*PI/NP)
     +-CEXP(-S*M*PI/NP))*A2
      A(M+NZP1,N+NZP1)=A(M+NZP1,N+NZP1)+FACT*(M-1.)/NP*SIN(ALPHAH)**2
10    CONTINUE
21    CONTINUE
      DO 20 N=1,N2
      A1=CMPLX(0.,0.) $ A2=A1
      B(1)=CMPLX(0.,0.)
      C(1)=B(1)
      DO 19 M=2,NZP1
      XL=M-1. $ XU=M
      CALL CIMCON(3,XL,XU,.01,100,FACT,NOI,ERR)
      A1=A1+FACT
      CALL CIMCON(4,XL,XU,.01,100,FACT,NOI,ERR)
      A2=A2+FACT
      B(M)=A1 $ C(M)=A2
19    CONTINUE
```

```
      DO 20 M=1,NZP1
      IF(M.EQ.NPP1) GO TO 20
      FACT=.5*(CEXP(S*M*PI/NP)+CEXP(-S*M*PI/NP))*(B(M)-B(NPP1))-.5*(CEXP
     +(S*M*PI/NP)-CEXP(-S*M*PI/NP))*(C(M)-C(NPP1))
      A(M,N+NZP1)=A(M,N+NZP1)+2.*FACT*(N-1.)/NP*SIN(ALPHA)**2
20    CONTINUE
      DO 22 N=2,NZ
      A1=CMPLX(0.,0.) $ A2=A1
      XL=1. $ XU=2.
      DO 22 M=1,NZP1
      IF(M.EQ.1) GO TO 22
      CALL CIMCON(5,XL,XU,.01,100,FACT,NOI,ERR)
      A1=A1+FACT
      CALL CIMCON(6,XL,XU,.01,100,FACT,NOI,ERR)
      A2=A2+FACT
      XL=XU $ XU=XU+1.
      FACT=.5*(CEXP(S*M*PI/NP)+CEXP(-S*M*PI/NP))*A1-.5*(CEXP(S*M*PI/NP)
     +-CEXP(-S*M*PI/NP))*A2
      A(M+NZP1,N)=A(M+NZP1,N)+FACT*(N-NPP1)/NP*SIN(ALPHA)**2
22    CONTINUE
      DO 30 M=1,NZP1
      A(M,1)=CEXP(S*(M-NPP1)*PI/NP)+CEXP(-S*(M-NPP1)*PI/NP)
      A(M,NZP1)=CEXP(S*(M-NPP1)*PI/NP)-CEXP(-S*(M-NPP1)*PI/NP)
      A(M,NTP2)=0.
30    CONTINUE
      DO 40 M=1,NZP1
      A(M+NZP1,1)=0.
      A(M+NZP1,NZP1)=CEXP(S*PI*(M-1.)/NP)-CEXP(-S*PI*(M-1.)/NP)
      A(M+NZP1,NTP2)=CEXP(S*PI*(M-1.)/NP)+CEXP(-S*PI*(M-1.)/NP)
40    CONTINUE
      DO 41 M=1,NTP2
      A(M,NTP3)=A(M,NPP1)/2.
      A(M,NPP1)=A(M,NTP3)
41    CONTINUE
      DO 42 N=1,NTP3
      A(NTP3,N)=0.
42    CONTINUE
      A(NTP3,NPP1)=1.
      A(NTP3,NTP3)=-1.
      A(NTP3,NZP2)=-2.
      FACT=A(2,2)
      DO 50 M=1,NTP3
      DO 50 N=1,NTP3
50    A(M,N)=A(M,N)/FACT
      RETURN
      END
C*****************************************************************
C FUNCTION TO COMPUTE THE INTEGRAND
C*****************************************************************
      COMPLEX FUNCTION F(INDEX,X)
      COMPLEX S
      COMMON/AN/AN
      COMMON/NUMBER/NP
      COMMON/ALPHA/ALPHA
      COMMON/Z/S
      COMMON/N/N
      PI=ATAN(1.)*4.
      IF(INDEX.NE.1.AND.INDEX.NE.2) GO TO 4
      DXN=N-X $ SXN=N+X-2.
      R2=PI*SQRT((DXN/NP*COS(ALPHA))**2+(SXN/NP*SIN(ALPHA))**2+AN**2)
      IF(INDEX.EQ.2) GO TO 3
      F=(PI/NP)**2*(CEXP(S*PI*X/NP)+CEXP(-S*PI*X
     +/NP))/2.*(1+S*R2)/R2/R2/R2*CEXP(-S*R2)
      RETURN
3     CONTINUE
      F=(PI/NP)**2*(CEXP(S*PI*X/NP)-CEXP(-S*PI*X
     +/NP))/2.*(1+S*R2)/R2/R2/R2*CEXP(-S*R2)
      RETURN
4     IF(INDEX.EQ.5.OR.INDEX.EQ.6) GO TO 5
      DXN=X-N-NP
      GO TO 6
5     DXN=X-N+NP
6     SXN=X+N-NP-2
      R1=PI*SQRT((DXN/NP*SIN(ALPHA/2.))**2+(SXN/NP*COS(ALPHA/2.))**2
     ++AN**2)
      IF(INDEX.EQ.4.OR.INDEX.EQ.6) GO TO 7
      F=(PI/NP)**2*(CEXP(S*PI*X/NP)+CEXP(-S*PI*X/NP))/2.
     +*(1.+S*R1)/R1/R1/R1*CEXP(-S*R1)
      RETURN
7     CONTINUE
      F=(PI/NP)**2*(CEXP(S*PI*X/NP)-CEXP(-S*PI*X/NP))/2.
     +*(1.+S*R1)/R1/R1/R1*CEXP(-S*R1)
      RETURN
      END
C*****************************************************************
C SUBROUTINE TO FIND THE MODAL CURRENT
C SEROOT: ND=DIMENSION OF MATRIX; ZEROS TO BE DELETED;
C N=COLUMN TO BE MOVED TO RIGHT HAND SIDE; AND I(N) SET TO 1
```

```
C***************************************************************
      SUBROUTINE CURMODE(S,ND,M,N,NN)
      COMPLEX S,I(152),A(152,1),B(152),IN
      COMMON/NUMBER/NP
      COMMON/R/R
      COMMON/RW/RW
      COMMON/MODE/MODE
      COMMON A
      COMMON/CURRENT/I
      NDP1=ND+1
      CALL SETFL(A(NDP1,NDP1))
      IF(MODE.EQ.1) CALL MET(S)
      IF(MODE.EQ.2) CALL METS(S)
      NDM1=ND-1
      NM1=N-1
      DO 10 J=1,ND
      B(J)=A(J,N)
10    CONTINUE
      DO 20 J=1,ND
      DO 21 K=N,NDM1
      KP1=K+1
      A(J,K)=A(J,KP1)
21    CONTINUE
      A(J,ND)=-B(J)
20    CONTINUE
      DO 30 J=M,NDM1
      DO 30 K=1,ND
      JP1=J+1
      A(J,K)=A(JP1,K)
30    CONTINUE
      CALL CMATRAC(-1,A,NDM1,1,DET,1.E-200)
      DO 40 J=1,NM1
      I(J)=A(J,ND)
40    CONTINUE
      I(N)=CMPLX(1.,0.)
      DO 50 J=N,NDM1
      JP1=J+1
      I(JP1)=A(J,ND)
50    CONTINUE
      IF(MODE.EQ.1) I(ND)=CMPLX(0.,0.)
      IF(MODE.EQ.2) I(1)=CMPLX(0.,0.)
      NZP1=NP*(1+R)+1
      IF(MODE.EQ.2) I(NZP1)=CMPLX(0.,0.)
      IF(MODE.EQ.2) I(NDM1)=CMPLX(0.,0.)
      IN=I(NN)
      DO 70 J=1,ND
      I(J)=I(J)/IN
70    CONTINUE
      RETURN
      END
*EOS
      PROGRAM MAIN(INPUT,OUTPUT,TAPE1)
C*****************************************************************
C TO FIND THE NATURAL FREQUENCIES BY USING NEWTON'S METHOD.
C*****************************************************************
      COMPLEX ROOT(1), DET,H
      EXTERNAL DET
      COMMON/MODE/MODE
      COMMON/NUMBER/NP
      COMMON/R/R
      COMMON/RW/RW
      COMMON/AN/AN
      COMMON/ALPHA/ALPHA
      PRINT*,"ENTER MODE TYPE: 1 FOR ANTI: 2 FOR SYM-"
      READ*,MODE
      PI=4.*ATAN(1.)
      PRINT*,"ENTER R-"
      READ*,R
      PRINT*,"ENTER RW-"
      READ*,RW
      PRINT*,"ENTER AN-"
      READ*,AN
      PRINT*,"ENTER NALPHA-"
      READ*,NALPHA
      ALPHA=PI/NALPHA
      PRINT*,"ENTER N-"
      READ*,N
      IF(MODE.EQ.2) NP=N
      PRINT*,"ENTER NR, # OF ROOTS-"
      READ*,NR
      DO 10 I=1,NR
      H=CMPLX(1.E-5,1.E-5)
      IF(MODE.EQ.1) NP=N*(2*I-1)
      IF(MODE.EQ.2.AND.I.GT.5) NP=N*5
      IF(MODE.EQ.1) ROOT(1)=CMPLX(0.,(2.*I-1.)/2.)
      IF(MODE.EQ.2) ROOT(1)=CMPLX(0.,I/2.)
      CALL NEWTON(DET,1.E-5,1.E-4,ROOT(1),H,500,500)
      PRINT 20,I,ROOT(1)
```

```
      WRITE(1,*) ROOT(1)
20    FORMAT(7H  ROOT(,I2,3H)=(,F10.4,1H,,F10.4,1H))
10    CONTINUE
      END
      COMPLEX FUNCTION DET(S)
C**********************************************************************
C TO EVALUATE DET(S) BY CALLING MET(OR METS) TO FIND THE MATRIX ELEMENTS
C AND CALLING CMATPAC TO FIND THE DETERMINANT.
C**********************************************************************
      COMPLEX A(152,1),S
      COMMON/NUMBER/NP
      COMMON/R/R
      COMMON/RW/RW
      COMMON/MODE/MODE
      COMMON A
      IF(MODE.EQ.1) GO TO 2
      N1=NP*R $ N2=NP*RW
      ND=NP+N1+N2+3
      NDP1=ND+1
      GO TO 3
2     ND=NP+1
      NDP1=NP+2
3     CALL SETFL(A(NDP1,NDP1))
      IF(MODE.EQ.1) CALL MET(S)
      IF(MODE.EQ.2) CALL METS(S)
      CALL CMATPAC(1,A,ND,0,DET,1.E-200)
      RETURN
      END
00.47.44.  00058 PAGES 007168 LINES PRINTED AT SITE MV
```

APPENDIX C
PROGRAM FOR IMPULSE RESPONSES

```
      PROGRAM MAIN(INPUT,OUTPUT,TAPE1,TAPE2,TAPE3)
C*********************************************************************
C THIS PROGRAM COMPUTES IMPULSE RESPONSE OF COUPLED WIRES
C TAPE1=ROOTS; TAPE2=MODAL CURRENTS; TAPE3=IMP RES OR STP RES
C IT IS CATALOGED AS IMPEW
C*********************************************************************
      COMPLEX S(20),CU(20,101),DP(20),D1(100),D,A(20,3,200),FACT,RES(20)
      COMPLEX FACTCU,RESCU(20),B(20,2,100)
      COMPLEX DA
      COMMON/DP/DP
      COMMON/MN/MN
      COMMON/TFR/TFR
      COMMON/TD/TD
      COMMON/AN/AN
      COMMON/DN/DN
      COMMON/ALPHA/ALPHA
      COMMON/A/A
      COMMON/B/B
      COMMON/RES/RES
      COMMON/RESCU/RESCU
      COMMON/CU/CU
      COMMON/CLASS/ICLASS
      COMMON/STP/ISTP
      COMMON/S/S
      COMMON/EXP/IEXP
      COMMON/ISO/ISO
      COMMON/SYM/ISYM
      COMMON/SKEW/ISKEW
      REWIND 1 $ REWIND 2 $ REWIND 3
C*********************************************************************
C INPUT PARAMETERS
C ICLASS=1 FOR CLASS1; 2 FOR CLASS2
C ISTP=0 FOR IMP RES; 1 FOR STP RES
C ISO=1 FOR ISOLATED WIRE
C ICU=1 FOR CURRENT; 0 FOR BACKSCATTERED FIELD
C ISKEW=0 FOR WIRE OVER GROUND; 1 FOR COUPLED WIRES
C IEXP=1 FOR CASES OF EXPERIMENTS( ZERO ASPECT-ANGLE )
C AN=A/L; DN=D/L; ALPHA=ORIENTATION ANGLE; THETA=ASPECT ANGLE
C*********************************************************************
      ICLASS=2
      ISTP=0
      ISO=0
      ICU=0
      ISKEW=0
      IEXP=1
      PI=4.*ATAN(1.)
      THETA=0.
      ALPHA=PI*89.9/180.
      AN=0.085
      DN=0.5
      TFR=2.*COS(THETA)
      IF(IEXP.EQ.1) TFR=2.*COS(ALPHA)
      TFRCU=TFR/2.
      TD=DN*SIN(THETA)
      N2=10
      IF(ISKEW.EQ.1) N2=20
      DO 5 N=1,N2
C***********************************************************
C        INPUT THE NATURAL FREQUENCY
C***********************************************************
      READ(1,100) S(N)
100   FORMAT(F10.4,5X,F10.4)
C***********************************************************
C        INPUT THE NATURAL MODE CURRENT
C***********************************************************
      MN=10*N
      IF(N.GT.10) MN=10*(N-10)
      MNP1=MN+1
      ISYM=0
      IF(N.GT.10) ISYM=1
      DO 6 I=1,MNP1
      READ(2,200) CU(N,I)
200   FORMAT(10X,E11.5,10X,E11.5)
6     CONTINUE
C***********************************************************
C        PRECOMPUTE D1(N) AND USE IT TO GET DP(N)
C***********************************************************
      DO 7 K=2,MN
      DKJ=K-2.
      D1(K)=D(S(N),DKJ)
7     CONTINUE
      DP(N)=CMPLX(0.,0.)
      DO 8 I=2,MN
```

```
      DO 12 J=2,I
      K1=IABS(I-J)+2
      DP(N)=DP(N)+D1(K1)*CU(N,I)*CU(N,J)*2.
12    CONTINUE
      DP(N)=DP(N)-D1(2)*CU(N,I)*CU(N,I)
8     CONTINUE
      IF(ISTP.NE.1) GO TO 50
       DO 29 I=2,MN
       DO 42 J=2,I
       DP(N)=DP(N)+DA(S(N),I,J)*CU(N,I)*CU(N,J)*2.
42     CONTINUE
       DP(N)=DP(N)-DA(S(N),I,I)*CU(N,I)*CU(N,I)
29     CONTINUE
50     CONTINUE
       IF(ISTP.EQ.1) DP(N)=DP(N)*S(N)*PI
C******************************************************************
C PRECOMPUTE ARRAY A FOR THE FUTURE USE IN RESIDUE
C******************************************************************
       MNM2=MN*2
       DO 9 IN=1,3
       DO 9 IPK=4,MNM2
       A(N,IN,IPK)=FACT(S(N),IN,IPK)
9      CONTINUE
       DO 17 IN=1,2
       DO 17 I=2,MN
       B(N,IN,I)=FACTCU(S(N),IN,I)
17     CONTINUE
C**********************************************
C       GET RESIDUE
C**********************************************
       RES(N)=CMPLX(0.,0.)
       K1=MN/2+1
       RESCU(N)=CMPLX(0.,0.)
       DO 15 I=2,MN
       RESCU(N)=RESCU(N)+CU(N,I)*CU(N,K1)*B(N,2,I)
       DO 11 K=2,MN
       IPK=I+K
       RES(N)=RES(N)+CU(N,I)*CU(N,K)*A(N,3,IPK)
11     CONTINUE
15     CONTINUE
       RES(N)=RES(N)/DP(N)
       RESCU(N)=RESCU(N)/DP(N)
5      CONTINUE
C************************************************************
C       DESIRED COMPUTATIONS BEGIN
C************************************************************
       DO 10 K=1,100
       TN=K*.05
       R=G(ICU,TN)
       IF(IEXP.EQ.1) R=R*4.
       IF(ISKEW.EQ.1) R=R/2.
       WRITE(3,200) TN,R
10     CONTINUE
       END
C*******************************************************************
C FUNCTION TO TAKE CARE OF TIME-DELAY BETWEEN WIRES
C*******************************************************************
       FUNCTION G(INDEX,X)
       COMMON/ISO/ISO
       COMMON/SKEW/ISKEW
       COMMON/EXP/IEXP
       COMMON/TD/TD
       TN=X
       IF(INDEX.EQ.1) GO TO 99
       TND=TN-2.*TD
       TND1=TND-2.*TD
       R=H(1,TN)
       IF(ISO.EQ.1.OR.IEXP.EQ.1) GO TO 222
       R=R-2.*H(1,TND)
       R=R+H(1,TND1)
       IF(ISKEW.EQ.1) R=R+H(2,TN)+2.*H(2,TND)+H(2,TND1)
       GO TO 222
99     TND=TN-TD
       R=HCU(1,TN)
       IF(ISO.EQ.1.OR.IEXP.EQ.1) GO TO 222
       R=R-HCU(1,TND)
       IF(ISKEW.EQ.1) R=R+HCU(2,TN)+HCU(2,TND)
222    CONTINUE
       G=R
       RETURN
       END
C*******************************************************************
C FUNCTIONS TO TAKE CARE OF DIFFERENT TURN-ON TIME FOR STEP FUNC.
C H FOR FIELD; HCU FOR CURRENT
C*******************************************************************
       FUNCTION H(INDEX,TN)
       COMPLEX S(20),RES(20),CO,CU(20,100),A(20,3,200)
       COMPLEX DP(20)
```

```
      COMMON/S/S
      COMMON/RES/RES
      COMMON/CU/CJ
      COMMON/A/A
      COMMON/TFR/TFR
      COMMON/DP/DP
      COMMON/CLASS/ICLASS
      PI=ATAN(1.)*4.
      H=0.
      IF(INDEX-2) 1,2,2
1     N1=1 $ N2=10
      GO TO 3
2     N1=11 $ N2=20
3     CONTINUE
      IF(ICLASS.EQ.1) GO TO 14
      IF(TN-TFR) 15,14,14
14    DO 20 N=N1,N2
      H=H+REAL(RES(N)*CEXP(S(N)*PI*TN))
20    CONTINUE
      GO TO 32
15    DO 33 N=N1,N2
      MN=10*N
      IF(N.GT.10) MN=10*(N-10)
      CO=CMPLX(0.,0.)
      DO 31 I=2,MN
      DO 31 K=2,MN
      IPK=I+K
      T1=(IPK-3.)/2./MN*TFR
      T2=(IPK-2.)/2./MN*TFR
      T3=(IPK-1.)/2./MN*TFR
      IF(TN.LT.T1) GO TO 31
      IF(TN.GE.T1) IN=1
      IF(TN.GE.T2) IN=2
      IF(TN.GE.T3) IN=3
      CO=CO+CU(N,I)*CU(N,K)*A(N,IN,IPK)
31    CONTINUE
      CO=CO/DP(N)
      H=H+REAL(CO*CEXP(S(N)*PI*TN))
33    CONTINUE
32    RETURN
      END
      FUNCTION HCU(INDEX,X)
      COMPLEX S(20),RESCU(20),COCU,CU(20,101),P(20,2,100)
      COMPLEX DP(20)
      COMMON/S/S
      COMMON/RESCU/RESCU
      COMMON/CU/CU
      COMMON/B/B
      COMMON/TFR/TFR
      COMMON/DP/DP
      COMMON/CLASS/ICLASS
      COMMON/STP/ISTP
      PI=ATAN(1.)*4.
      TN=X
      IF(INDEX-2) 1,2,2
1     N1=1 $ N2=10
      GO TO 3
2     N1=11 $ N2=20
3     CONTINUE
      HCU=0.
      TFRCU=TFR/2.
      IF(ICLASS.EQ.1) GO TO 14
      IF(TN-TFRCU) 15,14,14
14    DO 20 N=N1,N2
      HCU=HCU+REAL(RESCU(N)*CEXP(S(N)*PI*TN))
20    CONTINUE
      GO TO 32
15    DO 33 N=N1,N2
      MN=10*N
      IF(N.GT.10) MN=10*(N-10)
      K1=MN/2+1
      COCU=CMPLX(0.,0.)
      DO 31 I=2,MN
      T1CU=(I-1.5)/MN*TFRCU
      T2CU=(I-0.5)/MN*TFRCU
      IF(TN.LT.T1CU) GO TO 31
      IF(TN.GE.T1CU) IN=1
      IF(TN.GE.T2CU) IN=2
      COCU=COCU+CU(N,I)*CU(N,K1)*P(N,IN,I)
      IF(ISTP.NE.1) GO TO 999
      IF(IN.EQ.1) COCU=COCU-CU(N,I)*CU(N,K1)*CEXP(-S(N)*PI*TN)
999   CONTINUE
31    CONTINUE
      COCU=COCU/DP(N)
      HCU=HCU+REAL(COCU*CEXP(S(N)*PI*TN))
33    CONTINUE
32    RETURN
      END
```

```
C*****************************************************************
C UTILITY FUNCTIONS
C FACT HELPS TAKE CARE OF TURN-ON TIME FOR FIELD
C FACTCU HELPS TAKE CARE OF TURN-ON TIME FOR CURRENT
C D AND DA USED TO COMPUTE DENOMINATOR OF COUPLING COEFF.
C*****************************************************************
      COMPLEX FUNCTION FACT(S,INDEX,IPK)
      COMPLEX S,A1,A2,A3
      COMMON/MN/MN
      COMMON/TFR/TFR
      PI=4.*ATAN(1.)
      T1=(IPK-3.)/2./MN*TFR
      T2=(IPK-2.)/2./MN*TFR
      T3=(IPK-1.)/2./MN*TFR
      A1=CEXP(S*PI*(-T1))
      A2=CEXP(S*PI*(-T2))
      A3=CEXP(S*PI*(-T3))
      IF(INDEX.EQ.1) FACT=A1
      IF(INDEX.EQ.2) FACT=A1-2.*A2
      IF(INDEX.EQ.3) FACT=A1-2.*A2+A3
      RETURN
      END
      COMPLEX FUNCTION D(S,DIJ)
      COMPLEX S,E,E1,E2,CI,CJ,CK,EI,EI1,EI2
      COMMON/MN/MN
      COMMON/AN/AN
      COMMON/DN/DN
      COMMON/ISO/ISO
      COMMON/SYM/ISYM
      COMMON/EXP/IEXP
      PI=4.*ATAN(1.)
      DIJ1=DIJ+1.
      DIJ2=DIJ-1.
      R=SQRT((DIJ/MN)**2+AN**2)
      RI=SQRT((DIJ/MN)**2+AN**2+4.*DN**2)
      E=-S*PI*R
      EI=-S*PI*RI
      E1=-S*PI*SQRT((DIJ1/MN)**2+AN**2)
      EI1=-S*PI*SQRT((DIJ1/MN)**2+AN**2+4.*DN**2)
      E2=-S*PI*SQRT((DIJ2/MN)**2+AN**2)
      EI2=-S*PI*SQRT((DIJ2/MN)**2+AN**2+4.*DN**2)
      SQR=SQRT(1+(AN*MN)**2)
      CI=2.*CEXP(E)-CEXP(E1)-CEXP(E2)
      IF(DIJ.NE.0.) CJ=-2.*S*PI*CEXP(E)/MN/MN/R
      IF(DIJ.EQ.0.) CJ=2.*(S*PI/MN)**2-2.*(S*PI/MN)*
     +(ALOG((1.+SQR)/(-1.+SQR))-2.*SQR+2.*AN*MN)
      CK=(S*PI/MN)**2*CEXP(E)
      IF(ISO.EQ.1) GO TO 10
      IF(IEXP.EQ.1) GO TO 10
      IF(ISYM.EQ.1) GO TO 20
      CI=CI-2.*CEXP(EI)+CEXP(EI1)+CEXP(EI2)
      CJ=CJ+2.*S*PI*CEXP(EI)/MN/MN/RI
      CK=CK-(S*PI/MN)**2*CEXP(EI)
      GO TO 10
20    CI=CI+2.*CEXP(EI)-CEXP(EI1)-CEXP(EI2)
      CJ=CJ-2.*S*PI*CEXP(EI)/MN/MN/RI
      CK=CK+(S*PI/MN)**2*CEXP(EI)
10    CONTINUE
      D=CI+CJ+CK
      RETURN
      END
      COMPLEX FUNCTION FACTCU (S,INDEX,I)
      COMPLEX S,A1,A2
      COMMON/MN/MN
      COMMON/TFR/TFR
      TFRCU=TFR/2.
      PI=4.*ATAN(1.)
      T1CU=(I-1.5)/MN*TFRCU
      T2CU=(I-0.5)/MN*TFRCU
      A1=CEXP(S*PI*(-T1CU))
      A2=CEXP(S*PI*(-T2CU))
      IF(INDEX.EQ.1) FACTCU=A1
      IF(INDEX.EQ.2) FACTCU=A1-A2
      RETURN
      END
      COMPLEX FUNCTION DA(S,I,J)
      COMPLEX S,E1,E2,E3,E4,CI,CJ,CK
      COMMON/MN/MN
      COMMON/AN/AN
      COMMON/DN/DN
      COMMON/ALPHA/ALPHA
      PI=4.*ATAN(1.)
      DIJ=I-J $ SIJ=I+J-2
      DIJ1=I-J+1 $ SIJ1=I+J-1
      DIJ2=I-J-1 $ SIJ2=I+J-3
      R=SQRT((DIJ/MN*COS(ALPHA))**2+AN**2+(2*DN+SIJ/MN*
     +SIN(ALPHA))**2)
      E1=-S*PI*SQRT((DIJ/MN*COS(ALPHA))**2+AN**2+(2*DN*
```

```
     +SIJ1/MN*SIN(ALPHA))**2)
      E2=-S*PI*SQRT((DIJ/MN*COS(ALPHA))**2+AN**2+(2*DN+
     +SIJ2/MN*SIN(ALPHA))**2)
      E3=-S*PI*SQRT((DIJ1/MN*COS(ALPHA))**2+AN**2+(2*DN+
     +SIJ/MN*SIN(ALPHA))**2)
      E4=-S*PI*SQRT((DIJ2/MN*COS(ALPHA))**2+AN**2+(2*DN+
     +SIJ/MN*SIN(ALPHA))**2)
      CI=-CEXP(E1)-CEXP(E2)+CEXP(E3)+CEXP(E4)
      CJ=2.*S*PI*CEXP(-S*PI*R)/MN/MN/R*COS(2.*ALPHA)
      CK=-(S*PI/MN)**2*CEXP(-S*PI*R)*COS(2.*ALPHA)
      DA=CI+CJ+CK
      RETURN
      END
03.46.47.  00048 PAGES 005608 LINES PRINTED AT SITE MV
```

```
      PROGRAM MAIN(INPUT,OUTPUT,TAPE1,TAPE2,TAPE3)
C*****************************************************************
C THIS PROGRAM COMPUTES IMPULSE RESPONSE FOR ANTISYM MODE OF CROSS
C IT IS CATALOGED AS IMPCROSSF.
C MODE ALWAYS SET TO 1
      TAPE1=ROOTS; TAPE2=MODAL CURRENTS; TAPE3=IMP RES
C*****************************************************************
      COMPLEX S(10),CU(10,50),DP(10),D1(100),D
      COMPLEX DA
      COMPLEX DB
      COMPLEX DC
      COMMON/MN/MN
      REAL RES(10)
      COMMON/AN/AN
      REWIND 1 $ REWIND 2 $ REWIND 3
      PRINT*,"ENTER MODE="
      READ*,MODE
      PI=4.*ATAN(1.)
      RW=0.8
      AN=0.01
      IF(MODE.EQ.2) AN=AN*RW
      NR=5
      IF(MODE.EQ.2) NR=10
      DO 5 N=1,NR
C*****************************************************
C       INPUT THE NATURAL FREQUENCY
C*****************************************************
      READ(1,*) S(N)
C*****************************************************
C        INPUT THE NATURAL MODE CURRENT
C*****************************************************
      IF(MODE.EQ.1) MN=5*(2*N-1)
      IF(MODE.EQ.2) MN=8
      IF(MODE.EQ.2.AND.N.GT.5) MN=12
      IF(MODE.EQ.1) ND=MN+1
      IF(MODE.EQ.2) ND=MN*3+3
      DO 6 I=1,ND
      READ(2,200) CU(N,I)
200   FORMAT(10X,E11.5,10X,E11.5)
6     CONTINUE
C*****************************************************
C       PRECOMPUTE D1(N) AND USE IT TO GET DP(N)
C*****************************************************
      DO 7 K=2,MN
      DKJ=K-2.
      D1(K)=D(S(N),DKJ)
7     CONTINUE
      DP(N)=CMPLX(0.,0.)
      DO 9 I=2,MN
      DO 12 J=2,I
      K1=IABS(I-J)+2
      DP(N)=DP(N)+D1(K1)*CU(N,I)*CU(N,J)*2.
12    CONTINUE
      DP(N)=DP(N)-D1(2)*CU(N,I)*CU(N,I)
9     CONTINUE
      DO 28 I=2,MN
      DO 42 J=2,I
      DP(N)=DP(N)+DA(S(N),I,J)*CU(N,I)*CU(N,J)*2.
42    CONTINUE
      DP(N)=DP(N)-DA(S(N),I,I)*CU(N,I)*CU(N,I)
28    CONTINUE
      GO TO 97
      DO 17 I=2,MN
      DP(N)=DP(N)+2.*CU(N,1)*CU(N,I)*DB(S(N),I)
17    CONTINUE
      DP(N)=DP(N)+CU(N,1)*CU(N,1)*DC(S(N))
97    CONTINUE
C**************************************************
C       GET RESIDUE
C****************************************
      RES(N)=CMPLX(0.,0.)
      DO 15 I=2,MN
      RES(N)=RES(N)+CU(N,I)*CEXP(-S(N)*PI*.5*(I-1.)/MN)
15    CONTINUE
      RES(N)=RES(N)*(CEXP(S(N)*PI/4./MN)-CEXP(-S(N)*PI/4./MN))
      RES(N)=RES(N)+CU(N,1)*(1.-CEXP(-S(N)*PI/4./MN))
      RES(N)=RES(N)*RES(N)
      RES(N)=RES(N)/DP(N)
5     CONTINUE
C*****************************************************
C       DESIRED COMPUTATIONS BEGIN
C*****************************************************
      IF(MODE.EQ.1) TRR=0.5
```

```
      IF(MODE.EQ.2) TFR=SQRT(2.)
      DO 10 K=1,100
      TN1=TFR+.06*K
      IF(MODE.EQ.1) FACT=2.0
      IF(MODE.EQ.2) FACT=1.5
      TN=TN1*FACT
      R=0.
       DO 99 N=1,NR
       R=R+REAL(RES(N)*CEXP(S(N)*PI*TN))
99     CONTINUE
       WRITE(3,200) TN1,R
10     CONTINUE
       END
C**********************************************************************
C FUNCTIONS USED TO COMPUTE DENOMINATOR OF COUPLING COEFF.
C**********************************************************************
       COMPLEX FUNCTION D(S,DIJ)
       COMPLEX S,E,E1,E2,CI,CJ,CK
       COMMON/MN/MN
       COMMON/AN/AN
       PI=4.*ATAN(1.)
       DIJ1=DIJ+1.
       DIJ2=DIJ-1.
       R=SQRT((DIJ/MN)**2+AN**2)
       E=-S*PI*R
       E1=-S*PI*SQRT((DIJ1/MN)**2+AN**2)
       E2=-S*PI*SQRT((DIJ2/MN)**2+AN**2)
       SQR=SQRT(1+(AN*MN)**2)
       CI=2.*CEXP(E)-CEXP(E1)-CEXP(E2)
       IF(DIJ.NE.0.) CJ=-2.*S*PI*CEXP(E)/MN/MN/R
       IF(DIJ.EQ.0.) CJ=2.*(S*PI/MN)**2-2.*(S*PI/MN)*
      +(ALOG((1.+SQR)/(-1.+SQR))-2.*SQR+2.*AN*MN)
       CK=(S*PI/MN)**2*CEXP(E)
       D=CI+CJ+CK
       RETURN
       END
       COMPLEX FUNCTION DA(S,I,J)
       COMPLEX S,E1,E2,E3,E4
       COMMON/MN/MN
       COMMON/AN/AN
       PI=4.*ATAN(1.)
       DIJ=I-J $ SIJ=I+J-2
       DIJ1=I-J+1 $ SIJ1=I+J-1
       DIJ2=I-J-1 $ SIJ2=I+J-3
       R=SQRT((DIJ/MN)**2/2.+AN**2+(SIJ/MN)**2/2.)
       E1=-S*PI*SQRT((DIJ/MN)**2/2.+AN**2+(SIJ1/MN)**2/2.)
       E2=-S*PI*SQRT((DIJ/MN)**2/2.+AN**2+(SIJ2/MN)**2/2.)
       E3=-S*PI*SQRT((DIJ1/MN)**2/2.+AN**2+(SIJ/MN)**2/2.)
       E4=-S*PI*SQRT((DIJ2/MN)**2/2.+AN**2+(SIJ/MN)**2/2.)
       DA=-CEXP(E1)-CEXP(E2)+CEXP(E3)+CEXP(E4)
       RETURN
       END
       COMPLEX FUNCTION DB(S,I)
       COMPLEX S,E1,E2,E3,E4,CI,CJ,CK
       COMMON/MN/MN
       COMMON/AN/AN
       PI=4.*ATAN(1.)
       R=SQRT(((I-1.)/MN)**2+AN**2)
       E1=-S*PI*R
       E2=-S*PI*SQRT(((I-1.)/MN)**2/2.+AN**2+(1./MN+I)**2/2.)
       E3=-S*PI*SQRT(((I-2.)/MN)**2+AN**2)
       E4=-S*PI*SQRT(((I-2.)/MN)**2/2.+AN**2+((I-1.)/MN)**2)
       CI=CEXP(E1)-CEXP(E2)-CEXP(E3)+CEXP(E4)
       CJ=-S*PI*CEXP(E1)/MN/MN/R
       CK=0.5*(S*PI/MN)**2*CEXP(E1)
       DB=CI+CJ+CK
       RETURN
       END
       COMPLEX FUNCTION DC(S)
       COMPLEX S,CI,CJ,CK
       COMMON/MN/MN
       COMMON/AN/AN
       PI=4.*ATAN(1.)
       CI=CEXP(-S*PI*AN)-CEXP(-S*PI*SQRT((1./MN)**2/2.+AN**2))
       SQR=SQRT(1.+(AN*MN*2.)**2)
       CJ=2.*(S*PI/MN/2.)**2-S*PI/MN*(ALOG((1.+SQR)/(-1.+SQR))
      +-2.*SQR+4.*AN*MN)
       CK=(S*PI/MN/2.)**2*CEXP(-S*PI*AN)
       DC=CI+CJ+CK
       RETURN
       END
01.15.45.   0013 PAGES 000243B LINES PRINTED AT SITE  V
```

```
      PROGRAM MAIN(INPUT,OUTPUT,TAPE1,TAPE2,TAPE3)
C*****************************************************************************
C THIS PROGRAM COMPUTES IMPULSE RESPONSE FOR SYM MODE OF CROSS
C IT IS CATALOGED AS IMPCROSSSYMEW
C TAPE1=ROOTS; TAPE2=MODAL CURRENTS; TAPE3=IMP RES
C*****************************************************************************
      COMPLEX S(10),CU(10,50),DP(10),D1(100),D
      COMPLEX DA
      COMPLEX DB
      COMPLEX CZ(10,50)
      COMMON/N4/N4
      REAL RES(10)
      COMMON/AN/AN
      REWIND 1 $ REWIND 2 $ REWIND 3
      PI=4.*ATAN(1.)
      AN=0.008
      NR=10
      DO 5 N=1,NR
C*****************************************************************
C       INPUT THE NATURAL FREQUENCY
C*****************************************************************
      READ(1,*) S(N)
C*****************************************************************
C        INPUT THE NATURAL MODE CURRENT
C*****************************************************************
      IF(N-5) 1,1,2
1     MN=6 $ N4=10 $ N1=6 $ N2=8 $ GO TO 3
2     MN=12 $ N4=15 $ N1=9 $ N2=12
3     ND=3*MN+3
      DO 6 I=1,ND
      READ(2,200) CU(N,I)
200   FORMAT(10X,E11.5,10X,E11.5)
6     CONTINUE
      NZ=N4+N1
C*****************************************************************
C       PRECOMPUTE D1(N) AND USE IT TO GET DP(N)
C*****************************************************************
      NZP2=NZ+2
      DO 4 I=1,NZP2
      IF(I.LE.N4) CZ(N,I)=CU(N,I)
      IF(I.GT.N4+1) CZ(N,I)=CU(N,I+1)
      CZ(N,N4+1)=0.5*(CU(N,N4+1)+CU(N,N4+2))
4     CONTINUE
      DO 7 K=2,NZ
      DKJ=K-2.
      D1(K)=D(S(N),DKJ)
7     CONTINUE
      DP(N)=CMPLX(0.,0.)
      DO 8 I=2,NZ
      DO 12 J=2,I
      K1=IABS(I-J)+2
      DP(N)=DP(N)+D1(K1)*CZ(N,I)*CZ(N,J)*2.
12    CONTINUE
      DP(N)=DP(N)-D1(2)*CZ(N,I)*CZ(N,I)
8     CONTINUE
      DO 35 K=2,MN
      DKJ=K-2.
      D1(K)=D(S(N),DKJ)
35    CONTINUE
      DO 36 I=2,MN
      DO 37 J=2,I
      K1=IABS(I-J)+2
      DP(N)=DP(N)+D1(K1)*CU(N,I+NZ+2)*CU(N,J+NZ+2)*4.
37    CONTINUE
      DP(N)=DP(N)-D1(2)*CU(N,I+NZ+2)*CU(N,I+NZ+2)*2.
36    CONTINUE
      DO 29 I=2,MN
      DO 42 J=2,I
      DP(N)=DP(N)+DA(S(N),I,J)*CU(N,I+NZ+2)*CU(N,J+NZ+2)*4.
42    CONTINUE
      DP(N)=DP(N)-DA(S(N),I,I)*CU(N,I+NZ+2)*2.*CU(N,I+NZ+2)
29    CONTINUE
      DO 17 I=2,MN
      DO 17 J=2,NZ
      DP(N)=DP(N)+4.*CU(N,I+NZ+2)*CZ(N,J)*DB(S(N),I,J)
17    CONTINUE
C*************************************************************
C       GET RESIDUE
C*********************************************
      RES(N)=CMPLX(0.,0.)
      DO 15 I=2,MN
      RES(N)=RES(N)+CU(N,I+NZ+2)*CEXP(-S(N)*PI*.5*(I-1.)/.4)
15    CONTINUE
```

```
      RES(N)=RES(N)*(CEXP(S(N)*PI/4./N4)-CEXP(-S(N)*PI/4./N4))
      RES(N)=RES(N)+CU(N,N2+3)*(1.-CEXP(-S(N)*PI/4./N4))
      RES(N)=RES(N)-CU(N,N4+1)*.5*(1.-CEXP(-S(N)*PI/2./SQRT(2.)/N4))
      RES(N)=RES(N)-CU(N,N4+2)*.5*(CEXP(S(N)*PI/2./SQRT(2.)/N4)-1.)
      DO 56 I=2,N4
      RES(N)=RES(N)-.5*(CEXP(S(N)*PI/2./SQRT(2.)/N4)-CEXP(-S(N)*PI/2.
     +/SQRT(2.)/N4))*CEXP(S(N)*PI/SQRT(2.)*(I-1.-N4)/N4)*CU(N,I)
56    CONTINUE
      DO 57 I=2,N1
      RES(N)=RES(N)-.5*(CEXP(S(N)*PI/2./SQRT(2.)/N4)-CEXP(-S(N)*PI/2.
     +/SQRT(2.)/N4))*CEXP(S(N)*PI/SQRT(2.)*(I-1.)/N4)*CU(N,I+N4+1)
57    CONTINUE
      RES(N)=RES(N)*RES(N)
      RES(N)=RES(N)/DP(N)
5     CONTINUE
C***************************************************************
C        DESIRED COMPUTATIONS BEGIN
C***************************************************************
      TFR=SQRT(2.)
      DO 10 K=1,100
      TN1=TFR+.06*(K-1)
      FACT=1.6
      TN=TN1*FACT
      R=0.
      DO 99 N=1,NR
      R=R+REAL(RES(N)*CEXP(S(N)*PI*TN))
99    CONTINUE
      WRITE(3,200) TN1,R
10    CONTINUE
      END
      COMPLEX FUNCTION D(S,DIJ)
      COMPLEX S,E,E1,E2,CI,CJ,CK
C**********************************************************************
C FUNCTIONS USED TO COMPUTE DENOMINATOR OF COUPLEING COEFF.
C**********************************************************************
      COMMON/N4/N4
      COMMON/AN/AN
      PI=4.*ATAN(1.)
      DIJ1=DIJ+1.
      DIJ2=DIJ-1.
      R=SQRT((DIJ/N4)**2+AN**2)
      E=-S*PI*R
      E1=-S*PI*SQRT((DIJ1/N4)**2+AN**2)
      E2=-S*PI*SQRT((DIJ2/N4)**2+AN**2)
      SQR=SQRT(1+(AN*N4)**2)
      CI=2.*CEXP(E)-CEXP(E1)-CEXP(E2)
      IF(DIJ.NE.0.) CJ=-2.*S*PI*CEXP(E)/N4/N4/R
      IF(DIJ.EQ.0.) CJ=2.*(S*PI/N4)**2-2.*(S*PI/N4)*
     +(ALOG((1.+SQR)/(-1.+SQR))-2.*SQR+2.*AN*N4)
      CK=(S*PI/N4)**2*CEXP(E)
      D=CI+CJ+CK
      RETURN
      END
      COMPLEX FUNCTION DA(S,I,J)
      COMPLEX S,E1,E2,E3,E4
      COMMON/N4/N4
      COMMON/AN/AN
      PI=4.*ATAN(1.)
      DIJ=I-J $ SIJ=I+J-2
      DIJ1=I-J+1 $ SIJ1=I+J-1
      DIJ2=I-J-1 $ SIJ2=I+J-3
      R=SQRT((DIJ/N4)**2/2.+AN**2+(SIJ/N4)**2/2.)
      E1=-S*PI*SQRT((DIJ/N4)**2/2.+AN**2+(SIJ1/N4)**2/2.)
      E2=-S*PI*SQRT((DIJ/N4)**2/2.+AN**2+(SIJ2/N4)**2/2.)
      E3=-S*PI*SQRT((DIJ1/N4)**2/2.+AN**2+(SIJ/N4)**2/2.)
      E4=-S*PI*SQRT((DIJ2/N4)**2/2.+AN**2+(SIJ/N4)**2/2.)
      DA=CEXP(E1)+CEXP(E2)-CEXP(E3)-CEXP(E4)
      RETURN
      END
      COMPLEX FUNCTION DB(S,I,J)
      COMPLEX S,E1,E2,E3,E4
      COMPLEX CI,CJ,CK
      COMMON/N4/N4
      COMMON/AN/AN
      PI=4.*ATAN(1.)
      A=COS(PI/8.)
      B=SIN(PI/8.)
      DIJ=I-J+N4 $ SIJ=I+J-2-N4
      DIJ1=I-J+1+N4 $ SIJ1=I+J-1-N4
      DIJ2=I-J-1+N4 $ SIJ2=I+J-3-N4
      R=SQRT((DIJ/N4*B)**2+AN**2+(SIJ/N4*A)**2)
      E1=-S*PI*SQRT((DIJ/N4*B)**2+AN**2+(SIJ1/N4*A)**2)
      E2=-S*PI*SQRT((DIJ/N4*B)**2+AN**2+(SIJ2/N4*A)**2)
      E3=-S*PI*SQRT((DIJ1/N4*B)**2+AN**2+(SIJ/N4*A)**2)
      E4=-S*PI*SQRT((DIJ2/N4*B)**2+AN**2+(SIJ/N4*A)**2)
      CI=CEXP(E1)+CEXP(E2)-CEXP(E3)-CEXP(E4)
      CJ=SQRT(2.)*S*PI*CEXP(-S*PI*R)/N4/N4/R
      CK=-(S*PI/N4)**2/SQRT(2.)*CEXP(-S*PI*R)
```

```
1510=         DB=CI+CJ+CK
1520=         RETURN
1530=         END
00.59.55.     00023 PAGES 0002756 LINES PRINTED AT SITE MV
```

APPENDIX D

PROGRAM FOR REQUIRED INCIDENT WAVEFORMS

```
      PROGRAM EIREQD(INPUT,OUTPUT,TAPE1,TAPE2)
C**********************************************************************
C THIS PROGRAM SYNTHESIZES THE REQURIED WAVEFORM USING PULSE-EXPANSION
C IT IS CATALOGED AS EIREQDEW
C TAPE1=NATURAL FREQUENCIES; TAPE2=REQUIRED WAVEFORM
C**********************************************************************
      DIMENSION A(50,50),SIG(25),W(25)
      COMPLEX ROOT
      DOUBLE T
      DOUBLE A,DET
      DOUBLE Z(50)
      DOUBLE B(50),RCOND
      INTEGER IPVT(50)
      DOUBLE SIG,W,FACT,PI,D,E,E1,PHI,PHI1
      REWIND 1 $ REWIND 2
C**********************************************************************
C INPUT PARAMETERS AND ROOTS
C MODE=MODE # TO BE SYNTHESIZED
C IF ICOS=1 COSINE MODE EXCITATION
C IF IWIRE=1, FOR WIRE-TARGET ROOTS NORMALIZED BY PI*C/L
C IF IWIRE=0, FOR NON-WIRE NO PI IN ROOTS
C IF IANTI=1, ANTISYM MODE FOR CROSS; IANTI=2 FOR SYM MODE
C N=# OF MODES USED; INDEX=1 FOR INFINITE CYL TWO EXP TERMS ARE USED
C TE=ONE PERIOD OF FIRST MODE MULTIPLIED BY FACT
C IT IS ARRANGED TO USE LINPACK NOW; WITHOUT *EQS BEFORE
C SUBROUTINE MATPAC. WE CAN USE MATPAC BY CHANGE OF SOME STATEMENTS
C*********************************************************************
      PI=ATAN(1.)*4.
      PRINT*,"WHICH MODE DO YOU WANT TO EXCITE-"
      READ*,MODE
      ICOS=0
      IWIRE=1
      PRINT*,"ENTER IANTI FOR CROSSED WIRES-"
      READ*,IANTI
      PRINT*,"ENTER NUMBER OF MODES TO BE USED-"
      READ*,N
      K=1
      INDEX=0
      NT=N-INDEX
      FACT=1.
      N2=NT*2
      N2P1=N2+1
      DO 10 I=1,N
      IF(IANTI-2) 21,21,22
21    READ(1,*) ROOT
      SIG(I)=REAL(ROOT)$ W(I)=AIMAG(ROOT)
      GO TO 23
22    READ(1,100) SIG(I),W(I)
23    CONTINUE
      IF(IWIRE.NE.1) GO TO 10
      SIG(I)=PI*SIG(I) $ W(I)=PI*W(I)
      IF(IANTI-2) 40,50,10
40    SIG(I)=SIG(I)*2. $ W(I)=W(I)*2.
      GO TO 10
50    SIG(I)=SIG(I)*1.6 $ W(I)=W(I)*1.6
      GO TO 10
100   FORMAT(F10.5,5X,F10.5)
10    CONTINUE
C*********************************************************************
C SYNTHESIS OF WAVEFORM AND OUTPUT
C*********************************************************************
      DO 20 I=1,N
      IPN=I+N
      DO 20 J=1,N2
      JM1=J-1
      D=SIG(I)**2+W(I)**2
      E=-SIG(I)*PI*J/W(K)/NT $ E1=-SIG(I)*PI*JM1/W(K)/NT
      PHI=W(I)*PI*J/W(K)/NT $ PHI1=W(I)*PI*JM1/W(K)/NT
      E=E*FACT $ E1=E1*FACT $PHI=PHI*FACT $PHI1=PHI1*FACT
      A(I,J)=(DEXP(E)*(W(I)*DSIN(PHI)-SIG(I)*DCOS(PHI))
     *-DEXP(E1)*(W(I)*DSIN(PHI1)-SIG(I)*DCOS(PHI1)))/D
      A(IPN,J)=-(DEXP(E)*(SIG(I)*DSIN(PHI)+W(I)*DCOS(PHI))-
     *DEXP(E1)*(SIG(I)*DSIN(PHI1)+W(I)*DCOS(PHI1)))/D
20    CONTINUE
      DO 35 I=1,N2
      NPMODE=N+MODE
      IF(I.EQ.NPMODE) B(I)=1.0
      IF(I.NE.NPMODE) B(I)=0.0
      IF(ICOS.NE.1) GO TO 35
      IF(I.EQ.MODE) B(I)=1.0
      IF(I.NE.MODE) B(I)=0.0
35    CONTINUE
      CALL DGECO(A,50,N2,IPVT,RCOND,Z)
```

```
      PRINT *,"CONDNO=",1./RCOND
      T=1.0+RCOND
      IF(T.EQ.1.0) PRINT *,"WARNING. SINGULAR TO WORKING PRECISION"
      CALL DGESL(A,50,N2,IPVT,B,0)
      DO 30 I=1,N2
      TIME=PI/NT/W(K)*(I-.5)
      TIME=TIME*FACT
       PRINT 200,TIME,B(I)
       WRITE(2,200) TIME,B(I)
200    FORMAT(10X,E11.5,10X,E11.5)
30     CONTINUE
       END
*EOS
       SUBROUTINE MATPAC(IJOB,A,N,M,DET,EP)
C MATRIX OPERATIONS SUBROUTINE PACKAGE FOR REAL NUMBERS.
       DIMENSION A(50,50)
       DOUBLE A,B,C,D,S,CONST,DET
    30 FORMAT(1X,42HTHE DETERMINANT OF THE SYSTEM EQUALS ZERO./
      11X,35HTHE PROGRAM CANNOT HANDLE THIS CASE.//)
       DET=1.
       NP1=N+1
       NPM=N+M
       NM1=N-1
       IF(IJOB) 2,1,2
     1 DO 3 I=1,N
       NPI=N+I
       A(I,NPI)=1.
       IP1=I+1
       DO 3 J=IP1,N
       NPJ=N+J
       A(I,NPJ)=0.
     3 A(J,NPI)=0.
     2 DO 4 J=1,NM1
       C=DABS(A(J,J))
       JP1=J+1
       DO 5 I=JP1,N
       D=DABS(A(I,J))
       IF(C-D) 6,5,5
     6 DET=-DET
       DO 7 K=J,NPM
       B=A(I,K)
       A(I,K)=A(J,K)
     7 A(J,K)=B
       C=D
     5 CONTINUE
       IF(DABS(A(J,J))-EP) 14,15,15
    15 DO 4 I=JP1,N
       CONST=A(I,J)/A(J,J)
       DO 4 K=JP1,NPM
     4 A(I,K)=A(I,K)-CONST*A(J,K)
       IF(DABS(A(N,N))-EP) 14,18,18
    14 DET=0.
       IF(IJOB) 16,16,17
16     PRINT 30
    17 RETURN
    18 DO 11 I=1,N
    11 DET=DET*A(I,I)
       IF(IJOB) 10,10,17
    10 DO 12 I=1,N
       K=N-I+1
       KP1=K+1
       DO 12 L=NP1,NPM
       S=0.
       IF(N-KP1) 12,19,19
    19 DO 13 J=KP1,N
    13 S=S+A(K,J)*A(J,L)
    12 A(K,L)=(A(K,L)-S)/A(K,K)
       RETURN
       END
01.30.21.  00013 PAGES 000230B LINES PRINTED AT CITE  M
```

APPENDIX E

PROGRAM FOR CONVOLUTION

```
      PROGRAM CONV(INPUT,OUTPUT,TAPE1,TAPE2,TAPE3,TAPE4)
C*********************************************************************
C THIS PROGRAM CONVOLVES TWO DATA FILES: TAPE3=TAPE1*TAPE2.
C TAPE1=EI; TAPE2=H(T); (T IN H(T))*WRONG; WRONG>1.0-LONGER
C WRONG CAN BE USED TO READJUST TIME SCALE IN TAPE2
C TAPE4=PULSE-EXPANSION VERSION OF TAPE1
C IT IS CATALOGED AS SMOOTHEREW
C*********************************************************************
      REAL F1(3000),F2(3000),F3(3000),T(3000)
      REAL F(3000)
      COMMON/X/T
      COMMON/Y/Y
      REAL Y(3000),DF(3000),C(3000,3),WK(5000)
      REWIND 1 $ REWIND 2 $ REWIND 3
      REWIND 4
C******************************************************************
C INPUT PARAMETERS AND DATA
C******************************************************************
      PRINT*,"ENTER WRONG FOR TAPE2: >1.0 FOR LARGER L OR W-"
      READ*,WRONG
      PRINT*,"ENTER MULTIPLICATION FACTOR-"
      READ*,FACT
C FACT IS USED TO RESCALE THE RESULT SO THAT IT IS NOT TOO SMALL.
      PRINT*,"ENTER IPULSE-"
      READ*,IPULSE
C IF IPULSE=1, PULSE EXPANSION IS USED: EI=CONST FOR EACH SEGMENT.
      F1(1)=0. $ F2(1)=0.
      T(1)=0.
      DO 10 J=1,2
C N1=# OF PTS IN DATA FILE
      PRINT*,"ENTER N1-"
      READ*,N1
      N1P1=N1+1
      DO 25 I=1,N1
      IF(J.EQ.1) READ(1,100) T(I+1),F1(I+1)
      IF(J.EQ.1) F(I)=F1(I+1)
      IF(J.EQ.2) READ(2,100) T(I+1),F2(I+1)
      IF(J.EQ.2) T(I+1)=T(I+1)*WRONG
26    CONTINUE
      IF(T(2).EQ.0.) T(2)=T(3)/10.
C NOTE: IN SPLINE ROUTINE ICSSCU, TIME MUST BE IN INCREASING ORDER.
C AND T(1)=0. HAS BEEN SET.
      DT=T(N1P1)-T(N1)
      PRINT*,"DT=",DT
      DO 40 K=1,N1P1
      DF(K)=1.0
40    CONTINUE
      IC=N1 $ SM=0.3
      IF(J.EQ.2) GO TO 17
      IF(IPULSE.EQ.1) GO TO 25
C******************************************************************
C SMOOTH AND SPLINE
C******************************************************************
      CALL SMOOTH(T,F1,N1P1,DT)
C USING IMSL ROUTINE SMOOTH THE DATA
      CALL ICSSCU(T,F1,DF,N1P1,SM,Y,C,IC,WK,IER)
      GO TO 25
17    CALL SMOOTH(T,F2,N1P1,DT)
      CALL ICSSCU(T,F2,DF,N1P1,SM,Y,C,IC,WK,IER)
25    CONTINUE
C DTN=NEW TIME INCREMENT
      PRINT*,"ENTER DTN-"
      READ*,DTN
      NN=T(N1P1)/DTN
C NN=NEW # OF PTS AVAILABLE
      PRINT*,"NN=",NN
C*******************************************************************
C TAPE4 AS PULSE EXPANSION OF TAPE1, IN CASE PLOTTING IS DESIRED
C*******************************************************************
      DO 35 I=1,NN
      TN=DTN*I
      IF(IPULSE.EQ.1.AND.J.EQ.1) GO TO 27
      IF(J.EQ.1) F1(I)=SP(TN,N1,C)
      GO TO 29
27    II=TN/DT+1
      F1(I)=F(II)
      WRITE(4,100) TN,F1(I)
29    CONTINUE
      IF(J.EQ.2) F2(I)=SP(TN,N1,C)
35    CONTINUE
C NO=# OF OUTPUT PTS
      PRINT*,"ENTER NO-"
      READ*,NO
```

```
      NNP1=NN+1
      DO 55 I=NNP1,NO
      IF(J.EQ.1) F1(I)=0.
      IF(J.EQ.2) F2(I)=0.
55    CONTINUE
10    CONTINUE
C*****************************************************************
C DISCRETE CONVOLUTION
C*****************************************************************
      DO 20 I=1,NO
      S=0.
      DO 30 K=1,I
      S=S+F1(K)*F2(I-K+1)*DTN
30    CONTINUE
      S=S*FACT
      F3(I)=S
      TN=DTN*I
      WRITE(3,100) TN,F3(I)
20    CONTINUE
100   FORMAT(10X,E11.5,10X,F11.5)
200   FORMAT(1X,F10.4,5X,F30.10)
250   FORMAT(5X,E10.4,20X,E10.4)
260   FORMAT(1H ,E12.4,3H , ,G12.4)
270   FORMAT(1X,E10.4,1X,E10.4)
      END
      SUBROUTINE SMOOTH(X,Y,N1,DT)
C*****************************************************************
C        SUBROUTINE USING IMSL ROUTINE ICSMOU TO SMOOTH THE DATA
C*****************************************************************
      REAL X(N1),Y(N1),WK(3000)
      NX=N1 $ DIS=1.0 $ SC=0.0 $ MAXIT=N1
      CALL ICSMOU(X,Y,NX,DIS,SC,MAXIT,WK,IER)
      RETURN
      END
      FUNCTION SP(T,N,C)
C*****************************************************************
C FUNCTION TO GENERATE SPLINED DATA OF A DATA FILE
C*****************************************************************
      COMMON/X/X(3000)
      COMMON/Y/Y(3000)
      REAL C(N,3)
      DO 10 I=1,N
      IF(T.LT.X(I).OR.T.GT.X(I+1)) GO TO 10
      D=T-X(I)
      SP=((C(I,3)*D+C(I,2))*D+C(I,1))*D+Y(I)
      RETURN
10    CONTINUE
      END
00.52.57.  00018 PAGES 0000228 LINES PRINTED AT SITE MW
```

APPENDIX F

PROGRAM FOR DATA-PROCESSING OF EXPERIMENTAL RESULTS

```
      PROGRAM EXDATA(INPUT,OUTPUT,TAPE1,TAPE2,TAPE3,TAPE4,TAPE5,TAPE6,TA
     +PE7,TAPE8,TAPE9)
C**********************************************************************
C THIS  PROGRAM  PROCESSES THE DATA MEASURED BY TIME-DOMAIN RANGE.
C I/O FILES ARE DESCRIBED IN CHAP 5 OF THESIS OF C.I. CHUANG.
C ALL OUTPUT FILES ARE IN FORMAT(5X,E10.4,5X,E10.4,5X,E10.4).
C IT IS CATALOGED AS EXPOPEW
C**********************************************************************
      COMMON/X/X
      COMMON/Y/Y
      REAL FMAX(2),TMAX(2)
      REAL S1(1000)
      REAL S2(1000)
      DIMENSION HVD(1000),VVD(1000)
      REAL X(1000),F(1000),Y(1000),DF(1000),C(1000,3),WK(5000)
      REWIND 1 $ REWIND 2
      REWIND 3 $ REWIND 4
      REWIND 5 $ REWIND 6
      REWIND 7 $ REWIND 8
      REWIND 9
C**********************************************************************
C THIS OPTION MATCHES THE MAXIMA OF UNINTEGRATED DATA OF TAPES 5 & 7.
C**********************************************************************
      PRINT*,"DO YOU WANT TO MATCH THE MAXIMUM ? ENTER 1 IF YES-"
      READ*,IY
      PRINT*,"ENTER DISTANCE IN CM-"
      READ*,DIS
      TZ=DIS/15.
C**********************************************************************
C NOTE: TZ IS THE TWO-WAY PROPAGATION TIME BETWEEN TARGET AND PROBE IN
C       NS.
C IF NI=1 READ RAW DATA FOR EXP WITHOUT TARGET,
C IF NI=2 READ RAW DATA FOR EXP WITH TARGET.
C**********************************************************************
      DO 98 NI=1,2
      ND=0
10    ND=ND+1
      IF(NI-2) 99,97,97
99    READ(1,*) HVD(ND)
      READ(2,*) VVD(ND)
      GO TO 96
97    READ(5,*) HVD(ND)
      READ(6,*) VVD(ND)
96    CONTINUE
      IF(ND.EQ.1) GO TO 10
      IF((HVD(ND)-HVD(ND-1)).LT.-100.) GO TO 20
      GO TO 10
20    NS=ND-1
C NS=# OF AVAILABLE DATA PTS. BEFORE RETRACE.
      NZ=0
91    NZ=NZ+1
C IF THERE IS A SUDDEN RISE, THEN THIS IS THE TIME INCIDENT WAVEFORM
C HITS THE PROBE; NZ IS # OF PTS BEFORE THIS TIME. ALL THE FIRST
C NZ PTS WILL BE SET TO ZERO FOR CONSIDERATION OF ONLY TARGET RESPONSE.
      IF((VVD(NZ+1)-VVD(NZ)).GT.10.) GO TO 92
      GO TO 91
92    CONTINUE
C NE= # OF EXTRA PTS AFTER RETRACE TO BE AVERAGED TO EVALUATE THE DC
C LEVEL IN OPTION 2 & 3.
      PRINT*,"ENTER # OF EXTRA PTS, NE-"
      READ*,NE
      NEM1=NE-1
      DO 17 I=1,NEM1
      IF(NI.EQ.2) GO TO 93
      READ(1,*) HVD(NS+I+1)
      READ(2,*) VVD(NS+I+1)
      GO TO 95
93    READ(5,*) HVD(NS+I+1)
      READ(6,*) VVD(NS+I+1)
95    CONTINUE
17    CONTINUE
      HVI=HVD(1)
      HVF=HVD(NS)
      PRINT*,"NS=",NS
      PRINT*,"ENTER TPD IN NS-"
C TPD=TIME PER DIV ON SCOPE
      READ*,TPD
C DT=APPROX. TIME INCREMENT FOR EXP. ASSUMING TOTAL TIME OF A TRACE
C IS (TPD*10) NS AND THE LAST PT CORRESPONDS TO THE FULL SCALE OF TIME.
      DT=((HVF-HVI)/HVF)*10.*TPD/(NS-1)
      NZ=NZ+TZ/DT
C FOR TARGET RESPONSE, NZ PTS ARE SET TO ZERO SO THAT THE FIRST
C NONZERO PT IS DUE TO THE TARGET.
```

```
      PRINT*,"NZ=",NZ
C*************************************************************************
C EVALUATION OF DC LEVEL.
C*************************************************************************
      PRINT*,"WHAT OPTION DO YOU WANT?"
      PRINT*,"(1) AVE FIRST 10 (2) AVE LAST 10 (3) DO BOTH AND LIN INT"
      PRINT*,"(4) INTEGRATE THE RAW DATA AND ESTIMATE DC"
      PRINT*,"ENTER NOP-"
      READ*,NOP
      IF(NOP.EQ.4) GO TO 99
      IF(NOP-2) 51,53,51
51    II=1 $ IF=10
      GO TO 54
53    II=NS+NE-9 $ IF=NS+NE
54    CONTINUE
      DC=0.
      DO 11 I=II,IF
      DC=DC+VVD(I)
11    CONTINUE
      NP=IF-II+1
      DC=DC/NP
      PRINT*,"DC=",DC
      IF(NOP.NE.3) GO TO 55
      IF(II.EQ.1) DC1=DC
      IF(II.EQ.1) GO TO 53
      IF(IF.EQ.NS+NE) DC2=DC
55    CONTINUE
99    CONTINUE
C THE FOLLOWING IS PARAMETERS USED IN SPLINE ROUTINE ICSSCU
      X(1)=0. $ F(1)=0. $ DF(1)=1.
      IC=NS $ SM=0.0
      FMAX(NI)=0.
      IF(NOP.NE.4) GO TO 100
C NA=# OF PTS TO BE INTEGRATED IN OPTION 4
      PRINT*,"ENTER NA-"
      READ*,NA
      D=0.
      NZP1=NZ+1
      DO 77 I=NZP1,NA
      T=(I-NZ)*DT
      DP=.02*VVD(I)
      D=D+DP*DT
77    CONTINUE
      DC=D/T/0.02
      PRINT*,"DC=",DC
100   CONTINUE
      E=0.
C*************************************************************************
C SUB DC. FIND MAX, INTEGRATE AND OUTPUT TO TAPES 3 & 7
C*************************************************************************
      DO 12 I=1,NS
      T=(I-1)*DT+HVI/HVF*10.*TPD
      IF(NOP.EQ.3) DC=DC1+(DC2-DC1)*(I-5.5)/(NS+NE-10.)
      EP=.02*(VVD(I)-DC)
      IF(IY.NE.1) GO TO 14
      IF(EP.LE.FMAX(NI)) GO TO 14
      FMAX(NI)=EP $ TMAX(NI)=T
14    CONTINUE
      IF(I.LE.NZ) EP=0.
      E=E+EP*DT
      IP1=I+1
      X(IP1)=T $ F(IP1)=EP
      DF(IP1)=1.
      IF(NI.EQ.1) WRITE(3,40) T,EP,E
      IF(NI.EQ.2) WRITE(7,40) T,EP,E
40    FORMAT(5X,E10.4,5X,E10.4,5X,E10.4)
12    CONTINUE
C*************************************************************************
C MATCH MAX IF NECESSARY, SPLINE, SUB REFERENCE AND OUTPUT TO TAPES .
C*************************************************************************
      IF(IY.NE.1) GO TO 74
      PRINT*,"TMAX=",TMAX(NI)
      PRINT*,"FMAX=",FMAX(NI)
      IF(NI.EQ.1) GO TO 57
      TS=TMAX(2)-TMAX(1)
      RT=FMAX(2)/FMAX(1)
      PRINT*,"TIMESHIFT=",TS
      PRINT*,"RATIO=",RT
57    NSP1=NS+1
      IF(NI.EQ.1) GO TO 74
      DO 73 I=2,NSP1
      X(I)=X(I)-TS
      F(I)=F(I)/RT
73    CONTINUE
74    CONTINUE
      NSP1=NS+1
      CALL ICSSCU(X,F,DF,NSP1,SM,Y,C,IC,WK,IER)
      DTI=TPD/100.
```

```
      RES=0.
      DO 30 I=1,1000
C OUTPUT ONLY 500 PTS BUT INTEGRATE 1000 PTS TO GET MORE ACCURATE RESULT
      IW=I-I/2*2
      T=DT1*I
      IF(NI.EQ.2) GO TO 59
      A=S(T,NS,C)
      RES=RES+A*DT1
      S1(I)=A $ S2(I)=RES
      IF(IW.EQ.0) WRITE(4,40) T,A,RES
      GO TO 30
59    A=S(T,NS,C)
      RES=RES+A*DT1
      DIF1=A-S1(I) $ DIF2=RES-S2(I)
      IF(IW.EQ.0) WRITE(8,40) T,A,RES
      IF(IW.EQ.0) WRITE(9,40) T,DIF1,DIF2
30    CONTINUE
39    CONTINUE
      END
C**********************************************************************
C THIS IS THE RESULTING FUNCTION AFTER SPLINE
C T=TIME, N=# OF PTS  SPLINED, C=PARAMETER IN ICSSCU.
C**********************************************************************
      FUNCTION S(T,N,C)
      COMMON/X/X(1000)
      COMMON/Y/Y(1000)
      REAL C(N,3)
      DO 10 I=1,N
      IF(T.LT.X(I).OR.T.GT.X(I+1)) GO TO 10
      D=T-X(I)
      S=((C(I,3)*D+C(I,2))*D+C(I,1))*D+Y(I)
      RETURN
10    CONTINUE
      END
00.53.57.  00028 PAGES 0003165 LINES PRINTED AT SITE KV
```

BIBLIOGRAPHY

BIBLIOGRAPHY

[1] Kennaugh, E.K. and D.L. Moffatt, "Transient and Impulse Response Approximation," Proc. of IEEE, Vol. 53, pp. 893-901, August 1965.

[2] Moffatt, D.L. and R.K. Mains, "Detection and Discrimination of Radar Targets," IEEE Trans. on Ant. Prop., Vol. AP-23, No. 3, pp. 358-367, May 1975.

[3] Berni, A.J., "Target Identification by Natural Resonance Estimation," IEEE Trans. on Aerospace and Electronic Systems, Vol. AES-11, No. 2, pp. 147-154, March 1975.

[4] Young, J.D., "Radar Imaging from Ramp Response Signatures," IEEE Trans. on Ant. Prop., Vol. AP-24, No. 3, pp. 276-282, May 1976.

[5] Shubert, K.A., J.D. Young and D.L. Moffatt, "Synthetic Radar Imagery," IEEE Trans. on Ant. Prop., Vol. AP-25, No. 4, pp. 477-483, July 1977.

[6] Bennett, C.L. and W. Weeks, "A Technique for Computing Approximate Electromagnetic Impulse Response of Conducting Bodies," Purdue University, Lafayette, Indiana, Tech. Report TR-EE68-11, 1968.

[7] Repjar, A.G., A.A. Ksienski and L.J. White, "Object Identification from Multi-frequency Radar Returns," The Radio and Electronics Engineers, Vol. 45, No. 4, pp. 161-167, April 1975.

[8] Chuang, C.W. and D.L. Moffatt, "Natural Resonance of Radar Target via Prony's Method and Target Discrimination," IEEE Trans. on Aerospace and Electronic Systems, Vol. AES-12, No. 5, pp. 583-589.

[9] Baum, C.E., "The Signlarity Expansion Method," Transient Electromagnetic Fields, L.B. Felsen Ed., Springer-Verlag, New York, 1975, pp. 130-176.

[10] Tesche, F.M., "On the Analysis of Scattering and Antenna Problems Using the Singularity Expansion Techniques," IEEE Trans. on Ant. Prop., Vol. AP-21, No. 1, pp. 53-62, January 1973.

[11] Marin, L., "Natural-Mode Representation of Transient Scattering from Rotationally Symmetric Bodies," IEEE Trans. on Ant. Prop., Vol. AP-22, No. 2, pp. 266-274, March 1974.

[12] Van Blaricum, M.L. and R. Mittra, "A Technique for Extracting the Poles and Residues of a System Directly from its Transient Response," IEEE Trans. on Ant. Prop., Vol. AP-23, No. 6, pp. 777-781, November 1975.

[13] Chen, K.M., D.P. Nyquist, D. Westmoreland, C.I. Chuang and B. Drachman, "Radar Waveform Synthesis for Single-Mode Scattering by a Thin Cylinder and Application for Target Discrimination," IEEE Trans. on Ant. Prop., Vol. AP-30, No. 5, pp. 867-880, September 1982.

[14] Baum, C.E., "Toward an Engineering Theory of Electromagnetic Scattering: The Singularity and Eigenmode Expansion Methods," in Electromagnetic Scattering, P. Uslenghi Ed., Academic Press, New York, 1978, pp. 571-602.

[15] Baum, C.E., "On the Singularity Expansion Method for the Solution of Electromagnetic Interaction Problems," Interaction Note 88, December 1971.

[16] Marin, L., "Application of Singularity Expansion Method to Scattering from Imperfectly Conducting Bodies and Perfectly Conducting Bodies within a Parallel Plate Region," Interaction Note 116, June 1972.

[17] Chen, K.M., "Radar Waveform Synthesis Method - A New Radar Detection Scheme," IEEE Trans. on Ant. Prop., Vol. AP-29, No. 4, pp. 553-566, July 1981.

[18] Singaraju, B.K., D.V. Giri and C.E. Baum, "Further Developments in the Application of Contour Integration to the Evaluation of the Zeros of Analytic Functions and Relevant Computer Programs," Mathematics Note 42, March 1976.

[19] Collin, R.E., Field Theory of Guided Waves, McGraw-Hill, New York, 1960, pp. 49-51.

[20] Butler, C.M., "Currents Induced on a Pair of Skew Crossed Wires," IEEE Trans. on Ant. Prop., Vol. AP-20, No. 6, pp. 731-736, November 1972.

[21] Stratton, J.A., Electromagnetic Theory, McGraw-Hill, New York, 1941, p. 371.

[22] Abramowitz, M. and I.A. Stegun, Handbook of Mathematical Functions, Dover, New York, 1965.

[23] Watson, G.N., A Treatise on the Theory of Bessel Functions, Cambridge University Press, Cambridge, 1952.

[24] Luke, Y.L., "Approximate Inversion of a Class of Laplace Transforms Applicable to Supersonic Flow Problems," Quart. J. Mech. and Appl. Math., Vol XVII, Pt. 1, pp. 91-103.

[25] Churchill, R.V., Complex Variables and Applications, 2nd Ed., McGraw-Hill, New York, 1960.

[26] Drachman, B.C. and C.I. Chuang, "A Table of Two Hundred Zeros of the Derivative of the Modified Bessel Function $K_n(z)$ and a Graph of Their Distribution," J. Comp. and Appl. Math., Vol. 7, No. 3, pp. 167-171, September 1981.

[27] Goldstein, M., "Program Abstract on Bessel Functions for Complex Argument and Order (COMBES)," New York, November 1965.

[28] Chen, K.M. and D. Westmoreland, "Impulse Response of a Conducting Sphere Based on Singularity Expansion Method," Proc. IEEE, Vol. 69, No. 6, pp. 747-750, June 1981.

[29] Moffatt, D.L., "Impulse Response Waveforms of a Perfectly Conducting Right Circular Cylinder," Proc. IEEE, Vol. 57, No. 5, pp. 816-817, May 1969.

[30] Jones, D.S., Methods in Electromagnetic Wave Propagation, Oxford University Press, Oxford, 1979, pp. 572-578.

[31] Dongarra, J.J., C.B. Moler, J.R. Bunch and G.W. Stewart, Linpack Users' Guide, SIAM, Philadelphia, 1979.

[32] Harring, R.F., Field Computation by Moment Methods, Macmillan, 1968.

[33] Umashankar, K.R., T.H. Shumpert and D.R. Wiltin, "Scattering by a Thin Wire Parallel to a Ground Plane Using the Singularity Expansion Method," IEEE Trans. on Ant. Prop., Vol. AP-23, No. 2, pp. 178-184, March 1975.

[34] Crow, T.T., B.D. Graves and C.D. Taylor, "The Singularity Expansion Method as Applied to Perpendicular Crossed Wires," IEEE Trans. on Ant. Prop., Vol. AP-23, No. 4, pp. 540-546, July 1975.

[35] King, R.W.P. The Theory of Linear Antennas, Harvard Press, 1956.

[36] Dimoff, K., Statistical Plotting On-Line Command System User's Guide, Dept. of Entomology, Michigan State Univ., E. Lansing, 1981.

[37] Chen, K.M. and D. Westmoreland, "Radar Waveform Synthesis for Exciting Single-Mode Backscatters from a Sphere and Application for Target Discrimination," Radio Science, Vol. 17, No. 3, pp. 574-588, June 1982.

[38] Marin, L., "Major Results and Unresolved Issues in Singularity Expansion Method," Elecromagnetics, Vol. 1, No. 4, pp. 361-373, October-December 1981.